Arming vaccinia virus for pancreatic cancer oncolytic virotherapy

Hiley, Crispin

Barts & The London School of Medicine and Dentistry
Queen Mary University of London

Arming Vaccinia Virus for Pancreatic Cancer Oncolytic Virotherapy

PhD Thesis

Postgraduate Student: Crispin Hiley BSc (hons) MBChB (hons)
Supervisors: Dr Y Wang & Professor N Lemoine

Acknowledgements

Acknowledgments

I am most grateful for the support of my supervisors Dr Y Wang and Professor N Lemoine.

I would like to acknowledge the contribution of Dr Louisa Chard, who provided post-doctoral assistance during the design and construction of VV-ODD.

I would like to acknowledge the contribution of Dr A Braint, who constructed the pCMV-Neo-VEGF-165 and pCMV-Neo-Vector Control vectors.

I would like to acknowledge the contribution of Ms Heike Muller and Mr Vipul Bhakta who were responsible for large scale (CF-10) virus production after primary expansion.

All histology and immunehistochemistry was performed by the Institute of Cancer Pathology Department.

I am thankful to all the members of the Viral Gene Therapy Group and the Charterhouse Square Biological Services Unit for their assistance and suggestions during this project.

Finally I am most indebted to Cancer Research UK for financial support and the Molecular Pathology of Cancer Steering Committee for giving me this opportunity.

Abstract

Abstract

Vaccinia virus is a 250-300nm enveloped DNA virus from the poxvirus family and is used as a vector for oncolytic viral gene therapy. No unique cell surface receptor has been identified for Vaccinia virus and the reasons for its tropism for cancer cells are unclear. Pancreatic adenocarcinoma (PDAC) is resistant to conventional chemotherapy and typically contains areas that are profoundly hypoxic.

We have investigated the utility of Vaccinia virus as a vector for targeting hypoxic regions in pancreatic adenocarcinoma, as other viral vectors have been found to replicate poorly in hypoxia. We found that cytotoxicity was equivalent in normoxia and hypoxia in some PDAC cell lines but in others cytotoxicity was enhanced in hypoxia. This increase in cytotoxicity was only seen in cell lines where there was hypoxic induction of vascular endothelial growth factor (VEGF). Functional studies using over-expression and knockdown of VEGF in pancreatic cancer cell models showed that VEGF can augment viral transgene expression, cytotoxicity and replication *in vitro* and *in vivo*. We found that VEGF facilitates the internalisation of Vaccinia virus. These results show that VEGF is an additional factor involved in the tropism and pathogenesis of Vaccinia virus.

We then constructed an oncolytic Vaccinia virus to target hypoxic cancer cells using the HIF-1α oxygen degradation domain, encephalomyocarditis virus internal ribosomal entry site and the VEGF 3' un-translated region to regulate luciferase expression in hypoxia. We have shown a dose-, time- and oxygen-dependent effect using this construct and propose this may be adapted to regulate therapeutic genes, or produce a conditionally replicating Vaccinia virus, in hypoxic conditions.

Contents

Contents

List of Figures

List of Figures

List of Tables

List of Tables

List of Abbreviations

List of Abbreviations

Abbreviations	Definition
AMP	Adenosine Monophosphate
AMPK	AMP-activated protein kinase
ARCON	Accelerated radiotherapy with carbogen and nicotinamide
ATP	Adenosine TriPhosphate
BC	Breast Cancer
BCG	Bacillus Calmette-Guerin
BEGM	Bronchial Epithelial Growth Medium
BPE	Bovine Pituitary Extract
BRCA2	Breast Cancer 2
BSA	Bovine Serum Albumin
BSC-1	Kidney Epithelial Cells of Monkey Origin
CA	California
CALGB	Cancer And Leukaemia Group B
CAR	Coxsackie/Adenovirus receptor
CAT	Chloramphenicol Acetyl Transferase
CCS	Claire Hall Cell Services
CEACAM6	Carcinoembryonic antigen-related cell adhesion molecule 6
CEV	ell-associated enveloped virus
CH	Crispin Hiley
CIAP	Calf Intestinal Alkaline Phosphatase
CO_2	Carbon dioxide
CPE	Cytopathic Effect
CRUK	Cancer Research UK
CT	Computed Tomography
CXCL	CXC chemokine ligands
DAB	3,3'-diaminobenzidine tetrahydrochloride
DAPI	4',6-diamidino-2-phenylindole
DMEM	Dulbecco's modified Eagle's medium
DMOG	Dimethyloxaloyl glycine
DMSO	dimethyl sulfoxide
DNA	Deoxyribonucleic Acid
DTT	Dithiothreitol
EC50	Half maximal effective concentration
EDTA	ethylenediaminetetraacetic acid
EEV	Extracellular Enveloped Virus
EGF	Epidermal Growth Factor
EGFR	Epidermal Growth Factor Receptor
ELISA	Enzyme-Linked Immunosorbent Assay
EMCV	Encephalomyocarditis virus
EPC	Epithelial Progenitor Cell
ESPAC	European Study Group for Pancreatic Cancer
FCS	Foetal Calf Serum
FDA	Federal Drug Administration
FIH	Factor Inhibiting HIF
FITC	Fluorescein isothiocyanate
GADD34	Growth Arrest and DNA Damage-Inducible Protein 34
GAG	Glycos-aminoglycan

Abbreviations	Definition
GFP	Green Fluorescence Protein
GM-CSF	Granulocyte Macrophage Colony- Stimulating Factor
H&E	Hematoxylin and Eosin
HBV	Hepatitis B Virus
HCV	Hepatitis C Virus
HGF	Hepatocyte Growth Factor
HIF-1	Hypoxia inducible factor-1
HIV	Human Immunodeficiency Virus
HPV	Human Papilloma Virus
HRE	Hypoxia Response Elements
HRP	Horse radish peroxidase
HSPG	Heparan sulfate proteoglycan
HSV	Herpe Simplex Virus
HTLV	Human T-Cell Lymphotropic Virus
HUVEC	Human Umbilical Vein Endothelial Cell
IEV	Intracellular Enveloped Virus
IFN	Interferon
IHC	Immunohistochemistry
IL	Interleukin
IMRT	Intensity Modulated Radiotherapy
IMV	Intracellular Mature Virus
IP	Intra-peritoneal
IRES	Internal Ribosomal Entry Site
IV	Intra-venous
IVIS	In Vivo Imaging System
KDR	Kinase Domain Region/Flk-1
LB	Lysogeny Broth
LMP	Low Melting Point
LSM	Laser Scanning Microscope
LV	Leucovorin
MDR	Multi Drug Resistance
MOI	Multiplicity Of Infection
MTS	3-(4,5-Dimethylthiazol-2-yl)-2,5-diphenyltetrazolium bromide
MVA	Modified Virus Ankara
NHBE	Normal Human Bronchial Epithelial
NK	Natural Killer
NO	Nitric Oxide
NRP1	Neuropilin-1
NSCLC	Non Small Cell Lung Cancer
NYVAC	New York Health Board Vaccination Strain
O_2	Oxygen
OD	Optical Density
ODD	Oxygen Degradation Domain
PBS	Phosphate Buffered Saline
PCNA	Proliferating Cell Nuclear Antigen
PCR	Polymerase Chain Reaction
PDAC	Pancreatic Ductal Adenocarcinoma
PDGF	Platelet Derived Growth Factor
PECAM-1	Platelet Endothelial Cell Adhesion Molecule-1

Abbreviations	Definition
PHD	Prolyl Hydroxylase
PI3K	Phosphatidylinositol 3-kinases
PKR	Protein kinase R
PTEN	Phosphatase and tensin homolog
PVDF	Polyvinylidene Fluorid
RECIST	Response Evaluation Criteria In Solid Tumor
RES	Restriction Enzyme Site
RFP	Red Fluorescent Protein
RGB	Red-Green-Blue
RHP	Random Hexanucleotide Primers
RISC	RNA-Induced Silencing Complex
RNA	Ribonucleic acid
ROI	Region Of Interest
ROS	Reactive Oxygen Species
RT	Reverse Transcription
SDS	Sodium dodecyl sulfate
SEER	Surveillance Epidemiology and End Results
SEM	Standard error of the mean
SV40	Simian vacuolating virus 40
TAD	Trans-activating domain
TAE	Tris-acetate-EDTA
TBST	Tris-Buffered Saline and Tween 20
TCID50	50% Tissue Culture Infective Dose
TK	Thymidine Kinase
TSC	tuberous sclerosis complex
TUNEL	Terminal deoxynucleotidyl transferase dUTP nick end labeling
UTR	Untranslated region
VC	Vector Control
VEGF	Vascular endothelial growth factor-A
VEGF-E	Vascular endothelial growth factor-E
VEGFR	Vascular endothelial growth factor receptor
VGF	Vaccinia Growth Factor
VHL	Von Hippel Lindau
VLTF	Vaccinia Late Transcription Factor
VSV	Vesicular Stomatitis Virus
VV-488	Flourescently labelled Vaccinia virus
VVL	Vaccinia virus Lister strain
VVL15	TK deleted Vaccinia virus with fLuc reporter gene
VVL-488	Fluorescently labelled Vaccinia virus
VV-ODD	Hypoxia-targeting Vaccinia virus
WHO	World Health Organisation
WR	Western Reserve
YW	Yaohe Wang

Chapter 1

1 Introduction

1.1 Pancreatic Ductal Adenocarcinoma

1.1.1 Pancreatic Cancer Incidence & Epidemiology

Pancreatic ductal adenocarcinoma (PDAC) remains a disease with a dismal prognosis. Worldwide it is the 14th most common cancer but the fifth and sixth leading cause of cancer death in the USA and UK respectively. In the developed world incidence has risen three-fold since the 1920s, stabilising in the late 1970s. PDAC occurs at an incidence of 1.75:1 male to female ratio but this gender bias diminishes with increased age of onset. Approximately 30 percent of cases of PDACs are attributable to smoking. Diet and occupational carcinogens have been implicated but findings are not conclusive. Chronic pancreatitis is a known risk factor with the chronic inflammatory condition predisposing to malignant transformation(1).

1.1.2 Pathology and Molecular Biology

PDAC has a well-defined chronology of pathological and molecular changes during disease progression (Figure 1.1). Pre invasive lesions consist of pancreatic intra-epithelial neoplasia (PanIN) 1-3, after which loss of the integrity of the basement membrane is a sign of invasive carcinoma. The K-Ras oncogene is mutated in 95% of sporadic PDACs (2). It is located on chromosome 12p13 and mutations results in a constitutively active form which signals via the Ras-Raf-MEK pathway. The ErbB family of growth factor receptors have also been shown to be over expressed in PDAC, in particular epidermal growth factor receptor (EGFR) family members. Signalling via EGFR1 is increased due to greater production of its two ligands epidermal growth factor (EGF) and transforming growth factor-alpha (TGF-α). This results in signalling via the Ras-Raf-MEK signalling pathway (transmitting proliferative signals), the PI3K/Akt signalling pathway (mediating cell cycle progression and survival) and the signal transducer and activator of transcription (STAT) family of proteins which mediates a variety of

features conducive to cancer cell survival progression, including cell division, motility, invasion and adhesion (3). Loss of p16 function occurs in 80–95% of PDACs and results in abrogation of the pRB/p16 pathway, this means that p16 can no longer inhibit the formation of the cyclin D-cyclin-dependent kinase4/6 (CDK4/CDK6) complex resulting in cell cycle progression (4).

Later in the development of PDAC, loss of the tumour suppressor genes p53, DPC4 and BRCA2 is found (5). Smad4 mediates intercellular signalling for members of the TGFβ family of cytokines. There is a loss of heterozygosity of Smad4 in 70% of pancreatic cancers and a total loss of protein function in 50%. This mutation affects the tumour microenvironment and potentiates tumour invasion (6). Reactivation of the developmental signalling pathway through Notch and Hedgehog is found in PDAC and may be involved in a putative pancreatic cancer stem cell phenotype (7). In summary, a progression model for pancreatic cancer exists but the variety of molecular changes highlight the heterogeneity of PDAC.

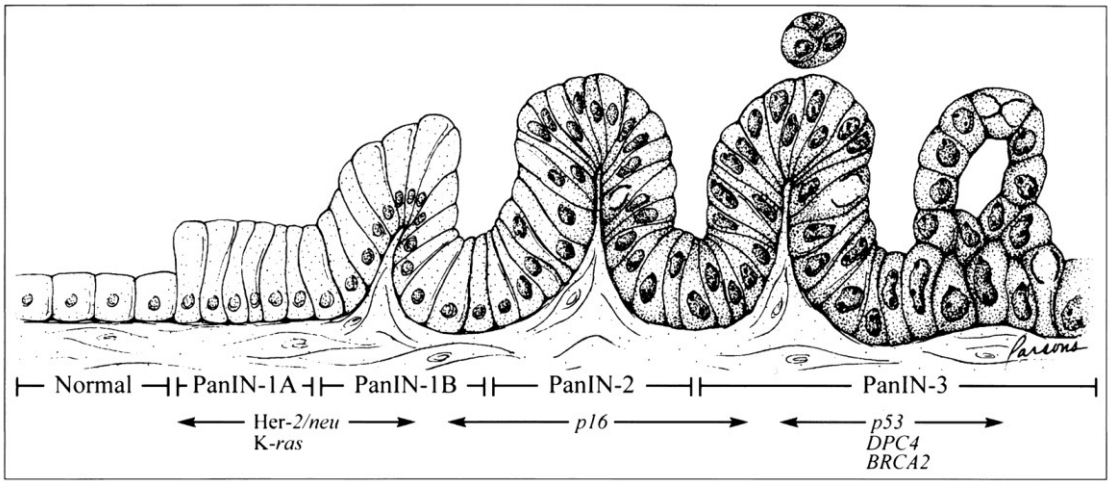

Figure 1.1: Progression model for pancreatic cancer.

Normal duct epithelium progresses to infiltrating cancer (*left* to *right*) through a series of histologically defined precursors. (5)

1.1.3 Pancreatic Ductal Adenocarcinoma Management

In the UK during 2004 there were 7398 new cases and 7238 deaths with outcomes being poor regardless of the therapeutic modality (8). Median survival for surgically resected patients is 11-15 months, 6-10 months for locally advanced disease and 3-5 months for metastatic disease(7).

Surgery remains the only curative therapy although only a minority (10-15%) of patients present early enough for resection. A Kausch-Whipple partial pancreatoduodenectomy or a pylorus-preserving partial pancreatoduodenectomy are considered the standard surgical procedures for resectable disease.

For adjuvant therapy of resectable disease, ESPAC-1 was the first study to show benefit for chemotherapy in this setting. ESPAC-1 demonstrated a 21% vs. 8% 5 year survival rate when patients received 5-florouracil (5-FU) and Leucovorin (LV) as opposed to observation (9). The CONKO-001 study showed a similar benefit for gemcitabine chemotherapy in the adjuvant setting (10). ESPAC-3 was designed to compare 5-FU/LV with gemcitabine in a head to head design. Both drug treatments improved 5 year survival in comparison to historical data, but no benefit was seen to favour either agent in the adjuvant setting (11). The standard of care for locally advanced or metastatic disease involves gemcitabine monotherapy, which has shown greater efficacy and lower toxicity compared to the previous regime of 5-flourouracil (12). A meta-analysis of clinical trials of chemotherapy for advanced pancreatic cancer have shown a small but significant survival advantage with combination regimes of gemcitabine with capecitabine (an oral 5-FU analogue) or a platinum-based drug over gemcitabine alone (13). A phase III randomized trial has recently demonstrated a 7.4 vs. 6.0 month (P=0.026) benefit for gemcitabine and capecitabine versus gemcitabine alone (14). Despite this, median survival times are still measured in months and consequently trials of biological agents targeting the molecular pathways involved in pancreatic cancer continue to be investigated. The EGFR inhibitor, erlotinib, was licensed by the Federal Drug Administration (FDA) after showing a

6.24 vs. 5.91 month improvement in mean overall survival when given with gemcitabine over gemcitabine alone (15). The anti-VEGF monoclonal antibody bevacizumab and the anti-EGFR monoclonal antibody cetuximab did not improve median survival in phase III trials of patients with metastatic and locally advanced PDAC (16, 17). Given this, there is a great need to develop effective systemic therapy, and consequently multiple novel immunotherapy and gene therapy strategies are being investigated.

The role of radiotherapy in the management of pancreatic cancer remains controversial. The ability to deliver high dose therapy is limited by the proximity of adjacent organs. More targeted radiotherapy techniques which allow greater dose delivery and account for organ motion may prove to be useful. These include 3D conformal radiotherapy and Intensity-Modulated Radiotherapy (IMRT) which improve targeting by using multiple lower energy beams to deliver a higher total dose at the point where the beams transect. Proton therapy uses ionised protons which, compared to conventional radiation therapy, allow more accurate tumour targeting and decreased deposition of energy in the normal tissue through which it passes before reaching the tumour. In addition incorporation of organ motion sensing during the breathing cycle into the treatment plan should allow delivery of greater radiotherapy doses without increased toxicity. In the adjuvant setting, combination chemoradiotherapy (5-FU and ~45Gy) has been widely used in some centres (18). Data from the Surveillance Epidemiology and End Results (SEER) registry suggest that there is a five-month improvement in overall survival with the addition of radiotherapy to treatment (17 month vs. 12 month median survival, $P<0.0001$) (19). However no benefit has been demonstrated in a phase III randomised trial and in the ESPAC-1 trial a detrimental effect was seen. Radiotherapy may still be useful in the adjuvant setting if combination regimes can be designed or dose delivery improved with advanced external beam technologies or radionucleotide strategies. For locally advanced pancreatic cancer, radiotherapy is beneficial when given in combination with 5-FU but there are limited data to support the addition of radiotherapy to gemcitabine (20). There is currently no role for radiotherapy in the metastatic setting except for palliation of symptoms.

There is clearly an unmet need in the treatment of PDAC both in the adjuvant and metastatic setting and virotherapy has emerged as a novel strategy to treat tumours resistant to conventional therapy (21). Vaccinia virus is a promising vector for gene delivery, viral oncolysis and cancer vaccines however, tumour hypoxia has been shown to reduce the efficacy of conventional therapy (22) and it is important also to investigate its effect on novel therapies.

1.2 Hypoxia and Cancer

Tissue hypoxia is the result of a mismatch of oxygen supply to cellular demand and can be multi-factorial in origin. Reduction in atmospheric oxygen concentration, decreased blood oxygen-carrying capacity, impaired perfusion of tissue vasculature and the distance over which molecular oxygen must diffuse from vessel to cell all limit the delivery of oxygen. The physiology and microenvironment of solid tumours are fundamentally different from normal tissue and are more prone to develop hypoxic regions because the disordered growth of tumours results in structural and functional distortions in the microcirculation which impairs the delivery of oxygen.

Normal tissues can maintain cellular function at a range of pO_2 from 10-80mmHg depending on the tissue type. In contrast, cancer cells can be exposed to pO_2 <10mmHg with moderate hypoxia being defined as $pO_2 \leq 1\%$ (~7mmHg), extreme hypoxia as $pO_2 \leq 0.1\%$ and anoxia as the absence of molecular oxygen (23). Tumours can be exposed to both chronic and acute hypoxia. Chronic hypoxia occurs when tumour cells are beyond the limit of oxygen diffusion (~150μm) which results from tumour growth extending beyond that of tumour vasculature, and this is defined as diffusion-limited hypoxia. In contrast, fluctuations in tumour blood supply caused by transient occlusion by intravascular thrombus, tumour cells or vasoconstriction result in periods of acute or perfusion-limited hypoxia. Thomlinson and Gray first described areas of hypoxia in histological sections of adenocarcinoma of the lung in 1955 (24). Since this time, areas of hypoxia have been found in the majority of solid tumours including malignant brain tumours

(25), melanomas (26), soft tissue sarcomas (27), prostate cancer (28), cervical cancer (29), invasive breast cancer (30), non-small cell lung cancer (NSCLC) (31), PDAC (32) and head and neck squamous cell carcinoma (HNSCC) (33). However, these areas are often heterogeneously distributed and may be located adjacent to normoxic regions.

1.2.1 Molecular Basis of Oxygen Sensing

The transcription factor hypoxia-inducible factor 1 (HIF-1) is an important regulator of the cellular response to hypoxic conditions (34-36). HIF-1 is a heterodimer composed of a α and β subunit. HIF-1β is constitutively expressed and not regulated by hypoxia. The transcription and translation of the HIF-1α subunit is mainly independent of oxygenation status (37) but proteolytic degradation is profoundly affected (38). In addition, the rate of HIF-1α translation is responsive to growth factor and oncogenic stimulation (39). The proteolytic regulation of HIF-1α is controlled via the oxygen-dependent degradation domain (ODD) (Figure 1.2). This region of HIF-1α contains two domains which are specifically hydroxylated at prolyl residues Pro402 and Pro 564. This hydroxylation is achieved via the actions of three prolyl hydroxylase domain (PHD) enzymes which require the presence of dioxygen as a substrate for this reaction in addition to other cofactors (2-oxoglutarate, iron and ascorbate) (40). This hydroxylation allows HIF-1α to bind the von Hippel-Lindau tumour suppressor protein (pVHL) which then functions as the substrate recognition component of the ubiquitin E3 ligase complex leading to proteolytic degradation of the HIF-1α-pVHL complex (41). In addition an asparaginyl residue, present in an N-terminal transactivation domain (TAD) of HIF-1α, is hydroxylated in the presence of molecular oxygen by factor inhibiting HIF (FIH). This FIH-dependent asparaginyl hydroxylation inhibits interactions with p300 co-activator and limits gene transcription (42).

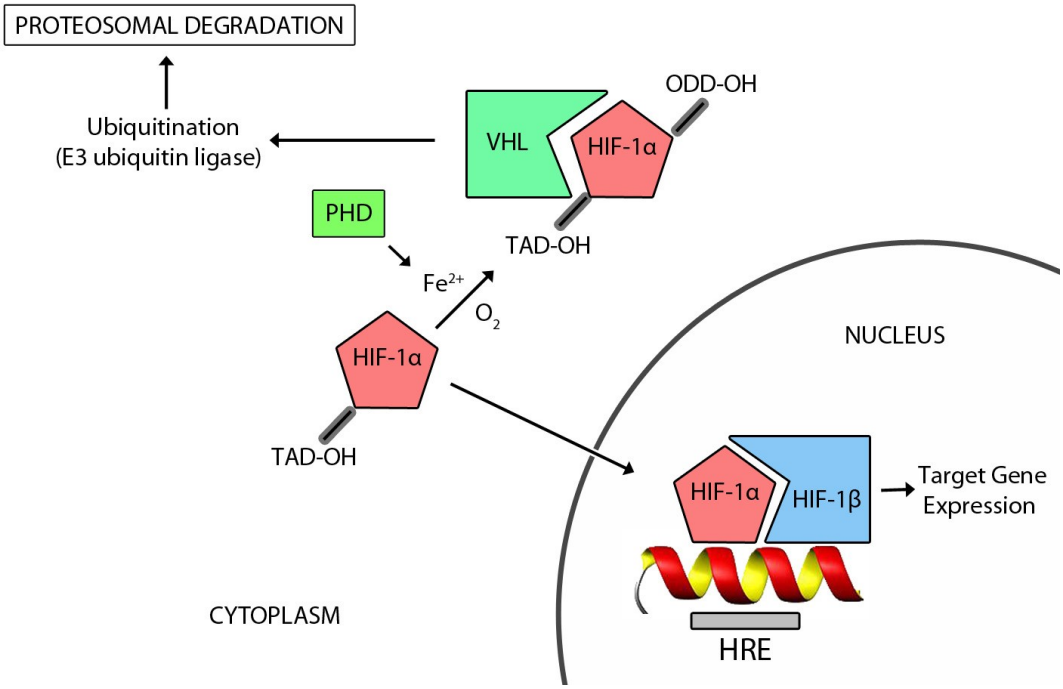

Figure 1.2: An overview of HIF-1α function and regulation.

In the presence of oxygen (O_2), prolyl hydroxylase (PHD) hydroxylates hypoxia-inducible transcription factor (HIF)-1α at the oxygen degradation domain. This allows it to interact with the von Hippel–Lindau (VHL) complex and it is this complex that mediates the ubiquitylation of HIF-1α . The ubiquitination targets HIF-1α for proteosomal degradation. In the absence of oxygen, prolyl hydroxylase cannot modify HIF-1α, and the protein remains stable. Stabilised HIF-1α, with an un-hydroxylated trans-activating domain (TAD) is translocated to the nucleus, where it interacts with cofactors including HIF-1β to bind to hypoxia-responsive elements (HREs) and activate transcription of target genes

Stabilisation of the HIF-p300/CBP complex leads to transcription of target genes containing hypoxia response elements (HRE). HRE sequences are present in the promoter region of some genes, and they contain the core sequence 5'-RCGTG-3' along with flanking regions that are recognised by HIF-1α and lead to the formation of the transcription complex (43). Consequently

this results in the transcription of genes with HREs within their promoters and this cellular response to hypoxia causes increased transcription of a number of genes involved in proliferation, apoptosis, energy metabolism and pH regulation (22). Gene expression studies of the response of both normal, non-transformed cells and cancer cells after exposure to hypoxia were published by Chi *et al.* (44). They defined both a gene signature pattern for the hypoxic response common to all cell types, and a distinct gene set which was specific to epithelial cells *versus* mesenchymal cells. Genes induced by hypoxia in an epithelial model included immune regulatory genes (HLADRB1, HLADRB3), complement inhibitors (SERPING1), solute transporters (MDR1), chemokines (CXCR4), genomic integrity (RAD50, RAD54B) and p53 target genes (caveolin, EGF-like transforming growth factor). Many of these have been implicated in the aetiology of cancer and the resistance to conventional therapy and are considered therapeutic targets. The "hypoxic signature" of Chi *et al* was shown to have independent prognostic significance for survival and progression-free survival in breast and ovarian cancer.

1.2.2 Hypoxia, Local Invasion and Metastasis of Cancer

Exposure of tumour cells to hypoxia results in a phenotypic change with increased local invasion, perifocal tumour spreading and an increased propensity to disseminate widely. In prostate cancer it has been shown to be independently predictive of shortened time to biochemical failure, a surrogate marker for disease progression (45). *In vitro* analysis of the LNCap prostate cancer cell line after exposure to hypoxia for 24 hours demonstrated increased phosphorylation of Akt/Protein Kinase B and reduced apoptotic potential (46). Immunohistochemical analysis of HIF-1α and extrinsic measures of hypoxia such as invasive microelectrode studies and the hypoxic marker pimonidazole (which is reduced and retained in hypoxic cells) can predict for increased invasion and a poor outcome in uterine cervical cancer (29, 47). Human papillomavirus, the causative agent in uterine cervical cancer, has been shown to stabilise HIF-1α and result in increased expression of the vascular endothelial growth factor

(VEGF) (48, 49). In NSCLC an endogenous marker of hypoxia, Carbonic Anhydrase IX, predicts for a poor outcome (31). Knockdown of HIF-1α in NSCLC cell lines, by lentiviral short-hairpin RNA, was found to reduce CXCR4 expression and result in reduced invasion and migration in response to its ligand CXCL12 (50).

The transition of cancer cells from an epithelial to a mesenchymal phenotype is now considered central to cancer migration, invasion and metastasis and is accompanied by the classical molecular hallmarks such as a fibroblastoid phenotype, loss of E-cadherin, β-catenin nuclear translocation and expression of vimentin (51). These changes can be induced by reactive oxygen species generation (ROS) secondary to hypoxic stress or by hypoxic upregulation of HIF-1α, hepatocyte growth factor (HGF), activation of Notch signalling or NFkB pathways or epigenetic changes (52, 53). This concept has great importance since it has been shown that anti-angiogenic strategies can elicit the malignant progression of tumours by causing hypoxia in tumours and promoting an epithelial to mesenchymal transition (54).

1.2.3 Hypoxia and Chemotherapy Response

Cytotoxic chemotherapies, as monotherapies or in combination, are central to modern cancer therapy however hypoxia reduces the efficacy of chemotherapy by multiple mechanisms. The cytotoxicity of some agents relies on the generation of superoxide radicals which results in DNA damage. Doxorubicin, mitomycin C, etoposide, cisplatin and docetaxel have all been shown to generate ROS. Although superoxide radicals can be generated from a number of molecules containing oxygen other than dioxygen a reduction in molecular oxygen availability has been shown to reduce efficacy (55, 56). Drug resistance can also result from hypoxia-induced cellular senescence. Many chemotherapies are only active against the proliferating tumour fraction and senescent cells which survive multiple cycles of chemotherapy will result in tumour regrowth (57). Hypoxic tumours also have disordered vasculature with greater diffusible distances between vessel and tumour cells. Both these factors can lead to poor distribution and

penetration of chemotherapy agents (58). The multiple alterations in gene expression after exposure to hypoxia can reduce the efficacy of chemotherapy. For example, hypoxia can increase the frequency of dihydrofolate reductase gene amplification and antagonise methotrexate cytotoxicity (59) and increase efflux of multiple chemotherapies by expression of the multi drug resistance protein (MDR) 1 (44).

1.2.4 Hypoxia and Radiotherapy

The response of both normal and malignant cells to ionizing radiation is dependent upon adequate oxygenation, a relationship was first described in 1953 by Gray et al (60). They defined the concept of the oxygen enhancement ratio i.e. the additional cytotoxicity induced by a given dose of radiation in normoxic vs. hypoxic cells *in vitro*. It was postulated that three times the amount of radiation was required to kill cells irradiated in the absence of oxygen. The magnitude of this effect at clinically relevant fractionation schedules (which are lower than those used in this original experiment) is not clear but the radio-resistance of hypoxic tumours has been well documented in a number of tumour types. Hypoxia has been shown to be independently predictive of a poor response to radiotherapy in cancer of the cervix (61), head and neck (33), prostate (62) and sarcoma (27, 63).

There are multiple mechanisms of resistance to radiotherapy in hypoxia. Radiation leads to the generation of DNA radicals either by direct ionisation or by radiolysis of water molecules resulting in production of hydroxyl radicals which then react with DNA molecules. This damage is then fixed in the presence of oxygen. In hypoxic conditions, reducing species can accept electrons and repair this damaged before it is permanently fixed. The genetic mechanisms behind radio-resistance are less well characterised than the radiobiological effects. Studies using individual pathway analysis have shown that, as with resistance to chemotherapy, the activation of PI3K/Akt/NF-kappa B signalling is associated with resistance to radiation-induced apoptosis (64). HIF-1α has also been used as a therapeutic target to restore

radiosensitivity. Knockdown of HIF-1α with siRNA *in vivo* using adenoviral gene transfer was found to cause a limited but significant improvement in radiosensitivity (65).

1.2.5 Evidence for hypoxia in PDAC

PDACs contain significant areas of hypoxia that have been measured intraoperatively using microelectrodes (32). Using intrinsic markers it has been shown that hypoxia and HIF-1α stabilisation is associated with a poor prognosis in PDAC (66, 67). *In vitro*, hypoxia is implicated in the resistance to gemcitabine, the current standard of care. Hypoxia causes resistance to the pro-apoptotic effects of gemcitabine by an increase in PI3K/Akt/NF-kappa B signalling (68).

1.3 Vascular Endothelial Growth Factor, Angiogenesis and Cancer

Angiogenesis is the growth of new blood vessels from existing vessels and neoangiogenesis is essential for the growth of all tumours beyond 2 or 3mm (69). The process of angiogenesis is regulated by the balance of angiogenic growth factors and inhibitors, released from endothelial cells, monocytes, platelets, smooth muscle and tumour cells (70). When there is an excess of growth factors in comparison to inhibitors, as is frequently the case in tumours, neoangiogenesis within the local tumour environment is initiated.

Proangiogenic growth factors released from tumours bind to receptors on both endothelial cells of nearby blood vessels and circulating, bone-marrow derived epithelial progenitor cells (EPC). This results in their activation, proliferation and co-ordinated growth via the interaction of integrins with extracellular matrix components. The endothelial cells then remodel and form tubes, which connect into loops through the tumours, forming completed blood vessels. Structural support cells such as smooth muscle cells follow, but these tumour blood vessels remain leaky and have a poorly formed basement membrane (71, 72).

Vascular endothelial growth factor-A (VEGF) is a diffusible mitogen that plays a critical role in angiogenesis by increasing blood vessel permeability, endothelial cell growth, proliferation, migration and differentiation (73-75). VEGF is a heparin-binding polypeptide growth factor that was identified and isolated in 1989 by Ferrara *et al* (76). They discovered a molecule that was secreted into the extracellular compartment and was mitogenic to endothelial cells. Further characterisation has discovered that this molecule exists in multiple isoforms (77) and that these isoforms differ in their molecular masses and their receptor binding (Figure 1.3). They have a variable pattern of binding to heparin or heparan-sulphate proteoglycans and to different VEGF receptors. The splice forms $VEGF_{121}$, $VEGF_{145}$ and $VEGF_{165}$ are secreted, whereas $VEGF_{189}$ is tightly bound to cell surface heparan-sulphate and $VEGF_{206}$ is an integral membrane protein. In

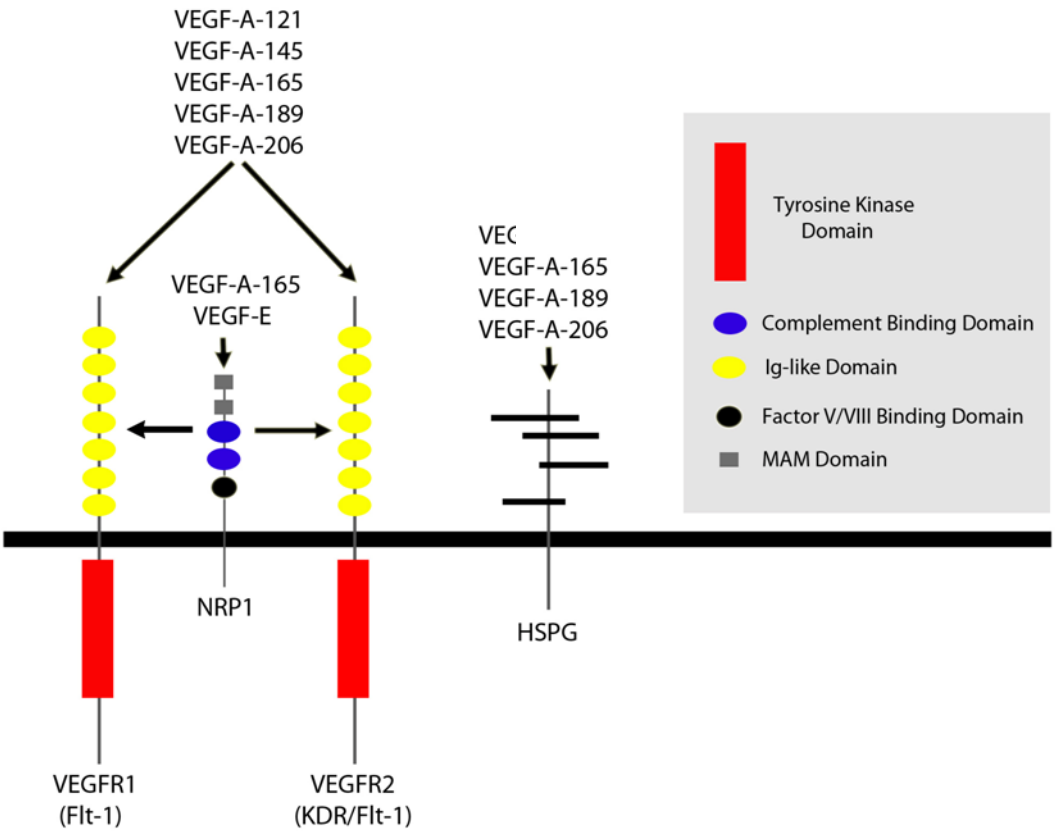

Figure 1.3: VEGF isoforms and their specificity for VEGFR1, VEGFR2, NRP1 and HSPGs.

VEGFA isoforms/VEGFE and their binding to VEGF receptor 1, VEGF receptor 2, Neuropilin 1 (NRP1) and heparan sulphate proteoglycans (HSPG) as relevant to this study. MAM Domain is a ~ 170 aa region important for NRP1 interaction with co-receptors.

contrast to the other forms, $VEGF_{121}$ and $VEGF_{145}$ do not bind to heparin or extracellular matrix proteoglycans. The signalling tyrosine kinase receptor FLT-1/VEGFR1 (fms-like tyrosine kinase-1) and KDR/VEGFR2 (kinase domain region/flk-1, foetal liver kinase-1) binds all isoforms of VEGFA but differ in their intracellular signalling. Signalling via VEGFR2 is responsible for most functions involved in angiogenesis. Neuropilin-1 acts predominantly as a co-receptor as it lacks the tyrosine kinase domain found in VEGFR1/2. Ligands for NRP1 include $VEGF_{165}$ and VEGFE, the Orf Virus VEGF homologue (78).

Elevated expression of VEGF has been detected in a variety of human tumours and this is associated with poor survival and an increased risk of recurrence (74). Up-regulation of VEGF occurs in response to a microenvironment of low oxygen conditions via the hypoxia inducible transcription factor HIF-1α (79). The 5' VEGF gene promoter regions contain hypoxia response elements that allow binding of HIF-1α and increased gene transcription (80). VEGF then stimulates endothelial migration via the PI3K isoform p110 alpha and subsequent activation of the Small GTPase RhoA (81). Expression of VEGF in response to hypoxia is central to angiogenesis and has led to VEGF being defined as the prime hypoxia-inducible angiogenic factor. VEGF is also induced by a number of cytokine growth factors such as epidermal growth factor (EGF), platelet derived growth factor (PDGF) and basic fibroblast growth factor (bFGF) (78). Mutations in *Ras* oncogenes, and p53 are also linked with increased VEGF expression, as are genetic alterations of the phosphatase and tensin homolog protein (PTEN) and the Von Hippel Lindau protein (pVHL) that increase HIF-1 activity in tumour cells, which may indirectly lead to increased levels of VEGF (82-87).

Although there is no known homologue of VEGF in the Vaccinia virus genome, *Orf* virus the type species of the *Parapoxvirus* genus, produces a protein with a high degree of similarity to other VEGF family members (88, 89). VEGF-E has been shown to have 25-43% sequence homology with other VEGF proteins but notably contains all six cysteine residues of the cysteine-knot motif which are conserved in all VEGF family members. Unique among the

VEGF family, receptor binding is restricted to VEGFR-2 and NRP1 (90, 91). This viral protein induces endothelial cell proliferation, vascular permeability, angiogenesis and lymphangiogenesis *in vitro*. *In vivo* it is responsible for the characteristic pustular dermatitis seen in sheep, goats and humans where there is extensive vascular and epithelial proliferation (92).

1.4 Viral Therapy for Cancer

Despite advances in conventional chemotherapy the response rates of PDAC is poor and five year survival limited. With the increasing knowledge of the molecular genetics of pancreatic cancer, gene therapy is developing as a new option for this extremely aggressive disease. Gene therapy strategies to repair isolated genetic defects in cancers, such as restoring wild type p53 status, showed promising *in vitro* results but have not been successful in clinical trials (93). The lack of efficacy of such single gene strategies is not unexpected given the complexity of genetic changes and abnormalities in signal transduction found in cancer cells. Given this lack of efficacy, the use or tumour-selective, replication-competent viruses or bacteria are being investigated as new agents for cancer therapy.

The concept that viruses may have some role in the treatment of cancer is not new. There are many examples in the literature where an acute viral illness or recent vaccination has resulted in the regression of a malignancy (94). Previous smallpox vaccination has also been shown to reduce the risk of melanoma incidence many years after vaccination implicating tumour specific immunity as a mechanism of action (95).

The central premise of viral oncolytic therapy is that the vector replicates specifically in cancer cells (Figure 1.4). Some viruses have an inherent tropism for cancer cells alternatively specific viral genes can be deleted which are essential for replication but are compensated for by abnormalities in cancer cells but not in normal tissue. These therapeutic effects can be mediated by multiple mechanisms in addition to cell lysis as a result of viral replication. These effects

include the expression of toxic proteins, local conversion of pro-drugs to active chemotherapy agents or re-sensitisation to conventional therapies and induction of host cell-mediated immunity.

The ideal vector would be highly tumour-selective so that it can target cancer cells without affecting surrounding normal cells. The efficiency of viral therapy can be enhanced by the use of a bystander effect. This is defined as induction of cell death, limitation of cell growth, inhibition of angiogenesis or an immune mediated effect by enhancing the host immune response to cancer cells (96). The ability to harness the host immune response against tumour cells has the potential not only to enhance local cancer cell death, but also to treat distant metastases.

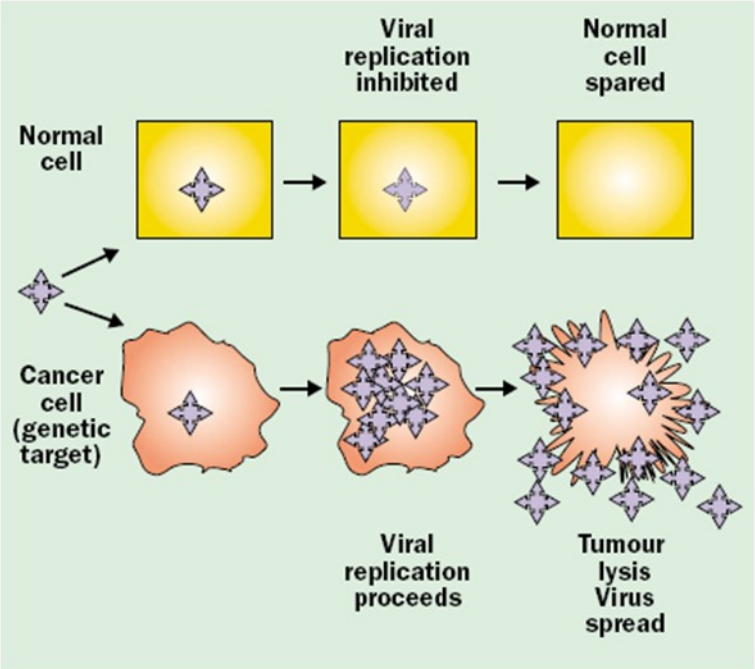

Figure 1.4: Replication-selective oncolytic viruses.

The premise of oncolytic viral therapy involves viral replication only in cancer cell due to an inherent tropism or deletion of critical viral genes rendering them tumour-specific. Viral replication leads to production of new infectious virions, lysis of infected cells and spread of virions to infect adjacent and potentially distant cancer cells. (Hawkins LK, Lemoine NR, Kirn D. Oncolytic biotherapy: a novel therapeutic plafform. The Lancet Oncology. 2002 January;3(1):17-26.)

Viruses have evolved over millions of years and gained the ability to evade our immune system, infect and replicate efficiently in and cause lysis of humans cells to facilitate viral spread (96). These vectors naturally induce oncolysis or stimulate apoptosis and are capable of expressing therapeutic genes at high transduction efficiencies and inducing tumour-specific, cell mediated immunity (21).

Many oncolytic viruses have been developed but there has been few successful clinical trials (97). Replication-selective oncolytic adenovirus is the most well-researched and Onyx 015/*dl*1520, or H101 in China, was approved as the world's first oncolytic virotherapy for head and neck cancer therapy (98). However, to date clinical trials using oncolytic viral therapy for pancreatic cancer have been disappointing. Two phase I/II trials using Onyx 015 (dl 1520), an adenovirus serotype 5 (Ad5) vector, with a deletion in the p53-binding protein E1B55kD to improve tumour selectivity, have shown minimal response when injected into pancreatic cancers endoscopically or under CT guidance (99, 100). There are many reasons for the poor performance of adenoviral vectors in clinical trials to date. The complexity of cancer cell signalling abnormalities and the effect of viral gene deletions are major factors and results may improve with future generations of adenoviruses.

Ultimately, for oncolytic viruses to become part of the cancer treatment paradigm the effect of the tumour microenvironment on viral delivery and pathogenesis will need to be considered. Studies looking more specifically at adenovirus biology under hypoxic conditions may partly explain its poor performance in clinical trials to date. Ad5, a group C adenovirus, shows attenuated viral replication in hypoxic conditions. Virus attachment and internalisation via Coxsackie/Adenovirus receptor (CAR) and α_v integrin expression is unaffected by hypoxia as is mRNA expression of viral proteins E1A and Hexon. However translation of viral mRNA to protein is reduced, resulting in a 10-100-fold reduction in the yield of infectious virus particles (101, 102). In addition the group B adenoviruses type 3 and 11 are attenuated in hypoxia displaying reduced lytic potential and production of virus particles independent of viral receptor

status and viral gene expression (103). Consequently, adenoviruses may not be the ideal vectors for pancreatic cancer and investigation of other vectors is warranted.

Vaccinia virus is an alternative viral vector with many attributes that make it an attractive vector for viral gene therapy. Townsley *et al*. found that exposure of cells to a low pH augmented viral uptake via an endosomal pathway. The tumour microenvironment is known to be hypoxic and genes involved in regulating intracellular pH are upregulated by HIF-1α (104). Given that pancreatic cancer has been shown to be one of the most hypoxic tumours (32) we have decided to investigate Vaccinia virus as an alternative vector for pancreatic cancer gene therapy and to characterise the effect of hypoxia on the viral life cycle.

1.4.1 Vaccinia Virus

Vaccinia virus is an enveloped, double-stranded DNA virus and a member of the genus *Orthopoxvirus* from the *Poxviridae* family. The true origin of Vaccinia virus remains unknown and it has no single natural host. In 1796, Edward Jenner created the first vaccine when he isolated cowpox virus from a milkmaid and used it to vaccinate others against smallpox. Vaccinia virus was probably derived from cowpox virus through multiple passages over time and became established as an effective smallpox vaccine (105). Vaccinia virus was used widely as the vaccine strain for the WHO smallpox eradication programme (106)

1.4.2 Strains of Vaccinia virus

Many strains exist, some of which have been sequenced (107). The Western Reserve (WR) strain of Vaccinia virus has been the most common strain used in laboratories for the construction of oncolytic Vaccinia viruses, based on its supposed superior lytic activity over other strains *in vitro* (108). However, this is not a vaccine strain and less is known of the safety

profile in humans. In addition, it has neurovirulence and is gonadotropic in murine models (109, 110).

Vaccine strains of Vaccinia virus such as the Lister, Wyeth, Modified Vaccinia virus Ankara (MVA), Copenhagen and its derivative New York Vaccinia virus (NYVAC) are less virulent than the WR strain and may offer a superior safety profile *in vivo*. The MVA, Copenhagen and NYVAC strains all require primary cells, such as chicken fibroblasts, for production (111). These are difficult to mass-produce and may be contaminated by other viruses. However, both the Lister and WR strains can be produced at a high yield in CV1 cells, a normal African Green Monkey Kidney Fibroblast Cells. This cell line can be easily stored and grown at high density in culture. Mass production of the Lister virus is therefore safer, easier and more cost-effective than other vaccine strains. The Lister strain was developed at the Elstree laboratories of the Lister Institute. This vaccine strain of Vaccinia virus was used safely as the smallpox vaccine throughout Europe, is highly attenuated and has recently been fully sequenced (112, 113). As a result the Lister strain is the Vaccinia strain used as the vector for oncolytic therapy in our laboratory.

1.4.3 Structure of Vaccinia virus and nomenclature of virions.

Vaccinia virus is a large DNA virus measuring 250-360nm in size and encodes over 200 proteins from a genome of approximately 200 kilobases (114, 115). The study of this virus is complicated by the fact that there are four forms of infectious virus particles and controversy surrounding the exact structure of these. The intracellular mature virus (IMV) is the initial particle formed in peri-nuclear viral factories and surrounded by a single lipoprotein membrane. The intracellular enveloped virus (IEV) which is a triple lipoprotein-enveloped virus produced after fusion with the trans-Golgi network or early endosomes. The cell-associated enveloped virus (CEV) is formed after the IEV fuses with the cell surface membrane and is retained at the cell surface membrane. The extracellular enveloped virus (EEV) is a double lipoprotein-

enveloped virus released from the cell membrane (116). Each particle contains an inner viral core containing a number of virus-encoded proteins including RNA polymerases, enzymes for RNA capping, methylation, polyadenylation and some early viral mRNA (117).

1.4.4 Overview of the Vaccinia virus life-cycle

Vaccinia virus replication occurs exclusively in the cell cytoplasm. Infection is a highly co-ordinated process from cell entry, viral mRNA transcription, protein translation, DNA replication, virion assembly through to release co-ordinated release of EEV/CEV or cell lysis and release of IMVs (Figure 1.5).

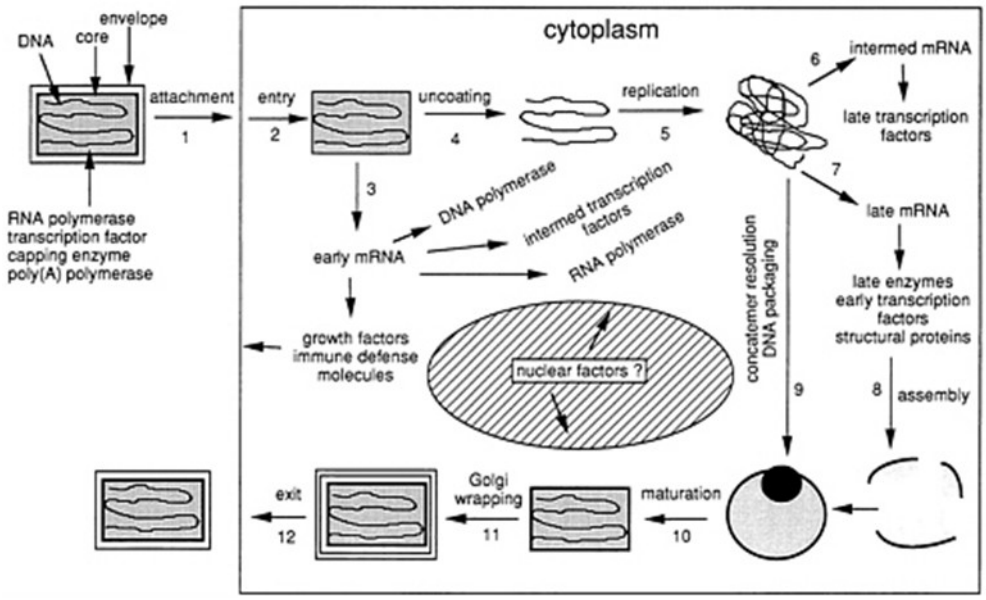

Figure 1.5: Overview of the Vaccinia virus lifecycle.

The Vaccinia virus lifecycle occurs in the cytoplasm of infected cells. Viral replication requires attachment and entry, temporal mRNA transcription, DNA replication, wrapping of viral cores with a cell-derived lipoprotein membrane and egress. (Moss B. Poxviridae: the viruses and their replication, Fields Virology. 4th Edition ed. Knie DM, Howley PM, editors. Philadelphia: Lippincott Williams and Wilkins; 2001.)

1.4.5 Viral Attachment and Internalisation

Vaccinia virus has a wide tropism and can enter most mammalian cell lines (118). However, a unique receptor for Vaccinia virus has not been identified. This is in contrast to adenovirus where attachment is via the coxsackievirus and adenovirus receptor (CAR) for Ad5 and CD46 for Group B adenoviruses (119, 120).

Several proteins present in the outer membrane of Vaccinia virus have been shown to be important in IMV cell entry (121). H3L, A27L and D8L all interact with cell surface glycosaminoglycans (GAG) and are involved in virus binding (122-124). However, the presence of these viral proteins is not essential and their effect on viral replication is dependent on cell type. Carter *et al* found that pre-incubation of purified IMV with various GAGs, to saturate these viral proteins, did not significantly impair the infectivity of BSC-1 cells (125). In contrast, Whitbeck *et al* found that heparin was able to inhibit IMV attachment in human HeLa cells, murine B78H1 and L cells but not BSC-1 and Vero cells (126). They also examined the effect of low pH on the rate of endosomal uptake of Vaccinia virus IMV. They used bafilomycin to inhibit the endosomal Na/H+ pump and thereby prevent acidification of the endosomal compartment. They found that they were able to reduce the entry of Vaccinia virus by 35-90%, depending upon the cell type. They concluded that Vaccinia virus may enter different cell types by different mechanisms and also use these different mechanisms simultaneously (both endocytosis and plasma membrane fusion) to enter a single cell type. This corroborates the findings of Townsley *et al* who showed that a low pH-dependent endosomal pathway was also responsible for the entry of Vaccinia virus IMV (127). Alternatively these findings may be the result of a mixture of IMVs and EEVs being used in the virus preparation. Vanderplasschen *et al* demonstrated that IMVs and EEVs enter cells via different mechanisms or receptors (128). They also suggested that only the EEV exhibits a low-pH-dependent entry mechanism where un-coating of the EEV occurs inside acidified endosomes (129). This would suggest that although EEVs represent only a small fraction (~2-5%) of standard preparations of

Vaccinia virus on a single sucrose gradient, they are responsible for a disproportionate amount of viral infection compared to IMVs. EEVs have an additional lipid layer making them more resistant to host immune inactivation. This improves infectivity after systemic delivery *in vivo* (130). In contrast, the comparative infectivity of IMV *versus* EEV particles *in vitro* has not been clearly demonstrated, partly due to the fragility of EEVs.

The epidermal growth factor receptor (EGFR) was initially proposed as a cellular receptor for Vaccinia virus because receptor occupation was shown to inhibit Vaccinia virus (131, 132). This hypothesis stemmed from the discovery of the viral protein Vaccinia Growth Factor (VGF). This is a polypeptide encoded in the viral genome with sequence homology to both the EGF and Transforming Growth Factor-α and is produced early after viral infection (133, 134). VGF is secreted extracellularly, induces auto-phosphorylation of the EGFR, and signals via MEK kinases resulting in cell survival and proliferation (135-137). The concept that EGFR is a receptor for Vaccinia virus has largely been disproved and there are no studies since the development of multi-channel fluorescence microscopy which show co-localisation of Vaccinia virus with the EGFR (138). The most likely conclusion is that VGF or EGF/TGF-α signalling via the EGFR stimulates cell signalling pathways that maintain cells in a more susceptible state for infection to maximise viral replication in epithelial tissues prior to the lytic step of the viral life cycle. A study by Vermeer *et al* used intact respiratory epithelium from cadaveric sources and monitored the effect of EGF on Vaccinia virus infection and respiratory epithelium morphology (139). In normal respiratory epithelium EGF is secreted via the apical membrane and acts on the basolaterally located receptors to stimulate cell proliferation and repair when epithelial integrity is lost. In the context of viral infection they showed that virally produced VGF or recombinant EGF was able to stimulate these basolateral receptors and maintain epithelial integrity, stimulate proliferation and consequently facilitate maximal viral replication at early time points after infection. Deletion of VGF now serves as one of the important strategies for improved tumour targeting of oncolytic Vaccinia virus. Mutant viruses with deletion in the VGF gene are attenuated but this deletion is compensated for in cancer cells with

constitutively active EGFR/Ras signalling pathways (140, 141). Due to concern about the use of smallpox in bioterrorist attacks this pathway has been targeted to reduce the lethality of respiratory inoculation. Vaccinia virus respiratory infection is used as a model of smallpox attack and Yang *et al* were able to show that pre-treatment with inhibitors of the ErbB1 receptor tyrosine kinase was able to reduce the lethality of a respiratory infection (142).

Lipid-rich membrane domains defined as lipid rafts have been implicated in the entry of enveloped viruses (143). Vaccinia virus co-localises with GM-1, a marker of lipid rafts, and depletion of the sphingomyelin and cholesterol domains impairs the binding of Vaccinia virus to the cell membrane (144).

1.4.6 Viral Internalisation and Movement.

Macropinocytosis, used by the IMV for cell entry, is a transient growth factor-induced, actin-dependent endocytic process that leads to internalisation of fluid and membrane into large vacuoles. It is associated with considerable cell-wide plasma membrane ruffling induced by the activation of actin and microfilaments connected to the plasma membrane. The ruffles take the form of lamellipodia, circular ruffles and plasma membrane blebs. These protrusions can fold back, forming fluid-filled cavities and undergo membrane fission forming closed vacuoles that are no longer connected with the plasma membrane. These macropinosomes have a diameter of 0.5–10 μm, larger than other pinocytic vesicles. This causes a transient increase in cellular fluid uptake and is often termed fluid phase endocytosis (145). The arginine-rich HIV-Tat protein also uses this mechanism for cell entry.

IMV can bind to filopodia and lamellapodia and move towards the cell body in a manner consistent with actin-based motility. Large transient plasma membrane blebs are formed when the IMV reaches the cell membrane. The formation of the structures appears to be stimulated by phosphatidylserine residues in the virus envelope. This mimics apoptotic bodies and induces a

macropinocytic response by the host cell. This requires Ras-related C3 botulinum toxin substrate 1 (Rac1), a member of the Rho family of GTPases and p21-activated kinase 1 (PAK1). The IMV induces phosphorylation of threonine 423 of PAK1 which is known to be essential for macropinocytosis (146). The stimulation of the cell entry mechanism allows virus cores to enter the cell. EEV entry does not require this co-ordinated entry mechanism and inhibition of molecules involved in this pathway does not reduce infectivity (147).

After internalisation, virus trafficking switches to microtubule-dependent transport. The pre-transcribed early viral mRNAs are released from the core on entry and are transported along with the intact viral core to the endoplasmic reticulum. Here these mRNAs are translated into proteins involved in core uncoating, release and then replication of viral DNA (148).

1.4.7 Viral Gene Expression and DNA Replication

The tropism of Vaccinia virus is determined both by the ability to enter cells but also to complete replication and form new virions. Following the entry of Vaccinia virus into the cell cytoplasm and trafficking to endoplasmic reticulum-associated, peri-nuclear viral factories, RNA polymerase and transcription factors already present in the virus facilitate early viral gene expression (114). Early Vaccinia virus mRNA is detected within 20 minutes of infection and peaks at 1.5 hours. Early mRNA transcripts produce further enzymes required for DNA transcription including thymidine kinase and ribonucleotide reductase, which synthesise any extra deoxyribonucleotides required for DNA replication. Soon after Vaccinia virus entry, all host protein synthesis is shut down following the expression of D9 and D10 Vaccinia proteins which destabilise cellular mRNA (149-151). This enhances viral replication by alleviating competition for nucleotides and protein synthesis machinery from cellular mRNAs, as depletions of pyrimidine nucleotide pools has been shown to limit Vaccinia virus DNA replication (152-154). Exposure of cancer cells to hypoxia is known to limit the availability of pyrimidine nucleotides (155).

Early transcription occurs exclusively under the control of viral transcription factors but host proteins contribute to the efficiency of intermediate and late gene transcription (118). Intermediate mRNA is seen from 1 hour after infection and peaks at 2 hours, resulting in the production of late transcription factors. Late mRNA is seen from 2 hours until 48 hours and encodes the structural proteins and enzymes required for viral assembly. New virions are coated with a single lipid layer containing viral proteins to form the IMV. This represents the majority of infectious viral particles as completion of the lytic viral life cycle will results in the release of these particles and allow infection of adjacent cells (116). Vaccinia proteins expressed on the surface of infected cells may mediate cell lysis by binding complement or natural killer (NK) cells although this is not completely characterised (156).

In order for viral replication to be efficient the virus must enter the cell and have sufficient time to replicate before virus-induced apoptosis or cell lysis occurs. The requirement of Akt activation to inhibit virus-induced apoptosis is a mechanism that is used by a number of viruses to facilitate maximal replication (157). Myxoma virus, a member of the poxvirus family, requires the presence of phosphorylated Akt or the induction of this phosphorylation on infection in order for viral replication to occur. An ankyrin-repeat viral protein, MT5 is responsible for phosphorylation of Akt (158). Soares *et al* were able to show that Vaccinia virus-induced Akt phosphorylation resulting in reduced virus-induced apoptosis as measured by caspase-3 and TUNEL assays (159). This was inhibited in the presence of LY294002, an inhibitor of PI3K/Akt.

1.4.8 Virus Egress

The majority of IMV are released on cell lysis. However some IMV are wrapped in a double layer of Golgi- or endosome-derived intracellular membrane to form IEV (160). These use microtubules to traffic to the cell surface where a single layer of the outer lipid membrane fuses

with the cell plasma membrane creating CEV (161). CEV induce the formation of actin tails at the cell surface, which facilitate their spread to surrounding cells. EEVs, which mediate long-range viral spread, are CEVs released from the cell membrane.

The molecular mechanisms of this transition have been clarified; the IEV binds via the unphosphorylated viral protein A36R to Kinesin which mediates the microtubule-dependent transport to the cell surface. When present at the membrane as a CEV the B5R protein stimulates Src or Abl family-mediated phosphorylation of A36R which causes recruitment of cell actin polymerization machinery including adaptor proteins Nck and Grb2, the scaffold protein N-WASP and the Arp2/3 nucleation complex. This results in a switch to actin-based motility and protrusion of actin tails from the cell membrane and can be inhibited using inhibitors of the Src or Abl families (162, 163). The release of EEV requires Abl but not Src family tyrosine kinase phosphorylation and can inhibited using STI-571 (Gleevec – an Bcr-Abl kinase inhibitor used in the treatment of chronic myeloid leukaemia) and reduces viral dissemination five-fold (163).

The replication of Vaccinia virus is fast, efficient and does not require the host transcriptional machinery. However the viral lifecycle is still regulated by interaction of viral proteins and intracellular signalling pathways. Selective modification of this can significantly affect viral pathogenesis. A greater understanding of the signalling pathways that facilitate Vaccinia virus infection could allow improvements in oncolytic viral therapy and present strategies to alter poxvirus pathogenesis.

1.4.9 Inherent tumour selectivity of systemically delivered Vaccinia virus

One of the greatest barriers to the clinical application of viral gene therapy is specific and efficient gene delivery. This can to some extent be achieved by direct delivery of the virus to primary tumours and metastases by intratumoural injection. However, for many tumours this is

not feasible or metastases are too small to be detectable and systemically delivered agents are required.

Wild-type Lister strain of Vaccinia virus has been shown to display inherent tumour specificity following intravenous delivery in both human tumour xenografts in nude mice and murine tumours in immunocompetent mice (164). This inherent specificity of Vaccinia virus for cancer cells is due to several factors; live *in vivo* imaging of systemically administered Vaccinia virus expressing the green fluorescence protein (GFP) confirmed that viral replication initially took place immediately surrounding tumour capillaries. These vessels differ from normal capillaries as they do not have an intact basement membrane and are leaky due to large gaps between endothelial cells (165). This may allow the large Vaccinia virus virions to enter the extravascular space. In support of this hypothesis, hyperthermia (to induce capillary dilation) improves the dissemination of Vaccinia virus (117). Additional factors include the constitutive activation of cell signalling pathways found in cancer cells, such as the EGFR pathway. In addition there are a range of host immunological factors, notably the loss of the interferon-gamma antiviral response, that contribute to the tropism of Vaccinia virus for cancer cells (166).

1.4.10 Current Status of Oncolytic Vaccinia Virus for Cancer Therapy

At present, there are three oncolytic Vaccinia viruses in clinical trials. The leading vector is JX-594, a Wyeth strain virus attenuated by deletion of the viral TK region and replacement with granulocyte/macrophage-colony stimulating factor (GM-CSF) to augment anti-tumour efficacy (167). A phase I trial of intratumoural injection of 22 heavily pre-treated patients (predominantly with hepatocellular carcinoma) was recently reported (168). All patients experienced grade I-III flu-like symptoms and four had transient, grade I-III, dose-related thrombocytopenia. Grade III hyperbilirubinemia was dose-limiting in two patients and the maximum tolerated dose was set at $1x10^9$ pfu. Only ten patients were evaluable for efficacy however, according to Response Evaluation Criteria in Solid Tumors (RECIST), three patients

had partial responses, six had stable disease, and one had progressive disease. These responses included patients who had been previously vaccinated for smallpox and had anti-Vaccinia antibodies before treatment. Secondly, viral replication was found in un-injected tumour cells distant to the site of initial injection showing that Vaccinia virus is capable of replication and spread to distant tumour sites. A phase II study is currently recruiting and a phase I study of this vector in patients with malignant melanoma has paused for interim analysis. Two other replicating Vaccinia viruses (see below) are in phase I clinical trials.

GLV-1h68 is a Lister strain virus with deletions of the viral TK and haemagglutinin gene and a phase I trial in patients with solid tumours using intravenous administration is currently recruiting. The trial plans to assess viral replication in primary/secondary lesions, evidence of immune response and traditional efficacy and toxicity outcomes.

JX-929 (vvDD-CDSR) is a Wyeth strain virus deleted for the viral TK and VGF genes, with two transgenes inserted in their place. The somatostatin receptor allows scintigraphic imaging and the cytosine deaminase transgene converts the pro-drug 5-fluorocytosine to the active metabolite 5-fluorouracil. A phase I study of intratumoural injection of this agent is currently recruiting (Data accessed www.clinicaltrials.gov 12th June 2010).

1.5 Hypoxia Targeting

1.5.1 Overview

Since the observations from pre-clinical data that hypoxia influences the phenotype of tumours and their response to therapies much has been done to target this issue. As the oxygen enhancement ratio demonstrates, hypoxia significantly reduces the efficacy the radiotherapy and consequently much of the work has focused on reversing this. Early clinical trials using hyperbaric oxygen chambers to increase the oxygen concentration of inspired air during radiotherapy showed benefit. A Medical Research Council study from 1978 showed a survival

benefit for hyperbaric oxygen therapy in combination with radiotherapy in cancer of the uterine cervix (169). However, patients must enter hyperbaric oxygen chambers prior to each dose of radiotherapy delivered. Consequently the logistics of delivering this kind of therapy make it an unfeasible solution.

Radiotherapy techniques have improved from this period and other ways of improving tumour oxygenation are being studied. A combination of the hyperoxic gas carbogen, to overcome diffusion-limited hypoxia, and the vasoactive agent nicotinamide, to circumvent perfusion-limited hypoxia have shown promise in phase II clinical trials using Accelerated Radiotherapy with Carbogen and Nicotinamide (ARCON) therapy (170). Phase III trial data should become available in the next few years and provide data to assess the efficacy of this approach.

An alternative is the use of radio-sensitizing agents to improve radiotherapy efficacy. A meta-analysis of their use has shown benefit in terms of local control and, in some tumour types, overall survival (171). The radio-sensitizing agent nimorazole is used in some centres in Europe for the management of supraglotic larynx and pharynx tumours after showing improved loco-regional control in phase III trials (172). Tirapazamine, a bio-reductive drug which becomes toxic preferentially in hypoxic cells, had shown benefit in phase II trials. A recent phase III trial in head and neck cancer using this agent in combination with cisplatin and radiotherapy has not shown benefit. However, this study has been criticised for its lack of biomarkers for selection of hypoxic tumours and poor radiotherapy delivery in some trial centres. In addition the aetiology of the disease has changed to more radiosensitive human papillomavirus (HPV)-induced tumours since the phase I/II data were collected.

An alternative approach to target hypoxia is to reduce hypoxia-induced gene transcription to reverse the phenotype that this causes. Some conventional chemotherapy agents have been shown to inhibit HIF function. Intervention with gene silencing or chemical inhibition of HIF has shown benefit *in vitro* (173). Development of these therapies may prove beneficial in future.

1.5.2 Hypoxia-Targeting Viral Therapy

Gene therapy strategies targeting hypoxia offer the potential of improved specificity and increased therapeutic ratios by restricting transgene expression to hypoxic regions. HIF-1α when stabilised in hypoxic conditions will bind to hypoxia regulatory elements (HREs) and initiate transcription. Hypoxia-induced genes such as erythropoietin (Epo-1), inducible nitric oxide synthetase (iNOS) and VEGF all have promoter sequences which include a HRE. Using these HREs as *cis*-acting elements in either 5' or 3' flanking locations allows hypoxia-specific transgene expression and has been demonstrated both *in vitro* and *in vivo* using both viral and non-viral vectors (174, 175). Post *et al* inserted HREs as part of the promoter sequence for E1A to make a conditionally replicating adenovirus (176). Gene transfer using adeno-associated virus as a transfer vector in cardiovascular disease has been used in a dual vector system to target ischaemia. Tang *et al* then created a transactivating fusion protein in the first vector that contains an ODD sequence, which under hypoxic conditions was able to bind to the inducible promoter in the second vector and increase transcription of the luciferase reporter gene (177).

Vaccinia virus encodes many of its own polymerases and therefore using HREs in a conventional hypoxia-targeting approach is not feasible. Given the advantages of Vaccinia as an oncolytic vector, in comparison to adenovirus or adeno-associated virus, a Vaccinia virus capable of targeting transgene expression or conditionally replicating in hypoxic conditions could be useful for cancer therapy.

1.6 Aims of Project

- To study the feasibility of Vaccinia virus as a therapeutic vector targeting hypoxic PDACs.
- To study the functional mechanisms by which hypoxia affects the potency of Vaccinia virus.
- To construct a novel hypoxia-targeting Vaccinia virus with the potential for re-sensitization of hypoxic tumours.

Chapter 2

2. Materials & Methods

2.1 Cell Lines

All cell lines were maintained in their respective media at 37°C in air supplemented with 5% carbon dioxide (CO_2) or were cultured in hypoxic conditions as indicated. Repeated experiments were performed using cells of similar passage. All cells were grown in media containing 0.06 µg/L penicillin and 0.1 µg/L streptomycin obtained from Cancer Research UK Central Cell Services (CRUK CCS, Clare Hall, Herts, UK) or PAA Laboratories GmbH (Pasching, Austria) and were regularly tested for mycoplasma.

2.1.1 Human cell lines

2.1.1.1 Pancreatic cancer cell lines

The pancreatic carcinoma cell lines Suit-2, CFPac1, MiaPaca2 and Panc1 were obtained from CRUK CCS and maintained in Dulbecco's Modified Eagle Medium (DMEM) with 10% foetal calf serum (FCS) (PAA Laboratories GmbH).

2.1.1.2 Primary cell lines

Normal human bronchial epithelial cells (NHBE) were obtained from Lonza (Lonza Group Ltd, Basel, Switzerland) and maintained in Bronchial Epithelial Growth Medium (BEGM) containing the following growth supplements: Bovine Pituitary Extract (BPE), 2 mL; Hydrocortisone, 0.5 mL; Human Epidermal Growth Factor (hEGF), 0.5 mL; Epinephrine, 0.5 mL; Transferrin, 0.5 mL; Insulin, 0.5 mL; Retinoic Acid, 0.5 mL; Triiodothyronine, 0.5 mL; GA-1000, 0.5 mL from Lonza (Basel, Switzerland). Lonza obtained these cells from their patient donation programme following the acquisition of informed consent for use of cells in research and were free of mycoplasma, HIV, HBV and HCV.

2.1.1.3 Monkey cell line

The immortalised non-transformed African Green Monkey kidney cell line CV1, was obtained from The American Tissue Culture Consortium (VA, USA) and cultured in DMEM with 10% FCS.

2.2 Vaccinia Virus Production

2.2.1 Wildtype Lister strain and recombinant thymidine kinase-deleted Vaccinia Virus

The Lister vaccine strain of Vaccinia virus (VVLister) and recombinant thymidine kinase (TK)-deleted Vaccinia viruses (VVL15) were a gift from Professor Istvan Fodor (Loma Linda University Campus, CA, USA). Fluorescently tagged Vaccinia virus-488 and VV-ODD were produced by Crispin Hiley (CH). Dr L Chard was involved in the design of VV-ODD and provided post-doctoral assistance during its construction.

VVLister was used as the backbone for production of other engineered viruses. VVL15 was produced by an *in vitro* intracellular recombination technique previously described (178). VVL15 was constructed by the insertion of the firefly luciferase and the lacZ reporter genes into the thymidine kinase (TK*)* region of VVLister downstream of the early–late Vaccinia p7.5 promoter.(179).

2.2.2 Fluorescently labeled Vaccinia virus - VV-488

Fluorescently tagged Lister strain Vaccinia virus (VV-488) was produced by CH following the protocol used by Warren *et al* to label the capsid of adenovirus (180). The Alexa Fluor® 488 (Invitrogen Ltd, Paisley, UK) 5-sulfodicholorphenol ester (1mg) was resuspended in 100 µL of DMSO in a foil-wrapped Eppendorf tube. The Lister strain Vaccinia virus was diluted to 0.885 $x10^{11}$ pfu/mL in 0.1 M sodium bicarbonate buffer to 2 mL in a 15 mL tube. This was vortexed slowly whilst adding the dye solution. This was then continuously vortexed for 1 hour at room temperature in a foil-wrapped tube. After 1 hour, the 2 mL volume was injected into a 10 kDa MWCO Slide-A-Lyzer dialysis cassette (Pierce Biotechnology Inc, IL, USA). This was

dialyzed overnight at 4°C against a total of two changes of 0.1 M Tris-HCL, pH 7.8, 0.1 M $MgCl_2$, 1.5 M NaCl, and 10% Sucrose and stored at -80°C in 10 µL aliquots prior to use.

2.2.3 Hypoxia-targeting virus - VV-ODD

The recombinant hypoxia-targeting Vaccinia virus VV-ODD was produced using intracellular homologous recombination as used for the construction of VVL15. The design and construction of VV-ODD are outlined in the results.

2.2.4 Vaccinia virus mass production

CV1 cells were cultured until 90% confluent and infected with 20 µL of purified virus to produce a primary expansion, and after this all further virus production was performed by Heike Muller. The primary expansion was harvested when significant cytopathic effect (CPE) was observed by cell detachment at 48-72 hours. A CF10 viral production factory (Nunc, NY, USA) was seeded with the cells from four 175 cm^2 flasks of CV1 cells at 90% confluence. After 72 hours, this was infected with the primary expansion in DMEM with 2% FCS until significant CPE was observed a further 72-96 hours later.

Cells harvested from the CF-10 were centrifuged in Sorvall centrifuge bottles (Sorvall, MA, USA) at 3500 revolutions per minute (rpm) for 15 minutes at 4°C. The cell pellet in each bottle was resuspended in 30 mL phosphate-buffered saline (PBS), transferred to a 50 mL tube and centrifuged in the same manner. The supernatant was again discarded and each pellet of cells resuspended in 7 mL of 10 mM Tris-HCl pH 9.0, then combined. Cell membranes were disrupted by three cycles of freezing in liquid nitrogen and thawing in a 37°C water bath, prior to homogenisation by 60 strokes with a Dounce homogeniser.

Cells were centrifuged at 900 rpm for 5 minutes at 4°C and the supernatant removed and saved. The cell pellet was resuspended in 3 mL of 10 mM Tris-HCl pH 9.0 prior to a second

centrifuge. Both supernatants were combined and the pellet discarded. This was sonicated in an ultrasound ice bath for 20 seconds (Grant Instruments, Herts, England) and diluted to 30 mL with 10 mM Tris-HCl pH 9.0. 7.5 mL was carefully layered onto 17 mL of 36% sucrose (w/v) 10 mM Tris-HCl pH 9.0 in each of four SW17 Beckman ultracentrifuge tubes (Beckman Coulter UK Ltd, Bucks, UK). After careful balancing by weight, these tubes were centrifuged at 13,500 rpm for 80 minutes at 4°C. Each supernatant was discarded and purified viral pellets resuspended in 1 mL of 1 mM Tris-HCl pH 9.0 prior to combination and storage at -80 °C. The viral titre was determined by $TCID_{50}$ plaque assay.

2.3 Hypoxia

For this study, hypoxia is defined as 1% oxygen unless otherwise stated. This equates to an approximate oxygen tension of 7 mmHg. This was achieved using a hypoxic incubator maintained at 94% nitrogen, 5% CO_2 and 1% Oxygen (Heto-Holten Cell Chamber 170, Surrey, United Kingdom).

2.4 RNA techniques

2.4.1 RNA extraction

Cells were lysed directly in wells using 1 mL of TRIzol (Invitrogen) reagent per 10 cm^2 of cells. Solutions were then pipetted into Eppendorf tubes and incubated for 5 minutes at 23 °C. 0.2 mL of chloroform per 1 mL of TRIzol was added to each Eppendorf. Tubes were shaken by hand and incubated for 2 minutes at 23°C. The reactions were centrifuged at 4°C in the Eppendorf 5471 refrigerated bench top centrifuge for 15 minutes at 14,000 rpm and the aqueous phase was transferred to a fresh tube. RNA was precipitated by mixing with 0.5 mL of isopropanol per 1 mL of TRIzol and incubated for 10 minutes at 4 °C. Samples were then centrifuged at 14,000 rpm for 10 minutes and the supernatant removed. Pellets were then washed with 75% ethanol and centrifuged at 14,000 rpm for 5 minutes at 4 °C. Pellets were air-dried and resuspended in 20 μL RNAse-free ddH_2O.

2.4.2 Reverse Transcription (RT) Polymerase Chain Reaction (PCR)

Purified total cellular and viral RNA (2 μg) was added to 1 μL random hexanucleotide primers (RHP) (50 ng/μL) (Roche) or gene-specific primers (2.5 μM) (Sigma), 1 μL of 10 mM dNTPs (Invitrogen) and made up to a total volume of 12 μL with nuclease-free dH_2O. The reactions were incubated at 65 ^oC for 5 minutes and chilled on ice. Then 4 μL of 5X first-strand buffer, 2 μL 0.1 M DTT and 1 μL of RNAseOUT (40 U/μL) were added to each sample. Samples were mixed and then incubated for 2 minutes at 42 ^oC for gene specific primers or 25 ^oC for random primers. 1 μL of SuperscriptII reverse transcriptase (Invitrogen) was added to each sample and incubated at 42 ^oC for 50 minutes for gene specific primers or 25 ^oC for 10 minutes for random primers. Superscript II reverse transcriptase was inactivated by heating to 70 ^oC for 15 minutes. The cDNA was stored at -20 ^oC until required.

2.5 DNA techniques

2.5.1 Agarose gel electrophoresis

Agarose gels (1%) were made using 1x TAE (40 mM Tris-acetate, 10 mM EDTA, pH 8.2) buffer and electrophoresis grade agarose powder (Invitrogen). Ethidium bromide (EtBr) (Sigma) was added to the molten agarose at a final concentration of 0.5 μg/mL before the gel was cast. Samples for analysis were added to 6x blue/orange loading dye (Promega) and dH_2O before being loaded into the wells. For reference, a 1 kb DNA ladder (5 μL) (Promega) was also run. Gels were run in 1x TAE buffer containing 0.5 μg/mL EtBr. Bands were visualised using a transilluminator and the GelDoc program (BioRAD).

2.5.2 Low melting point (LMP) gel electrophoresis

LMP agarose gels were used for purification of DNA. LMP agarose (1%) gels were made using 1x TAE buffer and electrophoresis grade LMP agarose powder (Invitrogen) (Appendix II). EtBr was added to the molten agarose at a final concentration of 0.5 μg/mL before the gel was cast. Gels were run in a 1x TAE buffer containing 0.5 μg/mL EtBr. The DNA bands were

observed under low intensity ultra violet (U.V.) light and the appropriate bands excised from the gel. The DNA was purified from the gel using the GE GFX^{TM} PCR DNA and Gel Band purification kit, according to the manufacturer's protocol. The DNA was eluted in 50 µL dH_2O and quantified by using a NanoDrop spectrophotometer to measure absorbance at 260 nm.

2.5.3 DNA extraction

DNA was extracted using the QIAamp DNA blood mini kit (QIAGEN Ltd, Crawley, UK) according to the manufacturers' instructions. Samples were lysed and DNA bound to a silica-gel membrane, while contaminants were washed away before the elution of purified DNA. Cell pellets samples were resuspended in 200 µL PBS. Viral standard samples consisted of 100 µL purified VVLister mixed with 100 µL PBS. 20 µL protein kinase K and 200 µL of lysis buffer AL were added to samples and mixed before incubating at 56 °C for 10 minutes. 200 µL ethanol was added, samples transferred into spin columns containing a silica-gel membrane, centrifuged at 800 rpm for 1 minute and filtrates discarded. Columns were placed in Eppendorfs and 500 µL wash buffer AW1 added to the columns, which were centrifuged as above and filtrates again discarded. Columns were washed in the same manner with 500 µL wash buffer AW2. Columns were placed in fresh Eppendorfs, samples eluted from membranes with 70 µL of elution buffer AE (10 mM TrisCl; 0.5 mM EDTA; pH 9.0) and stored at -20 °C. Sample DNA concentration and purity was determined using the Nanodrop® ND-Spectrophotometer and Nanodrop® v3.1.0 software (NanoDrop Technologies, Delaware, USA). DNA was accepted as adequately pure where the ratio of absorbance at 260 and 280 nm was ~1.8. Concentration was measured until three measurements within 4 ng were obtained and then an average taken.

2.5.4 Restriction digests

For analytical digests, 1 µg of plasmid DNA was added to an appropriate amount of each restriction enzyme (Promega/NEB), 2 µL of the supplied 10x enzyme buffer, 0.5 µL of bovine serum albumin as required and the reactions made up to 20 µL with dH_2O. Digests were

incubated for 2 hours at 37 ^{o}C and the sample mixed with 4 μL of blue/orange 6x loading dye and analysed by electrophoresis.

For preparative digests, 5 μg of the plasmid DNA and an appropriate amount of restriction enzyme were used in a 50 μL volume digest. Digests were incubated for 2 hours at 37 ^{o}C and 5 μL of the digest was analysed on a 1% agarose gel.

2.5.5 DNA polymerase I (Klenow fragment)

DNA polymerase I (Klenow fragment) was used for blunt end repair of DNA. 1 μL Klenow or (5 U/μL) (Promega) was added directly to 50 μL of preparative restriction digests, with 1.5 μL 10 mM dNTPs (from PCR nucleotide mix, Promega). The reaction was incubated at room temperature for 30 minutes.

2.5.6 Calf Intestinal Alkaline Phosphatase (CIAP) treatment

To remove 5' phosphate groups, the DNA was incubated for 30 minutes at 37 ^{o}C with 0.5 μL CIAP (1 U/μL) (Promega) and 5 μL 10x dephosphorylation buffer (Promega).

2.5.7 PCR

PCRs were performed using the primers listed in the appropriate results chapters. 50 μL reactions were used, containing 100 ng of template DNA, 10 pmol of each primer (forward and reverse), 5 μL 10x PCR reaction buffer, 2 μL of $MgSO_4$ (25 mM), 1 μL 10 mM PCR nucleotide mix and 1 U of KOD Hot Start DNA Polymerase. PCR cycles were performed using the program detailed in Table 2.1. The PCR products were analysed on a 1% agarose gel before the fragments were purified using LMP electrophoresis. Purified products were stored at -20 ^{o}C until required.

Table 2.1: Details of PCR cycles. [*1] The annealing temperature was adjusted according to the melting temperature (Tm) of the primers.

Step	Temperature	Time
1 Initial Denaturation	94 °C	2 minutes
2 Denaturation	94 °C	20 seconds
3 Annealing[*1]	56 °C	30 seconds
4 Elongation	72 °C	90 seconds/kb
	Go to 2, repeat 30 times	
5 Final Elongation	72 °C	7 minutes
6 Hold	4 °C	1 hour

2.5.8 Quantitative real-time PCR

2.5.8.1 Primers and probes

Primers and probes for VVLister Vaccinia Late Transcription Factor were designed manually using Primer Express® v3.0 software (Applied Biosystems, New Jersey, USA) and constructed by Sigma-Aldrich and Applied Biosystems respectively. Primers and probes were chosen for optimum PCR efficiency with minimal secondary structures with probe length 17-20 bp, Tm (Melting temperature) 68-70 °C, GC content 40-60% with repeats minimised. Primers were chosen to be 20-26 bp in length either side of the probe with Tm 58-60 °C and GC content 40-60%. Sequences were confirmed as unique within the Vaccinia virus and human genomes and are presented in the relevant results section.

2.5.8.2 Quantitative PCR (qPCR)

All samples were diluted to a concentration of 8 ng/µL of DNA. Samples, no template control (RNAse free water) and nine 10-fold serial dilutions of standards ($5x10^8$ to 5 viral genome copies diluted in 5µL RNAse free water) were tested in triplicate in each plate by qPCR. A 25µL reaction volume consisted of 5µL sample or standard and 20µL of Master mix (0.9 µM forward primer, 0.9 µM reverse primer, 0.2 µM probe in TaqMan® Universal PCR Master Mix). Reactions were performed in MicroAmp™ optical 96-well reaction plates sealed with optical adhesive covers and amplified using the 7500 Real-time PCR System (1 cycle of 48 °C for 30 minutes, 95 °C for 10 minutes then 40 cycles of 95 °C for 15 seconds, 60 °C for 1 minute).

Cycle thresholds (C_T) were determined using 7500 System SBS software (All Applied Biosystems, New Jersey, USA).

Standard and sample triplicates were accepted for analysis if their standard deviation was <0.3. Standard curves were created using mean cycle thresholds in Prism® and sample genome copy number determined accordingly. Standard curves were accepted as valid where $R^2 \geq 0.99$ with a slope of –3.30 to -3.32. Results were expressed in total genome copy number per sample. As the concentration of DNA used was constant the copy number represents the ratio of viral DNA to cellular DNA in any given sample. The mean of the qPCR triplicate was summed with the corresponding biological duplicate and presented as an average.

Reverse Transcriptase Quantitative PCR (rt-qPCR) for Vaccinia virus mRNA was performed as a two-step reaction with cDNA being produced as outlined. A multiplex reaction consisted of 40ng of template and a mastermix, as outlined above, with the inclusion of 1.25 µL of 20x eukaryotic 18S rRNA endogenous control (VIC/MGB Probe, Primer; Applied Biosystems) for each reaction. The comparative CT was used to compare the relative expression of VLTF mRNA to 18S overtime. A validation experiment was performed to confirm comparative efficiency of the target and reference amplification.

2.5.9 Annealing of oligonucleotides

5’ phosphorylated oligonucleotides (Sigma) were annealed for ligation into plasmid vectors. The details of these are given in the appropriate results chapters. 100 pmol of each of the forward and reverse primer were added to 18 µL dH_2O. The oligonucleotides were boiled at 100 ^oC for 2 minutes before being allowed to cool down to room temperature. 0.2 µL of the annealed oligonucleotides was used in subsequent ligation reactions.

2.5.10 Ligations

Ligations were carried out using 25-30 ng of vector and a quantified amount of purified insert at a ratio of 1:3. To this, 2 μL of 10x DNA ligase buffer (Promega) and 0.5 μL of T4 DNA ligase (3 U/μL) (Promega) were added and the reactions made up to 20 μL with dH_2O. The ligations were incubated at 16 ^oC overnight and then transformed into One Shot Top10 competent cells (Invitrogen). 'No insert' controls were performed for each vector used.

2.5.11 Transformation of competent cells

5 μL of each ligation reaction was added to 50 μL thawed One Shot Top10 competent cells and the mixture incubated on ice for 20 minutes. Each reaction was heat-shocked at 42 ^oC for 45 seconds then placed on ice for 5 minutes. 250 μL of warm SOC was added to each vial and then shaken horizontally for 1 hour at 225 rpm. Transformed bacteria were plated out on Lysogeny Broth (LB) agar plates containing the appropriate antibiotics and incubated overnight at 37 ^oC.

For midi preparations, the transformed cells were added to 50 mL LB media containing the appropriate antibiotic and incubated overnight at 37 ^oC in the shaker. Preparations were then pelleted by centrifugation at 8,000 rpm for 6 minutes and stored at -20 ^oC until purified.

2.5.12 Mini-preparation of plasmid DNA

Single colonies were picked from the LB agar plates and grown up overnight at 37 ^oC in 5 mL LB media containing an appropriate antibiotic. 1 mL of the overnight culture was centrifuged for 2 minutes at 14,000 rpm and the supernatant removed. The plasmid DNA was purified from the pelleted bacterial cells using the Qiagen Miniprep DNA purification system as described by the manufacturer. DNA was eluted in 50 μL dH_2O and 5 μL of the sample was analysed by restriction analysis and agarose gel electrophoresis.

2.5.13 Midi-preparation of plasmid DNA

For medium scale preparation of plasmid DNA, a 50 mL culture of transformed bacteria was grown overnight in LB broth containing the appropriate antibiotic. Cultures were transferred into 50 mL falcon tubes and centrifuged at 6000 rpm for 10 minutes. The supernatant was removed and the pellet used for purification of plasmid DNA.

Midi-prep DNA was obtained using the Qiagen Hi-Speed Plasmid Midi Prep Kit according to the manufacturer's protocol and the DNA eluted in 1 mL dH_2O. The DNA was then precipitated for 1 hour using 2.5 volumes 100% ethanol (EtOH) and 1/10th volume 3 M Sodium Acetate (NaOAC), before being washed once in 70% EtOH. The DNA was quantified using the Nanodrop spectrophotometer.

2.6 Protein techniques

2.6.1 Immunoblotting

2.6.1.1 Sample preparation for Western blot analysis

Nuclear extracts were isolated using the NE-PER Nuclear and Cytoplasmic extraction reagents (Pierce, Rockford, IL, USA) according to the manufacturer's instructions.

Whole cell extracts were collected by lysis of cells with NP40 cell lysis buffer (50 mM Tris pH7.4, 150 mM NaCl, 10 mM Ca^{2+}, protease inhibitor cocktail (Roche Applied Science, Mannheim, Germany) and 1% Nonidet P40 (Sigma Chemicals Co., Poole, UK). Lysis buffer for analysis of phosphorylated proteins also contained phophatase inhibitor cocktail (Roche Applied Science, Mannheim, Germany).

2.6.1.2 Protein quantification

Protein concentrations were determined using the Beckman protein assay. 5 µL of samples were mixed with 200 µL Bio-Rad protein assay indicator (Bio-Rad, Munich, Germany) and 795 µL of distilled water in cuvettes (Fisher Scientific, Leicester, UK). Following calibration with a

blank sample (200 µL Biorad indicator and 800 µL distilled water), the absorbance at 595 nm was measured using a spectrophotometer (Beckman Coulter UK Ltd, Bucks, UK). The protein concentration of samples was determined from a standard curve of protein concentration against absorbance of known quantities (1, 2, 4, 8, 16, 32 and 64 µg) of bovine serum albumin (Sigma Chemicals Co., Poole, UK) at 595 nm.

2.6.1.3 SDS-Polyacrylamide gel electrophoresis

30 µg of samples were mixed with 5 µL of 5x loading buffer (50 mM Tris, 4% SDS, 10% Glycerol, 5% Mercaptoethanol and 0.01% Bromophenol Blue) and distilled water to give a final volume of 25 µL. Samples were heated to 95 °C for 5 minutes and cooled on ice for 5 minute prior to loading into a denaturing 10% polyacrylamide gel in 1x Running buffer (3 g of Tris base, 14.4 g of glycine, 1 g of SDS diluted to 1 L of distilled water, pH 8.3) 10 µL of Rainbow® molecular weight marker (Amersham Biosciences, Bucks, UK) was loaded alongside the protein samples. Electrophoresis took place at 120 V for 60-70 minutes.

Proteins were sandwiched between blotting paper in the presence of transfer buffer (1% glycine and 10% methanol in distilled water) and transferred onto a Polyvinylidene Fluoride (PVDF) membrane (Immobilon-P, Millipore, Bedford, MA, USA) using a wet transfer system (Bio-Rad, CA, USA) at 100 V for 1 hour.

Membranes were blocked with a 5% BSA (Sigma Chemicals Co., Poole, UK) in a solution of 1% Tween®20 (Sigma Chemicals Co., Poole, UK) in PBS for thirty minutes at room temperature. The primary antibodies (Table 2.2) were diluted in the same blocking solution and incubated with the membrane at 4 ^{0}C overnight or at 37 ºC for 1 hour. Following removal of the primary antibody, membranes were washed three times for 10 minutes with TBST washing buffer (137 mM NaCl, 20 mM Tris, 0.1% Tween-20, pH 7.6). Secondary horseradish peroxidase (HRP)-conjugated antibodies were diluted in blocking solution and incubated with

membranes for 1 hour at room temperature. Three further TBST washes were performed following removal of the secondary antibody.

Chemiluminescent detection was performed using ECL Plus™ Detection reagent (GE Healthcare, Bucks, UK) according to the manufacturer's instructions. The signals were visualised by exposing membranes to Fuji Medical film Super RX (Fuji, Japan) for 1-10 minutes.

Membranes were placed in blocking solution for a further 30 minutes prior to incubation with proliferating cell nuclear antigen (PCNA), Ku-70 or β-actin (loading controls) using the same protocol.

Table 2.2: Antibodies used for western blots

Antibody	1º/ 2º	Species	Dilution	Supplier
VVLister coat protein	1º	Rabbit-pAb	1:1000	MorphoSys UK Ltd, Bath, UK
HIF-1α	1º	Murine-mAb	1:750	AbCam Plc, Cambridge, UK
PCNA	1º	Murine-mAb	1:1000	Santa Cruz Biotech Inc, California, USA
Ku-70	1º	Murine-mAb	1:1000	Santa Cruz Biotech Inc, California, USA
β-Actin (C4)	1º	Murine-mAb	1:3000	Santa Cruz Biotech Inc, California, USA
Anti-mouse HRP	2º	Goat	1:2000	Autogen Bioclear
Anti-rabbit HRP	2º	Goat	1:2000	Autogen Bioclear
Anti-goat HRP	2º	Donkey	1:2000	Autogen Bioclear

2.6.2 Enzyme-Linked Immunosorbant Assay (ELISA) for VEGFA

The Duoset® ELISA for human VEGFA (R and D Systems, Abingdon, UK) was used according to the manufacturers' instructions. 96-well microplates were coated with 100 µL/well of 1 µg/mL mouse anti-human VEGF antibody diluted in PBS. Plates were sealed overnight with plate sealers then aspirated and washed 3 times with 400 µL/well wash buffer (0.05% Tween 20® in PBS). Plates were blocked for 1 hour at 20 °C with 300 µL/well 1% bovine serum albumin (BSA; Sigma Chemicals Co., Poole, UK) in PBS and washed in the same manner.

Standards (recombinant human VEGF) and samples were diluted in PBS supplemented with 10% FCS. All samples were diluted 1:10. 100 µL of samples and seven 2-fold serial dilutions of standard (2000 pg/mL to 31.25 pg/mL) were added to 2 wells of each plate for 2 hours. Plates were washed, 100 µL/well of 100 ng/mL biotinylated goat anti-human VEGF added for 2 hours, 100 µL/well of 1:200 Streptavidin-HRP added and the plate kept in the dark for a further 20 minutes before washing. 100 µL/well of substrate solution (1:1 colour reagent A (H_2O_2) and colour reagent B (Tetramethylbenzidine)) was added and the plate kept in the dark for 20 minutes before the addition of 50 µL/well of stop solution ($2NH_2SO_4$) (R&D Systems, UK).

The OD of each well was determined using an Opsys MR 96-well plate absorbance reader (Dynex, VA, USA) at 450 nm and OD values at 540 nm subtracted to correct for optical plate imperfections. Mean OD values were used to create a standard curve using revelation software (Dynex, VA, USA), which was used to obtain human VEGF levels.

2.6.3 ELISA for Chloramphenicol Acetyltransferase (CAT)

A CAT Elisa kit (Roche) was used to quantify CAT levels in samples according to the manufactures instructions. Cells were lysed directly in wells with the lysis buffer provided. 200 µL of CAT standard or cell lysate was added to capture antibody labelled microplate modules and left for 1 hour at 37 °C. Cells were then washed 3 times with 250 µL of washing buffer. 200

μL of Anti-CAT-digoxigenin solution was added to each well and left for 1 hour at 37 °C. Cells were washed 3 times with 250 μL of washing buffer. 200 μL of anti-digoxigenin-peroxidase solutions was added to each well and left for 1 hour at 37 °C. Cells were washed 3 times with 250 μL of washing buffer. 200 μL of peroxidise substrate was then added to each well and left for 10 minutes at room temperature. Absorbance at 405 nm (using 490 nm as a reference) was determined using an Opsys MR 96-well plate absorbance reader (Dynex, VA, USA). Mean OD values were used to create a standard curve using revelation software (Dynex, VA, USA), which was used to obtain CAT levels.

2.6.4 In vitro bioluminescence quantification

Bioluminescence was originally measured using the IVIS camera (*In Vivo* Imaging System; Xenogen Corp., CA, USA). Media was aspirated and replaced with 150 μg/mL D-Luciferin (Xenogen Corp, CA, USA) in PBS at 37 °C and luminescence measured after 2 minutes. Light emission was quantified as the sum of all detected photon counts within uniform-sized regions of interest (ROI) with each well manually defined during post-data acquisition image analysis. This was measured in photons per second per cm^2 ($p/s/cm^2$) using Living Image software (Xenogen Corp., CA, USA).

During the course of this project a Perkin Elmer Victor II Multi-label plate-reader became available and was used for all luciferase reporter assays. Cells were lysed with passive lysis buffer (Promega), centrifuged at 6000 rpm for 3 minutes at 4 °C, kept on ice and used fresh for each assay. 20 μL of sample was added to each well of a white polystyrene plate (Corning Life Sciences) and warmed to 37 °C. 75 μL of luciferase reagent (Promega) was added to each well using the automated dispenser. Bioluminescence was measured for 1 second and samples were assayed in triplicate.

2.6.5 In vitro red fluorescent quantification

The Perkin Elmer Victor II Multi-label plate-reader was used to measure fluorescence using an excitation wavelength of 560 nm and an emission wavelength of 620 nm. Cells were lysed with passive lysis buffer (Promega), centrifuged at 6000 rpm for 3 minutes at 4 °C, kept on ice and used fresh for each assay. 50 µL of each sample was added to each well of a white polystyrene plate (Corning Life Sciences) and the fluorescence quantified in triplicate for each sample. The autofluorescence of control cells was subtracted from the average for each sample.

2.7 Tissue culture technique and viral assays

2.7.1 siRNA gene silencing

Gene silencing was performed using siGenome siRNA smartpools (Dharmacom, IL, USA). targeting four sequences unique to each gene. Sequences are shown in the relevant results chapter. Cells were seeded in antibiotic-free complete DMEM supplemented with 10% FCS at a density of $2x10^4$ cells per well in 24 well plates or $1x10^6$ cells per well in 6 well plates. Cells were then transfected 16 hours later with 25 nM of siRNA. The protocol for preparing siRNA transfection mix for one well of a 24 well plate was used as follows. A 5 µM siRNA solution in 1X siRNA Buffer (Dharmacon) was prepared from the stock reconstituted 20 µM solution using RNase-free water. In separate tubes 5 µM siRNA solution and DharmaFECT transfection reagent 1 were diluted with serum-free medium. Tube 1 – 2.5 µL of 5 µM siRNA and 47.5 µL serum-free medium. Tube 2 – 2 µL DharmaFECT reagent 1 and 48 µL of serum-free medium. The contents of each tube were incubated for 5 minutes at room temperature. Tube 1 and Tube 2 were combined and incubated for 20 minutes at room temperature. Sufficient antibiotic-free medium supplemented with 10% FCS was then added to make the final volume 500 µL. The culture medium was removed and replaced with 500 µL of medium containing siRNA. This protocol was then adapted for the volume of transfection medium required for each experiment. SiGenome RISC-free Control siRNA was used in place of as a negative control (Dharmacon, IL, USA). Minimal toxicity was noted on transfection of cells with DharmaFECT reagents. All reagents were purchased from Dhamacon, IL US.

2.7.2 Cytotoxicity of Vaccinia virus by MTS assay

The potency of viruses was determined by CellTiter 96® AQ_{ueous} Non-Radioactive Cell Proliferation (MTS) assay (Promega). Cells were infected with nine serial dilutions of virus in 96 well plates and the proportion of cells alive after 6 days at each viral concentration compared to a non-infected control following the addition of MTS reagents.

Cells were cultured in 90 μL of DMEM with 5% FCS in 96-well plates at a density of between $1x10^3$ and $5x10^3$ cells per well, depending on the rate of cell growth, to ensure that mock-infected wells were nearly confluent 6 days after infection. Plates included six replicates. Plates were incubated at 37 °C in normoxia or hypoxia and 16 hours later, infected with 10 μL of 9 serial dilutions of viruses (range optimised for each cell line) diluted in media with 5% FCS or mock-infected with media with 5% FCS alone and returned to normoxic or hypoxic conditions. 6 days following infection, MTS (3-(4,5-dimethylthiazol-2-yl)-5-(3-carboxymethoxyphenyl)-2-(4-sulfophenyl)-2H tetrazolium) was added to PMS (phenazine methosulfate; Promega, WI, USA) according to the manufacturer's instructions in a ratio of 20 MTS: 1 PMS. 20 μL was added to each well and plates incubated for 1 to 3 hours. Cell viability was determined by measuring the absorbance or optical density (OD) at 490 nm using an Opsys MR 96-well plate absorbance reader (Dynex, VA, USA). Cell viability was determined in infected cells in comparison to mock-infected cells (positive control) after correction for absorbance due to the media alone (negative control). All OD values in positive controls were greater than 1. The concentration of virus required to kill 50% of cells (half maximal effective concentration or EC_{50}) was then calculated for each cell line (section 2.11.1) and a dose-response curve created by non-linear regression using Prism® (GraphPad Software, CA, USA). Experiments were repeated in duplicate.

2.7.3 Viral replication assay

Cells were seeded in 3 wells of a 6-well plate in 2 mL of media with 10% FCS at a density of $2x10^5$ cells per well. One plate was seeded for each virus at time points 24, 48, 72, and 96 hours with a further control plate. All plates were incubated overnight at 37 °C in normoxic or hypoxic conditions.

Plates were infected by 2 mL of media with 2% FCS containing Vaccinia virus Lister strain at a multiplicity of infection (MOI) of 1 pfu/cell in human tumour cell lines. Cells and supernatant were harvested together by scraping from each individual well to give samples in triplicate at every time point. Samples were frozen in liquid nitrogen and thawed in a 37 °C water bath three times.

The titres of purified viruses and the replication of viruses in cell lines were determined by measuring the 50% tissue culture infective dose ($TCID_{50}$) of samples titrated onto indicator cells. $1x10^4$ CV1 cells were seeded in 200 µL of DMEM with 10% FCS into 96 well plates and incubated at 37 °C in air supplemented with 5% CO_2. 16 to 18 hours later, plates were infected with purified virus or viral burst assay sample lysates diluted to $1x10^{-5}$ or $1x10^{-3}$ respectively in DMEM supplemented with 10% FCS. 20 µL was added with a multi-tip pipette to all 12 wells of the top row and mixed. Following a change of pipette tips, serial 1:10 dilutions were made to the next 7 consecutive rows of CV1 cells up to a dilution of $1x10^{-11}$ for purified virus or $1x10^{-9}$ for burst assay sample lysates. Row H was left uninfected as a negative control.

The CPE of viruses on CV1 cells were determined by light microscopy 10 days after infection. Each well was scored 0 (no CPE) or 1 (any CPE) to make a score for each row out of 12. These were used to calculate the TCID50 using the established Reed-Meunch accumulate method (section 2.11.2). TCID50 plates were performed in duplicate for each sample, with three

samples at each time point. Purified viral titres were converted to pfu/mL and viral burst titres to pfu/cell based on the number of cells present at viral infection.

2.7.4 VVLister genome replication

For the assessment of Vaccinia virus DNA replication MiaPaca2-VEGF-165 and MiaPaca2-Vector Control cells were infected as for the viral replication assay indicated above. Cells were collected at 24, 48 and 72 hours post-infection, DNA extracted and qPCR performed as outlined.

2.7.5 Quantification of EEV production

Miapaca2-VEGFp165 and Miapaca2-Vector Control cell lines were seeded at a density of $2x10^5$ cells per well in 3 wells of a 24 well plate. After incubation for 16 hours at 37 ºC cells were infected with Vaccinia virus Lister strain at an MOI = 1 pfu/cell. 24 hours later before any CPE was evident only the supernatant was collected from the infected wells. This was then used without freeze-thawing to infect CV1 cells in a standard viral titration assay as outlined below. This method was previously used by Reeves *et al* to assess the effect of bcr-abl inhibition of EEV release (163).

2.7.6 Viral internalisation and attachment

Suit-2 cells were transfected with VEGF siRNA or control RISC-free siRNA for 72 hours before use. Miapaca2-VEGFp165 and Miapaca2-Vector control were cultured in 100mm dishes overnight in DMEM supplemented with 10% FCS. Cells were then trypsinised and suspended at a density of $1.5x10^5$ cells in a 1.5 mL Eppendorf in 100 µL of serum-free DMEM and kept on ice. Each cell type and time point was performed in duplicate and sufficient samples were prepared to assess viral attachment to the cell membrane and then internalisation at time points indicated in the results. Cells were then infected with an MOI = 10 pfu/cell of wild type Lister strain Vaccinia virus in 100 µL of buffer and left on a roller at 4 °C for 1 hour. For viral attachment samples cells were centrifuged at 3000 rpm for 5 minutes at 4 °C. The supernatant

was then removed and washed once with cold PBS supplemented with 1% BSA. This was repeated a second time to remove unattached virus before the cells were pelleted at -80 °C or used immediately for DNA extraction. The remaining samples were vortexed gently and placed in a normoxic incubator at 37 °C until the indicated time points, after which cells were centrifuged and washed in cold PBS supplemented with 1% BSA. Cells were then resuspended in PBS with Pronase (Roche, UK) at a dilution of 1.0 mg/mL for 30 minutes on ice to remove any attached but uninternalised virus (128). Cells were then centrifuged and washed once in cold PBS before pelleting for storage or DNA extraction and subsequent qPCR.

2.7.7 Immunofluorescence confocal microscopy

2.7.7.1 Validation of specific labelling of Vaccinia virus-488 with Alexa Fluor-488

Specificity of labelling of the viral envelope with Alexa Fluor-488 was performed by assessing co-localisation of the Alexa Fluor-488 probe with a Vaccinia virus-specific antibody. Suit-2 cells were seeded at a density of $5x10^4$ in three wells of a chamber slide in 500 µL of DMEM with 10% FCS. After 16 hrs, two chambers were infected with a 1:100 dilution of labelled Vaccinia virus-488 for 1 hour in DMEM supplemented with 5% FCS and the third chamber was mock-infected. The medium was removed and cells washed with PBS. These were then fixed with methanol for 10 minutes at -20 ºC. Cells were rinsed slowly three times with PBS and blocked for 1 hour at room temperature in PBS with 1% BSA. Cells were incubated with primary anti-Vaccinia virus rabbit polyclonal antibody at a 1:500 dilution (Serotac, USA) in PBS with 1% BSA for 1 hour at room temperature in one virally infected chamber and one mock-infected chamber. In the remaining virally infected chamber isotype control IgG at 1:500 (Santa Cruz, CA, USA) in PBS with 1% BSA was added for 1 hour at room temperature. Cells were rinsed slowly three times with PBS and incubated with secondary antibody Alexa Fluor 546 donkey anti-rabbit IgG (Invitrogen, USA) at 1:1000 dilution in PBS with 1% BSA for 1 hour at room temperature. This was rinsed slowly three times with PBS and once in dH_2O. Cells were protected with a cover slip mounted using Vectashield Mounting Media with DAPI (VectorLabs, USA), dried for 1 hour at 37 °C and protected from light until use. A Zeiss LSM

510 META laser scanning microscope was used for fluorescent 2D image and Z stack image capture and the Zeiss Zxiovision LE software for image presentation (Carl Zeiss Microimaging GmbH, Germany).

2.7.7.2 Assessment of viral attachment and internalisation using fluorescence confocal microscopy.

To assess attachment and binding of Vaccinia virus-488 to Suit-2 cells with or without VEGF knockdown, Suit-2 cells were seeded at a density of $2x10^4$ cells per chamber in 500 µL of DMEM supplemented with 10% FCS. Cells were seeded in all four chambers on each slide and incubated overnight at 37 °C in normoxia. Sufficient chamber slides were seeded to assess viral attachment and the internalisation at the indicated time points. Cells were then transfected with 100 nM concentration of SiGenome Smartpool hVEGF siRNA, Control RISC free siRNA, Dharmafect Reagent 1 only or DMEM only. After 72 hours cells were washed twice in cold PBS. Vaccinia virus-488 was diluted 1:170 in cold DMEM supplemented with 5% FCS. Cells were left to attach at 4 °C for 1 hour then washed x 3 with cold PBS. The first slide was fixed in methanol for 10 minutes at -20 °C. Warm DMEM was added to the remaining slides and left at 37 °C for 5 minutes, 15 minutes and 30 minutes. These slides were fixed in 100% methanol for 10 minutes and rinsed slowly three times with PBS. They were blocked for 1 hour at room temperature in PBS with 1% BSA and incubated with anti α-tubulin murine mAb at a 1:500 dilution (Sigma, UK) at room temperature for 1 hour in PBS with 1% BSA. Cells were rinsed slowly three times with PBS. Cells were incubated with Alexa Fluor 546 rabbit anti-mouse IgG at a dilution of 1:1000 at room temp for 1 hour in PBS with 1% BSA then rinsed slowly three times with PBS. Slides were mounted and imaged as outlined previously. Ten representative images of each experiment condition were taken with 63x lens on Zeiss Confocal Microscope. The ratio of internalised particles per cell and the number of infected *versus* uninfected cells was counted and results then analysed with Graph Pad Software using the students T-test for statistical analysis.

2.7.8 In vivo bioluminescent imaging

All imaging experiments were performed by CH at the Barts and The London School of Medicine and Dentistry Biological Services Unit (Charterhouse Square, London, UK) in accordance with the UK co-ordinating committee on cancer research guidelines and the Animals (Scientific Procedures) Act 1986 and the guidelines for the welfare and use of animals in cancer research (181). During all *in vivo* experiments, the general health of mice was assessed daily and animals sacrificed if signs of ill health were seen such as piloerection, hunched posture, 20% loss of body weight, diarrhoea or dyspnoea. Animals were also sacrificed if tumours ulcerated, impeded vital functions such as locomotion and excretion or tumour size (maximum length x maximum breadth) reached 1.4 cm^2.

Miapaca2-VEGFp165, Miapaca2-VEGFp121 and Miapaca2-Vector Control were used to establish tumour xenografts in the flank of 4-5 week-old Balb/c nude mice (Harlan UK Ltd., Bicester, Oxon, UK). $5x10^6$ cells in 150 µL of sterile PBS were injected using a 22 G needle into the right flank of each animal and there were five mice per group of each cell type. When tumours reached 0.4-0.5 cm each mouse received $1x10^7$ pfu of VVL15 in 100 µL of PBS via intravenous (IV) tail vein injection. The biodistribution of VVL15 was determined 1, 2, 3, 5 and 6 days following infection by measuring luciferase distribution by light emission with the IVIS camera according to the manufacturer's instructions. Mice were anaesthetised (2% isofluorane by inhalation in O_2 1 L/min and NO 1 L/min) and received an intraperitoneal (IP) injection of 150 mg/kg D-Luciferin at a concentration of 15 mg/mL (200 µL injection in 20 g mouse). Mice were placed on a stage pre-warmed to 37 °C in the light-free chamber housing the IVIS camera where anaesthesia was continued by nose-cone delivery.

10 minutes following D-Luciferin injection, grey-scale whole-body photographic images were collected (field of view 15 cm; exposure 0.2 seconds; binning medium; f/stop 16) followed by acquisition and overlay of a colour image representing the spatial distribution of the detected photons emitted from the field (field of view 15 cm; exposure 0.5-120 seconds; binning

medium; f/stop 1). The length of bioluminescence imaging varied between 0.5 and 120 seconds in order to ensure that a non-saturated image was obtained. Tumours were defined as ROI and light emission quantified (p/s/cm^2) using Living Image software. Results were analysed using Prism®.

2.8 Histology and immunohistochemistry (IHC)

All histology and IHC procedures were performed by Vipul Bhakta, Mohammed Ikram and Keyur Trivedi (Pathology Service, Barts CR-UK Centre, QMUL, London) and all slides reviewed by CH and YW.

2.8.1 Sample processing

Tumour xenografts and organs were collected from mice immediately after sacrifice and were fixed in 10% formaldehyde and then paraffin-embedded. Samples were cut into 4 μm sections using a Leica EG1160 microtome. Slides were stained with haematoxylin and eosin (H&E) according to standard protocols using a Leica autostainer XL. Further sections were cut for IHC, which was performed using the Ventana® Discovery staining module (Ventana, Tucson, USA). This system used biotin-free secondary antibodies, which were already conjugated to streptavidin-HRP. These were visualised with a hydrogen peroxide (H_2O_2) substrate and 3,3'diaminobenzidine tetrahydrochloride (DAB) chromogen, which produced a dark brown product visible by light microscopy.

Table 2.3: Primary Antibodies used for IHC

Antibody against	1º/ 2º	Species	Optimised dilution	Supplier
VVLister coat protein	1º	Rabbit	1:200 (paraffin)	MorphoSys UK Ltd, Bath, UK
Pecam-1 (ab56299)	1º	Rabbit	1:200	Abcam Ltd. Cambridge. UK.

2.8.2 IHC in paraffin-embedded sections for Vaccinia virus and Pecam-1.

All staining was performed using the Ventana® Discovery staining module (Ventana, Tucson, USA). Slides were deparaffinised using EZ Prep™ (Ventana) at 75 °C for 8 minutes. Slides were heated to 95 °C for 8 minutes in the presence of conditioning solution 1 (CC1; Tris-EDTA-based buffer). A 1:200 dilution of primary antibody (Table 2.3) was applied to sections for 60 minutes at 37 °C. Omnimap anti-Rabbit HRP was then applied 16 minutes. Sections were then incubated with 3,3'-Diaminobenzidine (DAB) and hydrogen peroxide for 8 minutes. Sections were counterstained with haematoxylin and bluing agent for two minutes. Sections were washed between each step.

2.8.3 Quantification of Pecam-1 immunostaining

Five tumours per group were used for analysis. Samples were collected and stained as described using a Pecam-1 mAb (Abcam, Cambridge, UK). Two sections were taken from the centre of each tumour 200 μm apart. The Zeiss Axioplan microscope (Carl Zeiss International, Gottingen, Germany) was used at 20x magnification to take sufficient images to cover the entire section. The edges of tumours, folding of sections or any images showing sample degradation were not included in the analysis. The images from each section were reconstructed into a montage using the Image J Software (National Institute of Health, Bethesda, USA) (182). Montages were then split into RGB channels. The blue channel was selected as giving greatest distinction between Pecam-1-positive staining and background. The threshold analysis tool was used to select vessels and any contaminating (non-vessel) stray pixels were excluded. Each montage was measured to give the area of Pecam-1-positive immuno-staining as a percentage of the total area. Measurements were combined for each group for analysis.

2.9 Data handling and statistical analysis

2.9.1 EC50 and variable slope non-linear regression

$$EC_{50} = ((X \text{ where } Y=\text{top}) - (X \text{ where } Y=\text{bottom}))*0.5$$

$$Y = \text{Bottom} + \frac{(\text{Top}-\text{Bottom})}{(1+10^{((\text{LogEC50}-X)*\text{HillSlope})})}$$

X = log[virus] ;Y = %cells alive; Hillslope=steepness of curve

Top/Bottom = Maximum/Minimum Y value (or cell death)

2.9.2 TCID50

The Reed-Muench method of TCID50 calculation is based on the adding the proportionate distance between CPE scores of rows above and below 6 out of 12 to the log of the viral dilution where CPE is 6 or less. Viral dilutions range from 10^{-3} to 10^{-9} for viral replication samples.

$$\log TCID_{50} = \log(\text{viral dilu}^{n} \text{ at row above 50\% CPE}) - \frac{(\%\text{ CPE next above } 50\%)-50\%}{(\%\text{ CPE next} > 50\%)-(\%\text{ CPE next} \leq 50\%)}$$

This is converted to pfu/mL for purified viral titres:

Since volume of sample inoculated into the first row = 0.02 mL

$$TCID_{50}/mL = (1/ TCID_{50})*(1/0.02)$$

$$TCID_{50}\ PFU/mL = TCID_{50}/mL*0.69$$

This is then converted into PFU/cell for viral replication titres.

$$TCID_{50}\ (PFU/cell) = \frac{TCID_{50}\ PFU/mL}{\text{number of cells at infection}}$$

2.9.3 Statistical analysis

Data sets were initially confirmed as normally distributed or not using the D'Agostino and Pearson test of normality. Comparisons were then performed using two-tailed unpaired t-tests or a Mann-Whitney U test as appropriate. A repeated measures two way ANOVA with a bonferroni correction was used to compare bioluminescence for in-vivo time course experiments.

Chapter 3

3 Hypoxia and Vaccinia Virus

Many tumours are known to contain areas of hypoxia due to poorly developed vasculature. Adenovirus, the most commonly used oncolytic vector has been shown to replicate poorly in hypoxia. We wanted to assess the effect of hypoxia on the life cycle VVLister to assess its potential as an oncolytic viral vector in hypoxia.

3.1 Validation of Hypoxic Conditions

Hypoxia-inducible factor 1 alpha (Hif-1α) is the key protein mediating the response of cells to a hypoxic microenvironment. In the presence of oxygen Hif-1α is hydroxylated at specific proline residues which results in its interaction with the Von Hippel–Lindau gene product and subsequent ubiquitination and degradation (41). In the absence of ambient oxygen this degradation does not occur and subsequent nuclear localisation results in the transcription of Hif-1α target genes and cellular adaptation to hypoxia. Vaccinia Virus is becoming an increasingly common vector for viral gene and oncolytic therapy. However its ability to replicate in hypoxia has not been reported to date. In this project, hypoxic conditions were simulated with the use of a hypoxic incubator (Cell Chamber 170, Heto-Holten, Surrey, UK) maintaining the ambient oxygen concentration at 1% pO_2. To validate the response of Hif-1α in our *in vitro* system, immunoblotting for Hif-1α in nuclear extracts of three pancreatic cancer cell lines Suit2, MiaPaca-2 and CFPac1 was carried out. This demonstrated stabilisation of the Hif-1α protein and nuclear localisation only when exposed to 1% pO_2 (Figure 3.1). The predicted molecular weight of Hif-1α is 92 kDa but this antibody, H1alpha67, detects a protein of approximately 120 kDa and it is assumed that this is due to post-translational modification of the protein (183). This demonstrates that a hypoxic environment can be maintained using our incubator and this was used to simulate a hypoxic environment in all future experiments unless otherwise stated. The use of the term hypoxia refers to a pO_2 of 1%, 5% pCO_2 and 94% pN_2 unless otherwise stated.

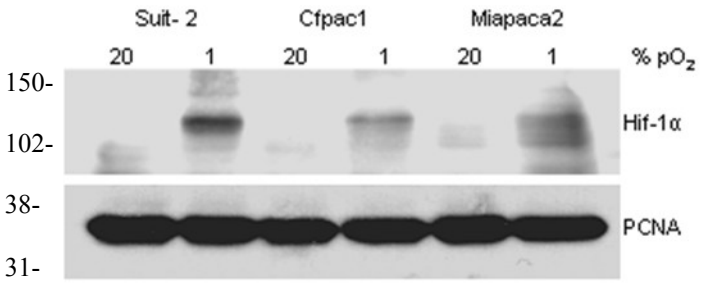

Figure 3.1: Stabilisation and nuclear translocation of Hif-1α under hypoxic conditions.

Cell lines were incubated in normoxic conditions (20% pO_2) or hypoxia (1% pO_2) for 16 hours before harvesting of nuclear extracts for immunoblotting. Lysates were probed for Hif-1α and proliferating cell nuclear antigen (PCNA) expression as a loading control. pO_2 = Oxygen Partial Pressure.

3.2 Viral Protein Production in Hypoxia

Hypoxia has been shown to limit the total amount of protein synthesis (184). Consequently we investigated whether production of viral proteins in pancreatic cancer cell lines exposed to hypoxic conditions would be altered. CFPac1 and MiaPaca2 cell lines were infected with VVLister at an MOI=1 pfu/cell or mock infected and lysates were harvested at 24h, 48h and 72h post-infection. Using an anti-VVL polyclonal antibody similar levels of Vaccinia virus protein were detected at 72 hours when exposed to normoxia or hypoxia as shown in lanes 6 & 7 of Figure 3.2. This result confirms that viral proteins are translated efficiently in hypoxic conditions.

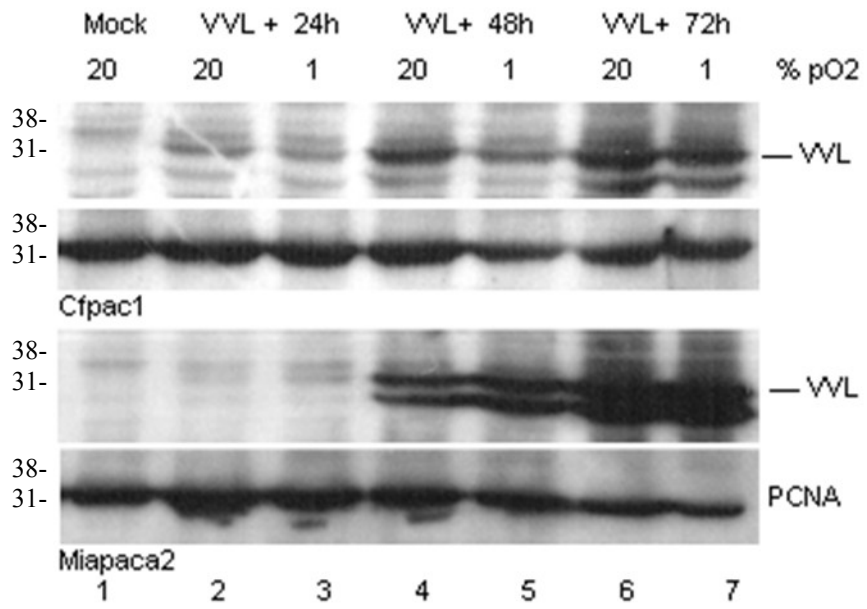

Figure 3.2: Western Blot of Vaccinia virus protein expression in MiaPaca2 and CFPac1 in normoxia and hypoxia.

Cells were maintained in normoxic or hypoxic conditions before and after viral infection. Cells were infected with VVLister at an MOI of 1 pfu/cell or mock infected with vehicle buffer alone. Membranes were probed for Vaccinia virus proteins with an anti-Vaccinia polyclonal antibody. This antibody detects most reliably a viral protein ~35-37 kDa in size which is likely to represent the 37 kDa Vaccinia virus major envelope protein. Human proliferating cell nuclear antigen (PCNA) was used as a loading control.

3.3 Viral Replication in Hypoxia

The ability of replication-competent, oncolytic viruses to infect, multiply, lyse and subsequently infect neighbouring cells is crucial for their anti-tumour efficacy. There has been concern that hypoxia may present a barrier to this (185). We investigated the replication of VVLister in pancreatic cancer cell lines Suit-2, Miapaca2 and CFpac1 when exposed to normoxia or hypoxia prior to and post viral infection. Cells and supernatant were collected at 24, 48, 72 and 96 hours post-infection. The number of pfu/cell produced for each cell line in different conditions was determined using a TCID50 assay as described in the Materials and Methods. Viral replication in Miapaca-2 and CFpac1 cells is unaffected at any point by hypoxic conditions (Figure 3.3). Suit-2 cells show a similar pattern at 24h and 48h producing a high titre of infectious viral particles in both hypoxia and normoxia. At 72 and 96 hours post-infection even higher titres are achieved when replication occurs in ambient oxygen concentrations ($P=0.01$ and $P=0.04$ respectively). In summary high viral titres of VVLister (approximately 100 pfu/cell) were achievable in all pancreatic cancer cell lines tested in both normoxia and hypoxia.

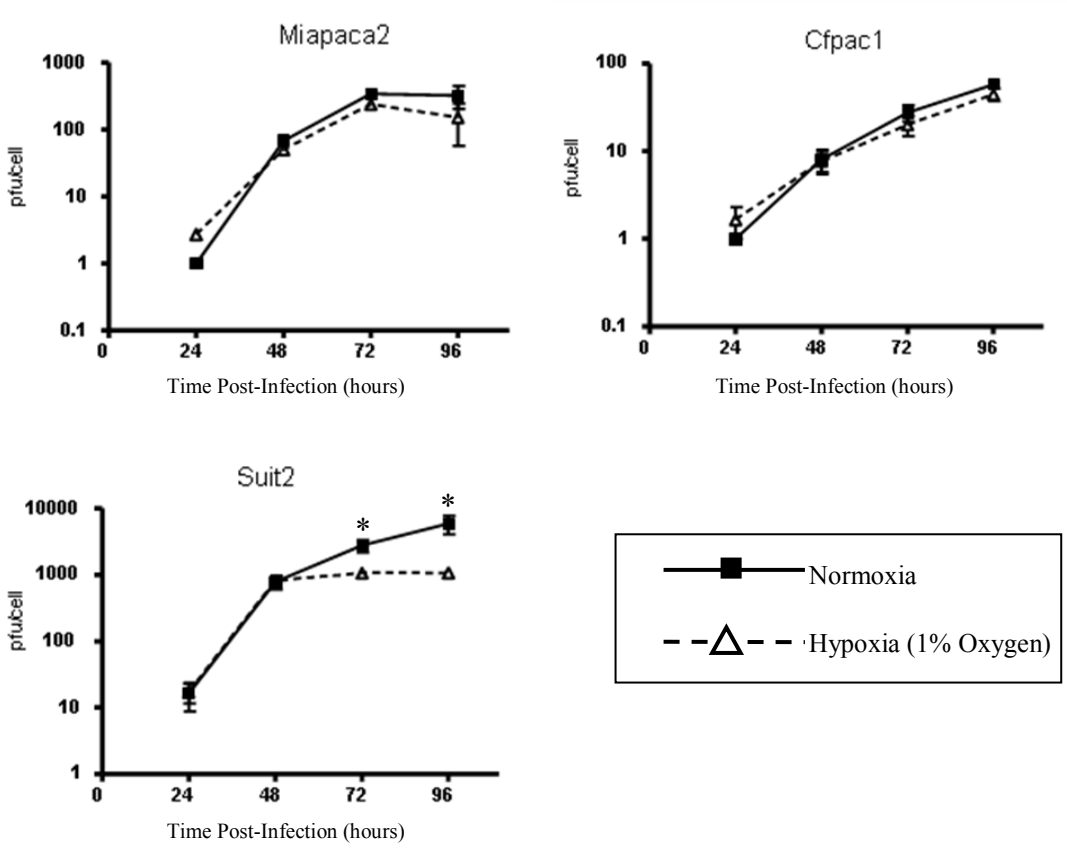

Figure 3.3: Viral replication of VVLister in normoxic and hypoxic conditions in PDAC cell lines.

Viral replication was measured by TCID50 (50% tissue culture infective dose) assay of viral burst assays. Cell lines were exposed to normoxic (solid line) or hypoxic conditions (dashed line) before and after infection with an MOI=1 of VVLister. Burst assay samples were collected at 24, 48, 72 and 96 hours post-infection. TCID50 assays were performed on CV1 green monkey kidney cells. Experiments were performed in triplicate for each cell line, time point and condition. Results are presented as mean ± SEM.

3.4 Cytotoxicity of Wildtype Vaccinia Virus in Hypoxia

Effective lysis of infected tumour cells is the ultimate aim of oncolytic therapy. We used the 3-(4,5-dimethylthiazol-2-yl)-5-(3-carboxymethoxyphenyl)-2-(4-sulfophenyl)-2H-tetrazolium (MTS) assay to determine the EC50 (dose of virus required to kill 50% of cells) for four pancreatic cancer cell lines using wild type Vaccinia virus. Cells were infected and maintained in the indicated oxygen conditions for the duration of the experiment and cell viability was analysed at 6 days post-infection. EC50 values were calculated (Figure 3.4).

In Suit2 the EC50 in normoxia was 1.5 pfu/cell and 1.8 pfu/cell in hypoxia ($P = 0.48$). In Panc1 the EC50 in normoxia was 1.2 pfu/cell and 0.8 pfu/cell in hypoxia ($P = 0.07$). For these two cell lines there was no statistically significant effect of hypoxia on viral replication. In MiaPaca2 the EC50 in normoxia was 187.0 pfu/cell and 9.0 pfu/cell in hypoxia ($P \leq 0.0001$). In CFPac1 the EC50 in normoxia was 3.7 pfu/cell and 1.1 pfu/cell in hypoxia ($P \leq 0.0001$). These values represent a statistically significant increase in Vaccinia virus cytotoxicity in Miapaca2 and CFPac1 cell lines maintained under hypoxic conditions, with an approximately 20-fold and 3-fold reduction in EC50 respectively. These data suggest that the Lister strain Vaccinia Virus is a good agent for oncolytic viral therapy where hypoxia is likely to be present in the tumour microenvironment and represent a proportion of the tumour burden.

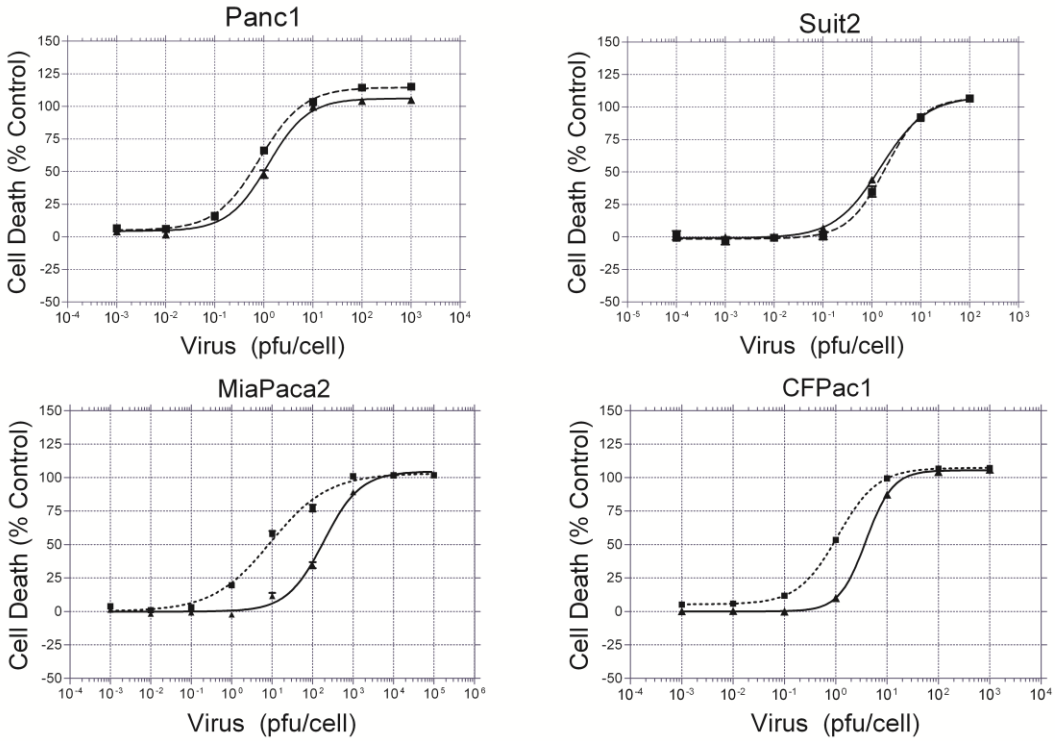

Figure 3.4: Effect of hypoxia on cytotoxicity of VVLister.

Pancreatic cancer cell lines were incubated in hypoxic or normoxic conditions for at least 16 hours, then infected with serial dilutions of VVLister and maintained under the same oxygen tension. The infected cells were assayed with MTS reagent at day 6 post-infection at 37 °C with 5% CO_2 for 2 hours. Viable cells were determined as a percentage of the uninfected controls and non-linear regression analysis was used to draw dose–response curves. The dotted line represents hypoxic conditions; the solid line represents normoxic conditions. Each assay contained six replicates and results are presented as mean ± SEM of four independent experiments.

3.5 Cytotoxicity of Recombinant Vaccinia Virus VVL15 in Hypoxia

VVL15 is a recombinant Vaccinia virus provided by Istvan Fodor (Loma Linda University Campus, CA, USA). VVL15 was made by insertion of the firefly luciferase (fLuc) and the lacZ reporter genes into the thymidine kinase (TK) region of VVLister. The firefly luciferase gene was placed under the control of the Vaccinia early/late promoter and lacZ under the control of the Vaccinia promoter p7.5. This virus is valuable for following transgene expression *in vitro* and *in vivo*. This virus was used in subsequent experiments so we wanted to verify if there was a similar effect of hypoxia on the cytotoxicity of this TK-deleted oncolytic virus in MiaPaca2 and CFPac1.

MTS assays were carried out as described previously. The EC50 values for VVL15 in MiaPaca2 were 183.8 pfu/cell and 7.7 pfu/cell in normoxia and hypoxia respectively ($P \leq 0.0001$). The EC50 values for CFPac1 were 7.9 pfu/cell and 2.4 pfu/cell in normoxia and hypoxia respectively ($P \leq 0.0001$) (Figure 3.5). Although there was some difference in the mean EC50 values for recombinant VVL15 versus wildtype VVLister a similar trend was observed. Both viruses were more cytotoxic under hypoxic conditions.

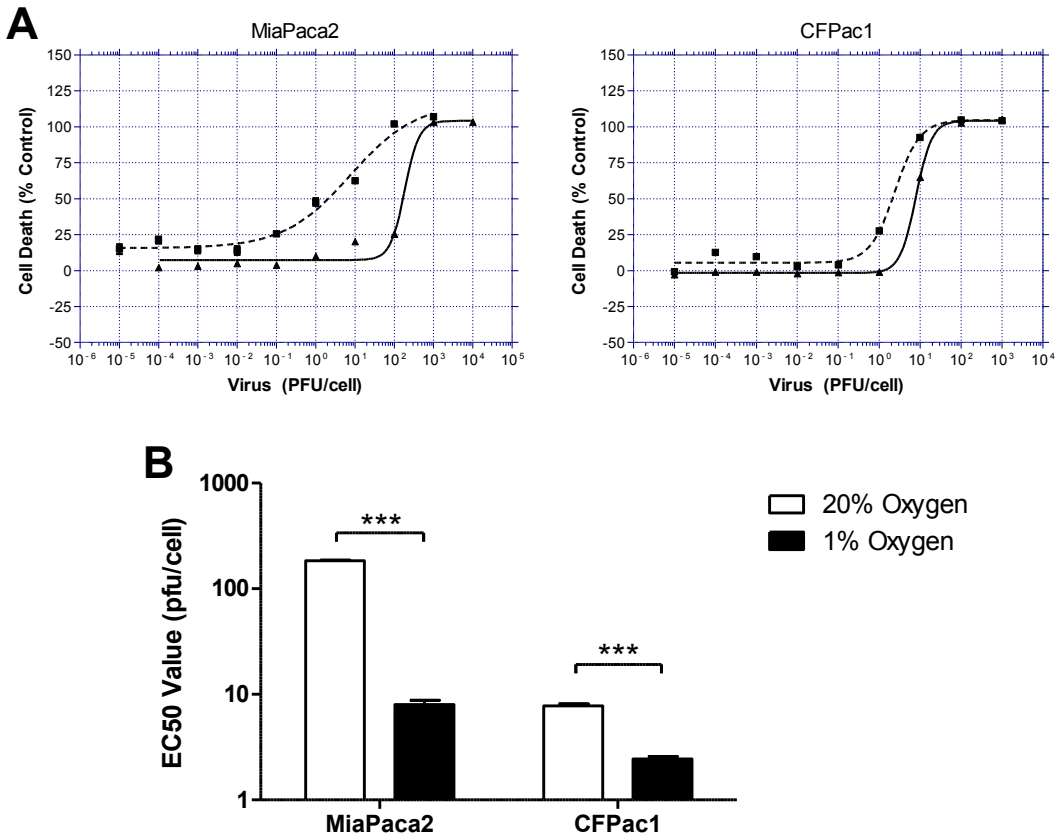

Figure 3.5: Effect of hypoxia on cytotoxicity of recombinant Vaccinia virus VVL15.

Pancreatic cancer cell lines were maintained in hypoxic or normoxic conditions for at least 16 hours, then infected with serial dilutions of VVLister and maintained under the same oxygen tension. The infected cells were assayed with MTS reagent at day 6 post-infection at 37 °C with 5% CO_2 for 2 hours. Viable cells were determined as a percentage of the uninfected controls and non-linear regression analysis was used to draw dose–response curves. The dotted line represents hypoxic conditions; the solid line represents normoxic conditions. Each assay contained six replicates and results are presented as mean ± SEM of four independent experiments.

3.6 Viral Transgene Expression in Hypoxia

Many replicating viruses used for oncolytic therapy have additional therapeutic transgenes inserted into the viral genome to increase their cytopathic effect. Examples include pro-apoptotic proteins, prodrug-converting enzymes and cytokines (186). One attraction of Vaccinia virus versus more conventional viral vectors such as adenovirus or adeno-associated virus is its large capacity for transgene insertion (187). Although we have seen that Vaccinia virus gene expression is unaffected by hypoxia it is important to determine the effect of hypoxia on transgene expression from replication-competent Vaccinia virus if this vector is to be of clinical use (184).

We used VVL15 to investigate the effect of hypoxia on firefly luciferase gene expression. Suit2, MiaPaca2, CFPac1 and Panc1 were all infected with VVL15 at an MOI=1 pfu/cell and samples collected at 24, 48 and 72 hours post-infection. In previous studies on the effect of hypoxia on other viruses isolated readings or early time points were used (103, 188). We felt it would be more appropriate to assay multiple and later time points to reflect the transgene expression that would be of interest in translational applications. The level of luciferase expression was largely unaffected by hypoxia (**Figure 3.6**). Only two of the four cell lines tested showed a significant difference between normoxia and hypoxia at two isolated time points. There was a decrease at 24 hours and increase at 48 hours in luciferase expression for CFPac1 and Panc1, respectively. However, this difference was not sustained at later time points. This result suggests that hypoxia does not compromise transgene expression from replication-competent Vaccinia virus.

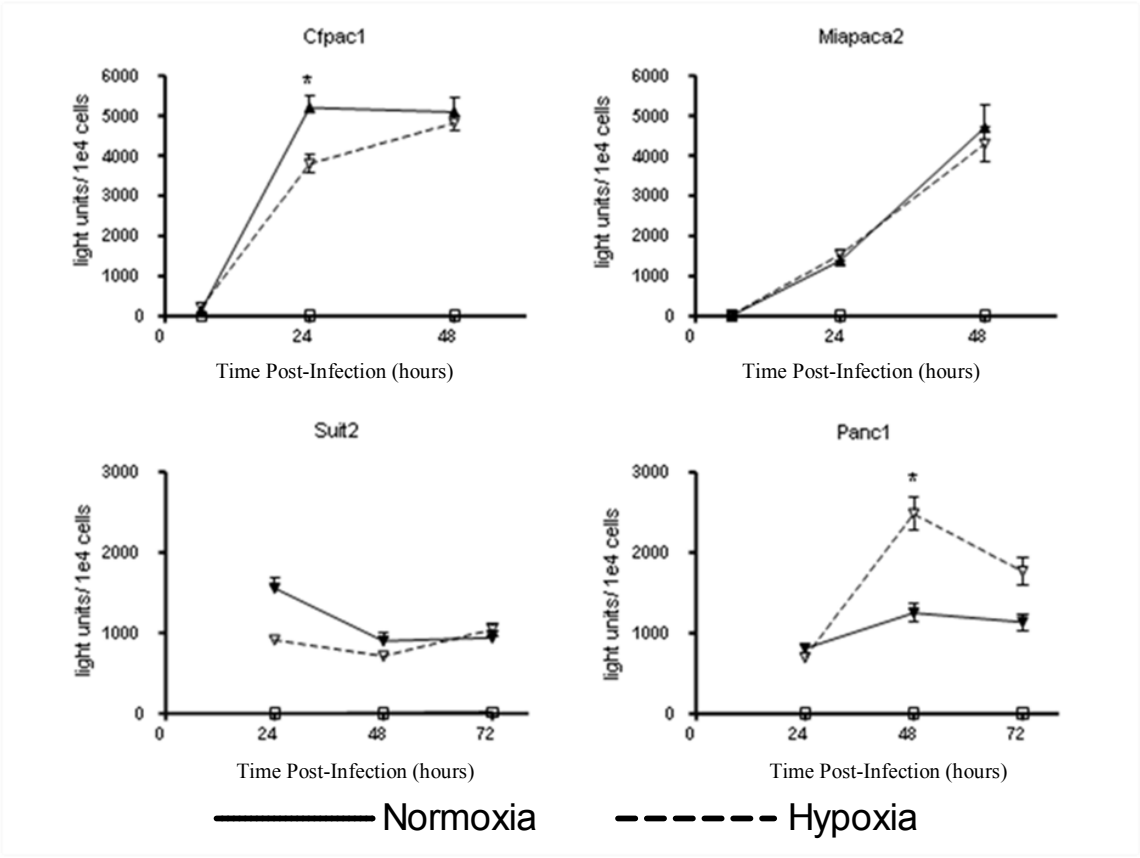

Figure 3.6: The effect of hypoxia on transgene expression from VVL15.

Cells were seeded at a density of $3x10^4$ per well in a 24 well plate and then infected with 1 pfu/cell of VVL15 24 hours later. Cells were lysed and luciferase activity was measured at 24, 48 and 72 hours post-infection using a luminometer (Perkin Elmer Victor II) after addition of D-Luciferin. The dashed line represents hypoxic conditions; the solid line represents normoxic conditions. All experiments were performed in triplicate and results represent the data from three separate experiments. Results are presented as mean ± SEM (solid line and triangle 20% pO2, dashed line and triangle 1% pO2. Light units=photons/second. * = $P \leq 0.05$).

3.6.1 Viral Transgene Expression in Hypoxia at an Early Time Point

The transcription of early poxvirus genes occurs inside the viral core at less than 4 hours post-infection using the virally encoded early transcription machinery that is packaged into the virion upon assembly. Intermediate and late viral gene expression occurs after peri-nuclear viral factories have been established at 4-5 hours post-infection (148).

We performed a luciferase assay to assess the effect of hypoxia on early viral gene expression in CFPac1 and MiaPaca2 (Figure 3.7). There was a statistically significant increase in early gene expression seen for both cell lines under hypoxic conditions ($P = 0.0004$ and $P \leq 0.0001$ respectively). Luciferase imaging was also performed with the IVIS imager to give a visual impression of Luciferase expression in normoxia and hypoxia using MiaPaca2 cell line imaged at 4 hours post-infection and a clear difference was noted (Figure 3.8). This suggests that hypoxia has an effect on the viral life cycle at an early time point prior to establishment of peri-nuclear viral factories. Additional effects at later time points are also possible.

As Vaccinia virus is an enveloped virus that contains cellular proteins accumulated in the virion during assembly it cannot be excluded that some of the effect on Luciferase expression is the result of luciferase being enveloped within the viral core during viral production in CV1 cells. Incorporating luciferase proteins inside infective virions has been used to study the effect of PI3K inhibitors on the cellular entry of Ebola Virus (189). If luciferase contained inside the infective virion is contributing to this finding it would suggest an effect of hypoxia on viral entry.

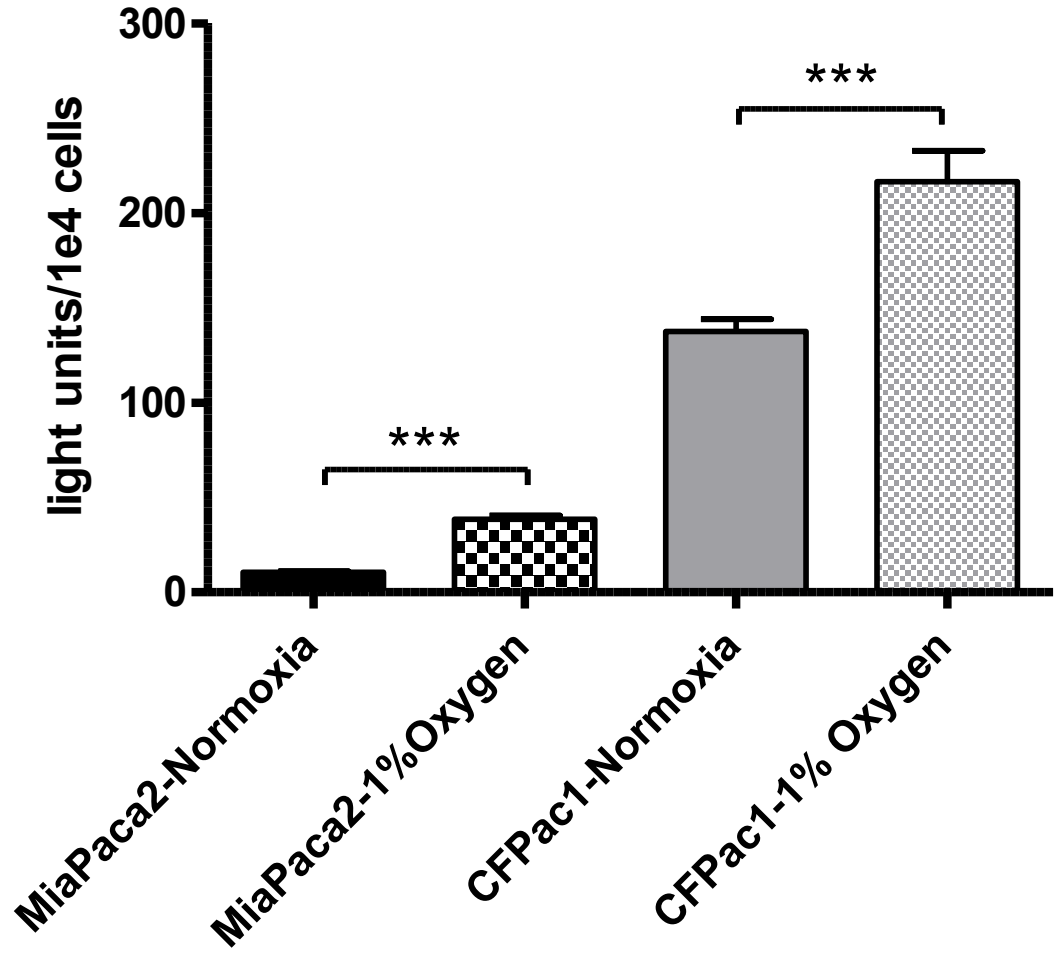

Figure 3.7: The effect of hypoxia on early transgene expression from VVL15.

Cells were seeded at a density of 3e4 per well in a 24 well plate and then infected with 1 pfu per cell of VVL15 four hours later. Cells were lysed and luciferase activity was measured at four hours post-infection using a luminometer (Perkin Elmer Victor II) after addition of D-Luciferin. All experiments were performed in triplicate and results represent the data from two separate experiments. An unpaired two-tailed students T-test was used to compare the mean bioluminescence. Results are presented as mean ± SEM. *** = $P \leq 0.001$.

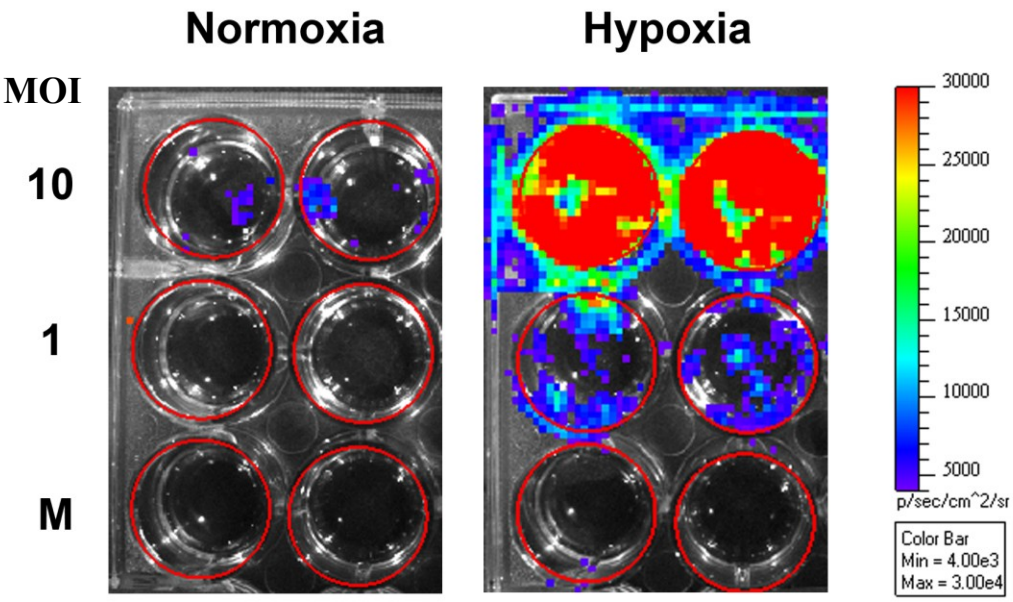

Figure 3.8: Representative images of bioluminescence from MiaPaca2 parental cell infected with VVL15 in normoxia and hypoxia.

MiaPaca2 cells were seeded in 6 wells plates and allowed to adhere overnight. Cells were then infected with VVL15 at an MOI of 10 pfu/cell, 1 pfu/cell or mock infected (M). Cells were then exposed to normoxia or hypoxia for 4 hours and imaged for luciferase expression using the IVIS imaging system. Wells are outlined in red and the same colorimetric scale is used for both images.

3.7 Summary of Vaccinia Virus and Hypoxia

We have demonstrated that the replication, protein production and transgene expression of the Lister strain Vaccinia virus is not negatively affected by hypoxia. Importantly, for translational applications, we found that viral cytotoxicity was augmented in two of four PDAC cell lines. Transgene expression from the recombinant virus VVL15 was increased in hypoxia versus normoxia early after viral infection. This suggests that hypoxia has a positive effect on an early stage of viral infection in some PDAC cell lines *in vitro*.

Chapter 4

4 Vaccinia Virus and VEGFA

4.1 The Effect of VEGFA Expression in PDAC Cell Lines

Vaccinia virus is a large virus and we hypothesised that the tropism of Vaccinia virus may be related to the increased permeability of blood vessels in tumours compared to normal tissue, allowing extravasation preferentially at tumours. VEGFA was initially discovered as a factor released by tumour cells that increased the permeability of blood vessels (73). To test this hypothesis, a cell line with a low endogenous level of VEGFA that could be engineered to overexpress VEGFA and used to establish an *in vivo* tumour model with increased vascular permeability was required. As in other solid tumours, it has been found that VEGF is over expressed in pancreatic cancer (190) and that this can be regulated by hypoxia as a transcriptional target of Hif-1α (191).

To verify the endogenous level of VEGF production and the effect of hypoxia on VEGF secretion by the PDAC cell lines, an ELISA was performed on the supernatant of uninfected cells. MiaPaca2, Suit2, CFPac1 and Panc1 cells were seeded in six well plates, allowed to adhere overnight and then incubated in normoxia or hypoxia for a further 24 hours. Experiments were designed so that all cells were at approximately 70% confluent when supernatant was taken to perform a subsequent ELISA. Suit2 and Panc1 had a relatively high level of VEGF secretion (>2000 ng/mL) compared to CFPac1 and MiaPaca2 (~1000 ng/mL). However, only in MiaPaca2 and CFPac1 was statistically significant hypoxic induction of VEGF observed and interestingly it is only in these two cell lines was a significant increase of viral cytotoxicity in hypoxia was noted (Figure 4.1).

Consequently we hypothesised that VEGF plays a role in the Vaccinia virus life cycle and could be involved in the effect of hypoxia on early gene expression. Orf virus, a member of the poxvirus family, produces VEGFE a vascular endothelial growth factor that is critical to viral infection (92). Although no homologue to VEGFA or VEGFE has been found in the Vaccinia

Lister strain genome it is known that another growth factor, epidermal growth factor, is important for Vaccinia virus infection, so we wanted to investigate if VEGFA played a role in the Vaccinia virus life cycle (133).

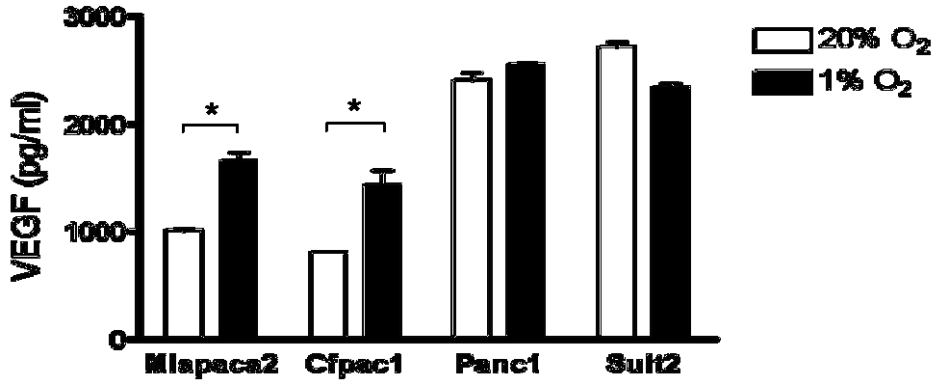

Figure 4.1: ELISA to assess VEGFA concentration in the supernatant of PDAC cell lines exposed to normoxia and hypoxia.

MiaPaca2, CFPac1, Panc1 and Suit2 were seeded in 6 well plates and exposed to the relevant oxygen conditions for 48 hours when the cells were all at approximately 70% confluence. Fresh supernatant was taken and used for a subsequent ELISA. Experiments were performed in duplicate and results represent the data from two separate experiments. An unpaired two tailed students T-test was performed to compare the mean VEGF levels. Results are presented as mean ± SEM. * = $P \leq 0.05$.

4.2 Manipulating VEGFA in PDAC cell lines

4.2.1 Silencing of VEGF Expression in Suit2 Cells

To establish cell models we selected Suit2, with a high endogenous level of VEGFA, and used a pool of four siRNA sequences to silence gene expression. Suit2 cells were transfected with Control siRNA, VEGFA siRNA (25 nM) or mock transfected and supernatant collected at 24, 48 and 72 hours later. An ELISA was used to detect the effectiveness of VEGF silencing and select the optimal time for viral infection. There was some off-target (or transfection reagent) effect on VEGFA expression in the control siRNA-transfected cells when compared to the parental cell line at 48 hours. However, at 72 after transfection there was a three-fold differential between control and VEGFA siRNA-treated cells and consequently 72 hours after siRNA transfection was selected as the optimal time point for viral infection (Figure 4.2). To further optimise the required concentration of siRNA and quantity of transfection reagent required for VEGFA gene silencing 25 & 50 nM of siRNA and 1 or 2 μL of transfrection reagent were used and VEGFA measured 72 hours later. A combination of 25 μM of siRNA and 2 uL of transfection was selected as optimal for VEGFA silencing (Figure 4.3). The sequences used for gene silencing of VEGFA are presented in Table 4.1.

Table 4.1: Sequence of VEGFA siRNA smartpool

GENE (Ref Seq)	siRNA Target Sequence
VEGFA (NM_001025366)	1-GCAGAAUCAUCACGAAGUGUU 2-GGAGUACCCUGAUGAGAUCUU 3-GAUCAAACCUCACC AAGGCUU 4-AGAAAGAUAGAGCAAGACAUU

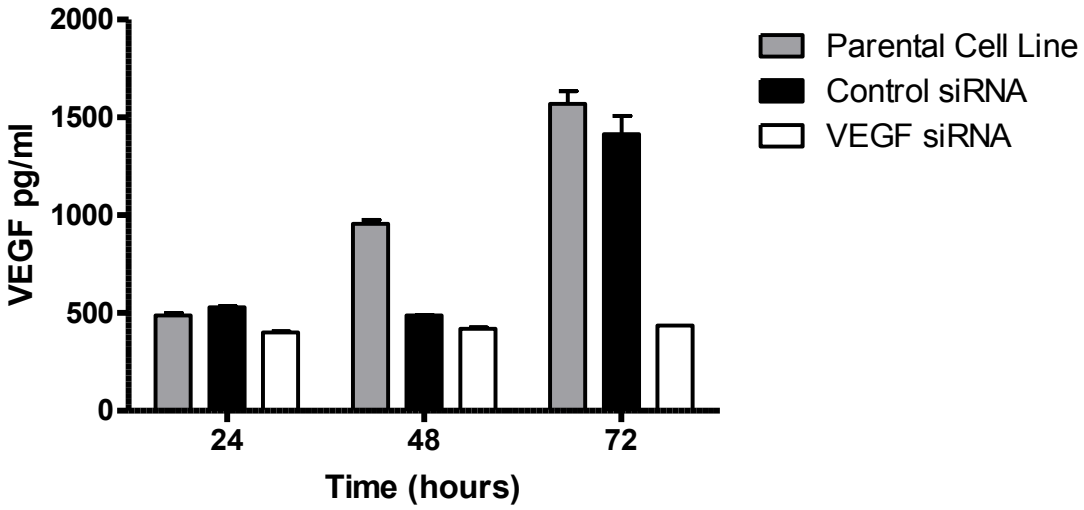

Figure 4.2: The effect of VEGFA siRNA in the Suit2 cell line.

To optimise timing for infection in the VEGFA-silenced Suit2 cell line, cells were transfected with VEGFA siRNA or siGENOME RISC-free control siRNA. Cells were transfected in 6 well plates using 50 nM of siRNA and 2 uL of transfection reagent per well. Supernatant was then collected for a VEGFA ELISA at 24, 48 and 72 hours. The untransfected parental cell line was also included for comparison. Experiments were performed in duplicate and results represent the data from two separate experiments. Results are presented as mean ± SEM. * = $P \leq 0.05$.

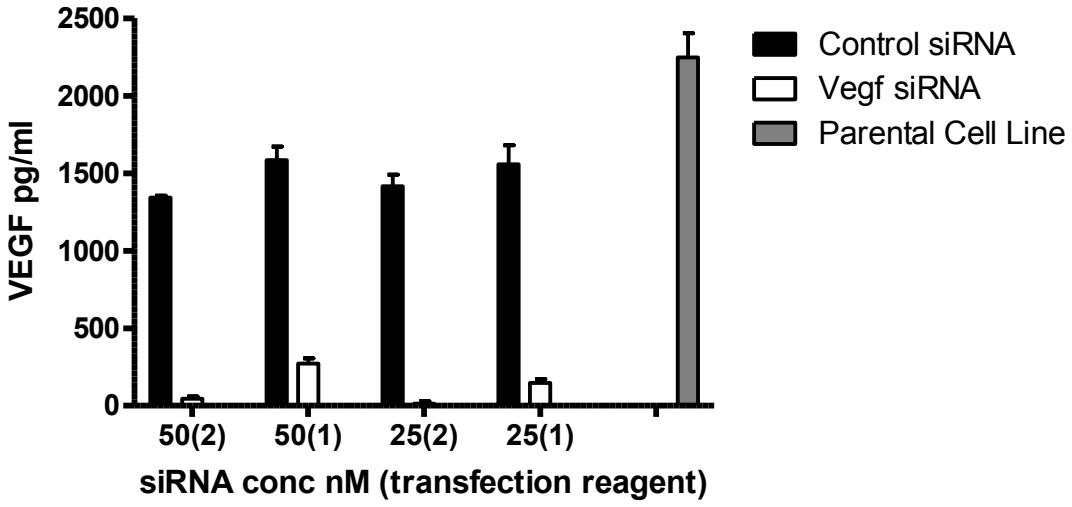

Figure 4.3: Optimisation of VEGFA siRNA in Suit2 cells.

Cells were transfected with 50 or 25 nM of VEGFA or Control siRNA using either 1 or 2uL of transfection reagent per well of a six well plate. Supernatant was collected 72 hours later and a VEGFA specific ELISA was used to measure VEGFA concentration. The VEGF level of the parental cell line at 72 hours is shown for comparison. Experiments were performed in duplicate and results represent the data from two separate experiments. Results are presented as mean ± SEM.

4.2.2 Over-expression of VEGF in MiaPaca2

In order to create a stable model, VEGFA- overexpressing and paired vector-control MiaPaca2 cells were selected as they have a relatively low endogenous level of VEGFA. The sequence NM_001025368.1 corresponding to Homo sapiens VEGFA transcript 4 coding for VEGF isoform p165 was used. This was supplied from the manufacturer in the Vector pCMV6-XL4 (Origene, Rockville MD, USA). The pCMV6-Neo vector was used for expression in eukaryotic cells (Origene, Rockville MD, USA). The Not1 restriction site was used to excise the VEGF sequence from the pCMV6-XL4 vector which was gel-purified and ligated into the pCMV-Neo eukaryotic expression vector creating the vector pCMV-Neo-VEGFp165. Restriction enzyme digestion with gel analysis and sequencing was performed to verify the integrity and orientation of the VEGF transcripts. MiaPaca2 cells were seeded at a density of $2x10^5$ cells per well in a 6 well plate. The Effectene transfection reagent (Qiagen, Valencia, CA, USA) was used at a ratio of 1 ug of DNA to 10 μL of Effectene reagent to transfect MiaPaca2 cells with pCMV-Neo-VEGFp165, pCMV-Neo control vector or no vector. Cells were cultured in the presence of G418 (Invitrogen) in DMEM supplemented with 10% FCS until cells in the untransfected wells were no longer viable. VEGF protein expression was then confirmed using Enzyme-linked immunosorbent assay (R&D Systems, Abingdon, UK). These cell lines will subsequently be referred to as Miapaca2-VEGF-165 and Miapaca2-Vector control.

To quantify the level of VEGF over-expression the stable cell lines were seeded in 6 well plates and supernatant collected for a VEGFA ELISA 48 hours later. There was a three-fold increase in VEGF A expression in MiaPaca2-VEGF-165 compared to MiaPaca2-Vector-Control (Figure 4.4). The stable cell line was assayed for VEGFA using an ELISA at regular intervals to confirm continued expression.

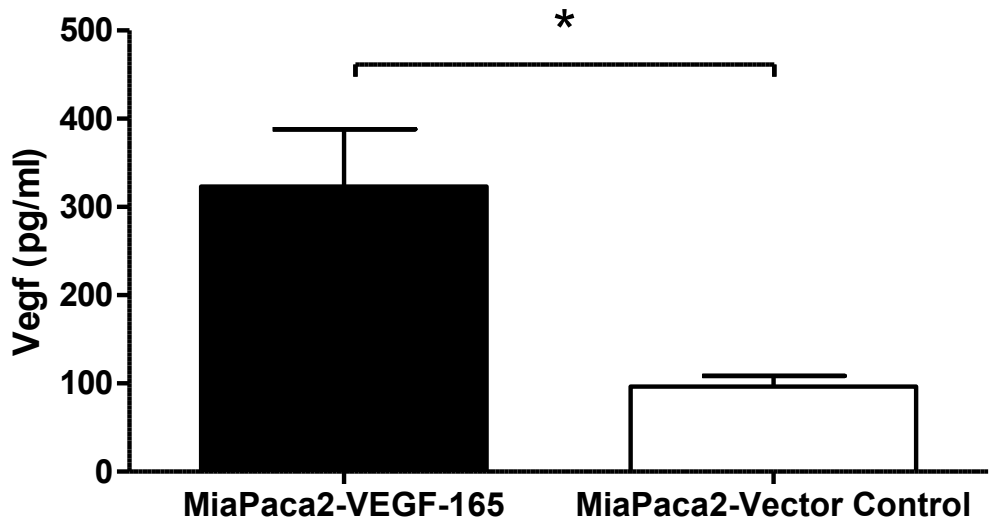

Figure 4.4: Quantification of VEGFA production in stable MiaPaca2 cell lines.

MiaPaca2 cells were transfected with pCMV-Neo-VEGF-165 or pCMV-Neo to establish the stable cell lines MiaPaca2-VEGF-165 and MiaPaca2-Vector Control respectively. Cells were seeded in 6 well plates and incubated in normoxic conditions for 24 hours. Supernatant was then collected and assayed for VEGF expression using an ELISA. Experiments were performed in triplicate. An unpaired two-tailed students T-test was used to compare the mean level of VEGF. * = $P \leq 0.05$.

4.3 The effect of VEGF expression on Vaccinia virus gene expression

To investigate whether VEGF plays a role in the viral life cycle *in vitro* we used the Suit2 cell model to assess the effect of VEGF gene silencing on luciferase expression from VVL15. Suit2 cells were seeded and allowed to adhere overnight, transfected with siRNA and infected 72 hours later with VVL15 at an MOI = 1, 0.1 or 0.01 pfu/cell, or mock-transfected. At 24 and 48 hours after infection, supernatant was removed, luciferin added and plates imaged immediately using the IVIS imaging system. VEGFA gene silencing resulted in a statistically significant log fold reduction of bioluminescence from VVL15. The bioluminescence from control siRNA-treated cells was comparable to the parental cell line. A reproducible effect was seen at both 24 and 48 hours and was consistent at all MOIs (Figure 4.5). A representative image taken at 48 hours after infection is shown in Figure 4.6.

To confirm these findings similar experiments were performed using MiaPaca2-VEGF-165 and MiaPaca2-Vector Control cell lines. Cells were seeded and allowed to adhere overnight and then infected with VVL15 at an MOI = 1 pfu/cell. Hypoxia affects bioluminescence from VVL15 as early as 4 hours post-infection. To see if hypoxic induction of VEGF may be implicated in VVL15 infection, cells were analysed for luciferase expression at 4, 24 and 48 hours post-infection. There was a statistically significant increase in bioluminescence in MiaPaca2-VEGF-165 verses MiaPaca2-Vector Control. The over expression of VEGF results in a greater than three-fold increase in luciferase expression from VVL15 at 4 hours post-infection and greater than two-fold increase at 24 hours post-infection. By 48 hours post-infection this finding had diminished and there was no significant difference between MiaPaca2-VEGF-165 and MiaPaca2-Vector Control (Figure 4.7).

These findings suggest that VEGF has a positive effect on the Vaccinia virus life cycle and that the mechanism operates early in the process of infection. However it is possible that VEGF may mediate effects at multiple points in the viral life cycle.

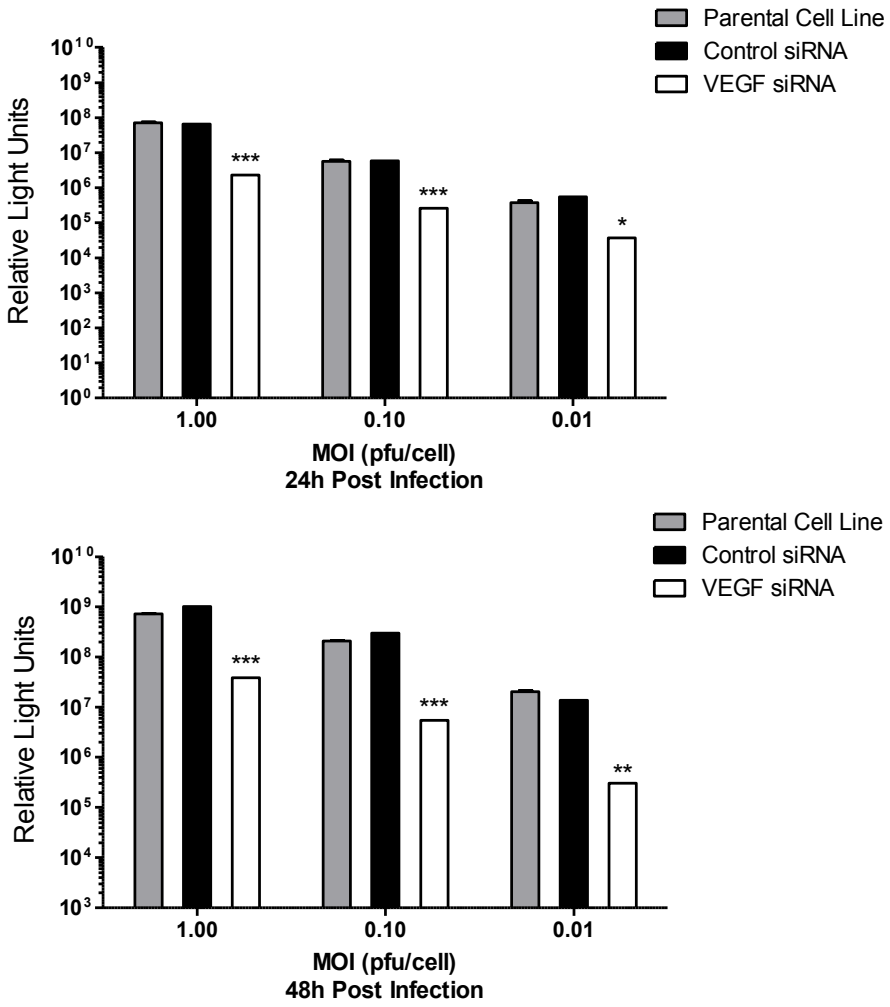

Figure 4.5. The effect of VEGFA silencing on expression of the firefly luciferase reporter gene from VVL15.

Suit2 cells were seeded in a 24 well plate. Cells were transfected with siRNA 24 hours later and then infected 72 hours after this with VVL15 at an MOI = 1, 0.1 or 0.01 or mock infected. Cells were lysed in the well and the substrate D-Luciferin was added. Plates were then imaged immediately using the IVIS imager and the baseline bioluminescence from mock infected cells was subtracted from infected wells. Cells were imaged at 24 and 48 hours post-infection. Experiments were performed in triplicate and results represent the data from two separate experiments. Results are presented as mean ± SEM. *** = $P \leq 0.001$, ** =

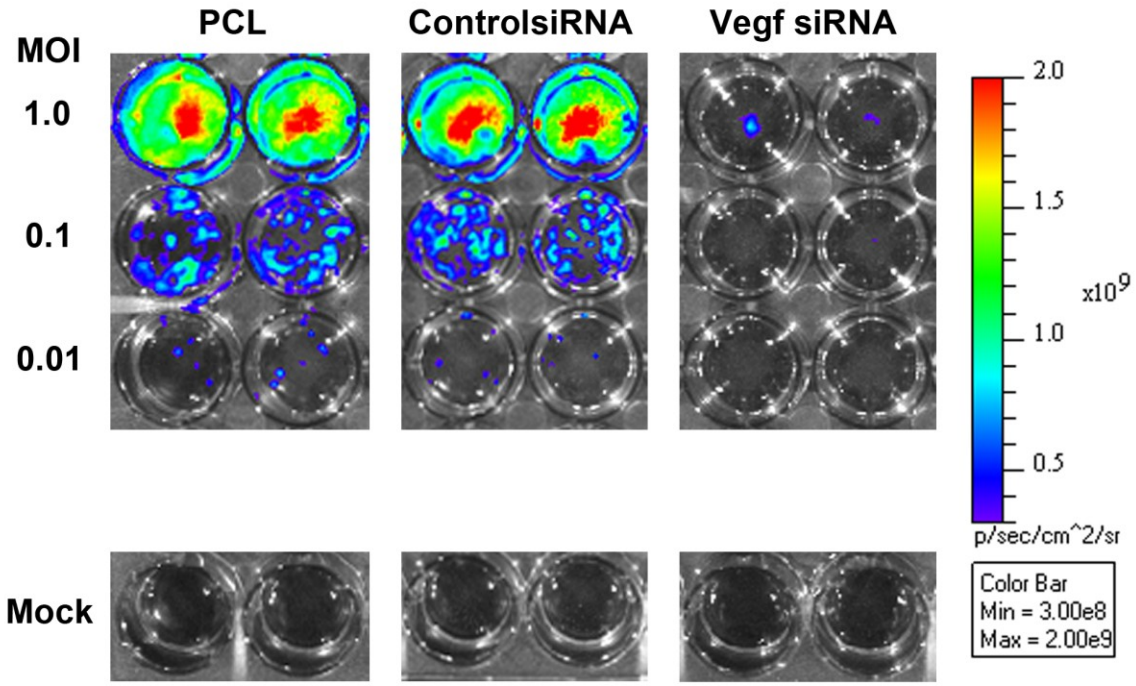

Figure 4.6: A representative image of the effect of VEGFA silencing on expression of the firefly luciferase reporter gene from VVL15.

Suit2 cells were seeded in a 24 well plate. Cells were transfected with siRNA 24 hours later and then infected 72 hours after this with VVL15 at an MOI = 1, 0.1 or 0.01 or mock infected. Cells were lysed in the well and the substrate D-Luciferin was added. Plates were then imaged immediately using the IVIS imager and the baseline bioluminescence from mock-infected cells was subtracted from infected wells. Cells were imaged at 48 hours post-infection. The same colorimetric scale was used for all images. PCL = parental cell line, Mock = mock-transfected.

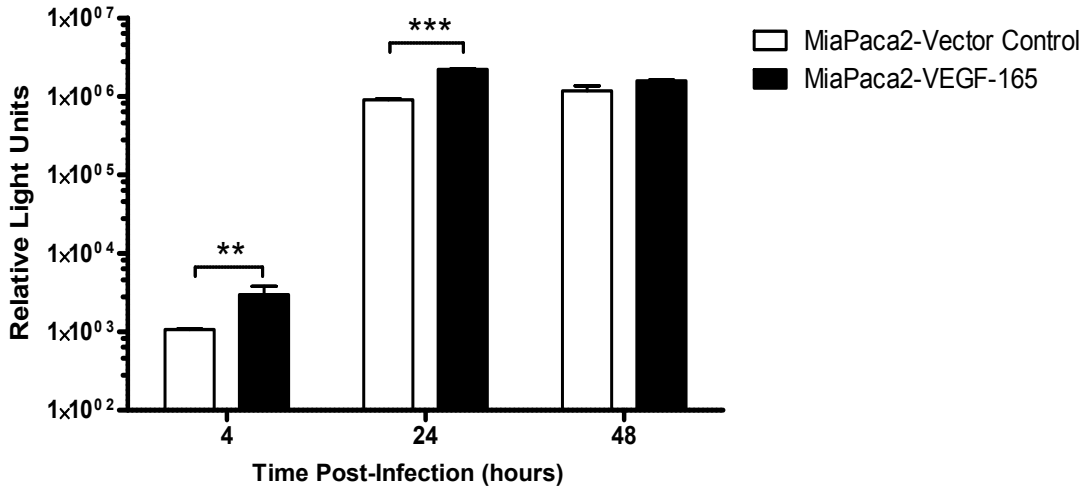

Figure 4.7: The effect of VEGF overexpression on the expression of the firefly luciferase reporter gene from VVL15.

MiaPaca2-VEGF-165 and MiaPaca2-Vector Control were seeded in a 24 well plate. Cells were infected 24 hours later with VVL15 at an MOI = 1 or mock infected. Cells were lysed in the well and the substrate D-Luciferin was added. Plates were then imaged immediately using the IVIS imager and the baseline bioluminescence from mock infected cells was subtracted from infected wells. Cells were imaged at 4, 24 and 48 hours post-infection. Experiments were performed in triplicate and results represent the data from two separate

4.4 The effect of VEGF expression on Vaccinia virus replication

We have determined that VEGF has a positive effect on luciferase expression from VVL15, but it is unclear whether this translates into an increase in production of infective virions. The effect of VEGF expression on wildtype Lister strain Vaccinia virus was investigated using the Suit2 and MiaPaca2 cell models. Suit2 cells were seeded in six well plates and allowed to adhere overnight. They were then transfected with VEGFA siRNA or Control siRNA and infected 72 hours after this with VVLister at an MOI=1 pfu/cell. Cells and supernatant were collected at 24, 48, 72 and 96 hours post-infection. CV1 green monkey kidney cells were used as indicator cells and infected with collected lysates in a TCID50 assay. There was a statistically significant reduction in infective virions produced in Suit2 cells after VEGF gene silencing at 48, 72 and 96 hours post-infection (Figure 4.8). A small amount of supernatant was also collected from all cells for a VEGF ELISA to verify that VEGF gene silencing was not lost towards the latter time points of the viral replication assay. Although there is a re-emergence of VEGFA secretion at 96 hours post-infection in the VEGF siRNA-treated Suit2 cells a large differential between Control siRNA and VEGF siRNA treated cells persists for the duration of the experiment (Figure 4.9).

MiaPaca2-VEGF-165 and MiaPaca2-Vector Control were also used to test the effect of VEGF overexpression on the replication of wildtype Lister strain Vaccinia virus. Cells were seeded in 6 well plates, allowed to adhere overnight then infected with VVLister at an MOI=1pfu/cell. Lysates were collected at 24, 48, 72 and 96 hours post-infection and CV1 cells used as indicator cells to determine a viral titre using a TCID50 assay. A statistically significant increase in viral replication was seen in MiaPaca2-VEGF-165 versus MiaPaca2-Vector Control at 48 and 72 hours post-infection (Figure 4.10). This difference was lost at 96 hours post-infection, similar to the loss of a statistically significant difference in gene expression at later time points in this model using VVL15. A small amount of supernatant was also used to verify persistent overexpression of VEGF during the viral replication assay and MiaPaca2-VEGF-165 produced 40-50% more VEGFA throughout the experiment (

Figure 4.11).

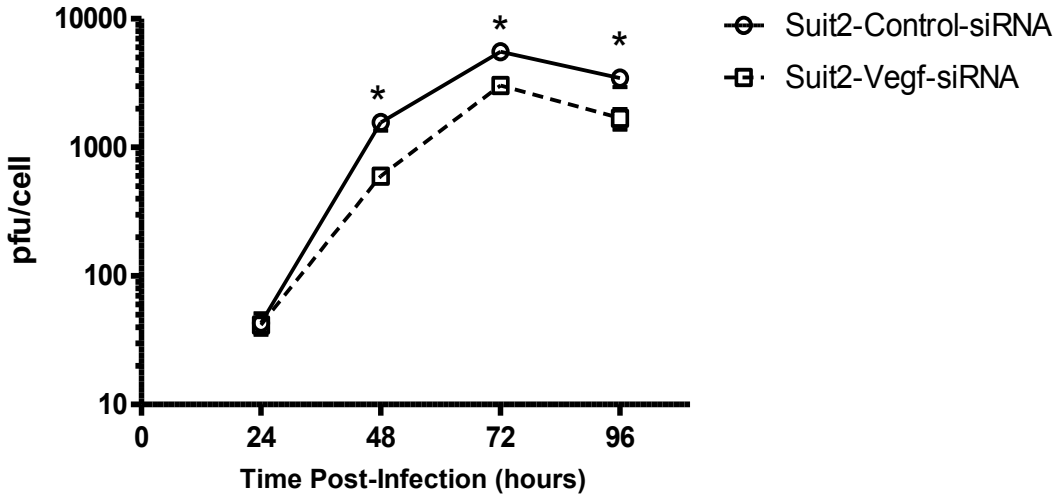

Figure 4.8: The effect of VEGFA gene silencing on VVLister replication.

Viral replication of VVLister in Suit2 cell line transfected with VEGFA siRNA (dashed line) or siGENOME RISC-free control siRNA (solid line) measured by TCID50 (50% tissue culture infective dose) assay of viral burst assays. Cell lines were infected with a multiplicity of infection (MOI) 1 of VVLister and burst assay samples were collected at 24, 48, 72 and 96 hours post-infection. TCID50 assays were performed on CV1 green monkey kidney cells. Experiments were performed in triplicate for each cell line, time point and condition. Results are presented as mean ± SEM. * = $P \leq 0.05$.

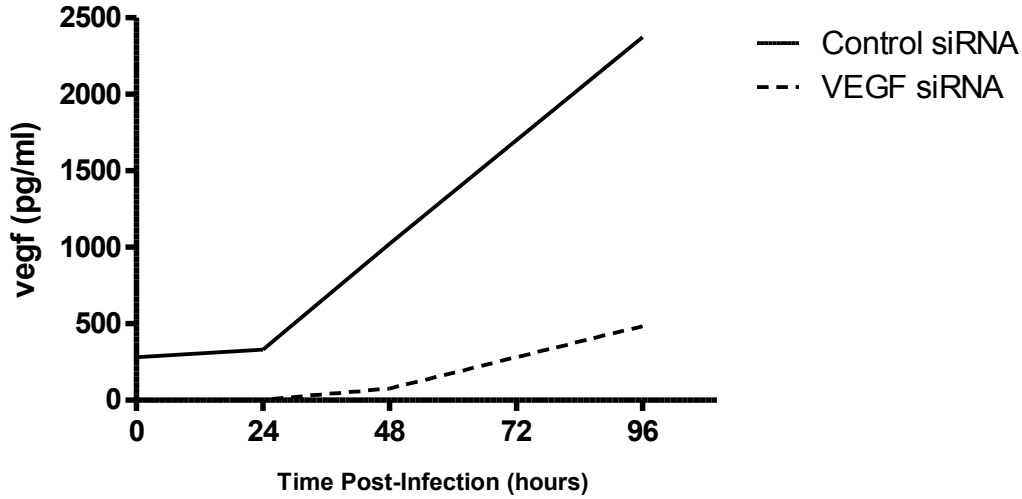

Figure 4.9: Confirmation of VEGFA silencing in Suit2 cell line during viral replication assay.

A sample of supernatant (50 µL) was taken from each viral burst assay before infection and then at 24, 48 and 96 hours post-infection. A VEGFA specific ELISA was used to quantify VEGF levels in the supernatant to ensure VEGF silencing had not been lost at later time points. Mean values are presented and experiments were performed in duplicate.

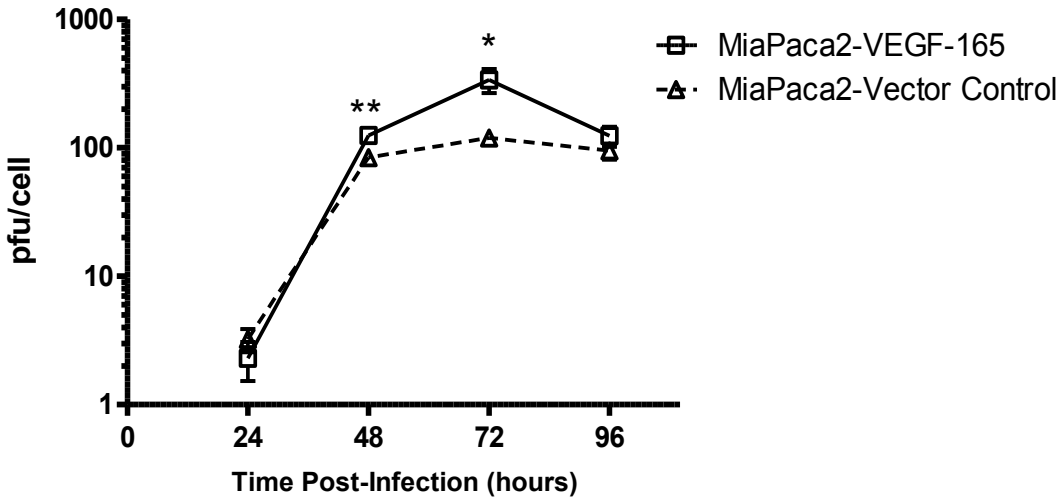

Figure 4.10: The effect of VEGFA over-expression on VVLister replication.

Viral replication of VVLister (Lister vaccine strain of Vaccinia virus) in MiaPaca2-VEGF-165 (solid line) and MiPaca2-Vector Control (dashed line) cells as measured by TCID50 assay of viral burst assays. Cell lines were infected with an MOI = 1 of VVLister and burst assay samples were collected at 24, 48, 72 and 96 hours post-infection. TCID50 assays were performed on CV1 green monkey kidney cells. Experiments were performed in triplicate for each cell line, time point and condition. Results are presented as mean ± SEM. ** = $P \leq 0.01$, * = $P \leq 0.05$.

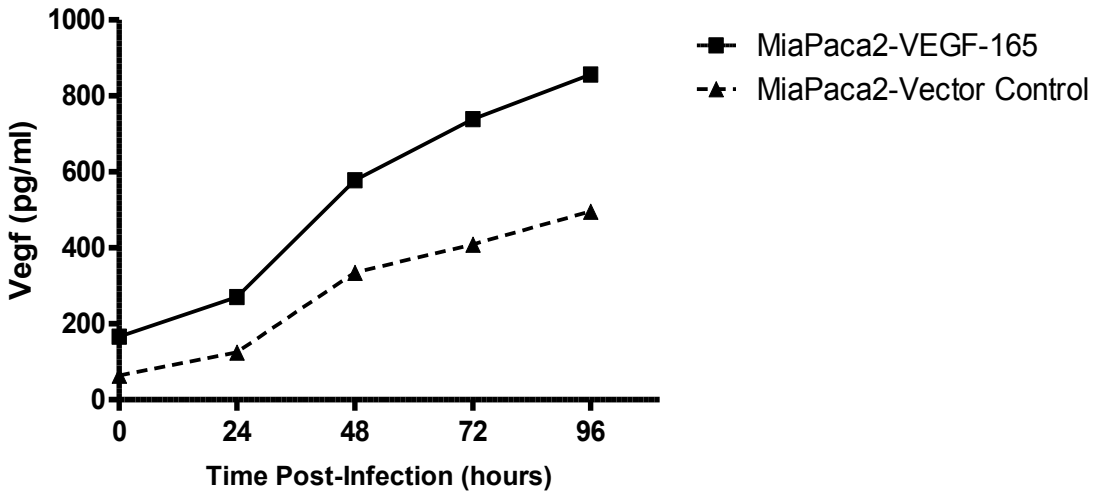

Figure 4.11: Confirmation of VEGFA expression in MiaPAca2-VEGF-165 and MiaPaca2-Vector Control cell lines during viral replication assay.

A sample of supernatant (50 μL) was taken from each viral burst assay before infection and then at 24, 48 and 96 hours post-infection. A VEGFA specific ELISA was then used to quantify VEGF levels in the supernatant. Mean values are presented and experiments were performed in

4.5 The effect of VEGF on Vaccinia virus cytotoxicity in PDAC

The presence of VEGF increases viral transgene expression and the production of infectious virions. The next question addressed was whether VEGF could affect the oncolytic ability of Vaccinia virus. MiaPaca2-VEGF-165 and MiaPaca2-Vector control cells were seeded in 96 well plates and infected with serial dilutions of wildtype Lister strain virus. An MTS assay was performed at 6 days post-infection to determine the percentage of viable cells remaining and a dose response curve was drawn in order to calculate an EC50 value (Figure 4. 12-A&B). The dose-response curve represents a composite of all experiments where as an EC50 value was calculated for each assay plate and the mean EC50 values for VVLister in MiaPaca2-VEGF-165 and MiaPaca2-Vector Control cells compared. A highly statistically significant reduction in the EC50 value, therefore increase in viral cytotoxicity, was seen for MiaPaca-VEGF-165 compared to MiaPaca2-Vector Control (26.5 vs. 122.4 pfu/cell, $P<0.0001$).

As CFPac1 cells showed a significant increase in viral cytotoxicity in hypoxia, recombinant human VEGF (rhVEGFA) was used to stimulate CFPac1 cells and see if any effect was seen on viral cytotoxicity. Cells were seeded in a 96 well plate format, stimulated with rhVEGFA and infected with serial dilutions of VVLister. A dose of 2 ng/mL was selected as this was the level of VEGFA found in other pancreatic cancer cell lines and therefore deemed to be an appropriate concentration (Figure 4.1). An MTS assay was performed 6 days after viral infection and a statistically significant increase in viral cytotoxicity was found in CFPac1 cells treated with rhVEGF versus untreated cells with EC50 values of 0.13 and 0.26 pfu/cell respectively ($P <0.001$) (Figure 4.13).

A 96 well plate format was more difficult to use with the Suit2 VEGF gene silencing cell model and results were not reproducible. Instead cells were seeded in 24 well plates and an MTS assay used to determine the percentage of cells killed at 3 days post-infection (Figure 4.15). A small

but statistically significant increase in the EC50 value was found in VEGF siRNA treated cells versus control siRNA treated cells (2.19 pfu/cell vs. 1.79 pfu/cell respectively).

These data show that modulating VEGF levels prior to viral infection using overexpression, siRNA knockdown or addition of recombinant human VEGF affects viral potency and that increased cytotoxicity is associated with increased VEGF.

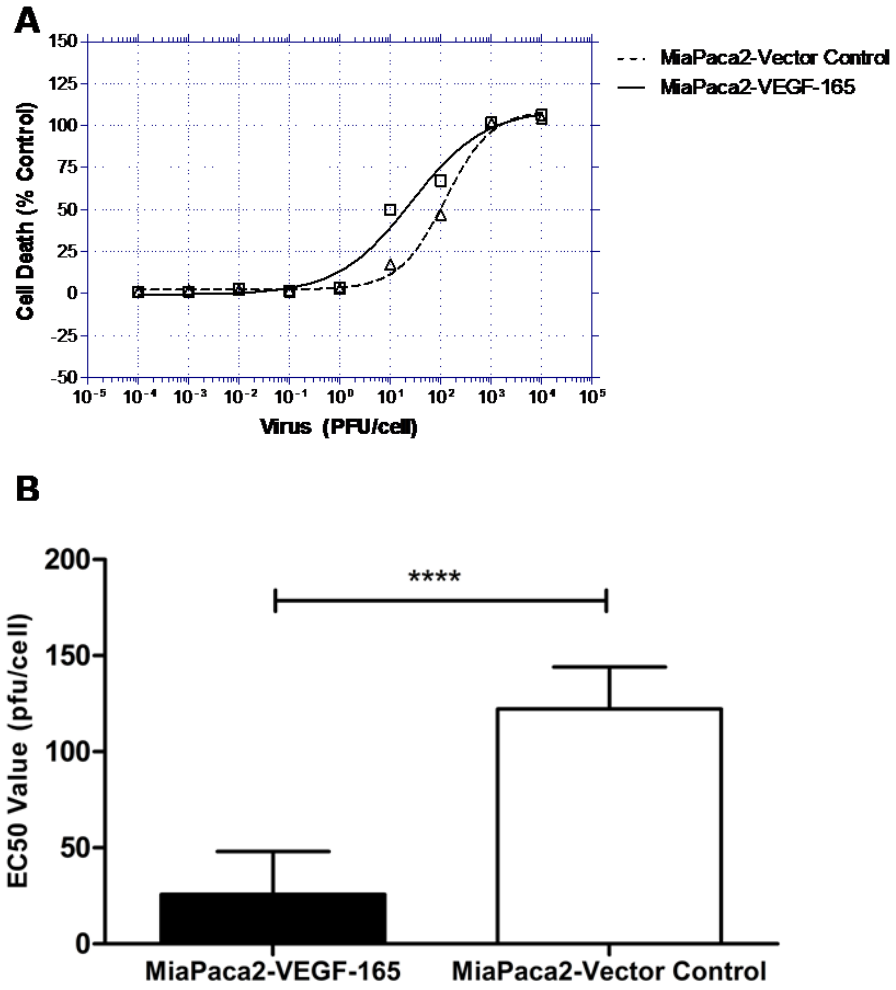

Figure 4. 12 : Effect of VEGF on the cytotoxicity of VVLister.

MiaPaca2-VEGF-165 and MiaPaca2-Vector Control cells were infected with serial dilutions of VVLister. The infected cells were assayed with MTS reagent at day 6 post-infection at 37 °C with 5% CO_2 for 2 hours. Viable cells were determined as a percentage of the uninfected controls and non-linear regression analysis was used to draw dose–response curves (A) and determine the EC50 value (B). Each plate contained six replicates, each assay used two 96 well plates. Each assay was repeated four times making a total of eight 96 well plates. For clarity the dose response curve shown is calculated from a combination of all the 48 replicates. The EC50 value is presented as the geometric mean of the eight plates with the 95% confidence interval**.** An unpaired students T-test was performed to compare geometric means **** = $P \leq 0.0001$.

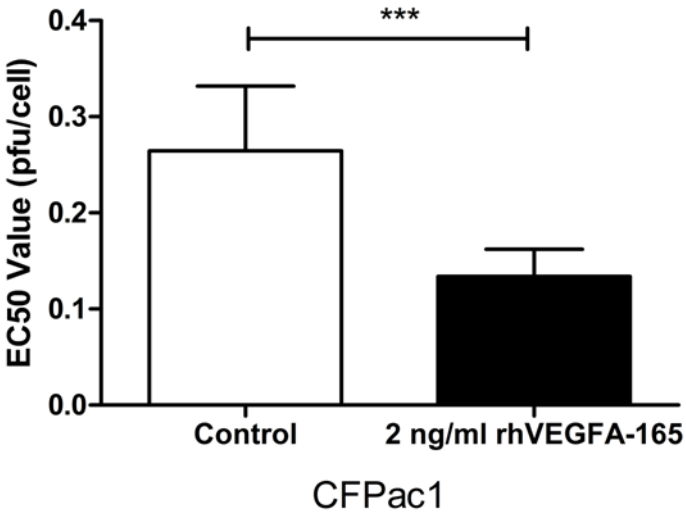

Figure 4.13 : The effect of rhVEGF on the cytotoxicity of VVLister in CFPac1 cells. Cells were stimulated with 2 ng/mL of rhVEGFA-165 for 5 minutes prior to infection with VVLister. An MTS assay was then used to assess cell viability at 72 hours post-infection. Viable cells were determined as a percentage of the uninfected controls and non-linear regression analysis was used to draw dose–response curves and determine the EC50 value. Each plate contained six replicates, each assay used two 96 well plates. Each assay was repeated twice making a total of 24 replicates. The EC50 value is presented as the geometric mean of the four plates with the 95% confidence interval**.** An unpaired students T-test was performed to compare geometric means *** = $P \leq 0.001$.

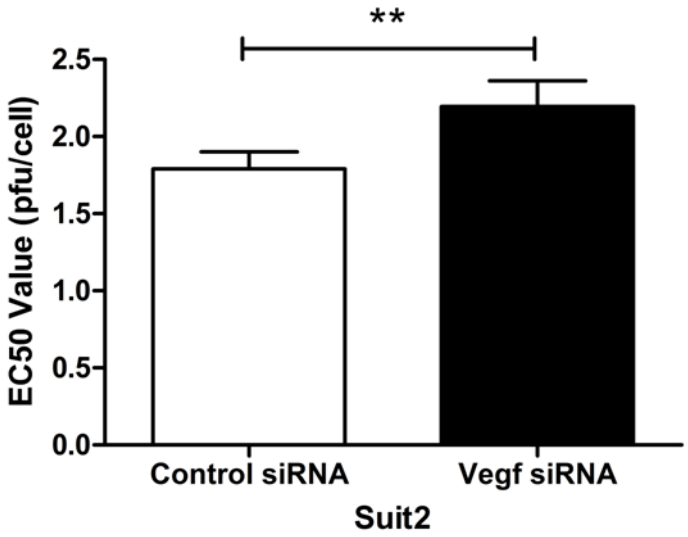

Figure 4.14: The effect of VEGF silencing on the cytotoxicity of VVLister.

Suit2 cells were seeded in 24 well plates and transfected with VEGF siRNA or siGENOME RISC free control siRNA. Cells were infected with VVLister at 72hours after siRNA transfection. The infected cells were assayed with MTS reagent at day 3 post-infection at 37 °C with 5% CO_2 for 1 hour. Viable cells were determined as a percentage of the uninfected controls and non-linear regression analysis was used to draw dose–response curves and determine the EC50 value. Each plate contained three replicates, each assay used two 24 well plates. Each assay was repeated twice making a total of 12 replicates. The EC50 value is presented as the geometric mean of the four plates with the 95% confidence interval**.** An Mann-Whitney U Test was performed to compare geometric means as results were not normally distributed ** = $P \leq 0.01$.

4.6 The effect of VEGF on viral replication in Normal Human Bronchial Epithelial cells.

Pox viruses are known to enter via the respiratory epithelium and it has been shown that EGF maintains epithelial integrity to allow viral replication in this context (139). Since it has been published that respiratory epithelium expresses VEGF and its receptors we were interested to determine whether exogenous VEGF could increase the susceptibility of cells to wildtype Vaccinia virus infection (192-194). Normal human bronchial epithelial (NHBE) cells were seeded in growth media without bovine pituitary extract which might potentially contain VEGF.

Viral replication in NHBE cells was performed using BEGM (without BPE and hEGF) or BEGM (without BPE and hEGF) supplemented with 10 ng/mL of rhVEGF (Peprotec, London, UK). Cells were infected with Lister strain Vaccinia virus at an MOI of 0.1 pfu/mL 10 minutes after the addition of rhVEGF. Collection and processing of samples was then performed as for other viral burst assays.

Significantly higher levels of viral replication were seen at 72 hours in the NHBE cells infected in the presence of rhVEGF (Figure 4.15). Although results were not as marked compared to the effect seen in PDAC cells, this suggests that VEGF may play a more fundamental role in Vaccinia virus infection and is not restricted to the infection of transformed cell lines.

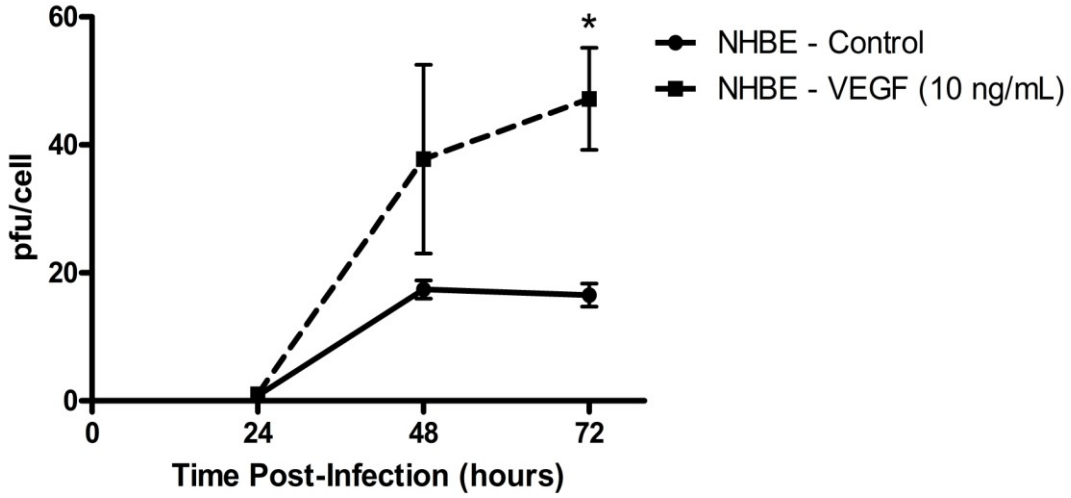

Figure 4.15: The effect of VEGF on the replication of VVLister in normal human bronchial epithelial (NHBE) cells as measured by TCID50 assay of viral burst assays.

Cells were seeded in growth mediator without growth factors and were then stimulated with 10 ng/mL of rhVEGFA-165 for 5 minutes prior to infection with VVLister. NHBE cells were infected with an MOI = 0.1 pfu/cell. Burst assay samples were collected at 24, 48 and 72 h post-infection. TCID50 assays were performed on CV1 green monkey kidney cells. Experiments were performed in triplicate for each cell line, time point and condition. Results are presented as mean ± SEM. * = $P \leq 0.05$.

4.7 Characterization of proteases to cleave bound Vaccinia virus from infected cells using Real-Time Quantitative PCR

The life cycle of Vaccinia virus begins with attachment to the cell membrane via an uncharacterized receptor followed by internalisation of the infectious viral particle. Attachment to the cell membrane is considered to be a passive process which can occur at 4 °C whereas internalisation is an active process requiring ATP and the co-ordination of complex actin dynamics occurring at 37 °C (121). DNA can be extracted from cells, after infection at 4 °C or after allowing internalisation to occur at 37 °C and the amount of viral DNA can be quantified as a surrogate for viral infection at these time points. However, in order to provide accurate results after returning cells to 37 °C for viral internalisation any virus particles which have not been internalised at the relevant time point need to be cleaved from the cell membrane so that only truly internalised particles are included for qPCR analysis. In a previous study using the International Health Department-J strain (IHD-J) of Vaccinia virus it has been demonstrated that trypsin is unable to cleave bound virus from infected cells where as pronase treatment was able to cleave 92% and 97% of bound IMV from rabbit kidney (RK_{13}) and HeLa cells respectively (128). Subtilisin has been used to cleave adenovirus from infected cells (195) but no data exist for the Lister strain Vaccinia virus. Consequently it was necessary to identify a suitable protease that could be used in subsequent internalisation assays to cleave and remove attached but un-internalised virus.

CV1 cells were infected with VVLister at an MOI = 30 pfu/cell at 4 °C for 1 hour after which unattached virus was removed by washing. At this point DNA was either extracted for assessment of internalisation or cells were treated with pronase (0.5, 1.0, 1.5 mg/mL), Subtilisin (2 mg/mL) or trypsin (0.5%) for 30 minutes at 4 °C and DNA extracted for qPCR to quantify the efficacy of these proteases at removing bound virions from infected cells. The Vaccinia late transcription factor 1 (VLTF-1) primer and probe set used and are shown in Table 4.2. As found in previous studies, trypsin does not cleave attached virus from infected cells (

Figure 4.16). Higher concentrations of trypsin were not used as this was the maximum that could be used without detaching cells during treatment. Both subtilisin and pronase are effective and are capable of removing 75% of bound virus after 30 minutes of treatment at the optimum concentrations. The remaining 25% may represent a proportion of virus that binds to cells in an alternative manner or could be removed if a more efficient protease was available. Although these results were not as impressive as published using the IHD-J they were considered sufficient for subsequent viral internalisations assays and a concentration of 1 mg/mL of pronase was used in all subsequent assays.

Table 4.2: Primers and probes used for qPCR, S = sense; AS = antisense. Vaccinia virus strain, Lister clone VACV107, complete genome (GenBank: DQ1211394.1) VLTF-1 Primers and probe =112800-112872 bp.

Gene	Primer or Probe	Sequence
VVLister VLTF-1	Probe (FAM)	ATTTTAGAACAGAAATACCC
	Primers	S 5'-AACCATAGAAGCCAACGAATCC AS 5'-TGAGACATACAAGGGTGGTGAAGT

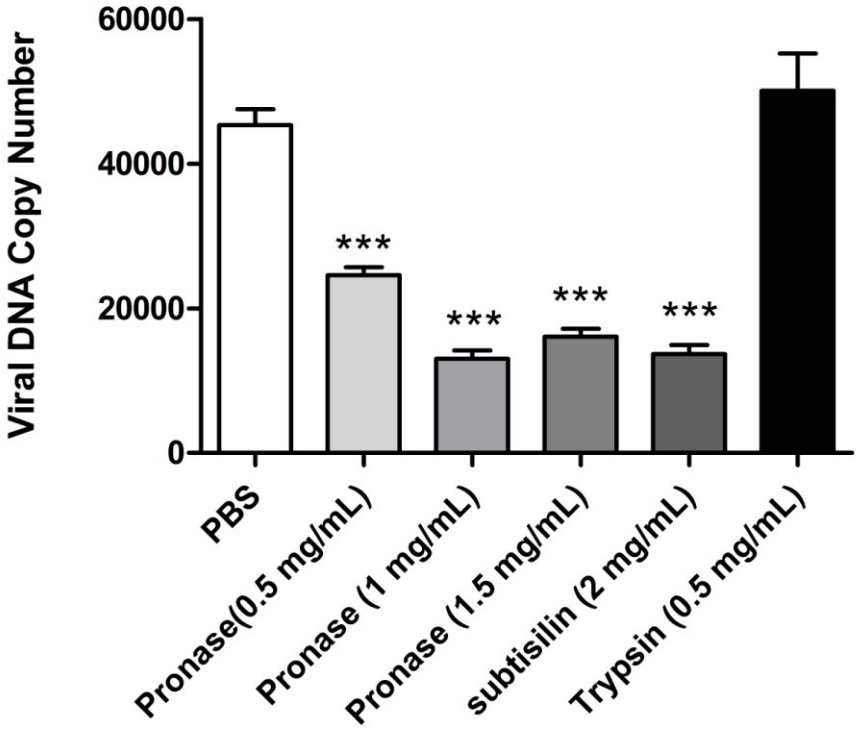

Figure 4.16: Comparison of proteases used to cleave virus attached to cells at 4°C.

CV1 cells were placed on ice and infected with VVLister at an MOI = 30 pfu/cell. Unattached virus was then removed and cells exposed to the relevant proteases for 30 minutes on ice. DNA was then extracted and 40 ng was used for qPCR using the VLTF-1 primer & probe set. Experiments were performed in biological duplicates and qPCR in triplicates. Results are presented as mean DNA copy number ± SEM. *** = $P \leq 0.001$.

4.8 The effect of VEGF on viral attachment and internalisation measured using Real-Time Quantitative PCR

To assess if VEGF has any effect on attachment or internalisation of Vaccinia virus a quantitative PCR assay was used to measure the proportion of viral DNA present in extracts from infected cells. MiaPaca2-VEGF-165 and MiaPaca2-Vector Control cells were infected with VVLister at an MOI = 10 pfu/cell for one hour at 4 °C. Cells were washed to remove uninternalised virus and DNA extracted immediately or cells returned to 37 °C for 5, 15 or 30 minutes. Cells were then treated with pronase to remove un-internalised virus and DNA extracted. As seen in Figure 4.17 there is no significant difference in the attachment of Vaccinia virus in the presence of VEGF. However after allowing internalisation to resume there is a highly significant increase in viral internalisation in the MiaPaca2-VEGF-165 versus MiaPaca2-Vector Control at 15 minutes ($P = 0.0032$) and 30 minutes ($P < 0.0001$). Suit2 cells were also used to investigate the effect of VEGF gene silencing on VVLister internalisation. Cells were infected with VVLister at 72 hours after siRNA treatment and virus was allowed to internalise for 30 minutes before pronase treatment and DNA extraction. There was a significant decrease in viral internalisation in the VEGF siRNA-treated Suit2 cells *versus* control siRNA treated cells ($P = 0.0027$) as shown in Figure 4.18.

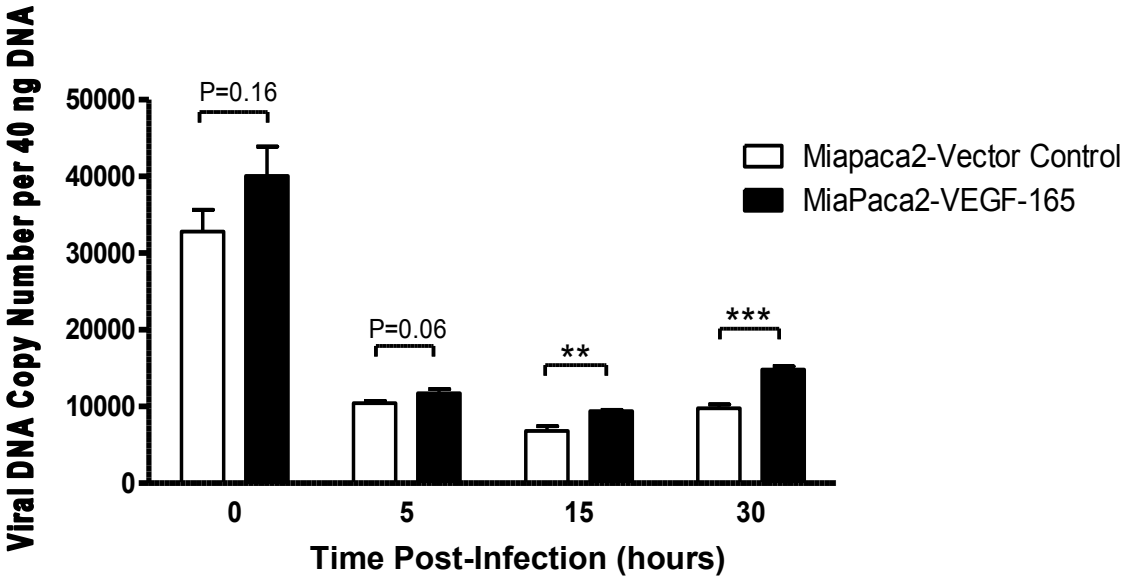

Figure 4.17: The effect of VEGF over expression on Vaccinia virus attachment and internalisation as measured by quantitative PCR.

MiaPaca2-VEGF-165 and MiaPaca2-Vector Control cells were infected with Vaccinia virus at an MOI of 10 pfu/cell for 1 hour at 4°C. Cells were washed and then DNA extracted for attachment analysis or treated with pronase (1 mg/mL) for 30 minutes at 4°C DNA and then warmed to 37 °C. Cellular and viral DNA was then extracted 5, 15 and 30 minutes later to assess viral internalisation. Quantitative real-time PCR was then used to determine the genome copy number using the VLTF-1 primer and probe set. Experiments were performed in triplicate for each time point and results are the combination of two experiments. Results are presented as mean ± SEM. *** = $P \leq 0.001$, ** = $P \leq 0.01$.

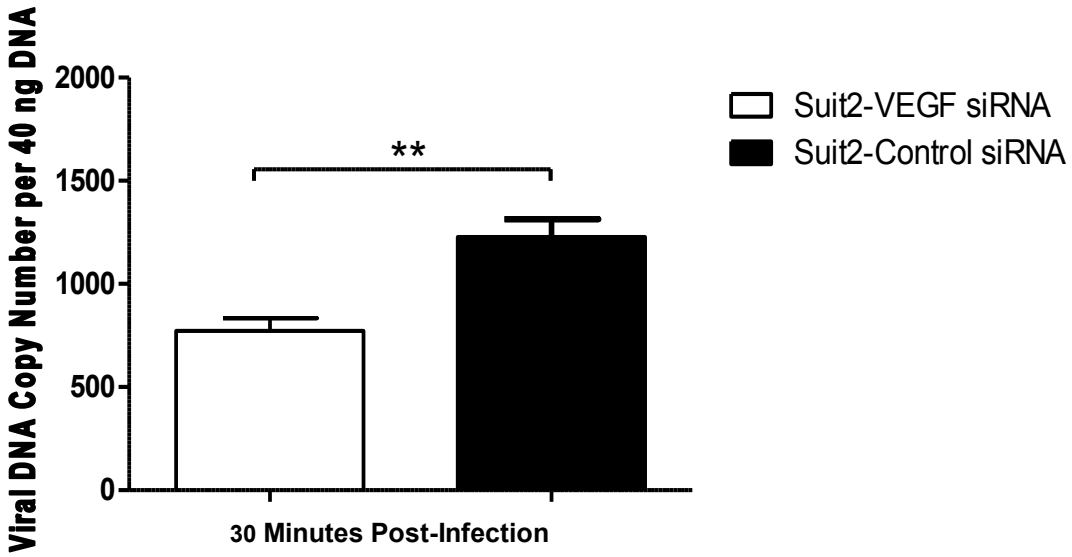

Figure 4.18: The effect of VEGF gene silencing on Vaccinia virus internalisation as measured by quantitative PCR.

Suit2 cells were transfected with VEGF siRNA or Control siRNA and then 72 hours later infected with Vaccinia virus at an MOI of 10 pfu/cell for 1 hour at 4 °C. Cells were washed and treated with pronase (1 mg/mL) for 30 minutes at 4 °C and then warmed to 37 °C. Cellular and viral DNA was then extracted 30 minutes later to assess viral internalisation. Quantitative real-time PCR was then used to determine the genome copy number using the VLTF-1 primer and probe set. Experiments were performed in triplicate for each time point and results are the combination of two experiments. Results are presented as mean ± SEM. ** = $P \leq 0.01$.

4.9 Development of fluorescently labelled Vaccinia virus VVL-488

In order to confirm, using an alternative technique, that viral internalisation was affected by VEGF we first made a fluorescently labelled Vaccinia virus to investigate attachment and internalisation of viral particles. To directly visualise the process of viral infection wildtype Lister strain virus was coated with Alexa Fluor® 488 (Invitrogen, USA) 5-sulphodicholorphenol ester which links the fluorescent marker to viral coat proteins. To verify the specificity and sensitivity of this technique CV1 cells were seeded onto a transwell on a microscope slide and infected with the Alexa Fluor labelled wild type Vaccinia virus (VVL-488) or mock-infected as shown in Figure 4.19-A and C. Samples were then fixed and probed with anti-Vaccinia polyclonal antibody or its isotype control as shown in Figure 4.19-A/C and B. The images show efficient labelling of Vaccinia virus with Alexa Fluor-488 (green) and this appears to be specific as these foci co-localise with staining for anti-Vaccinia antibody (red) although not all infective virions that are detected with anti-Vaccinia antibody were labelled with Alexa Fluor-488. In addition the foci VVL-488 vary markedly in size. As these are all labelled specifically with anti-Vaccinia virus antibody, it appears likely that our virus preparation produces individual infective virions but also virions grouped in clumps perhaps due to incomplete disruption of host cell membranes during virus production. However, this difference in size does not seem to affect virus attachment in these or subsequent images.

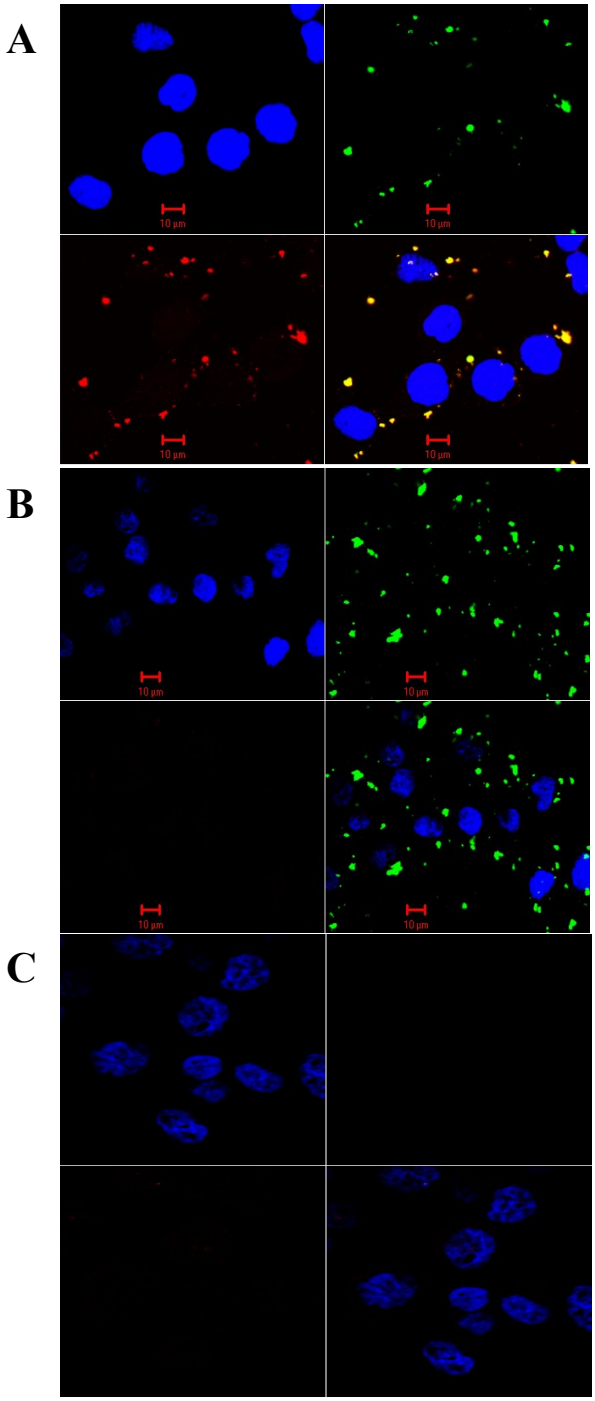

Figure 4.19: Validation of labelling of wild type lister strain virus with Alexa Fluor-488.

Split channels images: Top left=Dapi, Top right=488, Bottom left=546, Bottom right=combined image. Panel A - Split channel image of CV1 cells infected with VVL-488 (green) and stained with Vaccinia virus polyclonal rabbit IgG (red) and nuclear stain DAPI (blue). Panel B – Split channel image of CV1 cells infected with VVL-488 (green) and isotype control RbIgG (red). Panel C – Split channel image of mock-infected CVI cells counterstained with Vaccinia virus polyclonal rabbit (red). Images were taken at 64x magnification with Zeiss LSM 510 META laser scanning microscope.

4.9.1 The effect of VEGF on attachment and internalisation of VVL-488 assessed using confocal fluorescent microscopy

In order to assess visually if VEGF facilitates Vaccinia virus internalisation, the fluorescently labelled VVL-488 was used to infect Suit2 cells transfected with VEGF siRNA or Control siRNA. After returning cells to 37 °C previous experiments had indicated that 30 minutes was required before a difference was seen in viral internalisation, therefore images were taken at 30 minutes. Suit2 cells were seeded into chamber microscope slides and later transfected with control or VEGF specific siRNA. Three days after siRNA transfection cells were infected with a 1:200 dilution of VVL-488. Chamber slides were warmed to 37 °C and then fixed at 30 minutes post-infection for confocal microscopy. Images of VEGF siRNA treated cells (Figure 4.20) and a representative Z-stack image (Figure 4.21) show reduced attachment and internalisation of viral particles compared to control siRNA treated cells (Figure 4.22 & Figure 4.24). Membrane fusion and macropinocytosis have both been implicated in the internalisation of Vaccinia virus and although it is not possible to determine which GFP foci represent intact virions and which are viral membranes fused with cellular membranes VEGF siRNA cells are clearly less infectable at this time point. Quantification of attachment and internalisation was performed despite this caveat. Z-stack 3D representations of 10 fields of view were taken for the VEGF siRNA and control siRNA treated Suit2 cells. A clearly isolated GFP foci was counted as one virion and small or large foci counted equally. Two independent observers, who were blinded to sample group, scored images at the time of viral attachment and 30 minutes after internalisation was allowed to proceed at 37 °C. There was no significant difference in viral attachment but there was a significant ($P = 0.023$) increase in mean number of viral particles per cell after 30 minutes at 37 °C (Figure 4.24). Taken together with the quantitative PCR data it is clear that VEGF facilitates Vaccinia virus entry in PDAC cell lines *in vitro*.

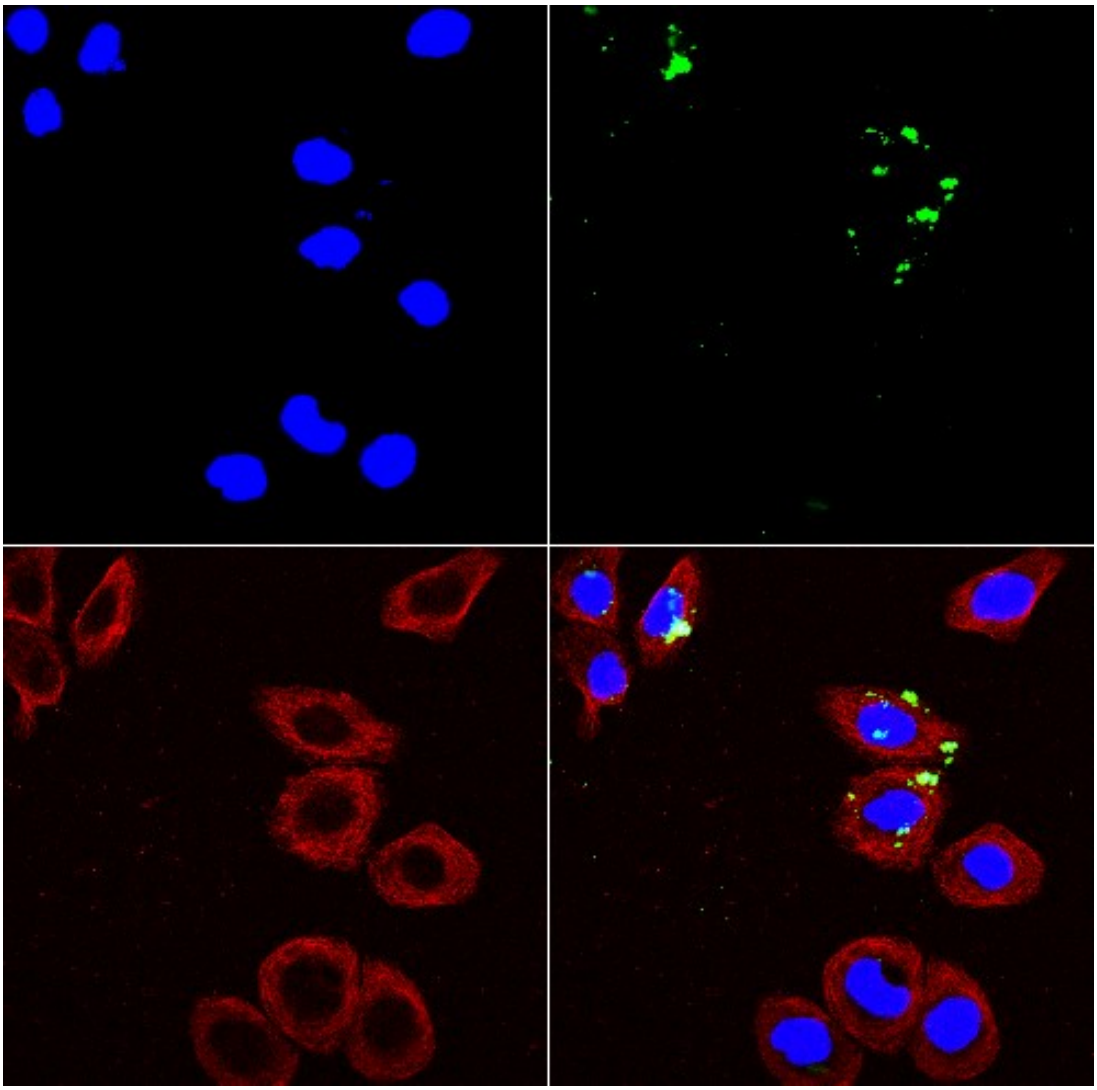

Figure 4.20: The effect of VEGF gene silencing on the internalisation of VV-488.

The Representative split channel image of Suit-2 cells transfected with VEGF siRNA and imaged at thirty minutes after warming of cells to 37 ºC to allow internalisation of viral particles. Nuclear material is stained blue with DAPI, alpha- tubulin (red) and VVL-488 (green). Images were taken at 64x magnification with a Zeiss LSM 510 META laser scanning microscope and displayed at a resolution of 1024 x 1024 dpi.

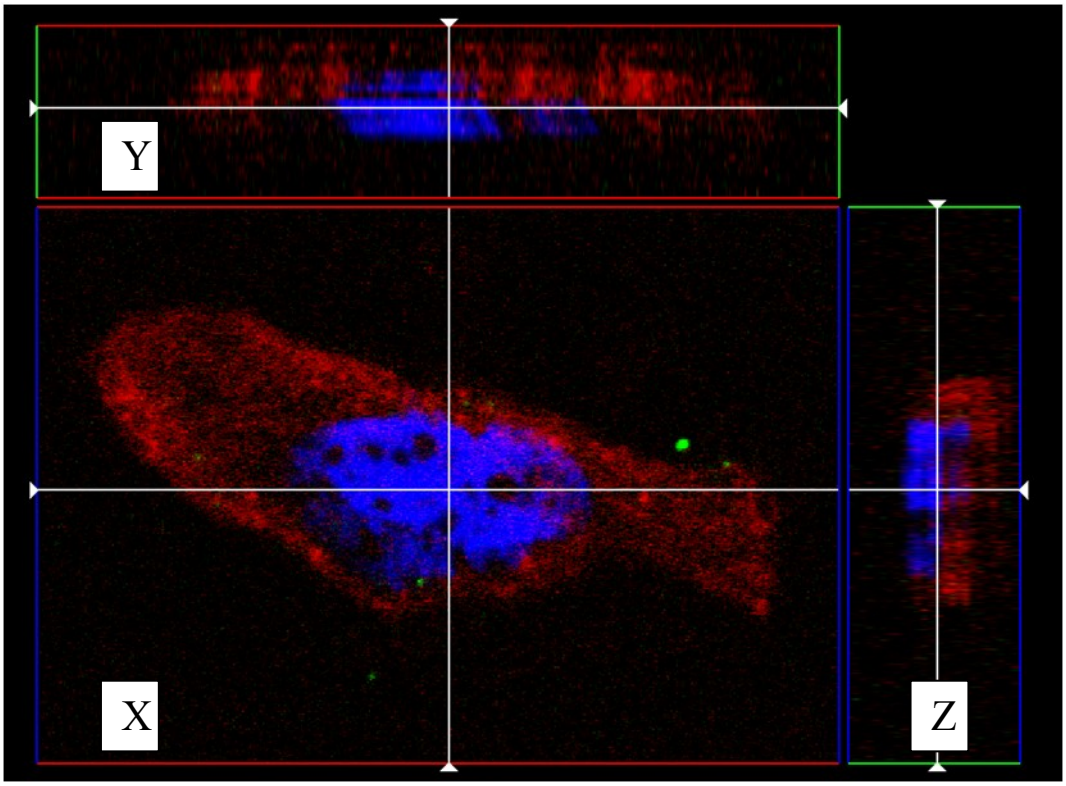

Figure 4.21: The effect of VEGF gene silencing on the internalisation of VV-488 (Z stack).

Representative Z stack image of Suit-2 cells transfected with VEGF siRNA and imaged at thirty minutes after warming of cells to 37 ºC to allow internalisation of viral particles. Nuclear material is stained blue with DAPI, alpha-tubulin (red) and VVL-488 (green). Images were taken at 100x magnification with a Zeiss LSM 510 META laser scanning microscope and displayed at a resolution of 1024 x 1024 dpi. Twenty-five images were taken to create each Z-stack. X, Y and Z dimensions are shown with viewpoint aligned through

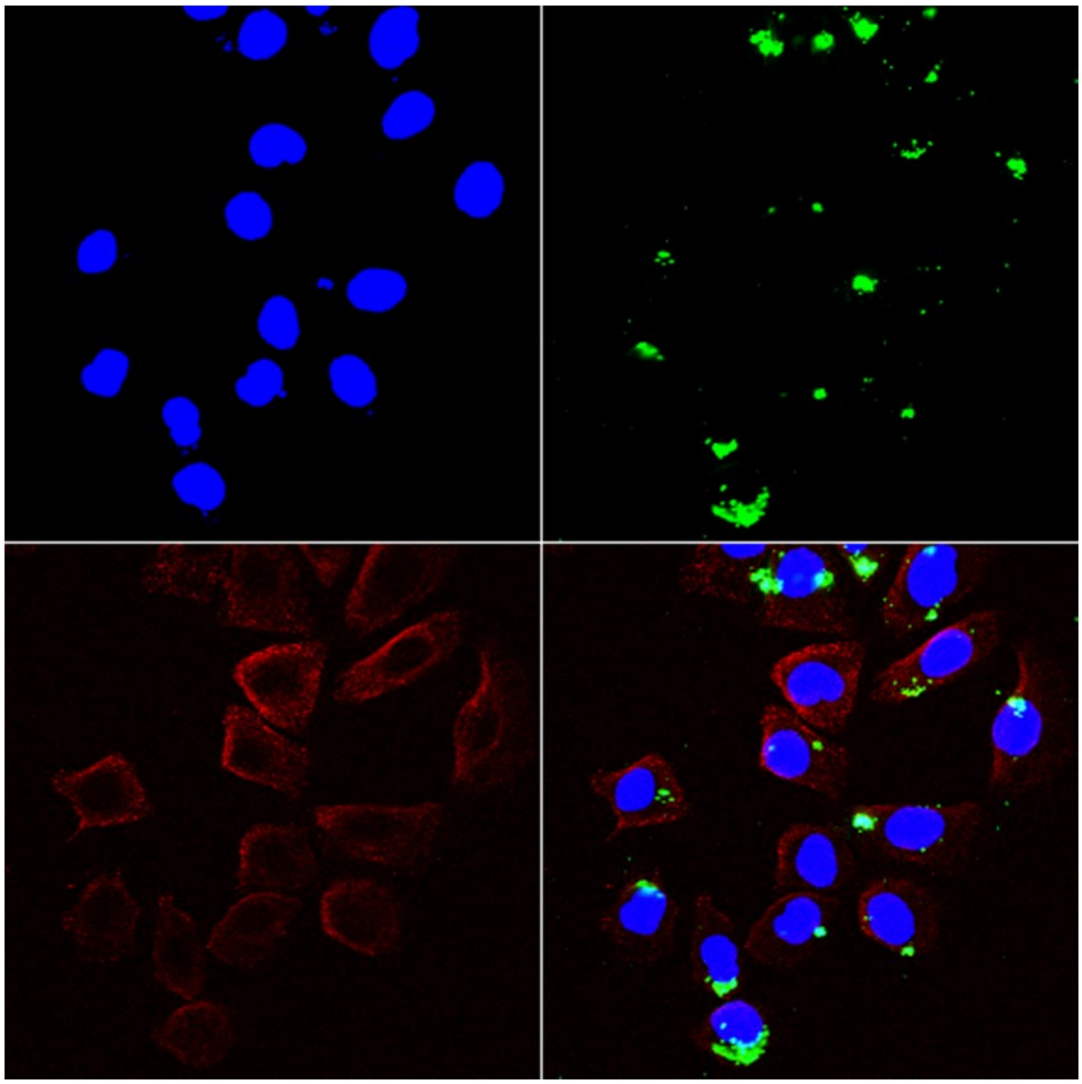

Figure 4.22: The effect of control siRNA on the internalisation of VV-488.

Representative split channel image of Suit-2 cells transfected with siGENOME RISC-free control siRNA and imaged at thirty minutes after warming of cells to 37 ºC to allow internalisation of viral particles. Nuclear material is stained blue with DAPI, alpha-tubulin (red) and VVL-488 (green). Images were taken at 64x magnification with a Zeiss LSM 510 META laser scanning microscope and displayed at a resolution of 1024 x 1024 dpi.

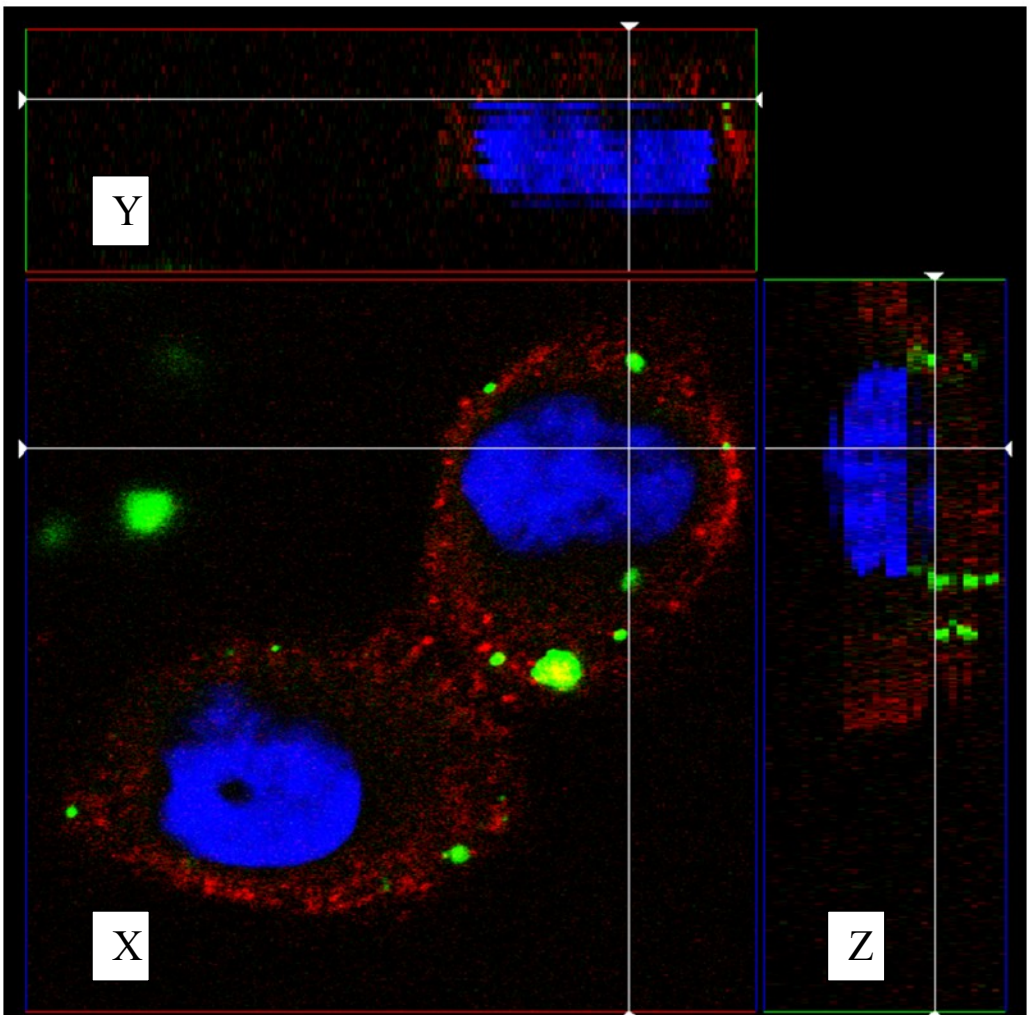

Figure 4.23: The effect of control siRNA on the internalisation of VV-488 (Z stack).

Representative Z stack image of Suit-2 cells transfected with Control siRNA and imaged at thirty minutes after warming of cells to 37 ºC to allow internalisation of viral particles. Nuclear material is stained blue with DAPI, alpha-tubulin (red) and VVL-488 (green). Images were taken at 100x magnification with a Zeiss LSM 510 META laser scanning microscope and displayed at a resolution of 1024 x 1024 dpi. Twenty-five images were taken to create each Z-stack. X, Y and Z dimensions are shown with viewpoint aligned through centre of cell as

Figure 4.24: Quantification of VVL-488 attachment & internalisation confocal images

Z-stack 3D representations of 10 fields of view were taken for the VEGF siRNA and control siRNA treated Suit2 cells. A clearly isolated GFP foci was counted as one virion and small or large foci counted equally. This was because we were not able to differentiate individual virions from those that could represent virion in complex with cellular membrane following viral preparation. Two independent observers, who were blinded to sample group, scored images at the time of viral attachment and at 30 minutes after internalisation was allowed to proceed at 37 °C. Images were taken at 64 x magnification with a Zeiss LSM 510 META laser scanning microscope and displayed at a resolution of 1024 x 1024 dpi for counting. * = $P \leq 0.05$ Two tailed students T-test.

4.10 The effect of VEGF on Vaccinia virus mRNA transcription

The next step in the Vaccinia life cycle is gene transcription, so to assess if VEGF can affect viral mRNA transcription we used a reverse transcription real-time quantitative PCR assay. MiaPaca2-VEGF-165 and MiaPaca2-Vector Control cells were infected for 1 hour with VVLister at an MOI = 10 pfu/cell. At 6 and 24 hours post-infection cells were harvested for RNA extraction. Quantitative PCR was then performed using the VLTF-1 primer and probe set (Table 4.2) and results were normalised to 18S RNA as detailed in the Material and Methods section of this thesis. The VTLF-1 primer and probe set were used firstly as no pre-transcribed early mRNA presents in viral particles would contaminate the assay and also as VTLF-1 mRNA would be transcribed only after the productions of early and intermediate mRNAs. This should give a picture more reflective of total viral mRNA transcription as opposed to early viral mRNA production.

A significant increase in mRNA production was noted in MiaPaca2-VEGF-165 compared to control at 6 hours after infection (Figure 4.25). However, given that VEGF facilitates Vaccinia virus internalisation in these cells a crude attempt was made to remove the effect of increased internalisation as a more rapid infection will undoubtedly result in greater mRNA transcription at early time points. The amount of mRNA present in MiaPaca2-VEGF-165 was normalised to the amount of virus internalised so that results were more comparable with MiaPaca2-Vector Control cells. When this was done there was no longer a significant affect of VEGF on viral mRNA transcription although a trend is present (Figure 4.26). On balance it is unlikely that VEGF has an effect of viral mRNA transcription other than accelerating the process by inducing earlier internalisation.

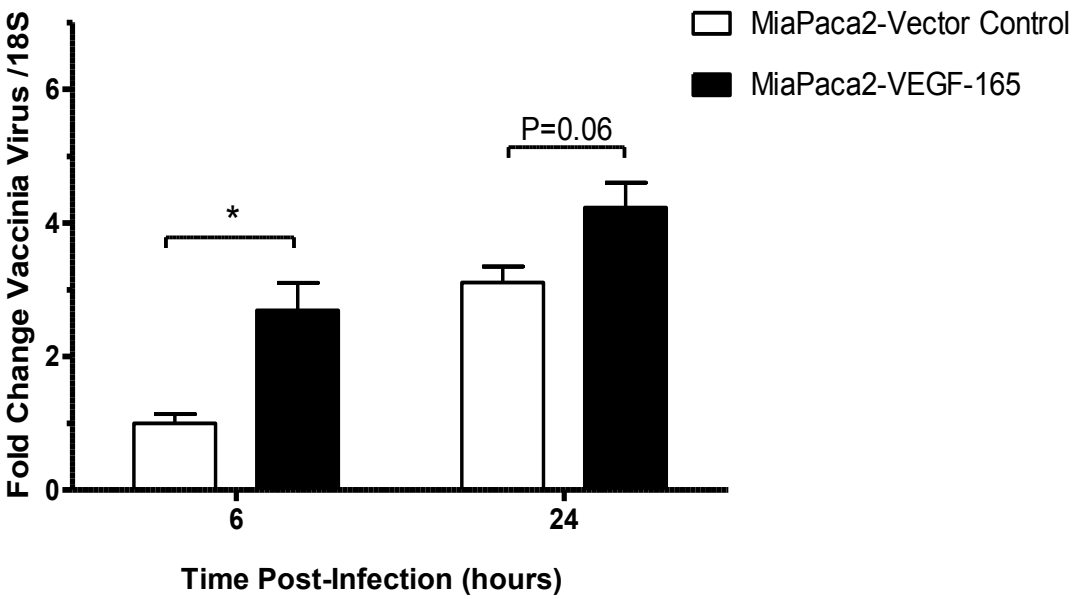

Figure 4.25: The effect of VEGF on Vaccinia virus mRNA expression.

MiaPaca2-VEGF-165 and MiaPaca2-Vector Control were infected for 1 hour with wild type Lister strain Vaccinia virus at an MOI = 10 pfu/cell. Cells were harvested at 6 and 24 hours for RNA extraction. RT-qPCR was performed for VLTF-1 and 18S and fold changes normalised to MiaPaca2-Vector Control at 6 hours post-infection. Relative quantification was used. * = P

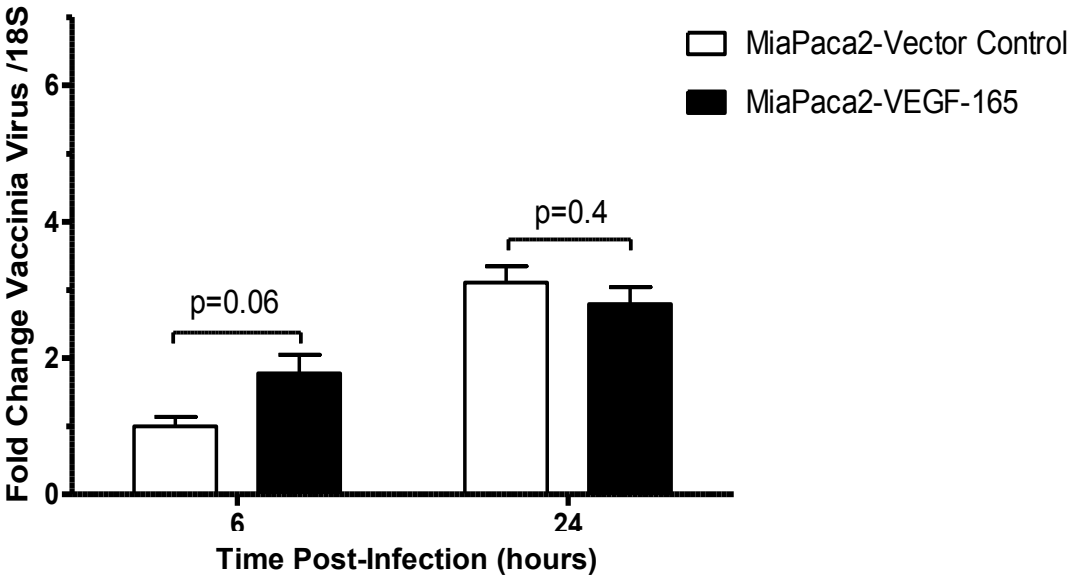

Figure 4.26: The effect of VEGF on Vaccinia virus mRNA expression.

MiaPaca2-VEGF-165 and MiaPaca2-Vector Control were infected for 1 hour with wild type Lister strain Vaccinia virus at an MOI = 10pfu/cell. Cells were then harvested at 6 and 24 hours for RNA extraction. RT-qPCR was performed for VLTF-1 and 18S then fold changes normalised to MiaPaca2-Vector Control at 6 hours post-infection. To control for increased internalisation of Vaccinia virus in MiaPaca2-VEGF-165 these ratios were transformed adjusting for this (values multiplied by 0.66). Relative quantification was used.

4.11 The effect of VEGF on Vaccinia virus DNA replication measured using qPCR

Replication of Vaccinia virus genomic DNA is required to in order to produce infective virions. To determine whether VEGF has any effect on DNA replication, MiaPaca2-VEGF-165 and MiaPaca2-Vector Control cells were infected with VVLister at an MOI = 1 pfu/cell. Cells were collected at 24, 48 and 72 hours post-infection and DNA extracted for Real-Time quantitative PCR using the VLTF-1 primer and probe set. Cells were not collected at 96 hours post-infection as significant cytopathic effect is seen at this time and DNA would be lost after cell lysis and release of virions.

A significant increase was seen in DNA replication in MiaPaca2-VEGF-165 compared to control cells at 24 ($P = 0.0033$), 48 ($P = 0.0016$) and 72 hours ($P = 0.003$) paralleling the viral replication as measured using viral burst and TCID50 assay (Figure 4.27).

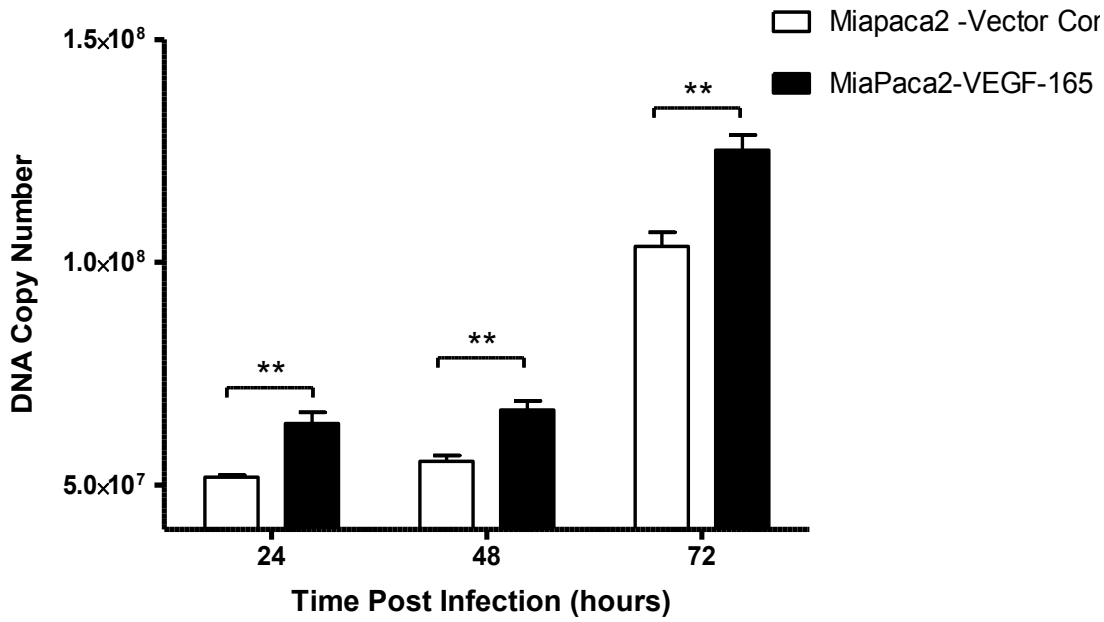

Figure 4.27: The effect of VEGF on the replication of Vaccinia virus genomic DNA. MiaPaca2-VEGF-165 and MiaPaca2-Vector Control were infected for 1 hour with wild type lister strain Vaccinia virus at an MOI = 1 pfu/cell. Cellular and viral DNA was then extracted at 24, 48 and 72 hours. The VLTF -1 primer and probe set was used to perform qPCR on 40 ng of DNA at each time point. ** = $P \leq 0.01$ Two tailed students T-test.

4.12 The effect of VEGF on Vaccinia virus EEV production measured using TCID50 assay

I have demonstrated that VEGF facilitates Vaccinia virus replication resulting in increased cytolysis and cytotoxicity. However EEV forms of Vaccinia are released without cytolysis early after infection and this process has been shown to be mediated in part by Abl-family tyrosine kinases (163). To assess whether VEGF affects the release of extracellular enveloped virus (EEV), MiaPaca2-VEGF-165 and MiaPaca2-Vector Control cells were infected with VVLister at an MOI = 1 pfu/cell. Supernatant was collected at 24 hours post-infection before any cytopathic effect was seen. Consequently any infective virions present in the supernatant represent EEV rather than the usual, predominant IMVs. This supernatant was then used in TCID50 assay to titrate the amount of EEV produced. As expected the amount of EEV produced was much lower than that of IMVs at this time point. There was no significant difference in the amount of EEV produced in the presence of increased VEGF (Figure 4.28). In summary our results show that VEGF facilitates the entry of oncolytic Vaccinia virus accelerating viral infection but does not directly affect other steps in the virus life cycle.

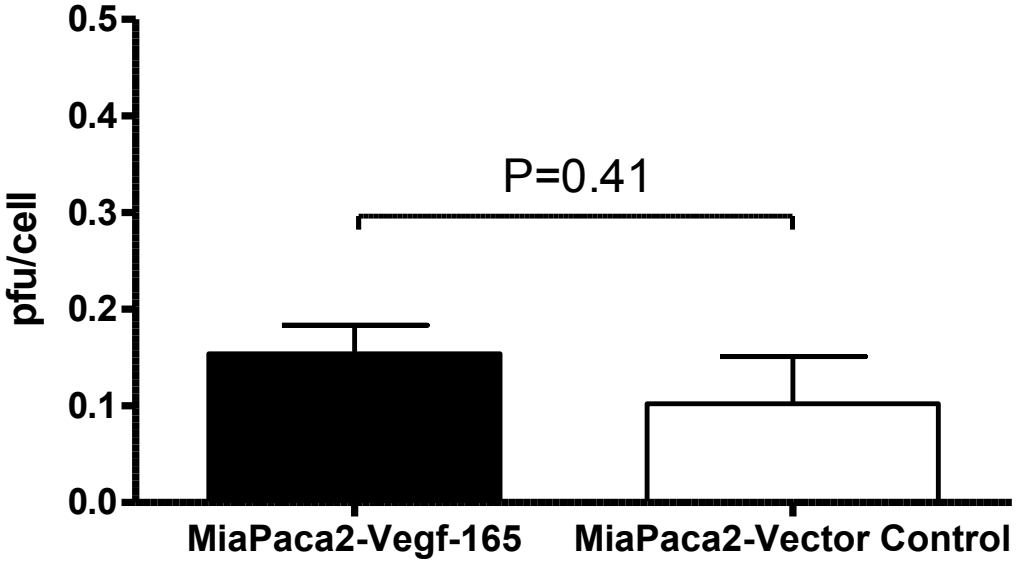

Figure 4.28: The effect of VEGF on the production of extracellular enveloped virus particles (EEV).

MiaPaca2-VEGF-165 and MiaPaca2-Vector Control were infected for 1 hour with wild type Lister strain Vaccinia virus at an MOI = 1 pfu/cell. Supernatant was then collected at 24 hours before any cytopathic effect and used to determine titre of EEVs by TCID50 on CV-1 indicator cells.

4.13 The expression of VEGF receptors on PDAC cell lines Suit2, MiaPaca2, Panc1 and CFPac1

To investigate the mechanism through which VEGF facilitates Vaccinia virus entry we firstly characterized the endogenous expression of VEGF receptors. There are many receptors that bind to VEGF ligands, but we restricted our analysis to those most implicated in VEGFA-165 biology, namely VEGFR1(Flt-1), VEGFR2(Flk-1/KDR) and neuropilin 1(NRP1) (78). Cells were seeded and allowed to adhere overnight, then exposed to normoxia or hypoxia for a further 24 hours. Protein was then extracted and probed for VEGFR1, VEGFR2, NRP1. Ku-70 was used as a loading control (Figure 4.29). Protein extract from human umbilical vein endothelial cells (HUVEC) was used as a positive control as they express all three receptors (196). The double bands of VEGFR1 and VEGFR2 represent differently glycosylated forms (197). NRP1 was highly expressed in CFPac1 cells compared to HUVECs in both normoxia and hypoxia. It was also present at a lower level in Suit2 and Panc1 and there is a slight increase in receptor expression after exposure to hypoxia. There is a faint band present in extracts of MiaPaca2 cells in both normoxia and hypoxia which is more clearly visible on the original radiograph. Li *et al* looked at NRP1 mRNA expression in Panc-1 and MiaPaca2 cells and their results are consistent with these. The immunoblotting for VEGFR1 and VEGFR2 is less clear. There are faint bands visible for VEGFR1 in Panc1 and CFPac1 cells and faint bands for VEGFR2 in Suit2/CFPac1cells exposed to hypoxia and MiaPaca2 cells exposed to normoxia. The expression of VEGFR1/2 is therefore likely to be low and variable across cell lines and as a consequence Western blotting may not be a sufficiently sensitive technique. This is consistent with the work of Itakura *et al* who found evidence for VEGFR2 in some PDAC cell lines but immunoprecipitation of protein was required to detect receptors with immunoblotting (190), although Wey *et al* have published that pancreatic cancer cell lines do express VEGFR1 and that density of receptor increases as cell become more confluent (198). Their experiments were performed using a polyclonal antibody for VEGFR1.

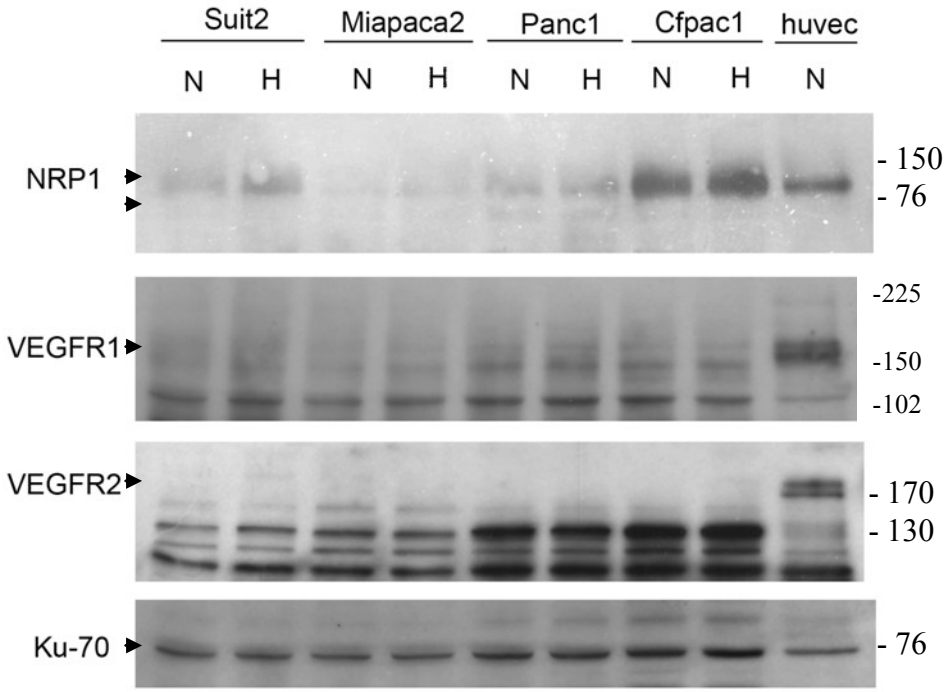

Figure 4.29: Western blot to determine VEGF receptor status of four pancreatic cancer cell lines in normoxia and hypoxia.

A reducing denaturing gel was used to separate 30ng of protein per well and transferred to a PVDF membrane. Membranes were then probed for VEGFR1, VEGFR2 and neuropilin 1 (NRP1) and Ku-70 used as a loading control. Human umbilical vein endothelial cells (HUVEC) known to express all three receptors were used as a positive control. Molecular weights are expressed as kDa. N=normoxia H=hypoxia.

4.14 The effect of NRP1 gene silencing in Vaccinia virus transgene expression in Suit2 and CFPac1

As NRP1 is the most abundant VEGF receptor we found on PDAC cell lines NRP1 gene silencing was used to look for any effect on Vaccinia virus transgene expression. The sequences used for siRNA gene silencing are shown in Table 4.3. Firstly the efficiency and timing of gene silencing was optimised in CFPac1 cells. Shown in Figure 4.30, cells were either mock transfected (1), transfected with transfection reagent only (2), NRP1 siRNA (25 nM) (3) or Control siRNA (25 nM) (4) and protein harvested 48 and 72 hours later. A Western Blot was then performed and membranes were probed with NRP1 mAb which show almost complete abolition of NRP1 protein expression at both time points. Cells were viable and did not show any unusual morphology. The double band on immunoblotting represents the soluble (90 kDa) and membrane-bound (130 kDa) form of NRP1 (199).

CFPac1 and Suit2 cells were then either mock-transfected with transfection reagent only, or transfected with NRP1 siRNA or control siRNA followed by infection 48 hours later with VVL15 expressing firefly luciferase. At 48 hours after infection, cells were lysed and samples measured for bioluminescence (using the Perkin Elmer Victor luminometer) and protein concentration. Bioluminescence is expressed per µg of protein in Suit2 (Figure 4.31) and CFPac1 (Figure 4.32) cells infected with VVL15 at an MOI = 0.1 pfu/cell. Unexpectedly there was a small but significant increase in viral transgene expression after NRP1 gene silencing compared to control siRNA in both Suit2 ($P < 0.0001$) and CFPac1 ($P < 0.0001$) cells. However, in CFPac1 the bioluminescence in the parental cell line is higher than in control siRNA or transfection-reagent treated cells suggesting a non-specific effect on viral transgene expression.

Table 4. 3: The siRNA sequences for NRP1 gene silencing

GENE (Ref Seq)	siRNA Target Sequence
NRP1 (NM_001024629)	1-CGAUAAAUGUGGCGAUACU 2-GGACAGAGACUGCAAGUAU 3-GUAUACGGUUGCAAGAUAA 4-AAGACUGGAUCACCAUAAA

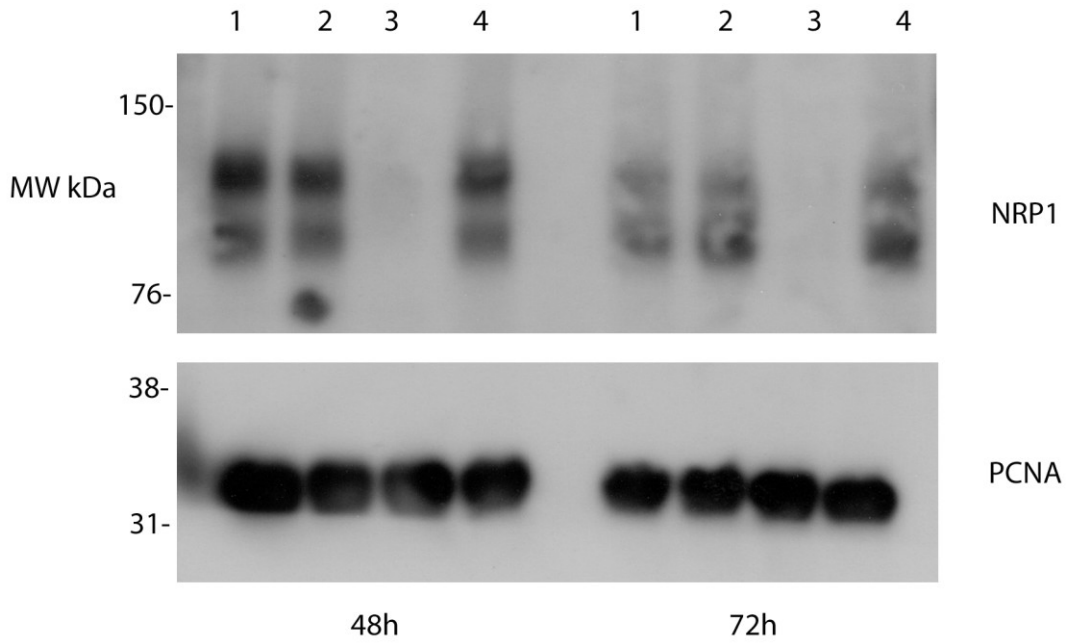

Figure 4.30: Western blot to confirm silencing of NRP1 with specific siRNA.

Protein from the parental cell line CFPac1 (1), cells exposed to transfection reagent only (2), NRP1 siRNA (3) or Control siRNA (4) were collected at 48 and 72 hours transfection. Lysates were then probed for neuropilin-1 (NRP1) or proliferating cell nuclear antigen (PCNA). The double band of NRP1 represents the membrane-bound form (130-135 kDa) and a soluble form (90 kDa).

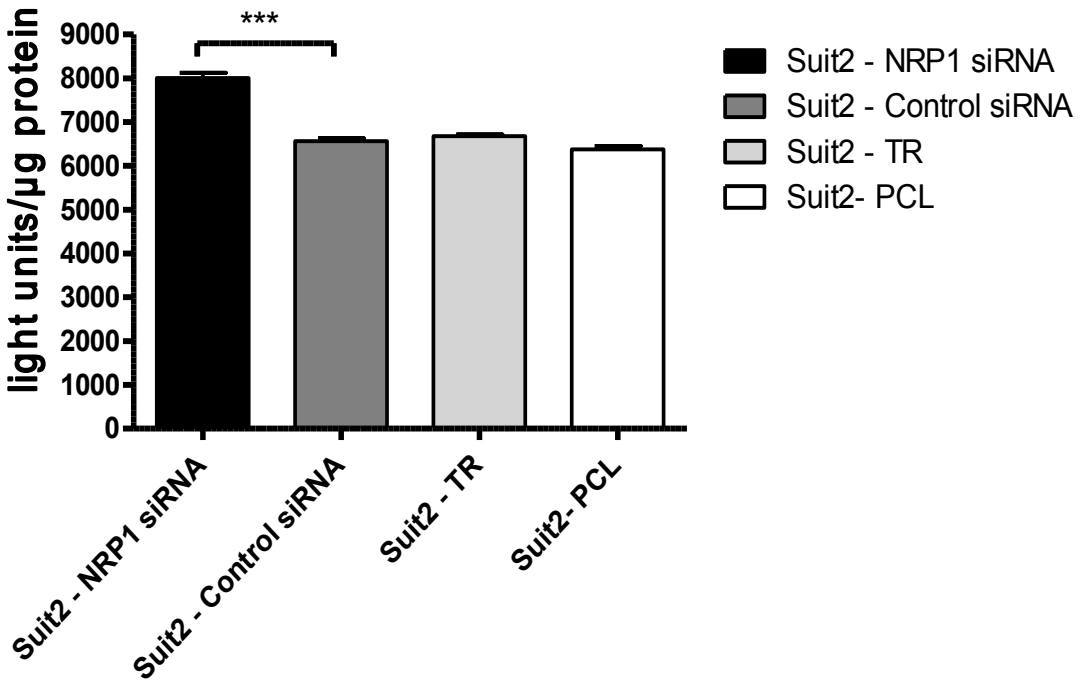

Figure 4.31: The effect of NRP1 gene silencing on the expression of the firefly luciferase reporter gene from VVL15.

Suit2 cells were seeded in a 24 well plates and transfected 24 hours later with NRP1 siRNA, control siRNA, transfection reagent only or mock-transfected. Cells were infected 48 hours later with VVL15 at an MOI = 0.1. Cells were lysed 48 hours post-infection and bioluminescence was quantified. Experiments were performed in triplicate and results represent the data from two separate experiments. Results are presented as mean ± SEM. TR= Transfection reagent only, PCL= parental cell line, *** = $P \leq 0.001$.

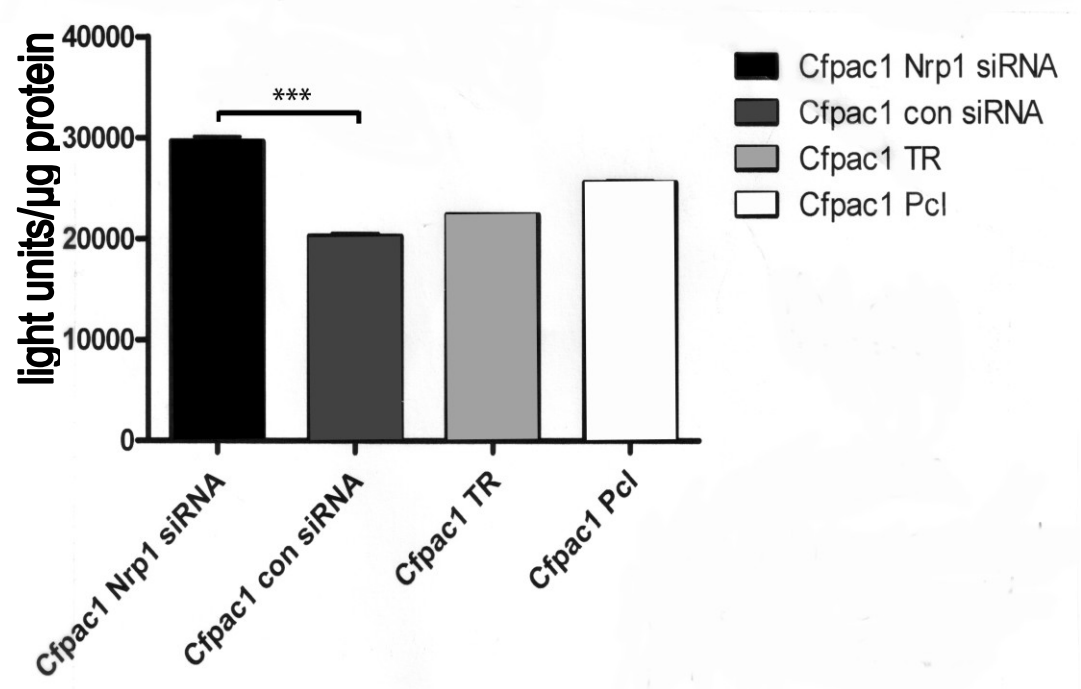

Figure 4.32: The effect of NRP1 gene silencing on the expression of the firefly luciferase reporter gene from VVL15.

CFPac1 cells were seeded in a 24 well plates and transfected 24 hours later with NRP1 siRNA, control siRNA, or transfection reagent only. Cells were infected 48 hours later with VVL15 at an MOI = 0.1. Cells were lysed 48 hours post-infection and used to quantify bioluminescence with a luminometer. Experiments were performed in triplicate and results represent the data from two separate experiments. Results are presented as mean ± SEM. TR= Transfection reagent only, PCL= parental cell line, *** = $P \leq 0.001$.

4.15 The effect of VEGF on Akt phosphorylation status in PDAC cells

The biology of VEGF receptor signalling is most well characterised in endothelial cells and it is known that VEGF acts via PI3K to phosphorylate Akt (78). However it has also been demonstrated that VEGF can increase Akt phosphorylation through NRP1 and via VEGFR1 in cancer cell lines (200, 201). The PI3K-Akt signalling pathways has additionally been shown to be important for viral infection and survival (157). We were interested to determine whether there was any difference between endogenous Akt phosphorylation in our PDAC cell lines. MiaPaca2-VEGF-165 and MiaPaca2-Vector Control cells were starved overnight and protein collected for western blotting with Fadu cell extracts used as a positive control. There was no clear difference in baseline Akt phosphorylation status (S473) in our cell lines (Figure 4.33).

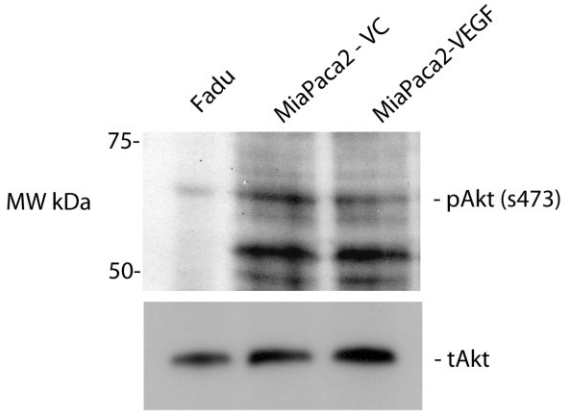

Figure 4.33: Western blot of Akt phosphorylation status (S473) in uninfected MiaPaca2-Vector Control (VC) and VEGFA-165 cell lines.

Cells were starved overnight before protein was collected and used for immunoblotting. Fadu was used as a positive control. pAkt = phospho Akt, tAkt = total Akt, MW kDa=Molecular Weight in Kilodaltons.

4.16 The effect of Akt inhibition on Vaccinia virus transgene expression

Although there was no difference in baseline Akt phosphorylation in our MiaPaca2 model we were interested to determine the effect of Akt inhibition on Vaccinia virus, as it had been shown previously that the infectivity of myxoma virus, another poxvirus, is dependent on Akt activation (158). MiaPaca2 and Suit2 cell lines were treated with Akt inhibitor VIII (202) at 5 or 10 μM or with the PI3K inhibitor Wortmannin for two hours prior to infection. Cells were then infected with VVL15 and lysed 24 and 48 hours later to measure bioluminescence. A highly significant and dose-dependent reduction in transgene expression after Akt inhibition was seen in both MiaPaca2 and Suit2 compared to DMSO-treated controls (Figure 4.34 A&B). This confirms that as with other viral species, Akt signalling plays an important role in infectivity. Wortmannin, an inhibitor of PI3K was used as it is known that PI3K can lead to phosphorylation of Akt, although Wortmannin does target other kinases (203). We found a limited effect on Vaccinia virus transgene expression at the dose used in our studies, with no effect on transgene expression in MiaPaca2 at 48 hours and a slight increase in Suit2 at this time point. This is consistent with the work of McNulty et al. who found that even at higher doses Wortmannin does not affect the plaque size of IHD-J strain Vaccinia virus (204).

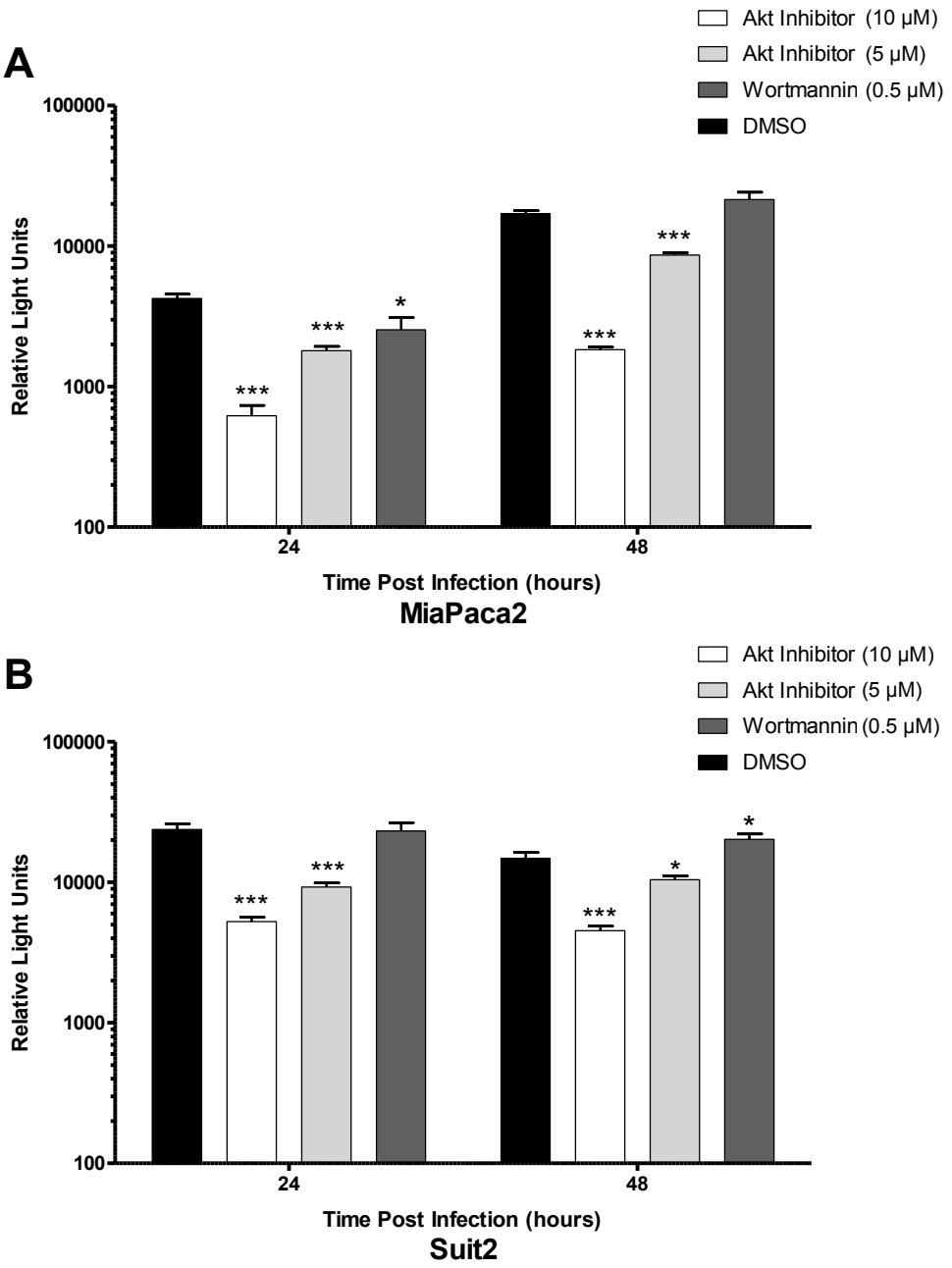

Figure 4.34: The effect of Akt and Wortmannin on Firefly luciferase expression from VVL15.

MiaPaca2 (A) and Suit2 (B) were pre-treated with Akt inhibitor VIII and Wortmannin for 2 hours prior to infection with VVL15 at MOI = 1 pfu/cell. Cells were lysed and bioluminescence quantified with a luminometer (Perkin Elmer Victor) at 24 and 48 hours post-infection. Experiments were performed in triplicate and results represent the data from two separate experiments. Results are presented as mean ± SEM. An unpaired, two-tailed students T Test was used to compare the difference to the mean of DMSO treated cells. * = $P \leq 0.05$, *** = $P \leq 0.001$.

4.17 The effect of Akt inhibiton on VEGF production

Akt has been shown to regulate VEGF production in both normoxia and hypoxia (39, 205). This regulation may be relevant in PDAC cells as Akt, in addition to its importance for viral infection outlined by Cooray et al, may indirectly slow viral internalisation by limiting VEGF production. Suit2 cells were treated with Akt inhibitor VIII (5 μM) or DMSO for 2 hours prior mock infection or infection with VVLister at an MOI = 1 pfu/cell. Akt inhibition resulted in a reduction in VEGFA productions as measured by ELISA after 2 hours of treatment and this was sustained at 24 hours after infection (Figure 4.35). Therefore, a reduction in Akt signalling may have an additional inhibitory effect on Vaccinia virus life cycle by reducing Vaccinia virus internalisation.

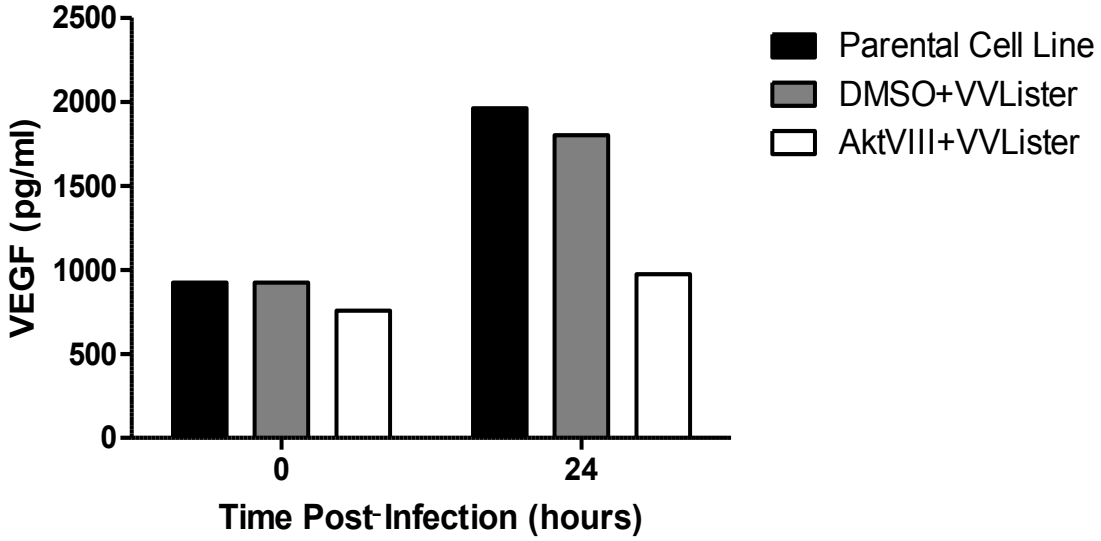

Figure 4.35: The production of VEGF during infection with Vaccinia virus and treatment with Akt InhibitorVIII.

Suit2 cells were pre-treated with Akt inhibitor VIII and then infected with VVL15 at an MOI = 1 pfu/cell. Supernatent was collected prior to treatment and a VEGFA-specific ELISA used to quantify the level of secreted VEGFA prior to treatment and at 24 and 48 hours after. DMSO = dimethyl sulfoxide, AktVIII = Akt Inhibitor VIII (5 μM).

4.18 The effect of Akt inhibition on VEGF internalisation measured using qPCR

To verify that Akt inhibition can affect Vaccinia virus internalisation, an internalisation assay was performed after Akt inhibitor treatment. Suit2 cells were treated with Akt Inhibitor VIII at 5 or 20 μM or with DMSO for 2 hours prior to infection with VVLister (MOI= 10 pfu/cell) at 4 °C for 1 hour. Internalisation was allowed to occur at 37 °C for 15 and 60 minutes after which cells were treated with pronase to remove un-internalised virions. There was a significant reduction in Vaccinia virus internalisation at 15 minutes post-infection with 20 μM, (the highest dose) of inhibitor (47% reduction vs DMSO, P = 0.009) and a trend with the lower dose (). At 60 minutes post-infection there was a 30% and 35% reduction in Vaccinia virus internalisation after treatment with Akt inhibitor VIII at 5 μM (P = 0.042) and 20 μM (P = 0.032) respectively. The effect of Akt inhibition at 60 minutes post-infection appears to be saturated suggesting that Akt is involved in one mode of Vaccinia virus entry but other forms are unaffected.

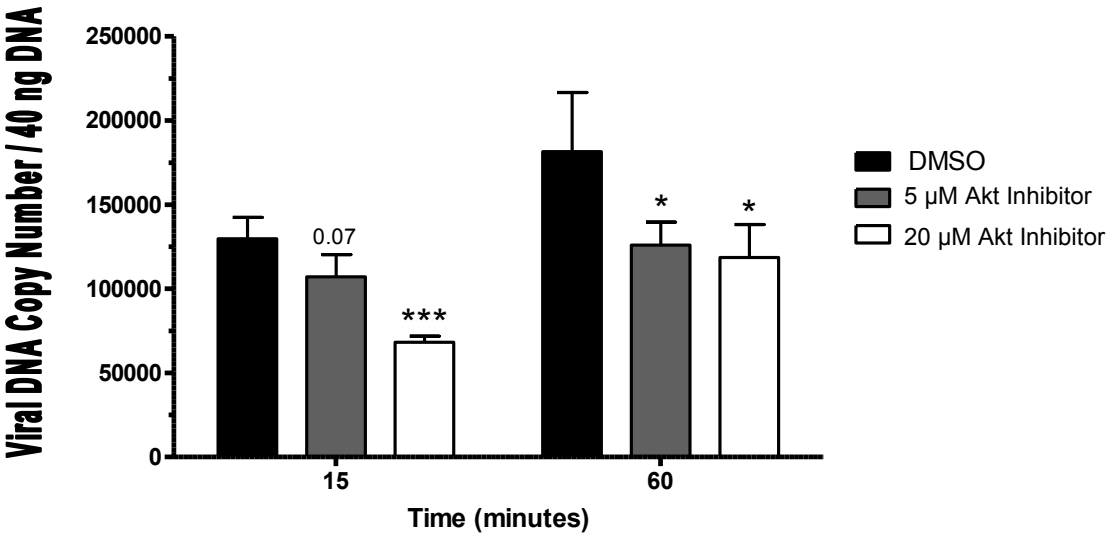

Figure 4.36: The effect of Akt inhibition on the rate of viral internalisation.

Suit2 cells were pre-treated for 2 hours with Akt inhibitor VIII at 5 or 20 µM and then infected with VVLister at an MOI = 10 pfu/cell for 1 hour at 4°C. Cells were warmed to 37°C to allow internalisation of attached viral particles. At 15, 30 and 60 minutes cells were treated with pronase (1 mg/ml) for 30 minutes at 4 °C and washed to remove uninternalised virus. Cellular and viral DNA was extracted simultaneously and 40 ng used for quantitative real-time PCR using the VLTF-1 primer and probe set. Each sample was assayed in triplicate for qPCR and each combination and time point were performed in biological duplicates. An unpaired two-tailed students T-test was used for statistical analysis and results are presented as mean +/- SEM. *** =$P < 0.001$, * = $P < 0.05$.

4.19 The effect of Akt inhibition on Vaccinia virus cytotoxicity

To verify if Akt inhibition has an effect on the oncolytic efficacy of Vaccinia virus we performed a MTS assay in the presence of this inhibitor. Suit2 cells were treated with 5 or 20 μM of Akt inhibitor VIII prior to infection with serial dilutions of Vaccinia virus and MTS reagent was added to assess cell viability at 3 days post-infection. There was a highly significant and dose-dependent effect of Akt inhibition on Vaccinia virus cytotoxicity (Figure 4.37). The EC50 value at 3 days after infection for DMSO treated cells was 93.6 pfu/cell versus 43.0 pfu/cell and 19.7 pfu/cell after treatment with 5 μM ($P<0.0001$) and 20 μM ($P<0.0001$) of Akt inhibitor VIII. This effect may be mediated in part by the reduction in VEGF produced after Akt inhibition but will almost certainly be caused by pleiotropic effects of Akt inhibition on the viral life cycle and also the host cell.

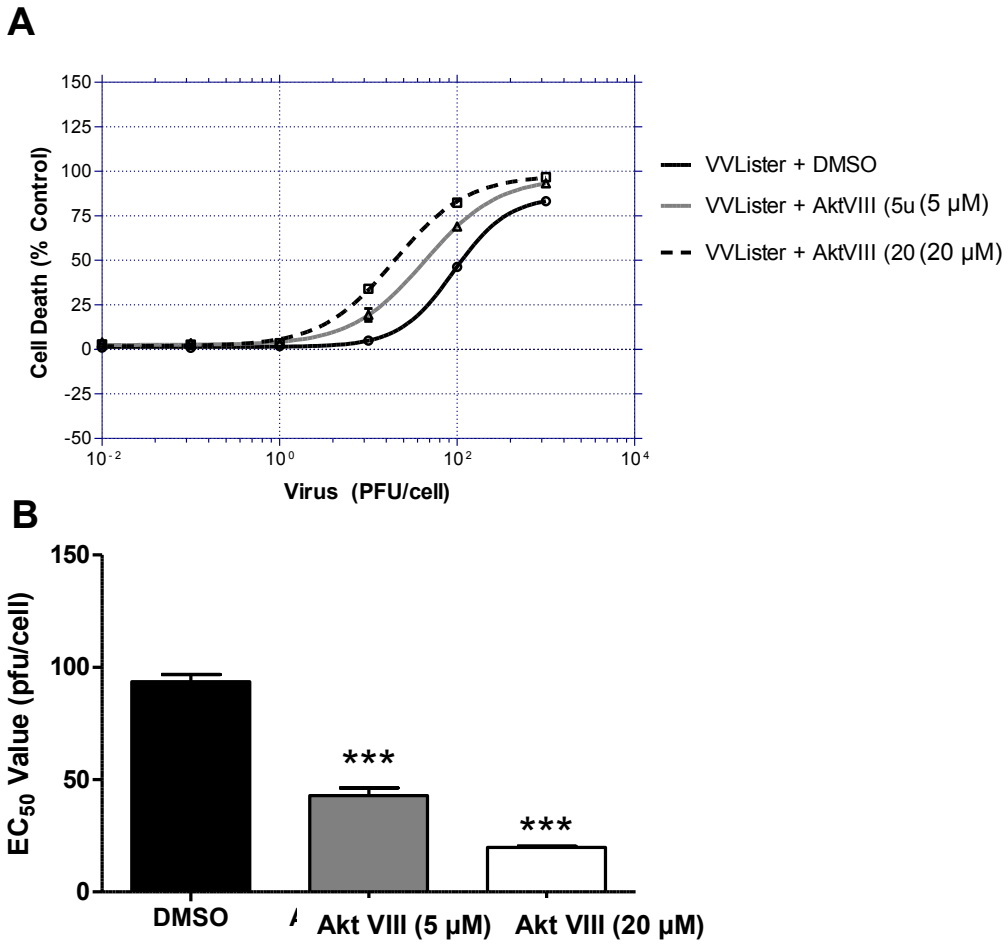

Figure 4.37: The effect of Akt Inhibition on Vaccinia virus cytotoxicity.

Suit2 cells were pretreated with Akt inhibitor VIII (5 µM or 20 µM) for 2 hours and then infected with serial dilutions of VVLister. The infected cells were assayed with MTS reagent at day 3 post-infection at 37 °C with 5% CO_2 for 2 hours. Viable cells were determined as a percentage of the uninfected controls and non-linear regression analysis was used to draw a dose–response curve (A) and determine the EC50 value (B). Each assay contained six replicates and results are presented as mean ± SEM of two independent experiments. An unpaired, two-tailed students T Test was used to compare the difference to the mean EC50 values. *** = $P \leq 0.0001$.

4.20 The effect of VEGF on Vaccinia virus transgene expression in vivo

VEGF facilitates Vaccinia virus entry and results in increased transgene expression and replication *in vitro*. To see determine whether this finding was reproducible *in vivo* and could therefore be partly responsible for the tropism of Vaccinia virus, the MiaPaca2 cell model was used to establish tumour xenografts. MiaPaca2-VEGF-165 and MiaPaca2-Vector Control cell lines were used to establish xenografts in the right flank of Balb/c mice (n = 5 per group). Mice were injected with $1x10^7$ pfu of VVL15 intravenously via the tail vein and subsequently imaged 12 to 132 hours later after the administration of D-luciferin. There was an increase in mean bioluminescent signal in MiaPaca2-VEGF-165 compared to vector control cells (Figure 4.38). This was statistically significant at 2.5 (P = 0.0019), 3.5 (P = 0.031), and 5.5 (P = 0.018) days post-infection and there was a trend towards statistical significance at 1.5 (P = 0.055) and 4.5 (P = 0.067) days post-infection.

A representative image at 2.5 days after infection is shown in Figure 4.39. This shows a clear difference between MiaPaca2-VEGF-165 and MiaPaca2-Vector Control xenografts. The bioluminescent signal seen in the oral region of some mice appears to be caused by oral contact by the mouse with an infected tumour or at the tail vein injections site as this occurs less commonly if animals are separated after infection. This does not seem to interfere with their eating or drinking habits.

Tumours were collected at the end of the experiment (5.5 days post-infection) to verify that the bioluminescent signal corresponded with positive immunohistochemistry for Vaccinia virus. A representative image, at low (100x) and high magnification (200x), of immunohistochemistry with an anti-Vaccinia polyclonal antibody and serial sections stained with haematoxylin and eosin (H&E) is displayed in Figure 4.40 A and B. This shows the characteristic foci of Vaccinia virus infection; Strong central staining and finger like projections of infection spreading out in all directions. The serial H&E sections show karyolysis in the central area of infection. This

finding confirms that VEGF does facilitate Vaccinia virus infection and is a relevant mechanism *in vivo*.

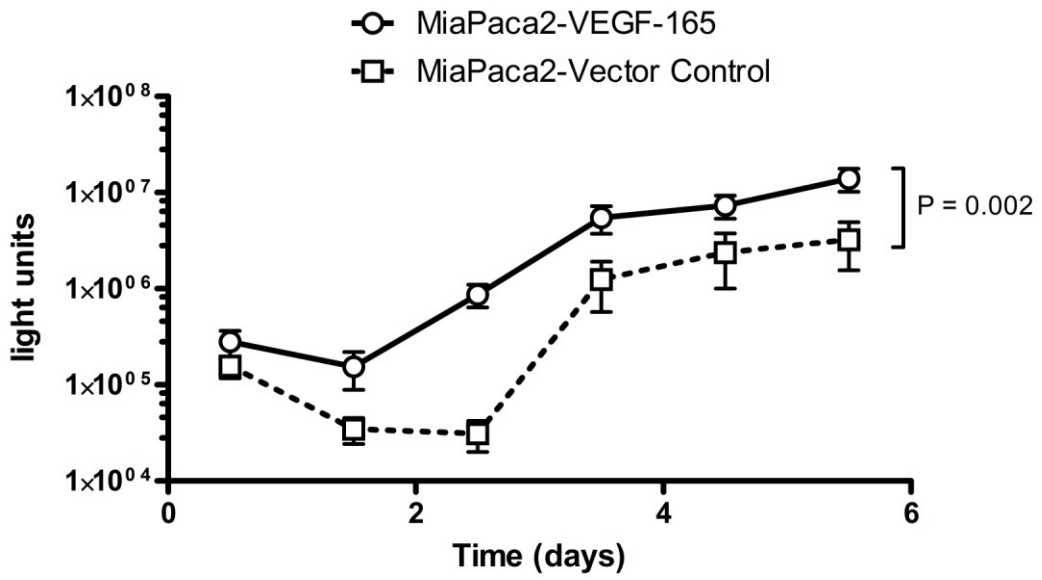

Figure 4.38: The effect of VEGFA on the tumour tropism of VVL15.

$5x10^6$ Miapaca2-VEGF-165 (solid line) and Miapaca2-Vector Control (dashed line) cells were injected into the right flank of balb/c nude mice. VVL15 at an MOI of $1x10^7$ pfu/mouse was injected once via the tail vein at day 0. The bioluminescence for each tumour was measured 12 hours after virus infection and every 24 hours after until 5.5 days post-infection using the IVIS imaging system. Results are presented as mean bioluminescent intensity ± SEM. A repeated measures two way ANOVA with a **bonferroni** correction was used to compare the two groups (n = 5 per group).

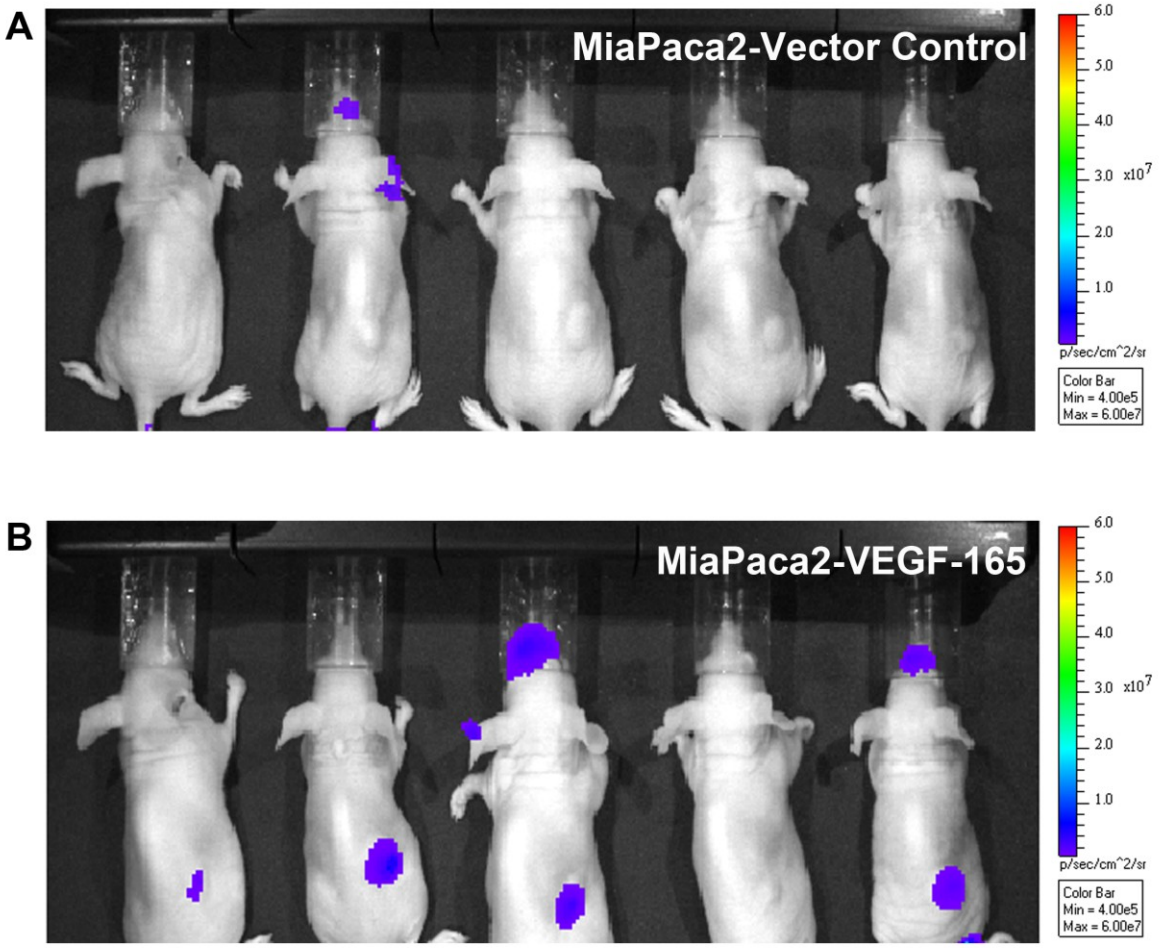

Figure 4.39: Representative image of the effect of VEGF on bioluminescence from VVL15.

$5x10^6$ Miapaca2-VEGF-165 and Miapaca2-Vector Control cells were injected into the right flank of balb/c nude mice. VVL15 at an MOI of $1x10^7$ pfu/mouse was injected once via the tail vein and this image was taken at 60 hours post-injection using the IVIS imaging system. Colour metric scale is the same for both images.

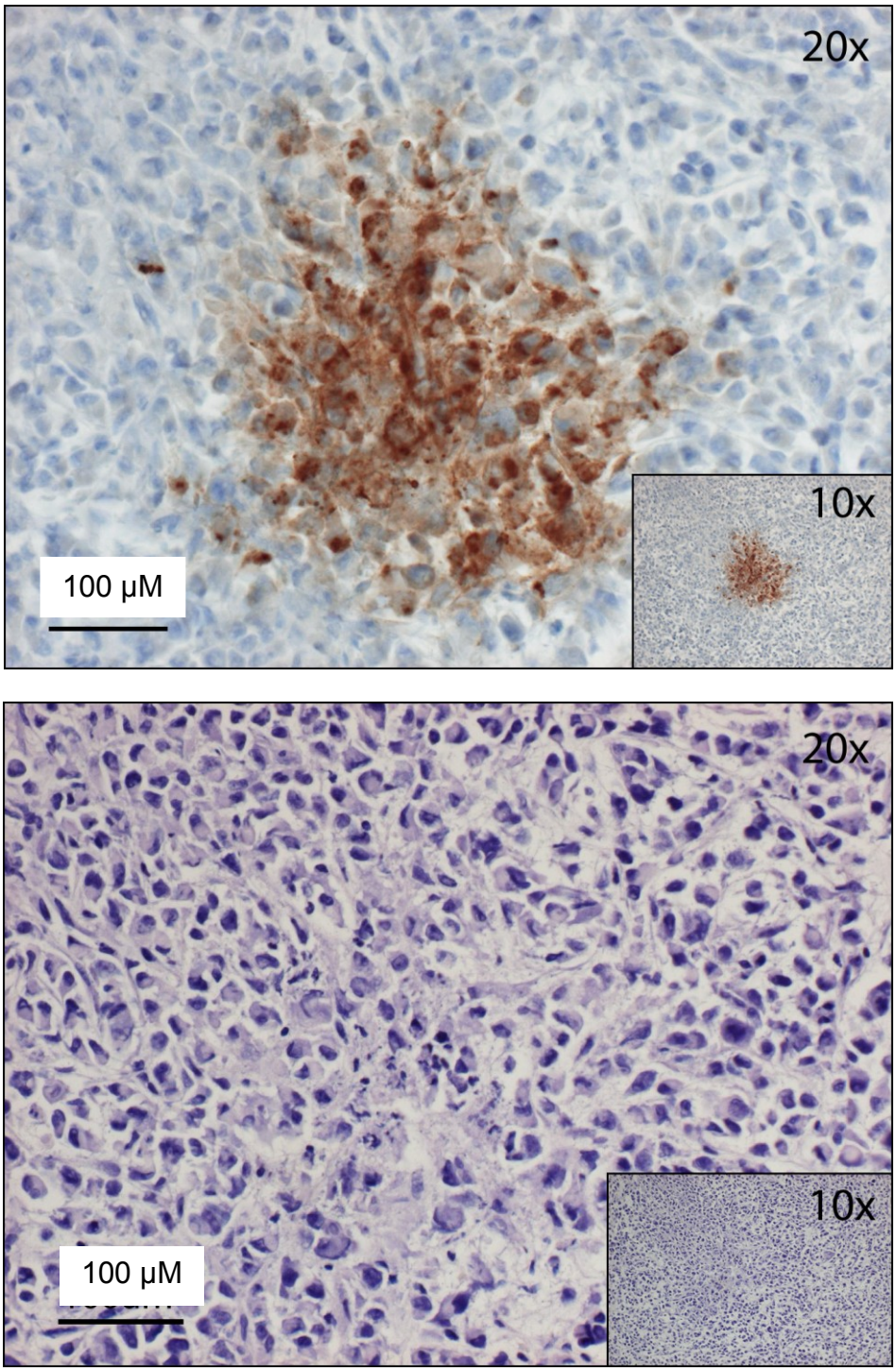

Figure 4.40: Immunohistochemistry for Vaccinia viral proteins and H&E staining.

MiaPaca2-VEGF-165 tumour xenografts were collected at day 6 post intravenous injection of VVL15. Images are representative of loci of viral infection found in tumours. Images were taken with 20x/0.5 and 10x/0.32 objectives on a Zeiss Axioplan microscope fitted with a Zeiss AxioCam MRc camera.

4.21 The effect of hVEGF production on vascularity in the MiaPaca2 xenograft model

VEGF facilitates Vaccinia virus infection *in vitro* and *in vivo,* however it is possible that other mechanisms may be important in animal models. Our original hypothesis was that VEGF would increase vascularity of tumours and therefore help improve the systemic distribution. MiaPaca2-VEGF-165 and MiaPaca2-Vector Control xenografts were stained for Pecam-1 a marker of murine endothelial cells (206). Two sections were taken from the centre of each tumour with a 200 μM distance between. The percentage of Pecam-1-positive cells was scored across the entirety of each section and the mean percentage of positive cells compared between the two groups. There is a greater than 90% homology between murine and human VEGFA with a high level of conservation at both N and C terminal regions. Thus we expected to see an increase in vascularity in the MiaPaca2-VEGF-165 xenografts. There was an increase in Pecam-1 positive cells and it was significantly greater than MiaPaca2-Vector Control cells, $P = 0.0037$ (Figure 4.41). A representative image of Pecam-1 staining from the MiaPaca2-VEGF-165 and MiaPaca2-Vector Control xenografts is shown in Figure 4.42. Although these results show there is increased vascularity in the presence of VEGF which could account for some of its effect on Vaccinia virus i*n vivo,* they do not give any indication as to the permeability of these vessels, which may also be important for Vaccinia virus spread.

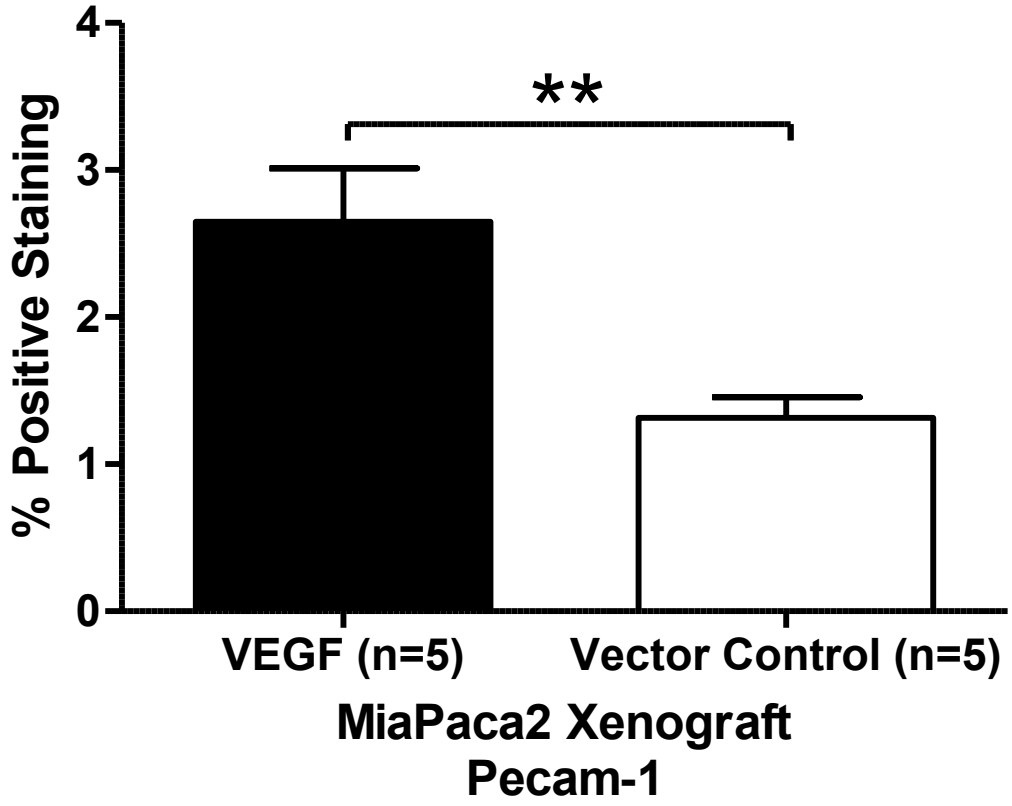

Figure 4.41: Quantification of Pecam-1 staining in MiaPaca2-VEGF-165 and MiaPaca2-Vector Control tumour xenografts in Balb/c nude mice.

Images were taken at 20x magnification to provide complete coverage of tumour sections, approximately 15-25 images per tumour. Quantification was performed on two sections separated by 200 μM for each tumour. There were five tumours per group. Data are presented as percentage area of Pecam-1 positive cells per tumour. **=P<0.01 A two-tailed, unpaired students t-test was used to compare the mean percentage of CD31 positivity. Results are presented as mean ± SEM. Please refer to Materials and Methods, section 2.8.3, for detailed explanation of the quantification procedure.

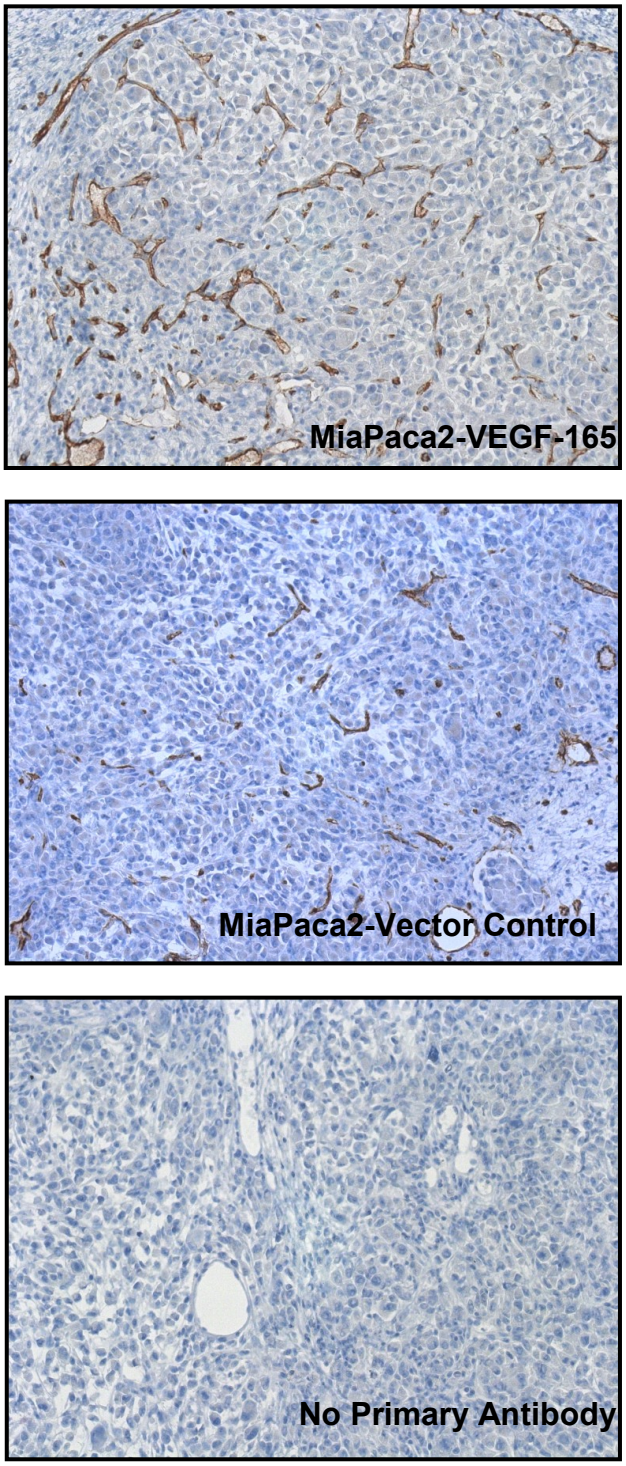

Figure 4.42: Representative images of CD31/Pecam-1 staining in MiaPaca2-VEGF-165 and MiaPaca2-Vector Control tumour xenografts in Balb/c nude mice.

Images were taken with 20x/0.5 objectives on a Zeiss Axioplan microscope fitted with a Zeiss AxioCam MRc camera.

Chapter 5

5 Construction of VV-ODD, a hypoxia targeting Vaccinia virus

5.1 Schema for VV-ODD

Having confirmed that Vaccinia virus is a potential vector targeting hypoxic tumours, we next sought how to improve the potency of this virus. One strategy is to arm the virus with a therapeutic gene however tight regulation of gene expression is required in order to minimise off target effects. Previously this has been achieved by limiting the tropism of recombinant viruses to cancer cells and by using conditional promoters to target therapeutic gene expression. In order to restrict gene expression to hypoxic conditions we designed a Vaccinia virus expressing a luciferase reporter gene regulated by hypoxia as a proof of principle. Limiting therapeutic gene expression to hypoxia offers an additional level of regulation that could enhance the therapeutic ratio as any off target effects in normoxic normal tissue would be minimised.

There are three levels of hypoxic regulation in this construct. Firstly it contains an IRES sequence to initiate protein translation, which is relatively more preserved than 5' methyl cap-dependent translation in hypoxia (207). Secondly the Luciferase reporter gene is fused to the oxygen degradation domain (ODD) of the HIF1α gene. This results in the hydroxylation, ubiquitination and consequent proteolytic degradation of the reporter gene in the presence of oxygen (208). Thirdly the 3'-untranslated region (UTR) from the VEGF gene is included as this has been shown to increase mRNA stability in hypoxia (209). The construct contains an unmodified red fluorescent protein (RFP) selection marker driven directly from the Vaccinia virus P7.5 promoter, and an SV40 poly A tail and is inserted into the TK region of the Lister strain virus (Figure 5.1). The shuttle plasmid has been designed so that elements including the transgene can be easily removed and replaced.

All PCR fragments were produced using Novagen KOD polymerase (Merck KGaA, Darmstadt, Germany) and all gene-specific primers were obtained from Sigma-Aldrich (St Louis, MO, USA). PCR primers for gene-specific reverse transcription from Suit2 DNA are shown in Table 5.1. All other PCR primers to amplify fragments and introduce restriction enzyme sites (RES) are shown in table 5.2.

The EMCV IRES bicistronic vector was used in a PCR reaction to produce a PCR fragment with SacI and AscI 5' and an RsrII, AsiSI, SacII and SacI RES 3' to the EMCV IRES sequence. pGem-Luc (Promega, Wisconsin, USA) was used as the source of the luciferase reporter gene. Gene-specific primers were designed to produce a PCR fragment with RsrII RES 5' and an FseI and AsiSI RES 3' to the luciferase coding sequence and to delete the stop codon. Suit2 cell mRNA was extracted using Trizol reagent (Invitrogen, Carlsbad, California, USA) and cDNA produced using superscript II reverse transcriptase (Invitrogen). This Suit2 cDNA was used as the source of the HIF1alpha ODD and gene specific primers were designed with a FseI RES 5' and a stop codon, NdeI and AsiSI RES 3' to the ODD coding sequence. These were designed so that the ODD sequence remained in frame with the Luciferase reporter gene. Suit2 cDNA was used as the source of the VEGFA 3'UTR, gene specific primers were designed to amplify the 130 bp sequence as published by Claffey *et al* (209). Primers were designed to introduce an NdeI RES 5' and a MluI and AsiSI RES 3' to the coding sequence. The SV40 polyA sequence was produced using gene-specific primers to introduce a MluI RES 5' and an AsiSI 3' to the coding sequence. All fragments were run on agarose gels with ethidium bromide to verify size and gel purified using the GFX PCR DNA purification kit (GE Healthcare Life Sciences, Bucks, UK). All fragments were subcloned into pTopo-CR-II blunt cloning vector (Invitrogen, Carlsbad, California, USA). All fragments were then cut from the pTOPO subcloning vector and gel purified. These were then sequentially ligated into the shuttle vector pSC65RFP.

The pSC65RFP Vaccinia shuttle vector constructed by Dr L Chard, developed originally from pSC65, which contains RFP driven from the p7.5 Vaccinia virus promoter in between the TK

left and right arm was used to create the pSC65RFP-ODD shuttle plasmid. The BamHI site after RFP was cut with its restriction enzyme and a short polylinker, produced by annealing two oligonucleotides (Sigma-Aldrich), was then used to insert a SacI and SacII restriction site to allow site-directed, sticky-end cloning. This was then cut using the relevant RE and dephosphorylated with calf intestinal phosphatase (NEBiolabs, Ipswich, MA, USA) and then run on an agarose gel with ethidium bromide and gel-purified.

Once completed the shuttle plasmid pSC65RFP-ODD was sequenced, using conventional Sanger sequencing by the QMUL Genome Centre, using 16 specific primers covering the TK left arm to the TK right arm. Vector NTI Software (Invitrogen, Carlsbad, CA, USA) was used to verify that the sequence was correct.

The recombinant hypoxia-targeting Vaccinia virus was produced by homologous recombination of the pSC65RFP-ODD shuttle plasmid with the Lister strain Vaccinia virus in CV1 cells. Cells were seeded in 6 well plates and the next day infected with VVLister at an MOI = 0.05 for one hour then removed. Cells were transfected two hours later with 1 μg of pSC65RFP-ODD using Effectene transfection reagent (Qiagen Inc, Valencia, CA, USA). When CPE was first visible 48 hours later, cell were collected and freeze thawed three times to release infectious virions. Serial dilutions of this were used to infect confluent CV1 cells which were then overlaid with a 50:50 mix of 2% low melting point (LMP) agrose and DMEM with 20%FCS. Wells were then observed for plaques that were positive for RFP using a fluorescent microscope. These were picked using a pipette tip, placed into 200 μL of DMEM and freeze-thawed three times. Serial dilutions were used to infect CV1 cells and overlaid with LMP agarose and DMEM mix and RFP-positive plaques picked again when visible. This process was repeated until all plaques at all serial dilutions used were RFP-positive to produce purified VV-ODD which was then used to produce a primary expansion as outlined in the methods.

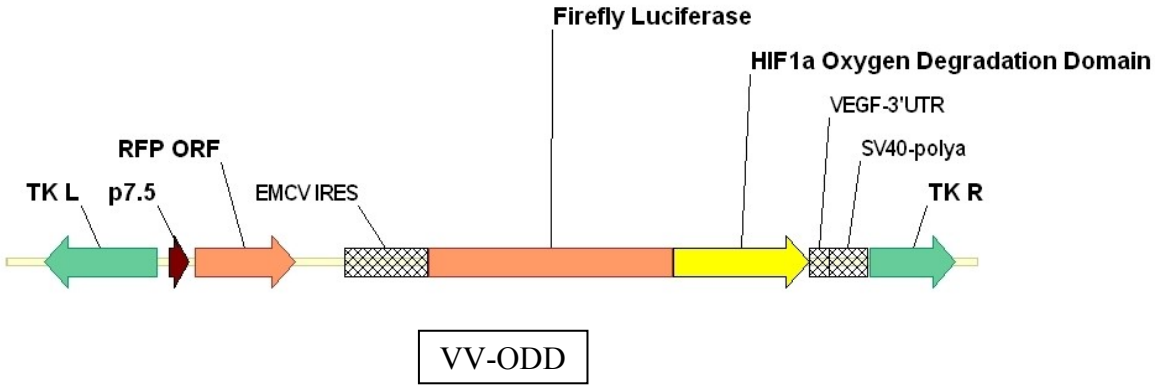

Figure 5.1: Schematic of VV-ODD.

The construct was inserted into the Vaccinia virus thymidine kinase region (J2R) to express the red fluorescent protein and firefly luciferase fused to the ODD from a single Vaccinia virus promoter. Three un-translated regions were included. TK L=Thymidine kinase gene left arm, TK R=Thymidine kinase gene right arm, RFP ORF=Red fluorescent protein open reading frame, EMCV IRES=Encephalomyocarditis virus internal ribosomal entry site, VEGF-3'UTR=Vascular endothelial growth factor three prime un-translated region, SV40-polyA=Simian virus 40 polyadenylation sequence.

Table 5. 1: Sequence of reverse transcription (RT) primers used first strand synthesis of the ODD sequence and VEGF 3'UTR from Suit2 mRNA.

Primer Name	Primer Sequence (5'-3')
RT Primer-ODD-Forward	CAGTGCATTGTATG
RT Primer-ODD-Reverse	AAGTGAACCATCATG
RT Primer-VEGF 3 'UTR-Forward	CCAGCACGGTCCCTC
RT Primer-VEGF 3 'UTR-Reverse	AAGATCATGCCAGAG

Table 5. 2: Sequence of primers used to produce fragments for the construction of VV-ODD

Primer Name	Sequence (5'-3')
Forward-SacI-AscI-EMCV	AAGAGCTCGGCGCGCCCCCTAACGTTACTGGCCGAA
Reverse-EMCV-RsrII-AsisI-Sac2	AGAGCTCTTCCGCGGGCGATCGCCGGTCCGATTATCATCGTGTTTTTCAA
Forward-Luciferase-RsrII	GTTTCGGACCGATGGAAGACGCCAAAAAC
Reverse-Luciferase-FseI-AsisI	CAAAGCGATCGCAGGCCGGCCCAATTTGGACTTTCCGCCC
Forward-ODD-FseI	GTTTGGCCGGCCACAACAAACAGAATGTGTCC
Reverse-ODD-NdeI-AsisI	CAAAGCGATCGCCATATGTCATGATGATGTGGCACTAG
Forward-VEGF 3'UTR-NdeI	GTTTCATATGTAGACACACCCACCC
Reverse-VEGF 3'UTR-AsisI-MluI	CAAAGCGATCGCACGCGTAACATTAGCACTGTTAA
Forward-SV40 PolyA-MluI	GTTTACGCGTTCGACATGATAAGATAC
Reverse-SV40 PolyA-AsisI	CAAAGCGATCGCGGATCTACCACATTTG

5.2 The use of Internal Ribosomal Entry Sites to drive protein translation in normoxia and hypoxia

Protein translation by internal ribosomal scanning has been shown to be preserved in times of cellular stress such has nutrient deprivation and hypoxia (210). The VEGFA gene 5' UTR contains an IRES sequence and is reported to be involved in hypoxic regulation of the protein (211). To see if the VEGF 5'UTR would function as an IRES in the context of Vaccinia virus infection, biscistronic vectors were created by Dr L Chard. They were all driven from a T7 promoter and contain the chloramphenicol acetyltransferase (CAT) and firefly luciferase reporter genes (fLuc).

Four bicistronic vectors were made (Figure 5.2):

A. CAT/fLuc with no IRES sequence to show baseline leaky scanning from the upstream promoter.
B. CAT/EMCV IRES/fLuc containing the encephalomyocarditis virus (EMCV) IRES a commonly used and well characterized IRES
C. CAT/VEGF IRES/fLuc containing the VEGF 5'UTR
D. CAT/VEGF IRES(AS)/fLuc containing the VEGF 5'UTR in the 3'-5' direction which should not function as an IRES.

Suit2 and MDA-231cells were transfected with one of the four bicistronic vectors and exposed to normoxic or hypoxic conditions for 16 hours. Cells were then infected with VTF7-3, a recombinant Vaccinia virus expressing the T7 RNA polymerase (212). Cells were lysed 24 hours after infection and assayed for luciferase expression and CAT expression. Results are presented as light units per nanogram of CAT in MDA-231 (Figure 5.3) and Suit2 (Figure 5.4). MDA-231 cells were found to be relatively resistant to Vaccinia virus gene expression and therefore fLuc/CAT ratios are much lower than the permissive cell line Suit2. The EMCV IRES functions in this cell line but there was a reduction, in fLuc expression, of approximately one

third under hypoxic conditions. In contrast the EMCV IRES does maintain protein translation in hypoxia in Suit2 cells with a significant increase, in fLuc expression, of almost 50 percent versus normoxia. The results of the VEGF IRES are less clear. There is a small but highly statistically significant increase in hypoxia using the VEGF IRES in the Suit2 cell line compared to normoxia. However there are also smaller but significant increases in the fLuc/CAT ratio in the CAT/fLuc (A) and CAT/VEGF-IRES (AS)/fLuc (B) vectors. This suggests that any difference is more likely to be due to the effect of hypoxia on Vaccinia virus or on the T7 RNA polymerase machinery. As the EMCV IRES did preserve protein translation in hypoxia this was used as the IRES sequence for VV-ODD.

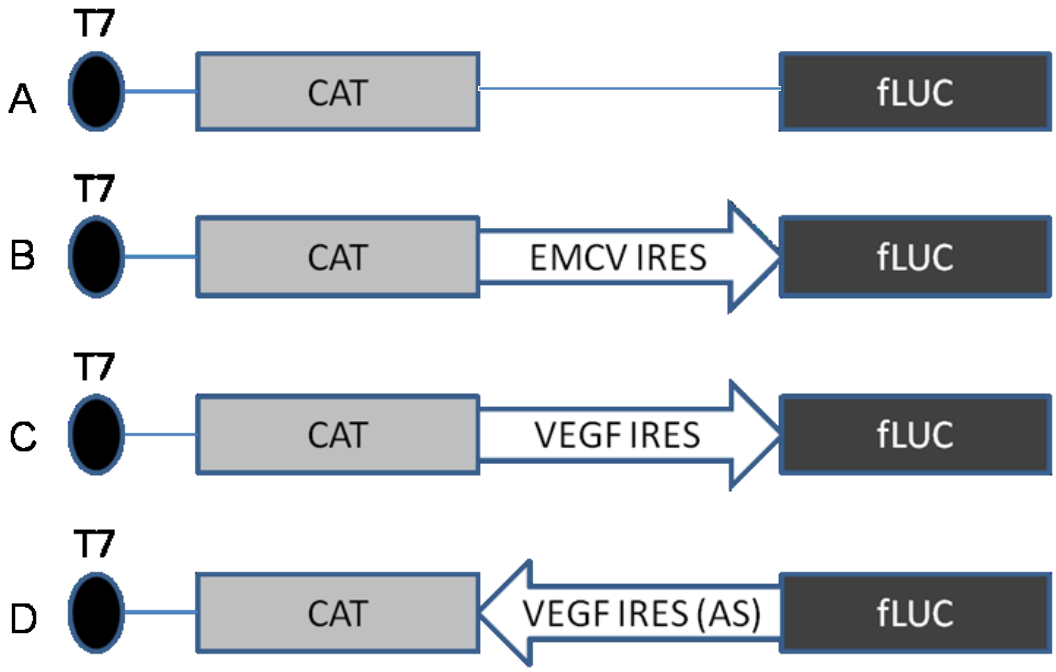

Figure 5.2: Schematic diagram of the bicistronic vectors used to analyse the ability of internal ribosomal entry sites to preserve protein translation in hypoxia.

A=CAT/LUC, B=CAT/EMCV-IRES/fLuc, C=CAT/VEGF-IRES/fLUC, D=CAT/VEGF-IRES-AS/fLUC. CAT = Chloramphenicol Acetyl Transferase, fLUC = firefly luciferase, EMCV = encephalomyocarditis virus internal ribosomal entry site, VEGF-IRES = vascular endothelial growth factor internal ribosomal entry site, VEGF IRES-AS = vascular endothelial growth factor internal ribosomal entry site in the anti-sense direction.

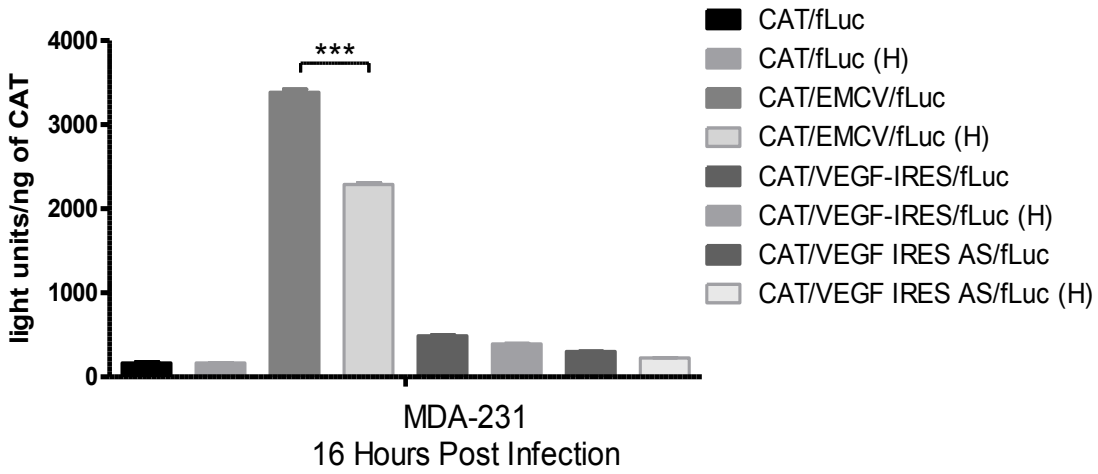

Figure 5.3: The use of a bicistronic vector to assess the efficacy of internal ribosomal entry sites in maintaining protein translation in hypoxia in MDA-231.

MDA-231 cells were transfected with the bicistronic vectors then infected with a Vaccinia virus expressing a T7 promoter. At 16 hours post-infection the expression of luciferase was measured with a bioluminescence assay and CAT with an enzyme-linked immunosorbent assay. CAT = Chloramphenicol Acetyl Transferase, fLuc = firefly luciferase, EMCV = encephalomyocarditis virus internal ribosomal entry site, VEGF-IRES = vascular endothelial growth factor internal ribosomal entry site, VEGF IRES AS = vascular endothelial growth factor internal ribosomal entry site in the anti-sense direction, H=hypoxia. An unpaired, two-tailed students T test was used to compare the mean bioluminescence and results are presented as mean ±SEM. *** = $P \leq 0.001$.

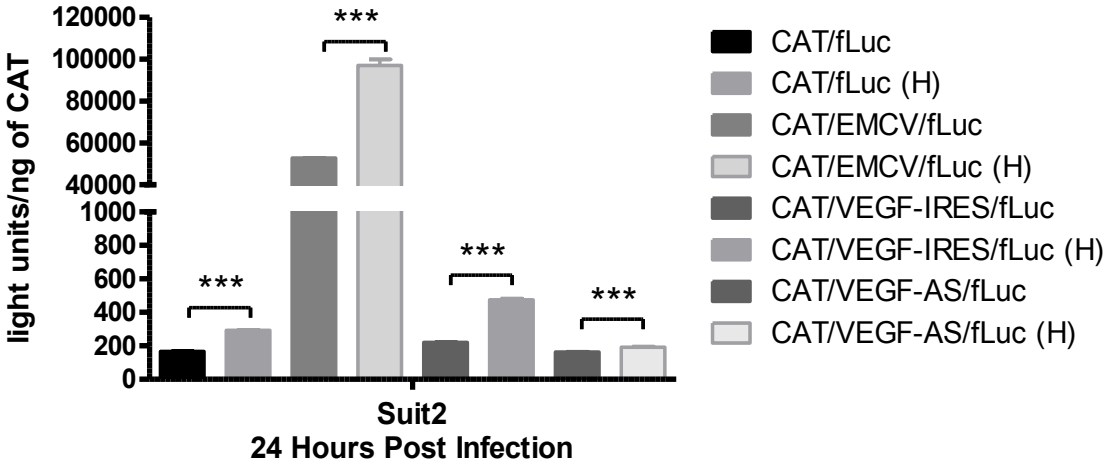

Figure 5.4: The use of a bicistronic vector to assess the efficacy of internal ribosomal entry sites in maintaining protein translation in hypoxia in Suit2.

Suit2 cells were transfected with the bicistronic vectors then infected with a vaccinia virus expressing a T7 promoter. At 16 hours post-infection the expression of luciferase was measured with a bioluminescence assay and CAT with an enzyme-linked immunosorbent assay. CAT = Chloramphenicol Acetyl Transferase, Luc = firefly luciferase, EMCV = encephalomyocarditis virus internal ribosomal entry site, VEGF-IRES = vascular endothelial growth factor internal ribosomal entry site, VEGF-AS = vascular endothelial growth factor internal ribosomal entry site in the anti-sense direction. An unpaired, two-tailed students T test was used to compare the mean bioluminescence and results are presented as mean ±SEM. *** = $P \leq 0.001$.

5.3 The efficacy of bioluminescence from VV-ODD and VVL15

Suit2 cells were used to compare the efficacy of bioluminescence from VV-ODD against the non-hypoxia-targeting virus VVL15. Cells were infected with either virus at an MOI = 1 pfu/cell, then exposed to normoxia or hypoxia for 24 hours. Evidence of increased bioluminescence was seen in this initial experiment and will be outlined in subsequent figures. However, the bioluminescent intensity from VV-ODD was 30 times lower than that seen in VVL15 (Figure 5.5). This may be a consequence of luciferase expression being transcribed through the IRES sequence rather than directly from the Vaccinia promoter or due to reduced luciferase protein efficacy once the ODD element was fused to it. In subsequent experiments VV-ODD was compared in normoxia and hypoxia and with VVL15.

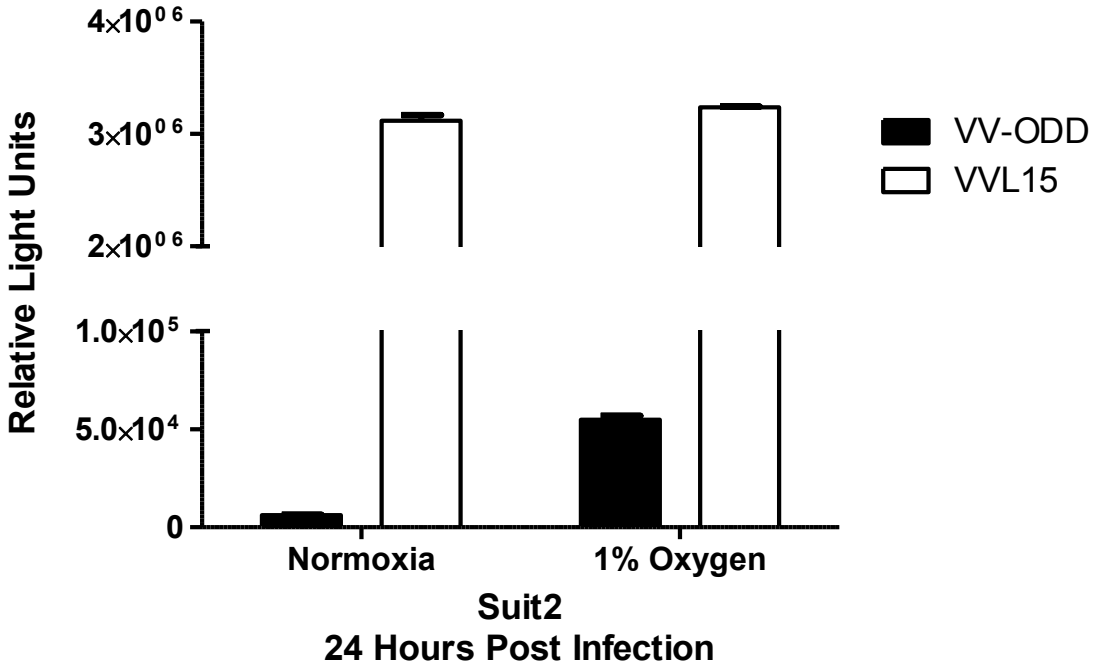

Figure 5.5: Comparison of bioluminescence from the oxygen sensitive VV-ODD and VVLI5

Suit 2 cells were infected with VV-ODD and VVL15 at an MOI = 1. Cell were then lysed at 24 hours post-infection and assayed for bioluminescence. An equal number of cells were seeded for each replicate and results are presented the mean bioluminescence ± SEM.

5.4 VV-ODD a hypoxia targeting Vaccinia virus shows efficacy in multiple cell lines

To verify the hypoxia targeting strategy, two PDAC cells lines and one breast cancer (BC) cell line were infected with VV-ODD. Suit2, MiaPaca2 (PDAC) and HeLa (BC) cells were infected with VV-ODD at an MOI=0.1pfu/cell and exposed to normoxia or hypoxia for 48 hours. Bioluminescence was measured using the Perkin Elmer Victor luminometer and normalised to RFP to give a ratio of hypoxia-targeting transgene expression over non-hypoxia-targeting. Values were normalised to the ratio of fLuc/RFP in each cell line and consequently the mean ratio in normoxia for each cell line is 1. There was a 10.2, 6.3 and 7.8 fold increase in bioluminescence in hypoxia in MiaPaca2, Suit2 and HeLa cell respectively, $P < 0.0001$ (Figure 5.6). This suggests that the hypoxia-targeting Vaccinia virus could be broadly applicable to multiple cell lines. However, this result does not show the individual contribution of each level of hypoxic regulation to the overall effect.

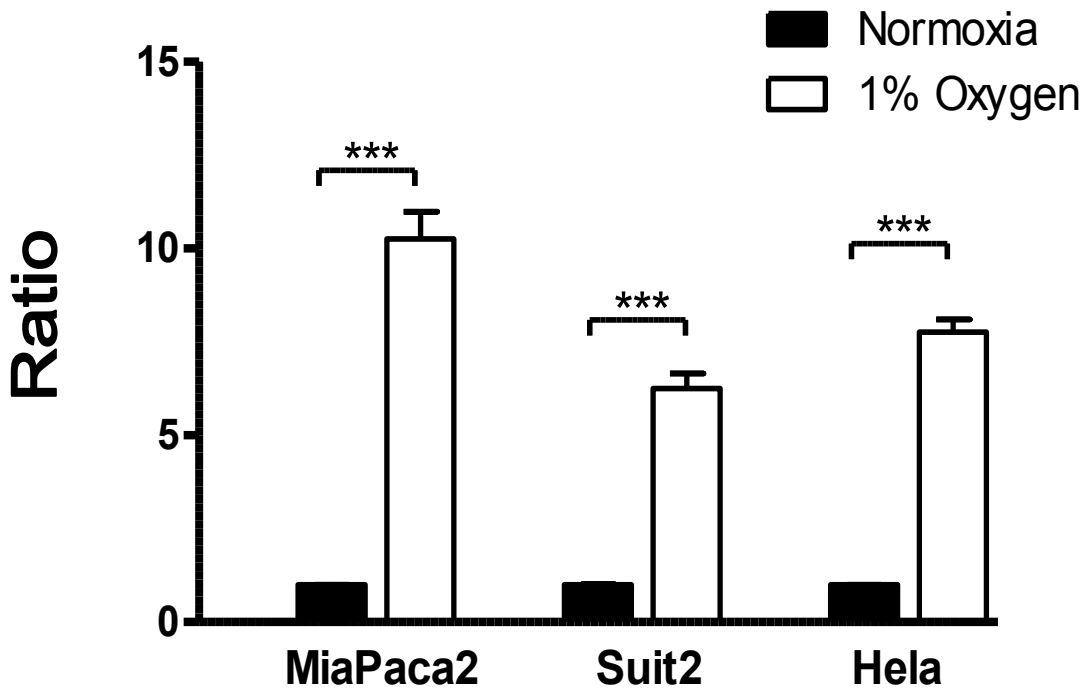

Figure 5.6: An example of the efficacy of VV-ODD in three different cell lines.

MiaPaca2, Suit2 and Hela cells were infected with VV-ODD at an MOI = 0.1 pfu/cell or mock infected. Cells were then incubated at the indicated oxygen concentrations for forty eight hours. Cells were then lysed and the luciferase activity and red fluorescence from VV-ODD was measured. Measurements were taken in duplicate from biological duplicates and normalised to the ratio in normoxia. The results are the combination of two independent experiments and presented as mean ± SEM. *** = $P \leq 0.001$ Students two tailed T-test.

5.5 A time-, dose- and oxygen concentration-dependent effect of VV-ODD

To show a time-dependent effect of VV-ODD, cells were infected with an MOI = 0.1 pfu/cell and exposed to normoxia or hypoxia. A time-dependent relationship with increasing relative difference between normoxic and hypoxic bioluminescence was seen in MiaPaca2 (Figure 5.7), Suit2 (Figure 5.8) and HeLa cells (Figure 5.9). The statistical significance was $P < 0.0001$ for all time points. In HeLa cells and Suit2 cells a 72 hour time point was not performed as in these cells lines significant cytopathic effect was seen.

To show a dose-dependent effect MiaPaca2 and Suit2 cells were infected with VV-ODD at an MOI=0.1, 1.0 and 5.0 pfu/cell and cells lysed at 24 hours post-infection (Figure 5.10 and Figure 5.11 respectively). An increase was seen from 0.1 to 1.0 pfu/cell indicating a dose-dependent effect. There was a further increase at 5 pfu/cell in Suit2 but the system appears to be saturated at this dose.

An oxygen-dependent increase was also noted when MiaPaca2 cells were infected with an MOI=0.1 pfu/cell. Infected cells were exposed to 0.1%, 1.0% and 5.0% oxygen for 24 hours. A small but significant increase in the bioluminescent ratio was seen in 5.0% oxygen compared to normoxia. However, more significant increases were seen at 1.0 and 0.1% oxygen (Figure 5.13). This is reassuring as this mimics the kinetics of HIF in different oxygen concentrations (213).

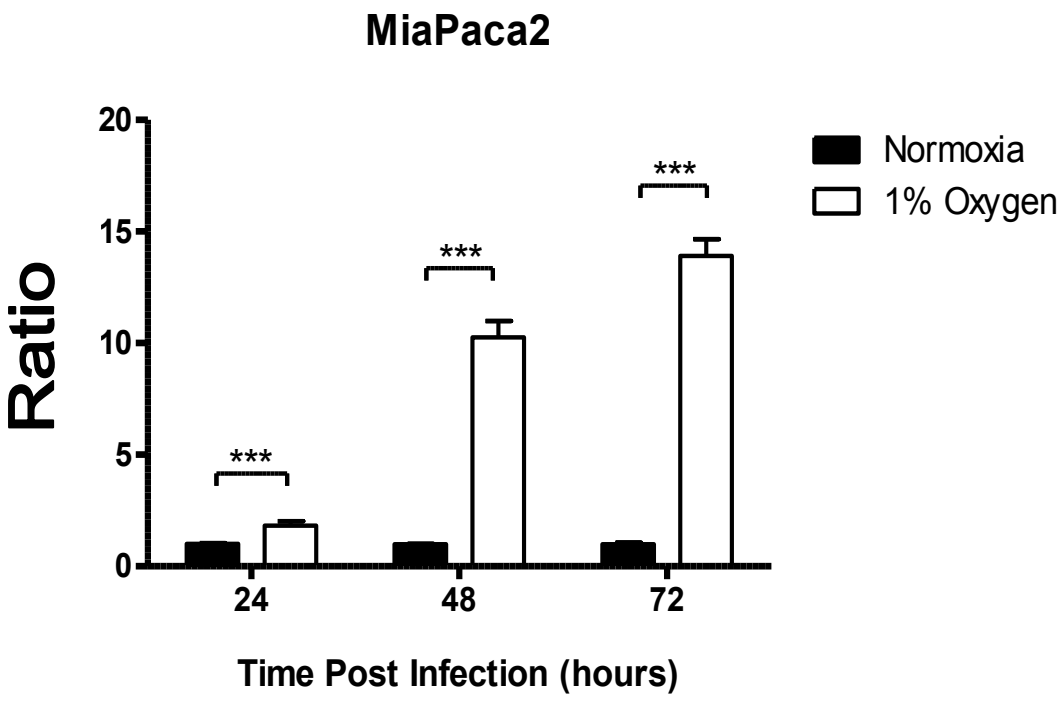

Figure 5.7: A time-dependent effect of luciferase expression from VV-ODD in MiaPaca2 cells.

Cells were infected with VV-ODD at an MOI=0.1 pfu/cell or mock infected. Cells were incubated at the indicated oxygen concentrations for 24, 48 and 72 hours. Cells were lysed and the luciferase activity and red fluorescence from VV-ODD was measured. Measurements were taken in duplicate from biological duplicates and normalised to the ratio in normoxia. The results are the combination of two independent experiments and presented as mean ± SEM. *** = $P \leq 0.001$ Students two tailed T-test.

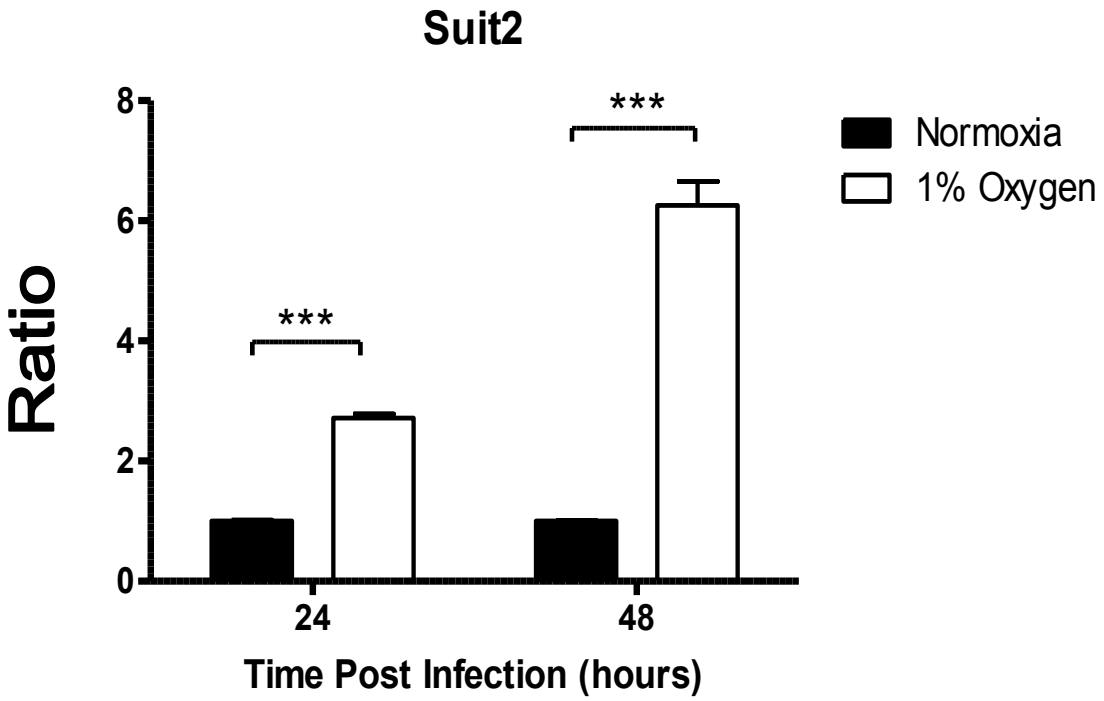

Figure 5.8: A time-dependent effect of luciferase expression from VV-ODD in Suit2 cells.

Cells were infected with VV-ODD at an MOI=0.1 pfu/cell or mock infected. Cells were incubated at the indicated oxygen concentrations for 24 and 48 hours. Cells were lysed and the luciferase activity and red fluorescence from VV-ODD was measured. Measurements were taken in duplicate from biological duplicates and normalised to the ratio in normoxia. The results are the combination of two independent experiments and presented as mean ± SEM. *** = $P \leq 0.001$ Students two tailed T-test.

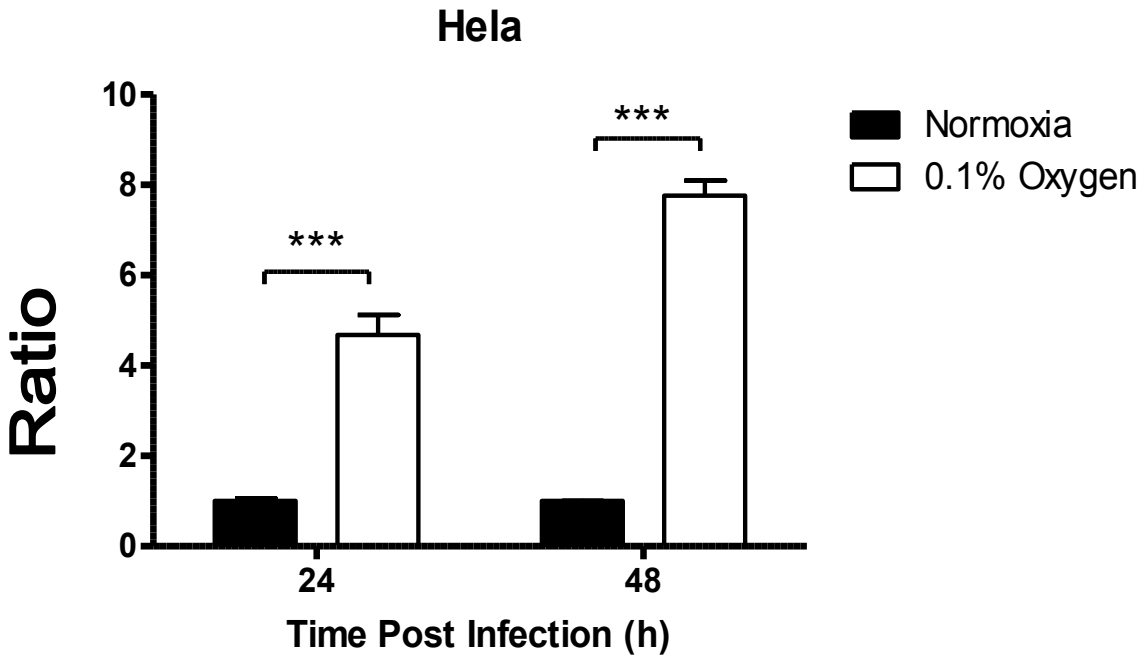

Figure 5.9: A time-dependent effect of luciferase expression from VV-ODD in Hela cells. Cells were infected with VV-ODD at an MOI = 0.1 pfu/cell or mock infected. Cells were incubated at the indicated oxygen concentrations for 24 and 48 hours. Cells were lysed and the luciferase activity and red fluorescence from VV-ODD was measured. Measurements were taken in duplicate from biological duplicates and normalised to the ratio in normoxia. The results are the combination of two independent experiments and presented as mean ± SEM. *** = $P \leq 0.001$ Students two tailed T-test.

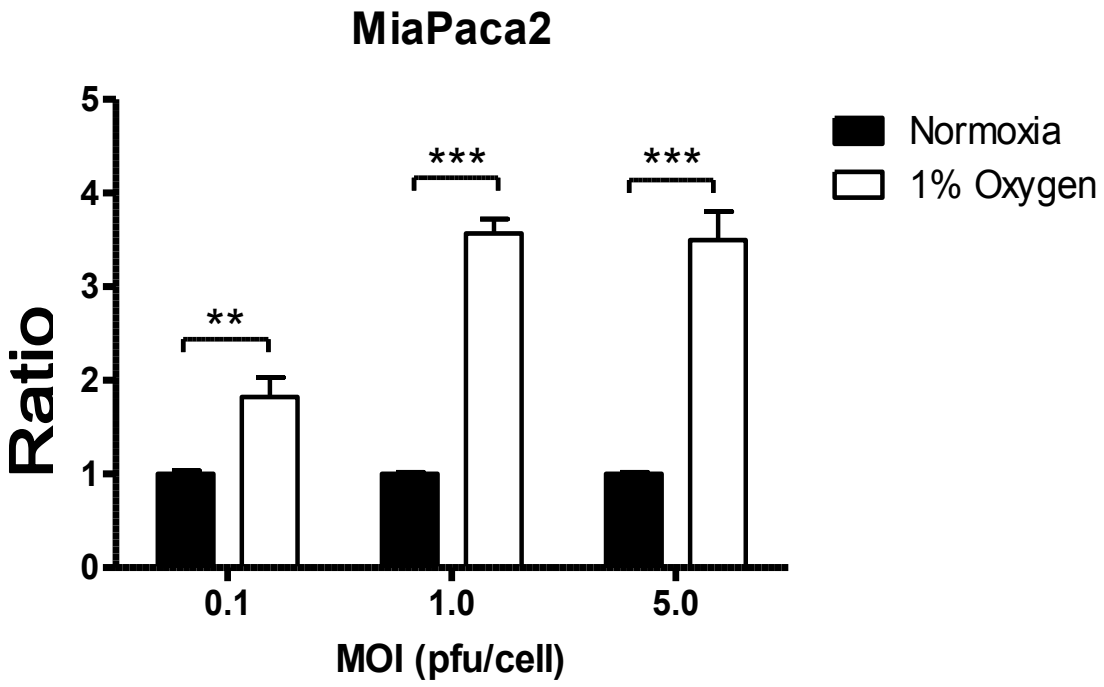

Figure 5.10: A dose-dependent effect of luciferase expression from VV-ODD in MiaPaca2 cells.

Cells were infected with VV-ODD at an MOI=0.1, 1.0 or 5.0 pfu/cell. Cells were incubated at 1% oxygen concentrations for 24 hours. Cells were lysed and the luciferase activity and red fluorescence from VV-ODD was measured. Measurements were taken in duplicate from biological duplicates and normalised to the ratio in normoxia. The results are the combination of two independent experiments and presented as mean ± SEM. *** = $P \leq 0.001$ Students two tailed T-test.

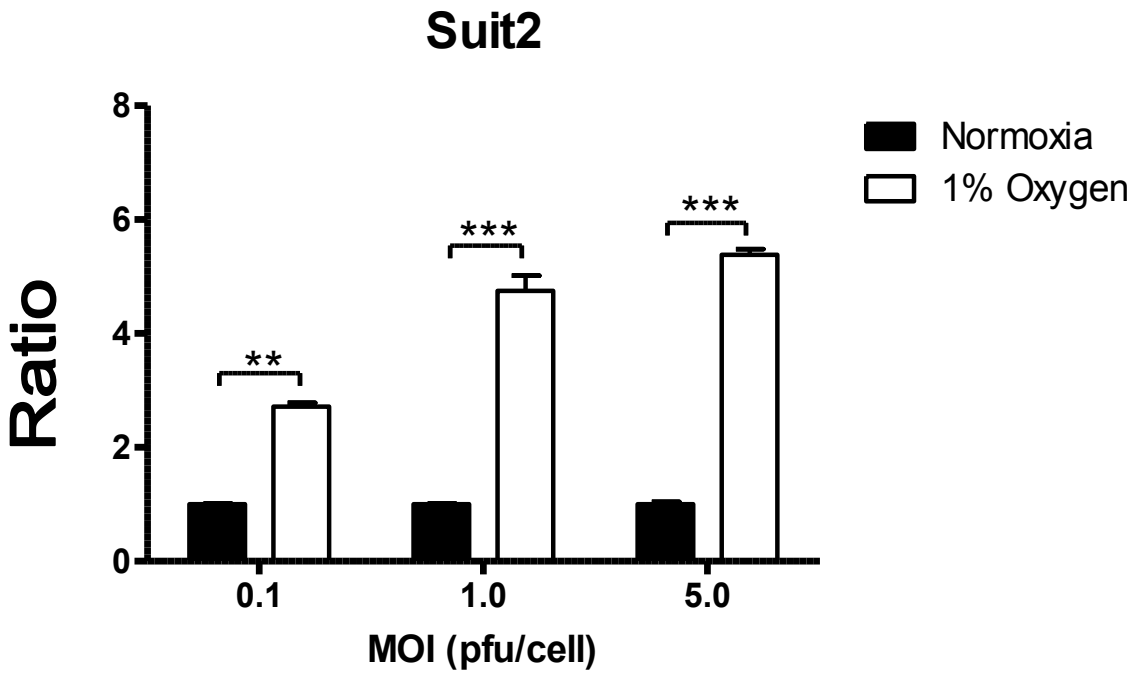

Figure 5.11: A dose-dependent effect of luciferase expression from VV-ODD in Suit2 cells.

Cells were infected with VV-ODD at an MOI = 0.1, 1.0 or 5.0 pfu/cell. Cells were incubated at 1% oxygen concentrations for 24 hours. Cells were lysed and the luciferase activity and red fluorescence from VV-ODD was measured. Measurements were taken in duplicate from biological duplicates and normalised to the ratio in normoxia. The results are the combination of two independent experiments and presented as mean ± SEM. *** = $P \leq 0.001$ Students two tailed T-test.

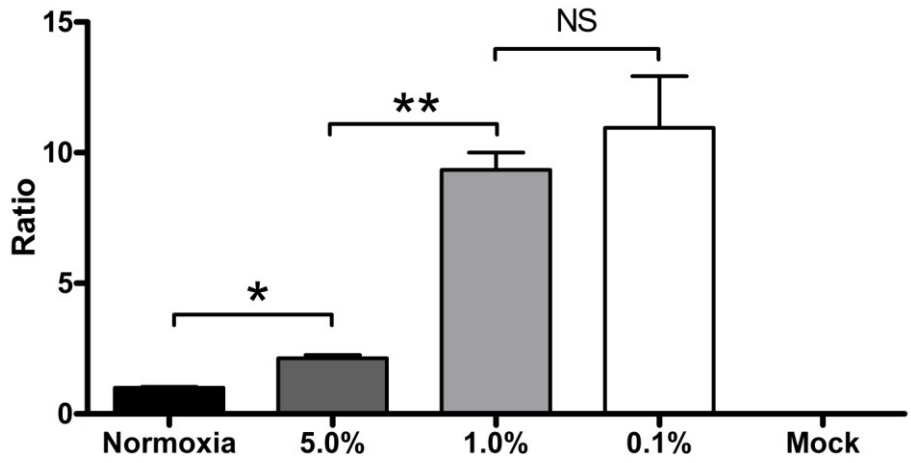

Figure 5.12: The effect of oxygen concentration on luciferase expression from VV-ODD.

MiaPaca2 cells were infected with VV-ODD at an MOI = 0.1 pfu/cell or mock-infected. Cells were then incubated at the indicated oxygen concentrations for forty eight hours. Cells were then lysed and the luciferase activity and red fluorescence from VV-ODD was measured. Measurements were taken in duplicate from biological duplicates and normalised to the ratio in normoxia. The results are the combination of two independent experiments and presented as mean ± SEM. * = $P \leq 0.05$, ** = $P \leq 0.01$. NS = not significant. Mann Whitney U test.

5.6 The effect of hypoxia mimetics and an inhibitor of proteasomal degradation on VV-ODD transgene expression

HeLa cells were infected with VV-ODD at an MOI = 1.0 pfu/cell and treated with the hypoxia mimetic Dimethyloxallyl Glycine (DMOG) at increasing concentrations for 48 hours. DMOG is a hypoxia mimetic that inhibits prolyl hydroxylase-dependent hydroxylation of the ODD (214). No cytotoxicity was seen at the concentrations used in HeLa cells. Cells were lysed at 48 hours after infection and a western blot for HIF-1α, the Luciferase-ODD fusion protein and the loading control B-actin was performed. As the concentration of DMOG increased stabilisation of HIF-1α was seen and increased levels of the Luciferase-ODD fusion protein were seen (Figure 5.13). The amount of Luciferase-ODD fusion protein present was quantified and is presented in Figure 5.14.

An alternative hypoxia mimetic Cobalt Chloride ($CoCl_2$) and the proteasomal inhibitor MG132 were also used to show the hypoxia-targeting ability of VV-ODD (213). These compounds were found to be cytotoxic on prolonged exposure so were used in a luciferase assay for 6 hours only. Hypoxia, at an oxygen concentration of 0.1% was used as a positive control. MiaPaca2 cells were infected with VV-ODD at an MOI = 0.1 pfu/cell or mock infected and then exposed to $CoCl_2$ (100 μM) and MG132 (10 μM). A significant increase was seen after treatment with both compounds showing that the ODD is functional in this fusion protein (Figure 5.15). However this assay may not utilise the 5' and 3' elements of the VV-ODD luciferase construct as these compounds are not known to have any effect on ribosomal scanning or mRNA stability unless indirectly through HIF-1α stabilisation and target gene transcription.

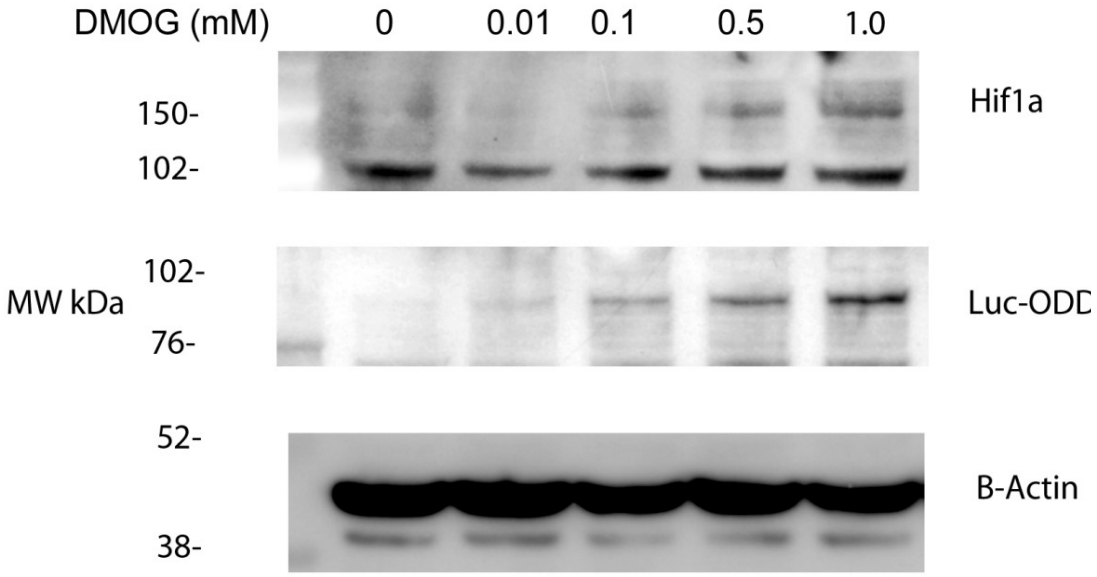

Figure 5.13: The effect of DMOG on VV-ODD fLuc stability.

Western blot of Hela cells infected with VV-ODD at MOI = 1 pfu/cell and then exposed to Dimethyloxallyl Glycine for 48 hours at the indicated concentrations or DMSO as control. Dimethyloxallyl Glycine is a cell-permeable competitive inhibitor of the HIF proyl hydroxylase enzymes and will stabilise luciferase expressed from VV-ODD. Membranes were probed for Hif1α, Luc-ODD and β-Actin. DMOG= Dimethyloxallyl Glycine, Luc-ODD=Luciferase/Oxygen degradation domain fusion protein.

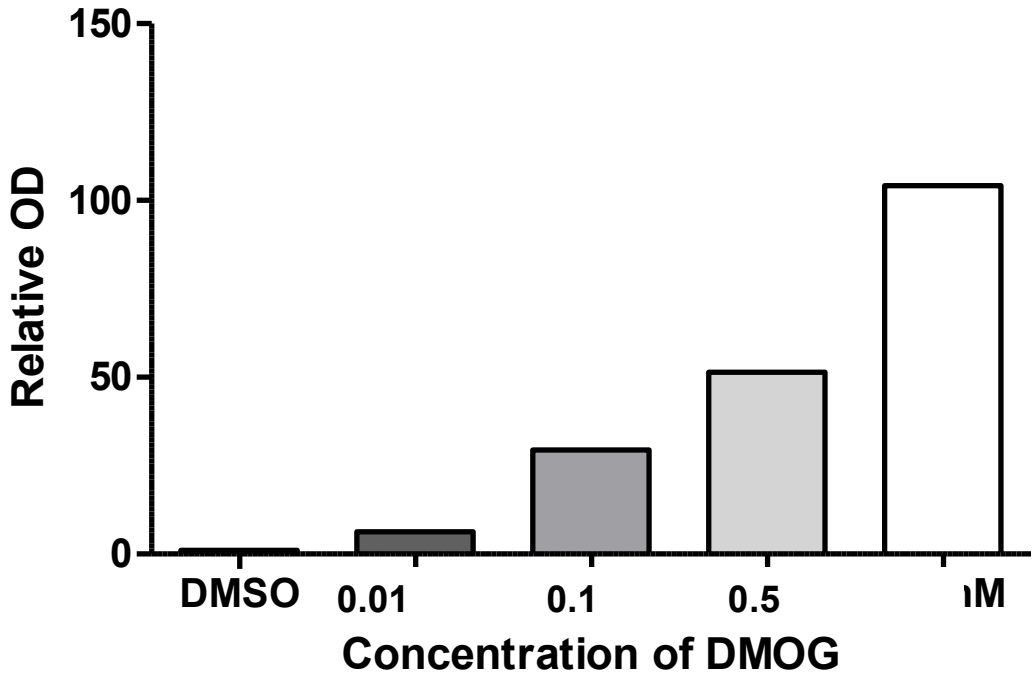

Figure 5.14: Quantification of the effect of DMOG on VV-ODD fLuc stability.

Quantification of Western blot of HeLa cells infected with VV-ODD (MOI = 1) and then exposed to DMOG at the indicated concentration (mM) for 48 hours. The optical density measurements are the ratio of Luciferase/Oxygen degradation domain fusion protein to that of the loading control Beta-Actin. Ratios were normalised to untreated cells. DMOG= Dimethyloxallyl Glycine, DMSO= Dimethyl sulfoxide.

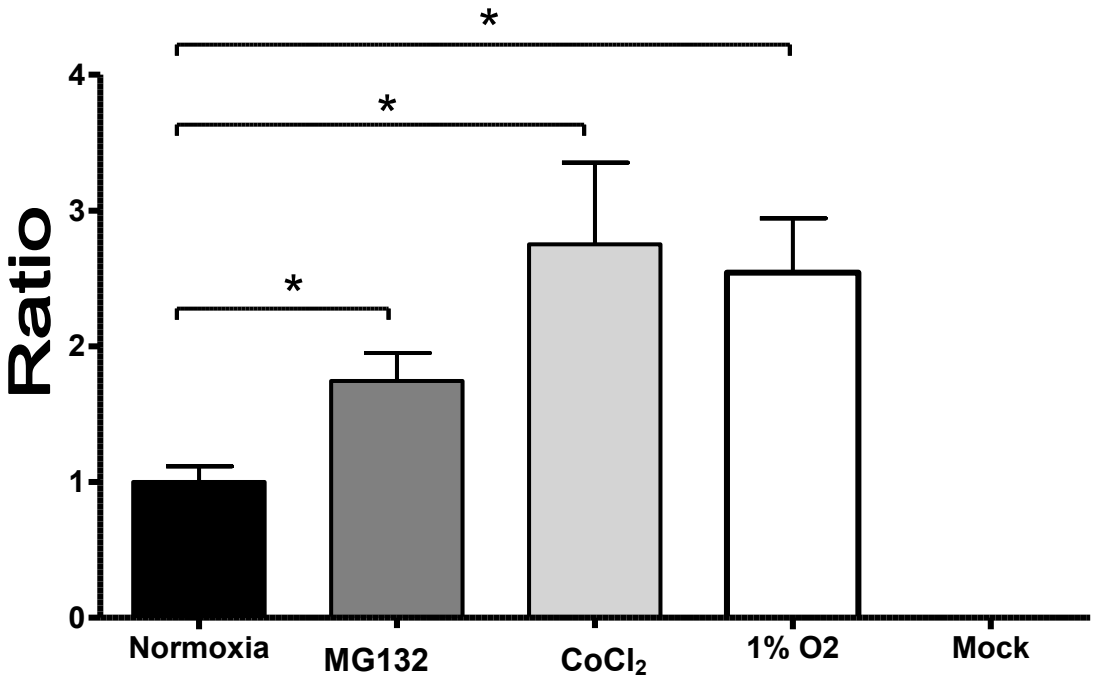

Figure 5.15: The effect of hypoxia mimetics and a proteasomal inhibitor on luciferase expression from VV-ODD.

MiaPaca2 cells were infected with VV-ODD at an MOI = 0.1 pfu/cell for twenty four hours or mock infected. They were then exposed to normoxia, 1% oxygen, the hypoxia mimetic Cobalt Chloride ($CoCl_2$) at 100 μM or the proteasomal inhibitor MG132 (10 μM) for six hours. Cells were lysed and the luciferase activity and red fluorescence from VV-ODD was measured. Measurements were taken in duplicate from biological duplicates and the results normalised to the ratio in normoxia. The results are the combination of two independent experiments and presented as mean ± SEM. * = $P \leq 0.05$ Students two tailed T-test**.**

Chapter 6

6 Discussion and Future Plan

6.1 Vaccinia Virus and Hypoxia

Wild-type Vaccinia virus has been well characterized and much of the molecular biology, genomic sequence, viral life cycle and immunology have been reported. Vaccinia virus has many inherent properties that make it an appealing candidate agent for oncolytic virotherapy. Vaccinia virus has a fast and efficient replication cycle with rapid cell-to-cell spread, a natural tropism for tumours, a strong lytic ability, large cloning capacity, is safe in humans and has good stability (167, 168, 215, 216). As outlined in the introduction, many tumours contain areas of hypoxia and these hypoxic regions contribute to the resistance of tumours to conventional therapy. Some oncolytic viruses have been shown to also be less effective in a hypoxic microenvironment. We have now demonstrated that hypoxia does not significantly affect viral gene expression, viral replication, cytotoxicity and it even enhances the tumour-killing activity in some PDAC cell lines by vaccinia virus.

We have demonstrated here that the Lister strain Vaccinia virus shows comparable efficacy in infection, replication and transgene expression in normoxia and hypoxia. It is important to highlight that hypoxic cells used in these experiments had been exposed to reduced oxygen concentration for at least 16 hours prior to infection. This is more likely to reflect cellular adaptation to hypoxia and model clinical Vaccinia virus infection than shorter exposure times that have been used for the study of other oncolytic viruses (101, 188). In addition, we found that effective tumour cell lysis was maintained after infection of hypoxic PDAC cell lines and in half of the cell lines tested there was a statistically significant improvement in viral cytotoxicity. In the metastatic cell line CFPac1 and the primary tumour cell line MiaPaca2 a 3.3-fold and 23-fold decrease in the EC50 value was seen, respectively, after 6 days of infection. This has implications for translational applications given that tumour lysis is the ultimate goal of oncolytic therapy and PDAC has been shown to contain areas of hypoxia (67).

Many groups have tried to target hypoxic fractions of tumours using hypoxia-specific promoters often containing hypoxia response elements (HRE) that facilitate HIF-1α binding and downstream gene transcription (176). Unfortunately such promoters are invariably less powerful drivers of gene expression than constitutive viral promoters and result in lower levels of gene expression and viral replication relative to wild-type viruses (174, 217). Our results show that Vaccinia virus has the capacity to infect and replicate in hypoxic tumour cells without the need for such approaches.

Conner *et al*. showed that Oncolytic Vesicular Stomatitis virus (VSV) has comparable viral replication in normoxic HeLa cells versus those exposed to 1% O2 for 2 hours prior to infection and only a slight reduction of virus-induced CPE on semi-quantitative analysis (188). It is a welcome finding that other oncolytic viruses are not affected by oxygen availability, this differs from adenovirus which is a commonly used oncolytic virus and has been shown to be attenuated in hypoxia (101, 103). However, our results suggest a several-fold, statistically significant improvement, rather than non-inferiority, in the oncolytic potential of Vaccinia virus in some pancreatic cell lines exposed to hypoxic conditions. Conner *et al* concluded that their results suggest an advantage of RNA viruses over DNA viruses in targeting hypoxic tumour cells because of a greater reduction of DNA synthesis in hypoxic cells (188). Vaccinia virus is a double-stranded DNA virus but like VSV replicates in the cytoplasm and encodes its own polymerases. Therefore our findings do not support their conclusion and suggest that the intracellular location of the viral life cycle could be an important factor in its potential as an oncolytic agent.

In contrast to Connor *et al*, Minami *et al* have found reduced replication of wildtype VSV in murine epidermal fibroblasts after exposure to hypoxia due to an increase in GADD34 (218). GADD34 is a cellular protein induced at times of cellular stress such as hypoxia and nutrient deprivation and was found to inhibit viral replication by inhibiting the mTOR pathway.

GADD34 was able to dephosphorylate and reverse the inhibitory effects of tuberous sclerosis complex 2 (TSC2) on the mTOR pathway, which regulated viral protein synthesis.

We have found similar replication of wildtype Lister strain Vaccinia virus in Panc1, MiaPaca2 and Suit2 cells in both normoxia and hypoxia. In Suit2, a permissive cell line, high titres were seen in both normoxia and hypoxia by 48 hours. However, at later time points up to four fold higher titres were seen in normoxic conditions. Interestingly this did not affect cytotoxicity in this cell line suggesting that either titres of 100pfu/cell are sufficient to cause cell lysis or that replication is not the rate-limiting step in cell death. In MiaPaca2 cells, an increase in cytotoxicity was found in hypoxic conditions but no significant increase in viral replication was seen, further supporting the idea that other factors affect cell lysis in addition to the burden of intracellular virions produced.

It is clear, however, that the effect of hypoxia on viral replication is specific to each virus. For example, in contrast to the observations for VSV, Aghi *et al* found that increased GADD34 in hypoxic conditions could significantly improve replication of the recombinant herpes simplex virus (HSV) G207 in the U87 glioma cell (219). This virus is deleted for the viral gamma 34.5 protein which normally stops the inhibition of protein translation during viral infection. The cellular GADD34 protein compensates for the deletion of this gene and so replication of the recombinant virus is increased in hypoxia relative to normoxia. The replication of wildtype HSV is similar in normoxia and hypoxia because of the presence of the γ34.5 gene and its replication is significantly higher than the recombinant virus. Therefore they suggest deletion of γ34.5 is a reason for the improved specificity of this virus in vivo. We have found that the cytotoxicity of both wildtype and a TK deleted recombinant Vaccinia virus (VVL15) can be increased, relative to normoxia, in some cell lines when exposed to 1% oxygen and is a beneficial property inherent to both wildtype and recombinant viral strains.

Viral infection induces innate anti-viral mechanisms that inhibit cellular protein synthesis and limit viral replication. This is similar to the effect of hypoxia on cells, which can also inhibit protein translation (184). Consequently viruses that have acquired mechanisms to subvert cellular protein synthesis for virus production during infection may be those most adaptable to hypoxic conditions. For example the oncolytic parvovirus, Minute virus of mice, has been shown to replicate poorly in hypoxia because it is unable to counteract the shutdown of protein translation (220). Protein kinase R (PKR) is a cellular protein involved in the anti-viral response and on viral infection it phosphorylates eIF2α inhibiting protein translation. Vaccinia virus however has two proteins E3L and K3L which act as pseudo-substrates, inhibiting the function of PKR (221). In our experiments we found that viral protein production was maintained in the CFPac1 and MiaPaca2 cell lines exposed to hypoxia. E3L and K3L mutant Vaccinia viruses have been produced (222) and assessing viral replication and cytotoxicty in hypoxia using these viruses would show if they are important for the oncolytic efficacy of Vaccinia virus in hypoxia.

This research shows the effect of 1% oxygen on Vaccinia virus replication and cytotoxicity. However, tumours are exposed to a range of oxygen tensions both acutely during temporary occlusion of the vasculature but also chronically when tumour cells are further than the diffusible distance of oxygen from a vessel. The effect of other forms and ranges of hypoxia on Vaccinia virus may be different and requires further investigation. Good transgene expression was seen at 0.1% oxygen using the hypoxia-targeting virus VV-ODD, suggesting that even lower concentrations of oxygen may not adversely affect Vaccinia virus. It is also unknown if the increase in cytotoxicity we have seen in hypoxia is HIF-1α dependent and further studies using RNAi strategies or HIF-null cells could be carried out to investigate this.

We were able to show a significant increase in bioluminescence from the recombinant virus VVL15 in MiaPaca2 cells after 4 hours of infection. This prompted us to look for a factor that regulates an early stage of the Vaccinia virus life cycle that could be affected by hypoxia. We

found that VEGF facilitates Vaccinia virus entry, however there are likely to be other factors regulated by hypoxia that affect both early and later stages of the Vaccinia virus life cycle and may contribute to the increased cytotoxicity found in MiaPaca2 and CFPac1 cell lines. For example, using an RNAi approach in a Drosophila model, AMP Kinase was recently identified as being involved in Vaccinia virus entry through the control of actin dynamics (223). Previously it has been shown that hypoxia can activate AMPK (224) and this may be another factor increasing viral cytotoxicity in hypoxia which could be confirmed by assessing AMPK activity in CFPac1 and MiaPaca2 cells exposed to hypoxia.

Our findings could also be relevant to others working more broadly on poxvirus biology. MiaPaca2 is a cell line relatively resistant to Vaccinia virus in normoxia with an EC50 of 183.4pfu/cell but becomes 23 fold more sensitive in hypoxia. This model could be used, through comparative gene expression and proteomic studies, to identify other host factors that are involved in the Vaccinia virus life cycle.

6.2 VEGF Facilitates the Vaccinia Virus Life Cycle

During the course of our investigation into the effect of hypoxia on Vaccinia virus we observed that increased cytotoxicity of the Lister strain virus was only found in those cell lines where there was a hypoxic induction of VEGF. Using VEGF gene silencing in Suit 2 (a cell line with a high endogenous VEGF level) and over expressing VEGF in MiaPaca2 (a cell line with a low endogenous VEGF level) we were able to show a functional relationship in PDAC cells *in vitro* and *in vivo*. Using these models we found that VEGF can affect Vaccinia virus replication, transgene expression and cytotoxicity. The cytotoxicity of Vaccinia virus was increased by over-expression of VEGF in MiaPaca2 cells and resulted in a 4.6 fold decrease in the EC50 value. This is not as great as the effect seen with hypoxia indicating that VEGF is only one of the factors modulated by hypoxia affecting Vaccinia virus efficacy. We were also able to increase viral cytotoxicity by the addition of exogenous rhVEGF-165 and decrease efficacy by VEGF gene silencing. However, the effect of VEGF gene silencing on the cytotoxicity of the Lister strain Vaccinia virus in Suit2 cells, although statistically significant, was small. Suit2 is a permissive cell line and supports high titres of Vaccinia virus replication, this suggests that the effect of VEGF on viral cytotoxicity may have more relevance to those cell lines that are more resistant to Vaccinia virus infection. This supports our hypothesis that once viral replication reaches moderate titres (~100pfu/cell) the maximal level of viral replication is no longer the main determinant of Vaccinia virus cytotoxicity.

Significantly we found that infection of MiaPaca2-VEGF-165 cells with the fLuc expressing virus VVL15 results in significantly higher bioluminescence at 4 hours post-infection compared to controls ($P < 0.01$). This mirrors the effect we had seen after exposure of VVL15 infected parental MiaPaca2 cells to hypoxia at this time point. It was apparent in our study, using both a quantitative PCR assay and fluorescent confocal microscopy to image internalisation of VVL-488, that VEGF facilitates the entry of the Lister strain Vaccinia virus. We did not find any effect of VEGF on viral attachment to cells, mRNA transcription or EEV release.

The innate interferon response, Ras pathway activity and the availability of cellular nucleotides are three cellular factors that are involved in pox virus tropism (225). Tumours produce higher levels of VEGF and other pro-angiogenic cytokines than normal tissue and hypoxia is an important regulator of VEGF production in this context (79).We propose that VEGF is an additional factor that is responsible for the tropism of Vaccinia virus for tumour cells by increasing the rate of viral internalisation. However, Vaccinia virus enters host cells by a number of mechanisms and it has been shown that cell entry is influenced by the form of virus used (IMV vs. EEV), the cell type infected and the strain of Vaccinia virus (128, 226, 227). Our virus preparations are prepared from lysed, infected CV1 cells after cytopathic effect is seen and will be predominately composed of IMVs. We have shown that VEGF affects the tropism of the Lister strain virus in PDAC cells but to ascertain whether this mechanism is more widely applicable to Vaccinia virus as a species and other cell types will require further investigation.

Primary infection with Vaccinia virus in a pathological context can occur through the respiratory tract. Vermeer *et al* have shown that EGF and the viral homologue VGF are important for Vaccinia infection of normal human bronchial epithelium (139).We were interested in whether VEGF affected Vaccinia virus infection in these non transformed cells so we used exogenous rhVEGF-165 to stimulate NHBE cells and found that viral replication was increased. This suggests that VEGF may have a wider role in the tropism of Vaccinia virus for different cell types. However internalisation of Vaccinia virus in NHBE cells was not directly analysed. Given that NHBE cells are likely to express more VEGFR1 and VEGFR2 than PDAC cells the mechanism may be different (193, 200).

Our finding that VEGF facilitates poxvirus infection is not surprising given that a number of poxviruses produce homologues to VEGF. VEGF-E was first described in the Orf virus, a member of the poxvirus family. VEGF-E is a 25 kDa protein that forms homodimers and binds to VEGFR2 and NRP1 but not VEGFR1 or VEGFR3 (89). It acts as a bridging molecule

between VEGFR2 and NRP1, which is thought to facilitate VEGF signalling and is important in Orf virus pathogenesis (92, 228). Subsequently it has been found that the genomes of other parapoxviruses, Bovine Papular Stomatitis Virus and Pseudocowpox virus all contain VEGF homologues (229). In contrast, there has been no reports of VEGF homologues in Vaccinia or any other orthopoxviruses but it is thought that the evolution of poxviruses has predominately been through gain and loss of eukaryotic genes from host cells. We have demonstrated that VEGF is able to increase viral internalisation, although this does not discount further mechanisms of action. VEGF secretion induced by hypoxia can also protect pancreatic cells from pro-apoptotic stimuli (230). Many viruses have mechanisms to inhibit virus-induced apoptosis, which facilitates maximal viral replication and also allows latent viral infection to occur (157). Future work could involve examining the effect of VEGF on the apoptotic fraction of virally infected cells by Annexin V or BrdU fluorescence-activated cell sorting analysis.

In vivo we were able to show that VEGF increases the bioluminescence of VVL15 in human xenografts in nude mice. Our group has found that bioluminescence is an effective surrogate for viral replication *in vivo*. VEGF improves Vaccinia virus replication in this mouse model, although viral recovery from tumours was not performed. In our mouse model of pancreatic cancer, VEGF may increase the rate of internalisation of Vaccinia virus as we have found *in vitro* but it also possible that it improves delivery to the tumour. VEGF increases vascular permeability and was originally named vascular permeability factor (73). The increased tumour targeting seen *in vivo* in this study may also be caused by better perfusion of the tumour with Vaccinia virus because of the more extensive vasculature which we have demonstrated in xenografts of MiaPaca-VEGF-165 compared to MiaPaca2-Vector Control. In addition more permeable tumour vasculature in VEGF-expressing stable cell lines could facilitate increased extravasation of this relatively large virus (200-250nm) at the site of tumours. The proportion of EEV re-entering the vasculature after subsequent rounds of viral replication could also be increased if surrounding vessels have been rendered more permeable by increased VEGF and would facilitate long-range spread of viral particles. We have not determined if these vessels are

more permeable and future work will involve the use of FITC dextran to see determine whether Vaccinia virus infection occurs more readily adjacent to areas of permeable vasculature in tumours.

VEGF has traditionally been thought to act in a paracrine fashion, being produced by tumour cells and ligating VEGF receptors on endothelial cells, so our finding that VEGF acts directly on PDAC cell *in vitro* was unexpected. However VEGF has been found to act in an autocrine factor through VEGFR1 and NRP1 on breast, colorectal and pancreatic cancer cell lines and seems to modulate cellular chemotaxis (198, 231, 232). Although we detected relatively low levels of VEGFR1 and no VEGFR2 a role cannot be excluded. An RNAi approach to silence and VEGF receptor expression could be performed to exclude any effect on Vaccinia virus internalisation. This would be preferable to VEGF receptor-blocking antibodies as others have shown that VEGF can act in an intracrine fashion on perinuclear VEGFR1 (201).

PDAC cells do express NRP1, which is a co-receptor for VEGF, which facilitates the binding of VEGF isoforms to VEGFR2. Previously, NRP1 was thought not to be involved directly in signalling, but to act as a co-receptor for VEGFR1 and VEGFR2, as it has a transmembrane but no intracellular domain itself (233). However, more recently it has been shown that it is a fairly promiscuous receptor and is involved in cell signalling by acting as a co-receptor with αVβ3 integrin or with C-Met (234-236). Interestingly, endocytic cycling of NRP1 has been shown to differ depending on the ligand. Studies to date on NRP1 and endocytosis have concentrated on endothelial cells. Salikhovaet *et al* showed that Nrp1 underwent clathrin-dependent endocytosis in response to VEGFp165 treatment, whereas its other ligand semaphorin 3C (sema3C) induced lipid raft-dependent endocytosis (237). Vaccinia virus uptake has been shown to occur at the site of lipd rafts, suggesting that NRP1 may act as a receptor or be involved in viral uptake (144). NRP1 has already been implicated in the entry and pathogenesis of another virus human T cell leukaemia virus (HTLV) (238). In this context NRP1 forms a ternary complex with HTLV-Env proteins, NRP1 and the hypoxia inducible gene Glucose transporter 1 (Glut1).

We effectively used NRP1 gene silencing to knockdown NRP1 protein expression however, NRP1 gene silencing actually increased Lister strain Vaccinia virus transgene expression by approximately twenty percent. Class 3 semaphorin family members have been shown to inhibit lammelipodia formation via NRP1, which can be blocked by heparin-binding forms of VEGF (239-241). It is tempting to speculate that VEGF may alter the balance of signalling via NRP1 with other ligands, semaphorins and plexins, resulting in a change in actin dynamics that favour virus internalisation. The possibility that NRP1 acts as a receptor or co-receptor for Vaccinia virus appears unlikely given our results but needs to be formally excluded by looking for NRP1 and Vaccinia virus co-localisation using fluorescent confocal microscopy. Investigating the role of class 3 semaphorins on Vaccinia virus infectivity could be performed, by overexpressing and silencing NRP1, in a similar manner to the viral assays described here for VEGF. This offers an intriguing possibility to augment Vaccinia virus potency as strategies to augments VEGF activity are unlikely to be approved by new drug regulatory agents whereas blocking of semaphorin activity prior to Vaccinia virus may be more acceptable.

VEGF may act via a non-receptor mediated effect as it interacts with cell surface GAGs via its heparin binding domain and alter their distribution or availability at the cell surface. GAGs have been implicated in Vaccinia virus pathogenesis and virus infectivity can be partially blocked by heparin and heparan sulphate (125, 227). One hypothesis could be that VEGF is able to bind heparin and heparans on the cell surface and block the inhibitory effects of GAGs on Vaccinia virus entry, thereby augmenting Vaccinia virus infectivity via a non signalling-dependent mechanism. We have confirmed that GAGs inhibit Lister strain infectivity (data not shown) but have been unable to use GAGs reproducibly in the internalisation assays outlined in this thesis to confirm if they antagonise the effects of VEGF. Further work to establish an assay to test this contention could use a self-quenching rhodamine B-labelled Vaccinia virus, a potentially more sensitive tool, to assess the interaction of GAGs and VEGF on virus membrane fusion with target cells ((242) & personal communication B Moss).

Akt is a central protein involved in actin dynamics, which acts downstream of NRP1, VEGFR2 and VEGFR1 (78, 243). Akt has recently been described as an important determinate of the susceptibility to infection by myxoma virus, a member of the Leporipoxvirus genus of poxviruses (158). Although we have been unable to clarify the receptor implicated in the effect of VEGF on Vaccinia virus internalisation, we have shown that Akt phosphorylation does affect Vaccinia virus infection. Inhibition of Akt reduces Vaccinia virus internalisation, transgene expression and cytotoxicity in a dose-dependent manner. Others have shown that Akt is phosphorylated early during Vaccinia virus infection and is also involved in later stages of the viral life cycle (159, 204). In addition we also show that Akt inhibition reduces VEGF production in the context of viral infection and may also affect the internalisation of Vaccinia virus in this manner.

During the course of the project, data have been published suggesting that one of the forms of cell entry used by Vaccinia virus is fluid phase endocytosis or macropinocytosis (146). Whether VEGF affects this mode of cell entry either by stimulating VEGF signalling pathway, acting as a scaffold for Vaccinia internalisation complex or reducing the inhibitory effect of GAGs is not clear. Mercer *et al* have shown that the Western Reserve (WR) strain Vaccinia virus induced membrane blebbing and the IHD-J strain induces filiopodia formation. They are both sensitive to inhibitors of actin polymerization and depolymerization (cytochalasin D and jasplakinolide) and myosin II (blebbistatin) but have different sensitivities to the effect of pH or GAGs on virus entry (226). Unlike WR IMVs, infection by IHD-J IMVs was not inhibited by genistein (tyrosine kinase inhibitor), nor by wortmannin (PI(3)-kinase inhibitor). Given these differences between strains, a full screen of inhibitors on the entry of the Lister strain Vaccinia virus needs to be performed to ascertain which mode of cell entry VEGF affects. Inhibitors of macropinocytosis, kinases and inhibitors of actin polymerization and depolymerisation could be used in an initial screen and then validated with siRNA gene silencing or transfection with dominant-negative proteins. Arginine rich cell penetrating peptides, originally identified from

the HIV tat protein, and now Vaccinia virus has been shown to use macropinocytosis as a mode of cell entry (244). Teesalu *et al* recently showed that the arginine-containing C-terminal of VEGF, which is not by definition arginine-rich, is important for cellular internalisation of NRP1 (245) and raises the possibility of a role for VEGF in macropinocytosis.

The results from this study to date are firstly that hypoxia does not significantly affect the efficacy of oncolytic Vaccinia virus. Furthermore, this study has highlighted a wider role for VEGF in the tropism of Vaccinia virus. These results are useful for the field of Vaccinia virus oncolytic therapy but may also have implication of Vaccinia virus based cancer vaccines and more general poxvirus pathogenesis. Although it has been demonstrated that increased internalisation of viral particles occurs in the presence of VEGF and that Akt inhibition can reverse this, the mode of internalisation and the signalling pathway through which it acts is unclear and requires further investigation.

6.3 The Hypoxia-Targeting Oncolytic Virus VV-ODD

This section outlines the structure and function of a novel hypoxia-targeting oncolytic Vaccinia virus. Other viral vectors have been constructed to target hypoxia using a hypoxia-responsive adenovirus for cancer therapy with a hypoxia-responsive adeno-associated virus for cardiovascular disease (176, 246). However, both these approaches utilise an HRE to drive expression in hypoxia. The use of an HRE results in a significantly reduced gene expression compared to endogenous viral promoters and because of Vaccinia's reliance on viral polymerases cannot be used in this vector. To produce VV-ODD, a construct was designed that incorporated three levels of hypoxic regulation; transcriptional regulation using the VEGF 3'UTR, translational regulation using an IRES sequence and post-translational regulation using the HIF-1α ODD.

A bicistronic vector system was used to compare the function of the EMCV IRES and the VEGF 5'UTR on transgene expression, in normoxia and hypoxia, using a CAT and luciferase reporter assay. Contrary to published reports, we found limited evidence that the 5 'UTR of the VEGFA gene functioned as an IRES sequence. There was a less than a two-fold difference between the fLuc/CAT ratio containing the VEGF 5'UTR and the control vector in both normoxia and hypoxia. Given that eukaryotic promoters would not drive a transgene located in the Vaccinia virus genome our results further suggest that the predominant feature of the 5' UTR is a cryptic promoter rather than an IRES. Our findings also support the more extensive report by Bert *et al* that shows the VEGF 5'UTR contains a cryptic promoter and has only minimal function as an IRES sequence in comparison the EMCV IRES (247). The EMCV IRES clearly functions as an IRES sequence in the context of viral infection using a T7 polymerase expressing Vaccinia virus to drive reporter gene expression. In the permissive PDAC cell line Suit2, there is an 84% increase in hypoxia of protein translation from the IRES compared to normoxia. Consequently the EMCV IRES was selected as the IRES sequence for VV-ODD.

When the bioluminescence from VV-ODD was compared to that of VVL15 there was a 30-fold decrease in bioluminescent signal using our virus. VVL15 contains an unmodified firefly luciferase reporter gene driven directly from the Vaccinia virus promoter with no intervening IRES sequence. It is unclear from our results if the decrease observed was caused by reduced enzymatic activity of the luciferase ODD fusion protein or reduced protein translation from the IRES in comparison to 5' methyl cap-dependent translation. Simple plasmid vector studies could be performed to compare the enzymatic activity of a modified *versus* unmodified luciferase protein. This highlights that the functionality of all new transgenes after being fused to the ODD will need to be reassessed *versus* control to demonstrate there is still sufficient biological efficacy. Future work will incorporate an amino acid spacer in between transgenes and the ODD as this has been demonstrated to preserve the biological function of fusion proteins (248).

It is equally as likely that the IRES, although functioning well in hypoxia, may not be sufficient for sufficient transcription of downstream genes. Our lab and others have found that the downstream sequence appears to be significantly more poorly expressed compared to the upstream sequence (249). Although IRES sequences allow the expression of multiple transgenes, in this context where highly efficient transgene expression is required, it does not add value in our vector design. The shuttle vector for this virus has been designed so that this sequence can be easily removed, making production of future generations of VV-ODD without an IRES sequence straightforward.

VV-ODD was used to infect two PDAC cell lines and HeLa cells to see if the concept of a hypoxia-targeting virus was feasible. We have demonstrated, using a reporter gene assay, that in all cell lines tested we are able to show a virus dose, time and oxygen-dependent effect. Significantly more luciferase expression is seen in cells infected with VV-ODD exposed to hypoxia at 24-72 hours post-infection and at MOIs from 0.1 – 5.0 pfu/cell. We have shown that the function of this construct mirrors the kinetics of HIF-1 when exposed to different oxygen

concentrations. Significantly more luciferase expression was seen at 0.1% oxygen versus 5.0% oxygen using VV-ODD. In the absence of a closed system for manipulation of cells in hypoxia, DMOG was used to inhibit PHD enzymes and stabilise the Luciferase-ODD fusion protein for Western blotting. We were able to demonstrate a dose-range effect with increasing concentrations on DMOG (0.01-1.0 mM) causing stabilisation of both HIF-1α and the Luciferase-ODD fusion protein. Using our reporter gene assay we were also able to show that another hypoxia mimetic ($CoCl_2$) and an inhibitor of proteasomal degradation (MG132) are able to increase bioluminescence from VV-ODD. In summary, we have shown through the use of different oxygen concentrations, hypoxia mimetics and inhibitors of HIF-1α degradation that the principle of our hypoxia-targeting Vaccinia virus is valid.

Our construct also contains a 3'UTR that has been reported to increase mRNA stability (209). We have used the smallest AU-rich region from the UTR in our construct but have not formally tested the contribution of this to our results. Future work will assess the requirement for this sequence by constructing reporter constructs expressing luciferase with or without the VEGF 3'UTR under the control of a Vaccinia virus promoter. Co infection/transfection studies with such reporter plasmids and the wildtype Lister strain Vaccinia virus in cells exposed to hypoxia/normoxia, both with and without an inhibitor of transcription (actinomycin D) would quantify the requirement for this sequence in future generations of viruses.

I have outlined above how the requirements for the IRES sequence and 3'UTR in future constructs will be assessed and subsequently modified. However, there maybe additional modifications that need to be introduced. Firstly our Vaccinia virus constructs contain two viral early termination sequences. These are strings of nucleotides (TTTTTNT) that signal termination of mRNA transcription by the Vaccinia virus ternary polymerase complexes when driven from an early promoter of Vaccinia virus (250). Two such sequences are present in our construct in the ODD sequence and the 3'UTR. Point mutations are possible that will remove these features without affecting the function of either sequence. Currently it is possible that

truncated fusions proteins are produced when transcription is driven from the early promoter. This means that a fraction of the luciferase reporter protein produced on infection with VV-ODD is not regulate by hypoxia and may result in increased baseline bioluminescence. Removing these early termination sequences may reduce any "leak" in this system and help improve specificity.

Recently it has been found the stabilisation of HIF-1α can also be caused by S-nitrosylation at Cysteine 533, independent of conventional hydroxylation by PHD enzymes (251). Li *et al* demonstrated that tumour-associated macrophages, after tumour irradiation, were a source of nitric oxide (NO) that stabilised HIF-1α in normoxia. This would be undesirable for our hypoxia-targeting virus and NO production is likely in the context of viral infection *in vivo*. In line with Li *et al* we have mutated the Cysteine to Serine in our fusion protein shuttle plasmid so that future generations of viruses would not be susceptible to this form of stabilisation. This is an important modification to make before any *in vivo* experiments are performed. *In vivo* experiments using systemically delivered VV-ODD and then luciferase imaging after hydralazine administration or carbogen inhalation to induce or reverse tumour hypoxia respectively will be required to validate the concept *in vivo* (252).

Although we have constructed a virus that is effectively able to target transgene expression to hypoxia it will also result in transgene expression in systems where the pathways for HIF-1α proteasomal degradation are disrupted. Such examples include loss of the VHL protein or PHD enzyme function. These mutations are often associated with malignancy and the loss of VHL is central to the pathogenesis of clear cell renal cell carcinoma (253). This system is unlikely to result in complete loss of transgene expression in normoxia and will increase the function of the transgene in hypoxia. Complete loss of transgene expression in normoxic cancer cells is undesirable and we anticipate that a combination of this construct and the dose delivered will result in a balance that will improve specificity and may reduce toxicity in translation applications.

A hypoxia-targeting virus would be a useful tool in the development of a clinically feasible oncolytic Vaccinia virus therapy. As initial clinical trial results show evidence of biological efficacy using replication-competent Vaccinia viruses, future generations of viruses will contain transgenes to improve efficacy. The principle, as demonstrated by VV-ODD, could be applied in several ways. Firstly, to create a conditionally replicating Vaccinia virus by applying this principle to a critical viral protein such as the viral ribonulceotide reductase (254). Alternatively, the luciferase reporter gene in VV-ODD could be replaced by a therapeutic transgene. Pro-drug converting enzymes such as NADPH:cytochrome P450 reductase are important in activating the bioreductive chemotherapy tirapazamine. Attempts to use adenovirus to target hypoxia in such a gene therapy approach have shown some specificity but limited efficacy (255) presumably as adenovirus replicate poorly in hypoxia. In contrast he VV-ODD concept could be used to deliver high levels of NADPH:cytochrome P450 reductase to hypoxic tumours. Hypoxia reduces the sensitivity of cells to radiotherapy and we are interested in using this concept to restore radiosensitivity to hypoxic tumours. Given the proximity of major vessels and other organs to the pancreas, the radiation doses delivered to patients with locally advanced PDAC are limited to 40-50Gy. Other tumour types, such as head & neck and prostate cancer, have shown significant responses when doses of radiation reach 80Gy. Even with more targeted delivery such as intensity-modulated radiotherapy (IMRT) and stereotactic radiotherapy, doses are still limited, as is access to this technology. Using the VV-ODD concept, transgene delivery specifically to tumour cells may allow us to restore radiosensitivity by augmenting cell death pathways or by restoring the oxygen enhancement ratio.

Hypoxia may be an important problem for viral therapy but offers possibilities to improve specificity (185). I have outlined the principle and demonstrated the function of the hypoxia-targeting virus VV-ODD. This could be used in many ways to treat the hypoxic component of pancreatic cancer and other tumour types with hypoxic regions although, like other oncolytic viruses, treatment is still limited by the ability to reach tumours. However, given the advantages

of Vaccinia virus for systemic delivery we believe that the concept of VV-ODD will be useful in the development of a clinically relevant oncolytic viral therapy.

7 References

1. Stewart B, Kleihues P. World Cancer Report. Stewart B, Kleihues P, editors. Lyon: IARC Press; 2003.

2. Almoguera C, Shibata D, Forrester K, Martin J, Arnheim N, Perucho M. Most human carcinomas of the exocrine pancreas contain mutant c-K-ras genes. Cell. 1988;53(4):549-54.

3. Marshall J. Clinical implications of the mechanism of epidermal growth factor receptor inhibitors. Cancer. 2006;107(6):1207-18.

4. Blasco F, Penuelas S, Cascallas M, Hernaindez JL, Alemany C, Masa M, et al. Expression profiles of a human pancreatic cancer cell line upon induction of apoptosis search for modulators in cancer therapy. Oncology. 2004;67(3-4):277-90.

5. Hruban RH, Goggins M, Parsons J, Kern SE. Progression Model for Pancreatic Cancer. Clin Cancer Res. 2000;6(8):2969-72.

6. Izeradjene K, Combs C, Best M, Gopinathan A, Wagner A, Grady W, et al. Kras(G12D) and Smad4/Dpc4 haploinsufficiency cooperate to induce mucinous cystic neoplasms and invasive adenocarcinoma of the pancreas. Cancer Cell. 2007;11(3):229-43.

7. Ghaneh P, Costello, E., Neoptolemos, JP. Biology and management of pancreatic cancer. Gut. 2007;56(8):1134.

8. UK-National-Statistics. Cancer Statistics registrations: registrations of cancer diagnosed in 2004, England. UK Office for National Statistics. 2007.

9. Neoptolemos JP, Stocken DD, Friess H, Bassi C, Dunn JA, Hickey H, et al. A Randomized Trial of Chemoradiotherapy and Chemotherapy after Resection of Pancreatic Cancer. N Engl J Med. 2004;350(12):1200-10.

10. Oettle H, Post S, Neuhaus P, Gellert K, Langrehr J, Ridwelski K, et al. Adjuvant Chemotherapy With Gemcitabine vs Observation in Patients Undergoing Curative-Intent Resection of Pancreatic Cancer: A Randomized Controlled Trial. JAMA. 2007;297(3):267-77.

11. Neoptolemos J, Buchler M, Stocken DD, Ghaneh P, Smith D, Bassi C, et al. ESPAC-3(v2): A multicenter, international, open-label, randomized, controlled phase

III trial of adjuvant 5-fluorouracil/folinic acid (5-FU/FA) versus gemcitabine (GEM) in patients with resected pancreatic ductal adenocarcinoma. J Clin Oncol (Meeting Abstracts). 2009;27(18S):4505.

12. Burris HA, 3rd, Moore MJ, Andersen J, Green MR, Rothenberg ML, Modiano MR, et al. Improvements in survival and clinical benefit with gemcitabine as first- line therapy for patients with advanced pancreas cancer: a randomized trial. J Clin Oncol. 1997;15(6):2403-13.

13. Sultana A, Smith CT, Cunningham D, Starling N, Neoptolemos JP, Ghaneh P. Meta-Analyses of Chemotherapy for Locally Advanced and Metastatic Pancreatic Cancer. J Clin Oncol. 2007;25(18):2607-15.

14. Cunningham D, Chau I, Stocken DD, Valle JW, Smith D, Steward W, et al. Phase III Randomized Comparison of Gemcitabine Versus Gemcitabine Plus Capecitabine in Patients With Advanced Pancreatic Cancer. J Clin Oncol. 2009;27(33):5513-8.

15. Moore MJ, Goldstein D, Hamm J, Figer A, Hecht JR, Gallinger S, et al. Erlotinib Plus Gemcitabine Compared With Gemcitabine Alone in Patients With Advanced Pancreatic Cancer: A Phase III Trial of the National Cancer Institute of Canada Clinical Trials Group. J Clin Oncol. 2007;25(15):1960-6.

16. Philip PA, Benedetti J, Corless CL, Wong R, O'Reilly EM, Flynn PJ, et al. Phase III Study Comparing Gemcitabine Plus Cetuximab Versus Gemcitabine in Patients With Advanced Pancreatic Adenocarcinoma: Southwest Oncology Group-Directed Intergroup Trial S0205. J Clin Oncol. 2010;28(22):3605-10.

17. Kindler HL, Niedzwiecki D, Hollis D, Sutherland S, Schrag D, Hurwitz H, et al. Gemcitabine Plus Bevacizumab Compared With Gemcitabine Plus Placebo in Patients With Advanced Pancreatic Cancer: Phase III Trial of the Cancer and Leukemia Group B (CALGB 80303). J Clin Oncol. 2010:1386.

18. Corsini MM, Miller RC, Haddock MG, Donohue JH, Farnell MB, Nagorney DM, et al. Adjuvant radiotherapy and chemotherapy for pancreatic carcinoma: the Mayo Clinic experience (1975-2005). J Clin Oncol. 2008;26(21):3511-6.

19. Hazard L, Tward JD, Szabo A, Shrieve DC. Radiation therapy is associated with improved survival in patients with pancreatic adenocarcinoma: results of a study from the Surveillance, Epidemiology, and End Results (SEER) registry data. Cancer. 2007;110(10):2191-201.

20. Huguet F, Girard N, Guerche CS-E, Hennequin C, Mornex F, Azria D. Chemoradiotherapy in the Management of Locally Advanced Pancreatic Carcinoma: A Qualitative Systematic Review. J Clin Oncol. 2009;27(13):2269-77.

21. Hawkins LK, Lemoine NR, Kirn D. Oncolytic biotherapy: a novel therapeutic plafform. Lancet Oncol. 2002;3(1):17-26.

22. Harris A. Hypoxia--a key regulatory factor in tumour growth. Nat Rev Cancer. 2002;2(1):38-47.

23. Hockel M, Vaupel P. Tumor Hypoxia: Definitions and Current Clinical, Biologic, and Molecular Aspects. J Natl Cancer Inst. 2001;93(4):266-76.

24. Thomlinson R, Gray L. The histological structure of some human lung cancers and the possible implications for radiotherapy. Br J Cancer. 1955;9(4):10.

25. Rampling R, Cruickshank G, Lewis AD, Fitzsimmons SA, Workman P. Direct measurement of pO2 distribution and bioreductive enzymes in human malignant brain tumors. Int J Radiat Oncol Biol Phys. 1994;29(3):427-31.

26. Lartigau E, Randrianarivelo H, Avril MF, Margulis A, Spatz A, Eschwage F, et al. Intratumoral oxygen tension in metastatic melanoma. Melanoma Res. 1997;7(5):400-6.

27. Nordsmark M, Alsner J, Keller J, Nielsen OS, Jensen OM, Horsman MR, et al. Hypoxia in human soft tissue sarcomas: adverse impact on survival and no association with p53 mutations. Br J Cancer. 2001;84(8):1070-5.

28. Movsas B, Chapman JD, Horwitz EM, Pinover WH, Greenberg RE, Hanlon AL, et al. Hypoxic regions exist in human prostate carcinoma. Urology. 1999;53(1):11-8.

29. Hutchison GJ, Valentine HR, Loncaster JA, Davidson SE, Hunter RD, Roberts SA, et al. Hypoxia-inducible factor 1alpha expression as an intrinsic marker of hypoxia: correlation with tumor oxygen, pimonidazole measurements, and outcome in locally advanced carcinoma of the cervix. Clin Cancer Res. 2004;10(24):8405-12.

30. Tomes L, Emberley E, Niu Y, Troup S, Pastorek J, Strange K, et al. Necrosis and hypoxia in invasive breast carcinoma. Breast Cancer Res Treat. 2003;81(1):61-9.

31. Swinson D, Jones J, Richardson D, Wykoff C, Turley H, Pastorek J, et al. Carbonic Anhydrase IX Expression, a Novel Surrogate Marker of Tumor Hypoxia, Is

Associated With a Poor Prognosis in Non-Small-Cell Lung Cancer. J Clin Oncol. 2003;21(3):473-82.

32. Koong AC, Mehta VK, Le QT, Fisher GA, Terris DJ, Brown JM, et al. Pancreatic tumors show high levels of hypoxia. Int J Radiat Oncol Biol Phys. 2000;48(4):919-22.

33. Nordsmark M, Overgaard M, Overgaard J. Pretreatment oxygenation predicts radiation response in advanced squamous cell carcinoma of the head and neck. Radiother Oncol. 1996;41(1):31-9.

34. Wang GL, Jiang BH, Rue EA, Semenza GL. Hypoxia-inducible factor 1 is a basic-helix-loop-helix-PAS heterodimer regulated by cellular O2 tension. Proc Natl Acad Sci U S A. 1995;92(12):5510-4.

35. Wang GL, Semenza GL. General involvement of hypoxia-inducible factor 1 in transcriptional response to hypoxia. Proc Natl Acad Sci U S A. 1993;90(9):4304-8.

36. Semenza GL, Wang GL. A nuclear factor induced by hypoxia via de novo protein synthesis binds to the human erythropoietin gene enhancer at a site required for transcriptional activation. Mol Cell Biol. 1992;12(12):5447-54.

37. Gorlach A, Camenisch G, Kvietikova I, Vogt L, Wenger RH, Gassmann M. Efficient translation of mouse hypoxia-inducible factor-1alpha under normoxic and hypoxic conditions. Biochim Biophys Acta. 2000;1493(1-2):125-34.

38. Sutter CH, Laughner E, Semenza GL. Hypoxia-inducible factor 1alpha protein expression is controlled by oxygen-regulated ubiquitination that is disrupted by deletions and missense mutations. Proc Natl Acad Sci U S A. 2000;97(9):4748-53.

39. Laughner E, Taghavi P, Chiles K, Mahon PC, Semenza GL. HER2 (neu) signaling increases the rate of hypoxia-inducible factor 1alpha (HIF-1alpha) synthesis: novel mechanism for HIF-1-mediated vascular endothelial growth factor expression. Mol Cell Biol. 2001;21(12):3995-4004.

40. Kaelin WG. Molecular basis of the VHL hereditary cancer syndrome. Nat Rev Cancer. 2002;2(9):673-82.

41. Masson N, Ratcliffe PJ. HIF prolyl and asparaginyl hydroxylases in the biological response to intracellular O2 levels. J Cell Sci. 2003;116(Pt 15):3041-9.

42. Lando D, Peet DJ, Whelan DA, Gorman JJ, Whitelaw ML. Asparagine hydroxylation of the HIF transactivation domain a hypoxic switch. Science. 2002;295(5556):858-61.

43. Semenza GL, Jiang B-H, Leung SW, Passantino R, Concordet J-P, Maire P, et al. Hypoxia Response Elements in the Aldolase A, Enolase 1, and Lactate Dehydrogenase A Gene Promoters Contain Essential Binding Sites for Hypoxia-inducible Factor 1. J Biol Chem. 1996;271(51):32529-37.

44. Chi J-T, Wang Z, Nuyten DSA, Rodriguez EH, Schaner ME, Salim A, et al. Gene Expression Programs in Response to Hypoxia: Cell Type Specificity and Prognostic Significance in Human Cancers. PLoS Med. 2006;3(3):e47.

45. Movsas B, Chapman JD, Hanlon AL, Horwitz EM, Greenberg RE, Stobbe C, et al. Hypoxic prostate/muscle pO2 ratio predicts for biochemical failure in patients with prostate cancer: preliminary findings. Urology. 2002;60(4):634-9.

46. Ghafar MA, Anastasiadis AG, Chen M-W, Burchardt M, Olsson LE, Xie H, et al. Acute hypoxia increases the aggressive characteristics and survival properties of prostate cancer cells. Prostate. 2003;54(1):58-67.

47. Hockel M, Schlenger K, Aral B, Mitze M, Schaffer U, Vaupel P. Association between tumor hypoxia and malignant progression in advanced cancer of the uterine cervix. Cancer Res. 1996;56(19):4509-15.

48. Nakamura M, Bodily JM, Beglin M, Kyo S, Inoue M, Laimins LA. Hypoxia-specific stabilization of HIF-1alpha by human papillomaviruses. Virology. 2009.

49. Tang X, Zhang Q, Nishitani J, Brown J, Shi S, Le AD. Overexpression of human papillomavirus type 16 oncoproteins enhances hypoxia-inducible factor 1 alpha protein accumulation and vascular endothelial growth factor expression in human cervical carcinoma cells. Clin Cancer Res. 2007;13(9):2568-76.

50. Liu YL, Yu JM, Song XR, Wang XW, Xing LG, Gao BB. Regulation of the chemokine receptor CXCR4 and metastasis by hypoxia-inducible factor in non small cell lung cancer cell lines. Cancer Biol Ther. 2006;5(10):1320-6.

51. Polyak K, Weinberg RA. Transitions between epithelial and mesenchymal states: acquisition of malignant and stem cell traits. Nat Rev Cancer. 2009;9(4):265-73.

52. Sahlgren C, Gustafsson MV, Jin S, Poellinger L, Lendahl U. Notch signaling mediates hypoxia-induced tumor cell migration and invasion. Proc Natl Acad Sci U S A. 2008;105(17):6392-7.

53. Cannito S, Novo E, Compagnone A, Valfre di Bonzo L, Busletta C, Zamara E, et al. Redox mechanisms switch on hypoxia-dependent epithelial-mesenchymal transition in cancer cells. Carcinogenesis. 2008;29(12):2267-78.

54. Pàez-Ribes M, Allen E, Hudock J, Takeda T, Okuyama H, Viñals F, et al. Antiangiogenic Therapy Elicits Malignant Progression of Tumors to Increased Local Invasion and Distant Metastasis. Cancer Cell. 2009;15(3):220-31.

55. Brown NS, Bicknell R. Hypoxia and oxidative stress in breast cancer. Oxidative stress: its effects on the growth, metastatic potential and response to therapy of breast cancer. Breast Cancer Res. 2001;3(5):323-7.

56. Mizumachi T, Suzuki S, Naito A, Carcel-Trullols J, Evans TT, Spring PM, et al. Increased mitochondrial DNA induces acquired docetaxel resistance in head and neck cancer cells. Oncogene. 2008;27(6):831-8.

57. Savage P, Stebbing J, Bower M, Crook T. Why does cytotoxic chemotherapy cure only some cancers? Nat Clin Pract Oncol. 2009;6(1):43-52.

58. Denekamp J, Dasu A, Waites A. Vasculature and microenvironmental gradients: the missing links in novel approaches to cancer therapy? Adv Enzyme Regul. 1998;38:281-99.

59. Rice GC, Hoy C, Schimke RT. Transient hypoxia enhances the frequency of dihydrofolate reductase gene amplification in Chinese hamster ovary cells. Proc Natl Acad Sci U S A. 1986;83(16):5978-82.

60. Gray LH, Conger AD, Ebert M, Hornsey S, Scott OC. The concentration of oxygen dissolved in tissues at the time of irradiation as a factor in radiotherapy. Br J Radiol. 1953;26(312):638-48.

61. Sundfor K, Lyng H, Rofstad EK. Tumour hypoxia and vascular density as predictors of metastasis in squamous cell carcinoma of the uterine cervix. Br J Cancer. 1998;78(6):822-7.

62. Hiley CT, Green MML, Shanks JH, Bottomley IC, West CML, Cowan RA, et al. Expression of vascular endothelial growth factor (VEGF) in locally invasive prostate

cancer is prognostic for radiotherapy outcome. Int J Radiat Oncol Biol Phys. 2007;67(1):84-90.

63. Nordsmark M, Hayer M, Keller J, Nielsen OS, Jensen OM, Overgaard J. The relationship between tumor oxygenation and cell proliferation in human soft tissue sarcomas. Int J Radiat Oncol Biol Phys. 1996;35(4):701-8.

64. Bussink J, van der Kogel AJ, Kaanders JH. Activation of the PI3-K/AKT pathway and implications for radioresistance mechanisms in head and neck cancer. Lancet Oncol. 2008;9(3):288-96.

65. Zhang X, Kon T, Wang H, Li F, Huang Q, Rabbani Z, et al. Enhancement of Hypoxia-Induced Tumor Cell Death In vitro and Radiation Therapy In vivo by Use of Small Interfering RNA Targeted to Hypoxia-Inducible Factor-1alpha. Cancer Res. 2004;64(22):8139-42.

66. Hoffmann A-C, Mori R, Vallbohmer D, Brabender J, Klein E, Drebber U, et al. High expression of HIF1a is a predictor of clinical outcome in patients with pancreatic ductal adenocarcinomas and correlated to PDGFA, VEGF, and bFGF. Neoplasia. 2008;10(7):674-9.

67. Kitada T, Seki S, Sakaguchi H, Sawada T, Hirakawa K, Wakasa K. Clinicopathological significance of hypoxia-inducible factor-1alpha expression in human pancreatic carcinoma. Histopathology. 2003;43(6):550-5.

68. Yokoi K, Fidler IJ. Hypoxia increases resistance of human pancreatic cancer cells to apoptosis induced by gemcitabine. Clin Cancer Res. 2004;10(7):2299-306.

69. Folkman J. Tumor Angiogenesis: Therapeutic Implications. N Engl J Med. 1971;285(21):1182-6.

70. Tandle A, Blazer D, Libutti S. Antiangiogenic gene therapy of cancer: recent developments. J Transl Med. 2004;2(1):22.

71. Hodivala-Dilke KM, Reynolds AR, Reynolds LE. Integrins in angiogenesis: multitalented molecules in a balancing act. Cell Tissue Res. 2003;314(1):131-44.

72. Dome B, Dobos J, Tovari J, Paku S, Kovacs G, Ostoros G, et al. Circulating bone marrow-derived endothelial progenitor cells: characterization, mobilization, and therapeutic considerations in malignant disease. Cytometry A. 2008;73(3):186-93.

73. Senger DR, Galli SJ, Dvorak AM, Perruzzi CA, Harvey VS, Dvorak HF. Tumor cells secrete a vascular permeability factor that promotes accumulation of ascites fluid. Science. 1983;219(4587):983-5.

74. Ferrara N. The role of vascular endothelial growth factor in pathological angiogenesis. Breast Cancer Res Treat. 1995;36(2):127-37.

75. Hicklin DJ, Ellis LM. Role of the vascular endothelial growth factor pathway in tumor growth and angiogenesis. J Clin Oncol. 2005;23(5):1011-27.

76. Ferrara N, Henzel WJ. Pituitary follicular cells secrete a novel heparin-binding growth factor specific for vascular endothelial cells. Biochem Biophys Res Commun. 1989;161(2):851-8.

77. Ladomery M, Harper S, Bates D. Alternative splicing in angiogenesis: the vascular endothelial growth factor paradigm. Cancer Lett. 2007;249(2):133-42.

78. Ferrara N, Gerber HP, LeCouter J. The biology of VEGF and its receptors. Nat Med. 2003;9(6):669-76.

79. Pugh CW, Ratcliffe PJ. Regulation of angiogenesis by hypoxia: role of the HIF system. Nat Med. 2003;9(6):677-84.

80. Levy AP, Levy NS, Wegner S, Goldberg MA. Transcriptional regulation of the rat vascular endothelial growth factor gene by hypoxia. J Biol Chem. 1995;270(22):13333-40.

81. Papakonstanti EA, Zwaenepoel O, Bilancio A, Burns E, Nock GE, Houseman B, et al. Distinct roles of class IA PI3K isoforms in primary and immortalised macrophages. J Cell Sci. 2008;121(Pt 24):4124-33.

82. Konishi T, Huang CL, Adachi M, Taki T, Inufusa H, Kodama K, et al. The K-ras gene regulates vascular endothelial growth factor gene expression in non-small cell lung cancers. Int J Oncol. 2000;16(3):501-11.

83. Okada F, Rak JW, Croix BS, Lieubeau B, Kaya M, Roncari L, et al. Impact of oncogenes in tumor angiogenesis: mutant K-ras up-regulation of vascular endothelial growth factor/vascular permeability factor is necessary, but not sufficient for tumorigenicity of human colorectal carcinoma cells. Proc Natl Acad Sci U S A. 1998;95(7):3609-14.

84. Bouvet M, Ellis LM, Nishizaki M, Fujiwara T, Liu W, Bucana CD, et al. Adenovirus-mediated wild-type p53 gene transfer down-regulates vascular endothelial growth factor expression and inhibits angiogenesis in human colon cancer. Cancer Res. 1998;58(11):2288-92.

85. Fujisawa T, Watanabe J, Kamata Y, Hamano M, Hata H, Kuramoto H. VEGF expression and its reguration by p53 gene transfection in endometrial carcinoma cells. Hum Cell. 2003;16(1):47-54.

86. Zundel W, Schindler C, Haas-Kogan D, Koong A, Kaper F, Chen E, et al. Loss of PTEN facilitates HIF-1-mediated gene expression. Genes Dev. 2000;14(4):391-6.

87. Maxwell PH, Pugh CW, Ratcliffe PJ. The pVHL-hIF-1 system. A key mediator of oxygen homeostasis. Adv Exp Med Biol. 2001;502:365-76.

88. Meyer M, Clauss M, Lepple-Wienhues A, Waltenberger J, Augustin HG, Ziche M, et al. A novel vascular endothelial growth factor encoded by Orf virus, VEGF-E, mediates angiogenesis via signalling through VEGFR-2 (KDR) but not VEGFR-1 (Flt-1) receptor tyrosine kinases. EMBO J. 1999;18(2):363-74.

89. Wise LM, Veikkola T, Mercer AA, Savory LJ, Fleming SB, Caesar C, et al. Vascular endothelial growth factor (VEGF)-like protein from orf virus NZ2 binds to VEGFR2 and neuropilin-1. Proc Natl Acad Sci U S A. 1999;96(6):3071-6.

90. Mercer AA, Wise LM, Scagliarini A, McInnes CJ, Battner M, Rziha HJ, et al. Vascular endothelial growth factors encoded by Orf virus show surprising sequence variation but have a conserved, functionally relevant structure. J Gen Virol. 2002;83(Pt 11):2845-55.

91. Pieren M, Prota AE, Ruch C, Kostrewa D, Wagner A, Biedermann K, et al. Crystal structure of the Orf virus NZ2 variant of vascular endothelial growth factor-E. Implications for receptor specificity. J Biol Chem. 2006;281(28):19578-87.

92. Savory LJ, Stacker SA, Fleming SB, Niven BE, Mercer AA. Viral vascular endothelial growth factor plays a critical role in orf virus infection. J Virol. 2000;74(22):10699-706.

93. Zeimet AG, Marth C. Why did p53 gene therapy fail in ovarian cancer? Lancet Oncol. 2003;4(7):415-22.

94. Rhim JH, Tosato G. Targeting the Tumor Vasculature to Improve the Efficacy of Oncolytic Virus Therapy. J Natl Cancer Inst. 2007;99(23):1739-41.

95. Krone B, Kölmel KF, Henz BM, Grange JM. Protection against melanoma by vaccination with Bacille Calmette-Guérin (BCG) and/or vaccinia: an epidemiology-based hypothesis on the nature of a melanoma risk factor and its immunological control. Eur J Cancer. 2005;41(1):104-17.

96. Young LS, Searle PF, Onion D, Mautner V. Viral gene therapy strategies: from basic science to clinical application. J Pathol. 2006;208(2):299-318.

97. Liu TC, Galanis E, Kirn D. Clinical trial results with oncolytic virotherapy: a century of promise, a decade of progress. Nat Clin Pract Oncol. 2007;4(2):101-17.

98. Garber K. China Approves World's First Oncolytic Virus Therapy For Cancer Treatment. J Natl Cancer Inst. 2006;98(5):298-300.

99. Mulvihill S, Warren R, Venook A, Adler A, Randlev B, Heise C, et al. Safety and feasibility of injection with an E1B-55 kDa gene-deleted, replication-selective adenovirus (ONYX-015) into primary carcinomas of the pancreas: a phase I trial. Gene Ther. 2001;8(4):308-15.

100. Hecht JR, Bedford R, Abbruzzese JL, Lahoti S, Reid TR, Soetikno RM, et al. A phase I/II trial of intratumoral endoscopic ultrasound injection of ONYX-015 with intravenous gemcitabine in unresectable pancreatic carcinoma. Clin Cancer Res. 2003;9(2):555-61.

101. Shen B, Hermiston T. Effect of hypoxia on Ad5 infection, transgene expression and replication. Gene Ther. 2005;12(11):902-10.

102. Pipiya T, Sauthoff H, Huang YQ, Chang B, Cheng J, Heitner S, et al. Hypoxia reduces adenoviral replication in cancer cells by downregulation of viral protein expression. Gene Ther. 2005;12(11):911-7.

103. Shen B, Bauzon M, Hermiston T. The effect of hypoxia on the uptake, replication and lytic potential of group B adenovirus type 3 (Ad3) and type 11p (Ad11p). Gene Ther. 2006;13(12):986-90.

104. Swietach P, Vaughan-Jones RD, Harris AL. Regulation of tumor pH and the role of carbonic anhydrase 9. Cancer Metastasis Rev. 2007;26(2):299-310.

105. Baxby D. The Origins of Vaccinia Virus. J Infect Dis. 1977;136(3):453-5.

106. Fenner F. Smallpox and Its Eradication (History of International Public Health, No. 6). Geneva: World Health Organization; 1988.

107. Goebel SJ, Johnson GP, Perkus ME, Davis SW, Winslow JP, Paoletti E. The complete DNA sequence of vaccinia virus. Virology. 1990;179(1):247-66, 517-63.

108. Guo ZS, Bartlett DL. Vaccinia as a vector for gene delivery. Expert Opin Biol Ther. 2004;4(6):901-17.

109. Luker KE, Hutchens M, Schultz T, Pekosz A, Luker GD. Bioluminescence imaging of vaccinia virus: Effects of interferon on viral replication and spread. Virology. 2005;341(2):284-300.

110. Hayasaka D, Ennis F, Terajima M. Pathogeneses of respiratory infections with virulent and attenuated vaccinia viruses. Virol J. 2007;4(1):22.

111. Tartaglia J, Perkus ME, Taylor J, Norton EK, Audonnet JC, Cox WI, et al. NYVAC: a highly attenuated strain of vaccinia virus. Virology. 1992;188(1):217-32.

112. Connor JD, McIntosh K, Cherry JD, Benenson AS, Alling DW, Rolfe UT, et al. Primary Subcutaneous Vaccination. J Infect Dis. 1977;135(1):167-75.

113. Garcel A, Crance J-M, Drillien R, Garin D, Favier A-L. Genomic sequence of a clonal isolate of the vaccinia virus Lister strain employed for smallpox vaccination in France and its comparison to other orthopoxviruses. J Gen Virol. 2007;88(7):1906-16.

114. Moss B. Poxviridae: the viruses and their replication, Fields Virology. 4th Edition ed. Knie DM, Howley PM, editors. Philadelphia: Lippincott Williams and Wilkins; 2001.

115. Cyrklaff M, Risco C, Fernandez JJ, Jimanez MV, Estaban M, Baumeister W, et al. Cryo-electron tomography of vaccinia virus. Proc Natl Acad Sci U S A. 2005;102(8):2772-7.

116. Roberts KL, Smith GL. Vaccinia virus morphogenesis and dissemination. Trends Microbiol. 2008;16(10):472-9.

117. Shen Y, Nemunaitis J. Fighting cancer with vaccinia virus: teaching new tricks to an old dog. Mol Ther. 2005;11(2):180-95.

118. McFadden G. Poxvirus tropism. Nat Rev Micro. 2005;3(3):201-13.

119. Gaggar A, Shayakhmetov DM, Lieber A. CD46 is a cellular receptor for group B adenoviruses. Nat Med. 2003;9(11):1408-12.

120. Bergelson J, Cunningham J, Droguett G, Kurt-Jones E, Krithivas A, Hong J, et al. Isolation of a Common Receptor for Coxsackie B Viruses and Adenoviruses 2 and 5. Science. 1997;275(5304):1320-3.

121. Moss B. Poxvirus entry and membrane fusion. Virology. 2006;344(1):48-54.

122. Hsiao J-C, Chung C-S, Chang W. Cell Surface Proteoglycans Are Necessary for A27L Protein-Mediated Cell Fusion: Identification of the N-Terminal Region of A27L Protein as the Glycosaminoglycan-Binding Domain. J Virol. 1998;72(10):8374-9.

123. Lin C-L, Chung C-S, Heine HG, Chang W. Vaccinia Virus Envelope H3L Protein Binds to Cell Surface Heparan Sulfate and Is Important for Intracellular Mature Virion Morphogenesis and Virus Infection In Vitro and In Vivo. J Virol. 2000;74(7):3353-65.

124. Chung C-S, Hsiao J-C, Chang Y-S, Chang W. A27L Protein Mediates Vaccinia Virus Interaction with Cell Surface Heparan Sulfate. J Virol. 1998;72(2):1577-85.

125. Carter GC, Law M, Hollinshead M, Smith GL. Entry of the vaccinia virus intracellular mature virion and its interactions with glycosaminoglycans. J Gen Virol. 2005;86(5):1279-90.

126. Whitbeck JC, Foo C-H, Ponce de Leon M, Eisenberg RJ, Cohen GH. Vaccinia virus exhibits cell-type-dependent entry characteristics. Virology. 2009;385(2):383-91.

127. Townsley A, Weisberg A, Wagenaar T, Moss B. Vaccinia Virus Entry into Cells via a Low-pH-Dependent Endosomal Pathway. J Virol. 2006;80(18):8899-908.

128. Vanderplasschen A, Smith G. A novel virus binding assay using confocal microscopy: demonstration that the intracellular and extracellular vaccinia virions bind to different cellular receptors. J Virol. 1997;71(5):4032-41.

129. Vanderplasschen A, Hollinshead M, Smith G. Intracellular and extracellular vaccinia virions enter cells by different mechanisms. J Gen Virol. 1998;79(4):877-87.

130. Kirn DH, Wang Y, Liang W, Contag CH, Thorne SH. Enhancing Poxvirus Oncolytic Effects through Increased Spread and Immune Evasion. Cancer Res. 2008;68(7):2071-5.

131. Eppstein DA, Marsh YV, Schreiber AB, Newman SR, Todaro GJ, Nestor JJ. Epidermal growth factor receptor occupancy inhibits vaccinia virus infection. Nature. 1985;318(6047):663-5.

132. Marsh YV, Eppstein DA. Vaccinia virus and the EGF receptor: A portal for infectivity? J Cell Biochem. 1987;34(4):239-45.

133. Brown JP, Twardzik DR, Marquardt H, Todaro GJ. Vaccinia virus encodes a polypeptide homologous to epidermal growth factor and transforming growth factor. Nature. 1985;313(6002):491-2.

134. Stroobant P, Rice AR, Gullick WJ, Cheng DJ, Kerr IM, Waterfield MD. Purification and characterization of vaccinia virus growth factor. Cell. 1985;42(1):383-93.

135. King CS, Cooper JA, Moss B, Twardzik DR. Vaccinia virus growth factor stimulates tyrosine protein kinase activity of A431 cell epidermal growth factor receptors. Mol Cell Biol. 1986;6(1):332-6.

136. Buller RM, Chakrabarti S, Moss B, Fredrickson T. Cell proliferative response to vaccinia virus is mediated by VGF. Virology. 1988;164(1):182-92.

137. Postigo A, Martin MC, Dodding MP, Way M. Vaccinia-induced epidermal growth factor receptor-MEK signalling and the anti-apoptotic protein F1L synergize to suppress cell death during infection. Cell Microbiol. 2009;11(8):1208-18.

138. Hugin AW, Hauser C. The epidermal growth factor receptor is not a receptor for vaccinia virus. J Virol. 1994;68(12):8409-12.

139. Vermeer PD, McHugh J, Rokhlina T, Vermeer DW, Zabner J, Welsh MJ. Vaccinia virus entry, exit, and interaction with differentiated human airway epithelia. J Virol. 2007;81(18):9891-9.

140. Buller RM, Chakrabarti S, Cooper JA, Twardzik DR, Moss B. Deletion of the vaccinia virus growth factor gene reduces virus virulence. J Virol. 1988;62(3):866-74.

141. McCart JA, Ward JM, Lee J, Hu Y, Alexander HR, Libutti SK, et al. Systemic Cancer Therapy with a Tumor-selective Vaccinia Virus Mutant Lacking Thymidine Kinase and Vaccinia Growth Factor Genes. Cancer Res. 2001;61(24):8751-7.

142. Yang H, Kim S-K, Kim M, Reche PA, Morehead TJ, Damon IK, et al. Antiviral chemotherapy facilitates control of poxvirus infections through inhibition of cellular signal transduction. J Clin Invest. 2005;115(2):379-87.

143. Rawat SS, Viard M, Gallo SA, Rein A, Blumenthal R, Puri A. Modulation of entry of enveloped viruses by cholesterol and sphingolipids (Review). Mol Membr Biol. 2003;20(3):243-54.

144. Chung C-S, Huang C-Y, Chang W. Vaccinia Virus Penetration Requires Cholesterol and Results in Specific Viral Envelope Proteins Associated with Lipid Rafts. J Virol. 2005;79(3):1623-34.

145. Mercer J, Helenius A. Virus entry by macropinocytosis. Nat Cell Biol. 2009;11(5):510-20.

146. Mercer J, Helenius A. Vaccinia Virus Uses Macropinocytosis and Apoptotic Mimicry to Enter Host Cells. Science. 2008;320(5875):531-5.

147. Locker JK, Kuehn A, Schleich S, Rutter G, Hohenberg H, Wepf R, et al. Entry of the Two Infectious Forms of Vaccinia Virus at the Plasma Membane Is Signaling-Dependent for the IMV but Not the EEV. Mol Biol Cell. 2000;11(7):2497-511.

148. Schramm B, Locker J. Cytoplasmic organization of POXvirus DNA replication. Traffic. 2005;6(10):839-46.

149. Rice AP, Roberts BE. Vaccinia virus induces cellular mRNA degradation. J Virol. 1983;47(3):529-39.

150. Parrish S, Moss B. Characterization of a Second Vaccinia Virus mRNA-Decapping Enzyme Conserved in Poxviruses. J Virol. 2007;81(23):12973-8.

151. Parrish S, Resch W, Moss B. Vaccinia virus D10 protein has mRNA decapping activity, providing a mechanism for control of host and viral gene expression. Proc Natl Acad Sci U S A. 2007;104(7):2139-44.

152. Deng L, Shuman S. Elongation properties of vaccinia virus RNA polymerase: pausing, slippage, 3' end addition, and termination site choice. Biochemistry (Mosc). 1997;36(50):15892-9.

153. Slabaugh M, Howell M, Wang Y, Mathews C. Deoxyadenosine reverses hydroxyurea inhibition of vaccinia virus growth. J Virol. 1991;65(5):2290-8.

154. Katsafanas GC, Grem JL, Blough HA, Moss B. Inhibition of vaccinia virus replication by N-(phosphonoacetyl)-L-aspartate: differential effects on viral gene expression result from a reduced pyrimidine nucleotide pool. Virology. 1997;236(1):177-87.

155. Amellem O, Loffler M, Pettersen EO. Regulation of cell proliferation under extreme and moderate hypoxia: the role of pyrimidine (deoxy)nucleotides. Br J Cancer. 1994;70(5):857-66.

156. Brooks CR, Elliott T, Parham P, Khakoo SI. The Inhibitory Receptor NKG2A Determines Lysis of Vaccinia Virus-Infected Autologous Targets by NK Cells. J Immunol. 2006;176(2):1141-7.

157. Cooray S. The pivotal role of phosphatidylinositol 3-kinase-Akt signal transduction in virus survival. J Gen Virol. 2004;85(5):1065-76.

158. Wang G, Barrett JW, Stanford M, Werden SJ, Johnston JB, Gao X, et al. Infection of human cancer cells with myxoma virus requires Akt activation via interaction with a viral ankyrin-repeat host range factor. Proc Natl Acad Sci U S A. 2006;103(12):4640-5.

159. Soares JAP, Leite FGG, Andrade LG, Torres AA, De Sousa LP, Barcelos LS, et al. Activation of the PI3K/Akt Pathway Early during Vaccinia and Cowpox Virus Infections Is Required for both Host Survival and Viral Replication. J Virol. 2009;83(13):6883-99.

160. Hollinshead M, Rodger G, Van Eijl H, Law M, Hollinshead R, Vaux DJT, et al. Vaccinia virus utilizes microtubules for movement to the cell surface. J Cell Biol. 2001;154(2):389-402.

161. Smith GL, Vanderplasschen A, Law M. The formation and function of extracellular enveloped vaccinia virus. J Gen Virol. 2002;83(12):2915-31.

162. Newsome TP, Scaplehorn N, Way M. Src Mediates a Switch from Microtubule- to Actin-Based Motility of Vaccinia Virus. Science. 2004;306(5693):124-9.

163. Reeves P, Bommarius B, Lebeis S, McNulty S, Christensen J, Swimm A, et al. Disabling poxvirus pathogenesis by inhibition of Abl-family tyrosine kinases. Nat Med. 2005;11(7):731-9.

164. Yu YA, Shabahang S, Timiryasova TM, Zhang Q, Beltz R, Gentschev I, et al. Visualization of tumors and metastases in live animals with bacteria and vaccinia virus encoding light-emitting proteins. Nat Biotechnol. 2004;22(3):313-20.

165. Jain RK. Barriers to drug delivery in solid tumors. Sci Am. 1994;271(1):58-65.

166. Moroziewicz D, Kaufman HL. Gene therapy with poxvirus vectors. Curr Opin Mol Ther. 2005;7(4):317-25.

167. Kim JH, Oh JY, Park BH, Lee DE, Kim JS, Park HE, et al. Systemic armed oncolytic and immunologic therapy for cancer with JX-594, a targeted poxvirus expressing GM-CSF. Mol Ther. 2006;14(3):361-70.

168. Park BH, Hwang T, Liu TC, Sze DY, Kim JS, Kwon HC, et al. Use of a targeted oncolytic poxvirus, JX-594, in patients with refractory primary or metastatic liver cancer: a phase I trial. Lancet Oncol. 2008;9(6):533-42.

169. Watson ER, Hainan KE, Dische S, Saunders MI, Cade IS, McEwen JB, et al. Hyperbaric oxygen and radiotherapy: a Medical Research Council trial in carcinoma of the cervix. Br J Radiol. 1978;51(611):879-87.

170. Kaanders JHAM, Bussink J, van der Kogel AJ. ARCON: a novel biology-based approach in radiotherapy. Lancet Oncol. 2002;3(12):728-37.

171. Overgaard J. Hypoxic Radiosensitization: Adored and Ignored. J Clin Oncol. 2007;25(26):4066-74.

172. Jens O, Hanne Sand H, Marie O, Lars B, Anne B, Lena S, et al. A randomized double-blind phase III study of nimorazole as a hypoxic radiosensitizer of primary radiotherapy in supraglottic larynx and pharynx carcinoma. Results of the Danish Head and Neck Cancer Study (DAHANCA) Protocol 5-85. Radiother Oncol. 1998;46(2):135-46.

173. Semenza GL. Defining the role of hypoxia-inducible factor 1 in cancer biology and therapeutics. Oncogene. 2009;29(5):625-34.

174. Binley K, Iqball S, Kingsman A, Kingsman S, Naylor S. An adenoviral vector regulated by hypoxia for the treatment of ischaemic disease and cancer. Gene Ther. 1999;6(10):1721-7.

175. Greco O, Patterson AV, Dachs GU. Can gene therapy overcome the problem of hypoxia in radiotherapy? J Radiat Res (Tokyo). 2000;41(3):201-12.

176. Post DE, Van Meir EG. A novel hypoxia-inducible factor (HIF) activated oncolytic adenovirus for cancer therapy. Oncogene. 2003;22(14):2065-72.

177. Tang Y, Schmitt-Ott K, Qian K, Kagiyama S, Phillips MI. Vigilant vectors: adeno-associated virus with a biosensor to switch on amplified therapeutic genes in specific tissues in life-threatening diseases. Methods. 2002;28(2):259-66.

178. Timiryasova TM, Chen B, Fodor N, Fodor I. Construction of recombinant vaccinia viruses using PUV-inactivated virus as a helper. Biotechniques. 2001;31(3):534, 6, 8-40.

179. Hung CF, Tsai YC, He L, Coukos G, Fodor I, Qin L, et al. Vaccinia virus preferentially infects and controls human and murine ovarian tumors in mice. Gene Ther. 2007;14(1):20-9.

180. Warren JC, Rutkowski A, Cassimeris L. Infection with replication-deficient adenovirus induces changes in the dynamic instability of host cell microtubules. Mol Biol Cell. 2006;17(8):3557-68.

181. Workman P, Aboagye EO, Balkwill F, Balmain A, Bruder G, Chaplin DJ, et al. Guidelines for the welfare and use of animals in cancer research. Br J Cancer. 2010;102(11):1555-77.

182. Shojaei F, Wu X, Qu X, Kowanetz M, Yu L, Tan M, et al. G-CSF-initiated myeloid cell mobilization and angiogenesis mediate tumor refractoriness to anti-VEGF therapy in mouse models. Proc Natl Acad Sci U S A. 2009;106(16):6742-7.

183. Zhong H, De Marzo AM, Laughner E, Lim M, Hilton DA, Zagzag D, et al. Overexpression of Hypoxia-inducible Factor 1 alpha ± in Common Human Cancers and Their Metastases. Cancer Res. 1999;59(22):5830-5.

184. Kraggerud SM, Sandvik JA, Pettersen EO. Regulation of protein synthesis in human cells exposed to extreme hypoxia. Anticancer Res. 1995;15(3):683-6.

185. Hay JG. The potential impact of hypoxia on the success of oncolytic virotherapy. Curr Opin Mol Ther. 2005;7(4):353-8.

186. Bhattacharyya M, Lemoine NR. Gene therapy developments for pancreatic cancer. Best Pract Res Clin Gastroenterol. 2006;20(2):285-98.

187. Thorne SH. Oncolytic vaccinia virus: from bedside to benchtop and back. Curr Opin Mol Ther. 2008;10(4):387-92.

188. Connor JH, Naczki C, Koumenis C, Lyles DS. Replication and cytopathic effect of oncolytic vesicular stomatitis virus in hypoxic tumor cells in vitro and in vivo. J Virol. 2004;78(17):8960-70.

189. Saeed MF, Kolokoltsov AA, Freiberg AN, Holbrook MR, Davey RA. Phosphoinositide-3 Kinase-Akt Pathway Controls Cellular Entry of Ebola Virus. PLoS Pathog. 2008;4(8).

190. Itakura J, Ishiwata T, Shen B, Kornmann M, Korc M. Concomitant over-expression of vascular endothelial growth factor and its receptors in pancreatic cancer. Int J Cancer. 2000;85(1):27-34.

191. Bachler P, Reber HA, Bachler M, Shrinkante S, Bachler MW, Friess H, et al. Hypoxia-inducible factor 1 regulates vascular endothelial growth factor expression in human pancreatic cancer. Pancreas. 2003;26(1):56-64.

192. Lee CG, Yoon HJ, Zhu Z, Link H, Wang Z, Gwaltney JM, Jr., et al. Respiratory Syncytial Virus Stimulation of Vascular Endothelial Cell Growth Factor/Vascular Permeability Factor. Am J Respir Cell Mol Biol. 2000;23(5):662-9.

193. Ahlbrecht K, Schmitz J, Seay U, Schwarz C, Mittnacht-Kraus R, Gaumann A, et al. Spatiotemporal Expression of flk-1 in Pulmonary Epithelial Cells during Lung Development. Am J Respir Cell Mol Biol. 2008;39(2):163-70.

194. Le A, Zielinski R, He C, Crow MT, Biswal S, Tuder RM, et al. Pulmonary Epithelial Neuropilin-1 Deletion Enhances Development of Cigarette Smoke-induced Emphysema. Am J Respir Crit Care Med. 2009;180(5):396-406.

195. Wang Y, Gangeswaran R, Zhao X, Wang P, Tysome J, Bhakta V, et al. CEACAM6 attenuates adenovirus infection by antagonizing viral trafficking in cancer cells. J Clin Invest. 2009;119(6):1604-15.

196. Li M, Yang H, Chai H, Fisher W, Wang X, Brunicardi F, et al. Pancreatic carcinoma cells express neuropilins and vascular endothelial growth factor, but not vascular endothelial growth factor receptors. Cancer. 2004;101(10):2341-50.

197. Alexander FB, Shane PH, Adam FO, Helen MJ, Nigel MH, Ian CZ, et al. Ligand-Stimulated VEGFR2 Signaling is Regulated by Co-Ordinated Trafficking and Proteolysis. Traffic.11(1):161-74.

198. Wey JS, Fan F, Michael JG, Todd WB, Marya FM, Ray S, et al. Vascular endothelial growth factor receptor-1 promotes migration and invasion in pancreatic carcinoma cell lines. Cancer. 2005;104(2):427-38.

199. Gagnon ML, Bielenberg DR, Gechtman Ze, Miao H-Q, Takashima S, Soker S, et al. Identification of a natural soluble neuropilin-1 that binds vascular endothelial growth factor: In vivo expression and antitumor activity. Proc Natl Acad Sci U S A. 2000;97(6):2573-8.

200. Hong T-M, Chen Y-L, Wu Y-Y, Yuan A, Chao Y-C, Chung Y-C, et al. Targeting Neuropilin 1 as an Antitumor Strategy in Lung Cancer. Clin Cancer Res. 2007;13(16):4759-68.

201. Lee T-H, Seng S, Sekine M, Hinton C, Fu Y, Avraham HK, et al. Vascular Endothelial Growth Factor Mediates Intracrine Survival in Human Breast Carcinoma Cells through Internally Expressed VEGFR1/FLT1. PLoS Med. 2007;4(6):e186.

202. Calleja Vr, Laguerre M, Parker PJ, Larijani B. Role of a Novel PH-Kinase Domain Interface in PKB/Akt Regulation: Structural Mechanism for Allosteric Inhibition. PLoS Biol. 2009;7(1):e1000017.

203. Workman P, Clarke PA, Raynaud FI, van Montfort RLM. Drugging the PI3 Kinome: From Chemical Tools to Drugs in the Clinic. Cancer Res. 2010;70(6):2146-57.

204. McNulty S, Bornmann W, Schriewer J, Werner C, Smith SK, Olson VA, et al. Multiple Phosphatidylinositol 3-Kinases Regulate Vaccinia Virus Morphogenesis. PLoS ONE. 2010;5(5):e10884.

205. Liang Z, Brooks J, Willard M, Liang K, Yoon Y, Kang S, et al. CXCR4/CXCL12 axis promotes VEGF-mediated tumor angiogenesis through Akt signaling pathway. Biochem Biophys Res Commun. 2007;359(3):716-22.

206. Newman PJ. The biology of PECAM-1. J Clin Invest. 1997;99(1):3-8.

207. Young RM, Wang S-J, Gordan JD, Ji X, Liebhaber SA, Simon MC. Hypoxia-mediated selective mRNA translation by an internal ribosome entry site-independent mechanism. J Biol Chem. 2008;283(24):16309-19.

208. Masson N, Willam C, Maxwell PH, Pugh CW, Ratcliffe PJ. Independent function of two destruction domains in hypoxia-inducible factor-alpha chains activated by prolyl hydroxylation. EMBO J. 2001;20(18):5197-206.

209. Claffey KP, Shih SC, Mullen A, Dziennis S, Cusick JL, Abrams KR, et al. Identification of a human VPF/VEGF 3' untranslated region mediating hypoxia-induced mRNA stability. Mol Biol Cell. 1998;9(2):469-81.

210. Baird SD, Turcotte M, Korneluk RG, Holcik M. Searching for IRES. RNA. 2006;12(10):1755-85.

211. Akiri G, Nahari D, Finkelstein Y, Le S-Y, Elroy-Stein O, Levi B-Z. Regulation of vascular endothelial growth factor (VEGF) expression is mediated by internal initiation of translation and alternative initiation of transcription. Oncogene. 1998;17(2):227-36.

212. Fuerst TR, Niles EG, Studier FW, Moss B. Eukaryotic transient-expression system based on recombinant vaccinia virus that synthesizes bacteriophage T7 RNA polymerase. Proc Natl Acad Sci U S A. 1986;83(21):8122-6.

213. Moroz E, Carlin S, Dyomina K, Burke S, Thaler HT, Blasberg R, et al. Real-Time Imaging of HIF-1alpha Stabilization and Degradation. PLoS ONE. 2009;4(4):e5077.

214. Xia M, Huang R, Sun Y, Semenza GL, Aldred SF, Witt KL, et al. Identification of Chemical Compounds that Induce HIF-1{alpha} Activity. Toxicol Sci. 2009;112(1):153-63.

215. Poland GA, Grabenstein JD, Neff JM. The US smallpox vaccination program: a review of a large modern era smallpox vaccination implementation program. Vaccine. 2005;23(17-18):2078-81.

216. Roenigk HH, Jr., Deodhar S, St Jacques R, Burdick K. Immunotherapy of malignant melanoma with vaccinia virus. Arch Dermatol. 1974;109(5):668-73.

217. Binley K, Askham Z, Martin L, Spearman H, Day D, Kingsman S, et al. Hypoxia-mediated tumour targeting. Gene Ther. 2003;10(7):540-9.

218. Minami K, Tambe Y, Watanabe R, Isono T, Haneda M, Isobe K-i, et al. Suppression of Viral Replication by Stress-Inducible GADD34 Protein via the Mammalian Serine/Threonine Protein Kinase mTOR Pathway. J Virol. 2007;81(20):11106-15.

219. Aghi MK, Liu T-C, Rabkin S, Martuza RL. Hypoxia Enhances the Replication of Oncolytic Herpes Simplex Virus. Mol Ther. 2008;17(1):51-6.

220. Servais C, Caillet-Fauquet P, Draps M-L, Velu T, de Launoit Y, Brandenburger A. Hypoxic-response elements in the oncolytic parvovirus Minute virus of mice do not allow for increased vector production at low oxygen concentration. J Gen Virol. 2006;87(5):1197-201.

221. Langland JO, Jacobs BL. The Role of the PKR-Inhibitory Genes, E3L and K3L, in Determining Vaccinia Virus Host Range. Virology. 2002;299(1):133-41.

222. Beattie E, Paoletti E, Tartaglia J. Distinct Patterns of IFN Sensitivity Observed in Cells Infected with Vaccinia K3L- and E3L- Mutant Viruses. Virology. 1995;210(2):254-63.

223. Moser TS, Jones RG, Thompson CB, Coyne CB, Cherry S. A Kinome RNAi Screen Identified AMPK as Promoting Poxvirus Entry through the Control of Actin Dynamics. PLoS Pathog. 2010;6(6):e1000954.

224. Laderoute KR, Amin K, Calaoagan JM, Knapp M, Le T, Orduna J, et al. 5'-AMP-activated protein kinase (AMPK) is induced by low-oxygen and glucose deprivation conditions found in solid-tumor microenvironments. Mol Cell Biol. 2006;26(14):5336-47.

225. Kirn DH, Thorne SH. Targeted and armed oncolytic poxviruses: a novel multi-mechanistic therapeutic class for cancer. Nat Rev Cancer. 2009;9(1):64-71.

226. Mercer J, Knabel S, Schmidt FI, Crouse J, Burkard C, Helenius A. Vaccinia virus strains use distinct forms of macropinocytosis for host-cell entry. Proc Natl Acad Sci U S A. 2009;107(20):9346-51.

227. Bengali Z, Townsley AC, Moss B. Vaccinia virus strain differences in cell attachment and entry. Virology. 2009;389(1-2):132-40.

228. Cébe-Suarez S, Grunewald FS, Jaussi R, Li X, Claesson-Welsh L, Spillmann D, et al. Orf virus VEGF-E NZ2 promotes paracellular NRP-1/VEGFR-2 coreceptor assembly via the peptide RPPR. FASEB J. 2008;22(8):3078-86.

229. Delhon G, Tulman ER, Afonso CL, Lu Z, de la Concha-Bermejillo A, Lehmkuhl HD, et al. Genomes of the Parapoxviruses Orf Virus and Bovine Papular Stomatitis Virus. J Virol. 2004;78(1):168-77.

230. Baek J, Jang J, Kang C, Chung H, Kim N, Kim K. Hypoxia-induced VEGF enhances tumor survivability via suppression of serum deprivation-induced apoptosis. Oncogene. 2000;19(40):4621-31.

231. Bachelder RE, Lipscomb EA, Lin X, Wendt MA, Chadborn NH, Eickholt BJ, et al. Competing Autocrine Pathways Involving Alternative Neuropilin-1 Ligands Regulate Chemotaxis of Carcinoma Cells. Cancer Res. 2003;63(17):5230-3.

232. Fan F, Wey JS, McCarty MF, Belcheva A, Liu W, Bauer TW, et al. Expression and function of vascular endothelial growth factor receptor-1 on human colorectal cancer cells. Oncogene. 2005;24(16):2647-53.

233. Ellis LM. The role of neuropilins in cancer. Mol Cancer Ther. 2006;5(5):1099-107.

234. Robinson SD, Reynolds LE, Kostourou V, Reynolds AR, da Silva RGa, Tavora B, et al. AlphaVBeta3 Integrin Limits the Contribution of Neuropilin-1 to Vascular Endothelial Growth Factor-induced Angiogenesis. J Biol Chem. 2009;284(49):33966-81.

235. Zhang S, Zhau H, Osunkoya A, Iqbal S, Yang X, Fan S, et al. Vascular endothelial growth factor regulates myeloid cell leukemia-1 expression through neuropilin-1-dependent activation of c-MET signaling in human prostate cancer cells. Mol Cancer. 2010;9(1):9.

236. Hu B, Guo P, Bar-Joseph I, Imanishi Y, Jarzynka MJ, Bogler O, et al. Neuropilin-1 promotes human glioma progression through potentiating the activity of the HGF//SF autocrine pathway. Oncogene. 2007;26(38):5577-86.

237. Salikhova A, Wang L, Lanahan AA, Liu M, Simons M, Leenders WPJ, et al. Vascular Endothelial Growth Factor and Semaphorin Induce Neuropilin-1 Endocytosis via Separate Pathways. Circ Res. 2008;103(6):e71-9.

238. Ghez D, Lepelletier Y, Lambert S, Fourneau J-M, Blot V, Janvier S, et al. Neuropilin-1 Is Involved in Human T-Cell Lymphotropic Virus Type 1 Entry. J Virol. 2006;80(14):6844-54.

239. Nasarre P, Constantin B, Rouhaud L, Harnois T, Raymond G, Drabkin HA, et al. Semaphorin SEMA3F and VEGF have opposing effects on cell attachment and spreading. Neoplasia. 2003;5(1):83-92.

240. Miao H-Q, Soker S, Feiner L, Alonso JL, Raper JA, Klagsbrun M. Neuropilin-1 Mediates Collapsin-1/Semaphorin III Inhibition of Endothelial Cell Motility. J Cell Biol. 1999;146(1):233-42.

241. Narazaki M, Tosato G. Ligand-induced internalization selects use of common receptor neuropilin-1 by VEGF165 and semaphorin3A. Blood. 2006;107(10):3892-901.

242. Bagai S, Lamb RA. Quantitative measurement of paramyxovirus fusion: differences in requirements of glycoproteins between simian virus 5 and human parainfluenza virus 3 or Newcastle disease virus. J Virol. 1995;69(11):6712-9.

243. Castro-Rivera E, Ran S, Brekken RA, Minna JD. Semaphorin 3B Inhibits the Phosphatidylinositol 3-Kinase/Akt Pathway through Neuropilin-1 in Lung and Breast Cancer Cells. Cancer Res. 2008;68(20):8295-303.

244. Schmidt N, Mishra A, Lai GH, Wong GCL. Arginine-rich cell-penetrating peptides. FEBS Lett. 2010;584(9):1806-13.

245. Teesalu T, Sugahara KN, Kotamraju VR, Ruoslahti E. C-end rule peptides mediate neuropilin-1-dependent cell, vascular, and tissue penetration. Proc Natl Acad Sci U S A. 2009;106(38):16157-62.

246. Phillips MI, Tang Y, Schmidt-Ott K, Qian K, Kagiyama S. Vigilant Vector: Heart-Specific Promoter in an Adeno-Associated Virus Vector for Cardioprotection. Hypertension. 2002;39(2):651-5.

247. Bert AG, Grapin R, Vadas MA, Goodall GJ. Assessing IRES activity in the HIF-1alpha and other cellular 5' UTRs. RNA. 2006;12(6):1074-83.

248. Ray P, Wu AM, Gambhir SS. Optical Bioluminescence and Positron Emission Tomography Imaging of a Novel Fusion Reporter Gene in Tumor Xenografts of Living Mice. Cancer Res. 2003;63(6):1160-5.

249. Ngoi SM, Chien AC, Lee CG. Exploiting internal ribosome entry sites in gene therapy vector design. Curr Gene Ther. 2004;4(1):15-31.

250. Yuen L, Moss B. Oligonucleotide sequence signaling transcriptional termination of vaccinia virus early genes. Proc Natl Acad Sci U S A. 1987;84(18):6417-21.

251. Li F, Sonveaux P, Rabbani ZN, Liu S, Yan B, Huang Q, et al. Regulation of HIF-1alpha Stability through S-Nitrosylation. Mol Cell. 2007;26(1):63-74.

252. Anna SEL, Johan B, Paulus FJWR, James AR, Juliana D, Albert JVDK. Changes in tumor hypoxia measured with a double hypoxic marker technique. Int J Radiat Oncol Biol Phys. 2000;48(5):1529-38.

253. Pugh CW, Ratcliffe PJ. The von Hippel-Lindau tumor suppressor, hypoxia-inducible factor-1 (HIF-1) degradation, and cancer pathogenesis. Semin Cancer Biol. 2003;13(1):83-9.

254. Gammon DB, Gowrishankar B, Duraffour S, Andrei G, Upton C, Evans DH. Vaccinia virus-encoded ribonucleotide reductase subunits are differentially required for replication and pathogenesis. PLoS Pathog. 2010;6(7):e1000984.

255. Cowen RL, Williams KJ, Chinje EC, Jaffar M, Sheppard FCD, Telfer BA, et al. Hypoxia Targeted Gene Therapy to Increase the Efficacy of Tirapazamine as an Adjuvant to Radiotherapy. Cancer Res. 2004;64(4):1396-402.

8 Publications

Gene Therapy (2009), 1–7

www.nature.com/gt

ORIGINAL ARTICLE

Lister strain vaccinia virus, a potential therapeutic vector targeting hypoxic tumours

CT Hiley[1], M Yuan[1], NR Lemoine[1,2] and Y Wang[1,2]

[1]*Centre for Molecular Oncology & Imaging, Institute of Cancer, Barts and the London School of Medicine and Dentistry, Queen Mary University of London, London, UK and* [2]*Sino-British Research Center for Molecular Oncology, Zhengzhou University, Zhengzhou, PR China*

Hypoxia contributes to the aggressive and treatment-resistant phenotype of pancreatic ductal adenocarcinoma. Oncolytic vaccinia virus has potential as an anti-tumour agent, but the ability to lyse hypoxic tumour cells is vital for clinical efficacy. We hypothesized that unique aspects of the poxvirus life cycle would protect it from attenuation in hypoxic conditions. We characterized and compared the viral protein production, viral replication, cytotoxicity and transgene expression of Lister strain vaccinia virus in a panel of pancreatic cancer cell lines after exposure to normoxic or hypoxic conditions. Viral protein production was not affected by hypoxia, and high viral titres were produced in both normoxic and hypoxic conditions. Interestingly, there was a 3.5-fold ($P < 0.001$) and 20-fold ($P < 0.0001$) increase in viral cytotoxicity for CFPac1 and MiaPaca2 cell lines, respectively, in hypoxic conditions. Cytotoxicity was equivalent in the remaining cell lines. Levels of transgene expression (luciferase reporter gene) from the vaccinia viral vector were comparable, regardless of the ambient oxygen concentration. The present study suggests that the vaccinia virus is a promising vector for targeting pancreatic cancer and potentially other hypoxic tumour types.
Gene Therapy advance online publication, 5 November 2009; doi:10.1038/gt.2009.132

Keywords: *human pancreatic cancer; vaccinia virus; hypoxia*

Introduction

Solid tumours are characterized by regions of hypoxia that are inherently resistant to both radiotherapy and chemotherapy.[1] Many studies have shown that a wide variety of tumour types exhibit hypoxia-related resistance mechanisms, resulting in a worse prognosis.[2,3] Pancreatic ductal adenocarcinoma (PDAC) remains a disease with a dismal prognosis. The majority of patients present with metastatic disease, and attempts to alter the natural history with conventional chemotherapy have shown limited benefit. Response rates of only 5–20% are seen and median survival for those with advanced disease remains less than six months.[4] PDACs contain significant areas of hypoxia that have been measured intraoperatively in a clinical setting.[5] In addition, hypoxia is associated with a poor prognosis in PDAC[6] and is implicated in the resistance to gemcitabine, the current standard of care.[7] Therefore, development of novel therapeutics to conquer this obstacle is pivotal to improve the survival from this lethal disease.

Replicating oncolytic viruses have a natural tropism for tumour cells. Further modification of viruses enables selective tumour targeting and offers the possibility of treating cancers that are resistant to conventional therapies. The oncolytic viruses are not subject to the same resistance mechanisms as conventional cytotoxic therapies, and are effective even if apoptosis is blocked.[8] Despite encouraging laboratory data, clinical trials using oncolytic viral therapy for pancreatic cancer have shown safety, but with limited efficacy. A replication-selective oncolytic adenovirus, Onyx 015 (*dl*1520), has been administered by intratumoral injection to patients with locally advanced pancreatic tumours in phase I/II trials. Although treatments were well tolerated, no objective responses were seen in patients after virus alone was administered, and only two of 21 patients showed objective responses when gemcitabine was used in combination.[9,10]

One major hurdle affecting oncolytic adenovirus potency is the tumour environment, which can affect different stages of the viral life cycle. Recent studies show that replication of Adenovirus serotype 5, the most commonly used oncolytic viral vector, is attenuated in hypoxic conditions. Expression of cell-surface receptors for adenovirus, Coxsackie/Adenovirus receptor and α_v integrins, is unaffected by hypoxia, as is the mRNA expression of critical viral genes such as E1A and Hexon. However, translation of viral mRNA to protein is reduced, resulting in a 10–100-fold reduction in the yield of infectious virus particles.[11,12] In addition, the group B adenoviruses, serotype 3 and 11, are attenuated in hypoxia with both reduced lytic potential and production of virus particles independent of viral receptor status or viral gene expression.[13] Consequently,

Correspondence: Professor NR Lemoine or Dr Y Wang, Institute of Cancer, Barts & The London School of Medicine, Queen Mary University of London, Charterhouse Square, London EC1 6BQ, UK.
E-mail: Director@qmcr.qmul.ac.uk or yaohe.wang@qmul.ac.uk
Received 13 June 2009; revised 7 September 2009; accepted 14 September 2009

adenoviruses may not be the ideal vectors for tumours with significant hypoxic fractions such as PDAC.

Vaccinia virus is an alternative oncolytic virus and has some potential advantages over other viral vectors. Vaccinia is a DNA virus with an extensive safety profile in humans, as the virus has been used in millions of people for the World Health Organization smallpox eradication programme.[14] In comparison to adenoviral vectors, the virion particle size and DNA organization of vaccinia virus allows insertion of multiple transgenes with less deleterious effects on subsequent viral DNA replication, virion packaging and dissemination.[15] As an *Orthopoxvirus*, the life cycle of vaccinia virus is entirely located in the cytoplasm of infected host cells, in contrast to other viral vectors that replicate in the nucleus and rely on host transcription factors for DNA replication.[16] In addition, the infectious virion is packaged with pre-transcribed early viral gene mRNA and ATP, consequently, viral replication is initiated early after infection and the life cycle of vaccinia virus is shorter than other oncolytic viruses.[17]

We hypothesized that, unlike adenovirus, the unique features of vaccinia virus would mean that its inherent oncolytic potential would not be deleteriously affected under hypoxic conditions. This hypothesis was further supported by two recent reports. First, it was shown that the entry of mature vaccinia virions into host cells is accelerated by brief low-pH through an endosomal pathway.[18] Second, the tumour microenviroment is known to be hypoxic, and genes involved in regulating intracellular pH are upregulated by hypoxia-inducible factor (Hif-1α).[19] Given that pancreatic cancer has been shown to be one of the most hypoxic tumours,[5] we therefore investigated the effect of hypoxia on the life cycle of vaccinia virus using pancreatic cancer as a model and characterized vaccinia virus as an alternative vector targeting hypoxic tumour cells.

Results

Hypoxia stabilizes Hif-1α and induces nuclear translocation

Hypoxia-inducible factor-1α is the key protein mediating the response of cells to a hypoxic microenvironment. In the presence of oxygen, Hif-1α is hydroxylated at specific proline residues, which results in its interaction with the Von Hippel–Lindau gene product and subsequent ubiquitination and degradation.[20] In the absence of ambient oxygen, this degradation does not occur and subsequent nuclear localization results in the transcription of Hif-1α target genes and cellular adaptation to hypoxia. Vaccinia virus is becoming an increasingly common vector for viral gene and oncolytic therapy. However, its ability to replicate in hypoxic conditions has not been reported to date. In the present study, hypoxic conditions were simulated with the use of a hypoxic incubator maintaining the ambient oxygen concentration at 1% pO_2. Immunoblotting for Hif-1α in nuclear extracts of three pancreatic cancer cell lines, shown in Figure 1, showed that nuclear localization of this protein was observed only when cells were exposed to 1% pO_2 and validates the use of this technique in subsequent experiments. This suggests that the environment used in the present study is suitably hypoxic.

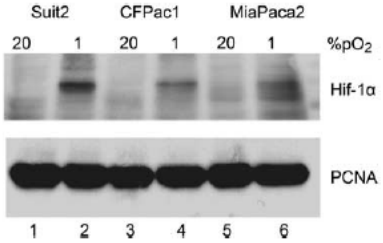

Figure 1 Stabilization and nuclear translocation of hypoxia-inducible factor 1α (Hif-1α) under hypoxic conditions. Cell lines were incubated in normoxic conditions (20% pO_2) (lanes 1, 3 and 5) or hypoxia (1% pO_2) (lanes 2, 4 and 6) for 16 h before harvesting of nuclear extracts for immunoblotting. Lysates were probed for Hif-1α and proliferating cell nuclear antigen (PCNA) expression as a loading control.

Vaccinia virus protein expression is not affected by hypoxic conditions

Given the fact that viral protein expression is the direct indicator of initiation of the viral life cycle and hypoxia has been shown to limit the total amount of protein synthesis,[21] we first investigated whether production of viral proteins in pancreatic cancer cell lines exposed to hypoxia would be altered. CFPac1 and Miapaca2 cell lines were infected with Lister vaccine strain of vaccinia virus (VVLister) at an multiplicity of infection (MOI) = 1 and cell lysates were harvested at 24 h, 48 h and 72 h after infection. Similar levels of vaccinia virus protein were present at 72 h when exposed to normoxic or hypoxic conditions, as shown in lanes 6 and 7 of Figure 2a. Immunoblotting for stabilization and nuclear translocation of Hif-1α from MiaPaca2 lysates was performed to confirm that exposure to hypoxia had been adequate during the experiment (Figure 2b). This result confirms that critical viral proteins are translated efficiently in hypoxic conditions. This also implies that the steps of the vaccinia virus life cycle before viral gene expression, such as attachment and internalization etc., may not be affected by hypoxia.

Vaccinia virus replication under hypoxic conditions

The ability of replication-competent viruses to infect, multiply, lyse and then subsequently infect neighbouring cells is crucial for them to spread throughout a tumour. There has been concern that hypoxia may present a barrier to this.[22] We investigated the replication of VVLister in pancreatic cancer cell lines, Suit-2, MiaPaca2 and CFPac1, when exposed to normoxic or hypoxic conditions before and after viral infection. Cells and supernatant were collected at 24, 48, 72 and 96 h post-infection. The number of plaque-forming units (pfu) per cell produced for each cell line in different conditions was determined using a TCID50 (50% tissue culture infective dose) assay, as described in the Materials and Methods section. The levels of viral replication in MiaPaca-2 and CFPac1 cells are unaffected at any point by hypoxic conditions (Figure 3). Suit2 cells show a similar pattern at 24 h and 48 h, producing a high titre of infectious viral particles in both hypoxic and normoxic conditions. At later time points, even higher titres are

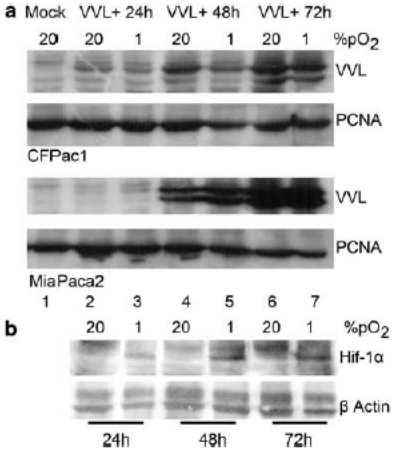

Figure 2 Viral gene expression of vaccinia virus in human pancreatic cancer after viral infection, and hypoxia-inducible factor 1α (Hif-1α) stabilization and nuclear translocation in normoxic or hypoxic cells. (**a**) Hypoxia does not affect viral gene expression of vaccinia virus. Cells were maintained in normoxic or hypoxic conditions before and after viral infection. Cells were infected with VVLister (Lister vaccine strain of vaccinia virus) at an multiplicity of infection (MOI) = 1 or mock infected with vehicle buffer alone. Vaccinia virus protein was measured using an anti-vaccinia polyclonal antibody. Human proliferating cell nuclear antigen (PCNA) was used as a loading control; (**b**), Hif-1α stabilization and nuclear translocation was shown on nuclear lysates from MiaPaca2 cells in normoxic (20% pO_2) or hypoxic cells (1% pO_2) over a time course. β-actin was used as a loading control.

achieved when replication occurs in ambient oxygen concentrations; however, there was no significant difference compared with those in hypoxia. In summary, high viral titres of VVLister (approximately more than 100 pfu per cell) were achievable in all pancreatic cancer cell lines tested in both normoxic and hypoxic conditions.

Enhanced cytotoxicity of vaccinia virus in hypoxia

Effective lysis of infected tumour cells is the ultimate aim of oncolytic therapy. We used the MTS (3-(4, 5-dimethylthiazol-2-yl)-5-(3-carboxymethoxyphenyl)-2-(4-sulfophenyl)-2H-tetrazolium) assay to determine the EC_{50} (dose of virus required to kill 50% of cells) for four pancreatic cancer cell lines. Cells were infected and maintained in the indicated oxygen conditions for the duration of the experiment and cell viability was analysed at 6 days post-infection. Dose–response curves and EC_{50} values were calculated, and the results were shown in Figure 4 and Table 1. Cytotoxicity of vaccinia virus in Suit-2 and Panc1 cell lines was maintained irrespective of a reduction in ambient oxygen concentration. Interestingly, for MiaPaca2 and CFPac1 cell lines, there was a statistically significant increase in vaccinia virus cytotoxicity in hypoxia with an ~20-fold ($P < 0.0001$) and 3.5-fold ($P < 0.001$) reduction in EC_{50}, respectively. These data suggest that VVLister is a potential agent for oncolytic virotherapy in which hypoxia occurs in the tumour microenvironment.

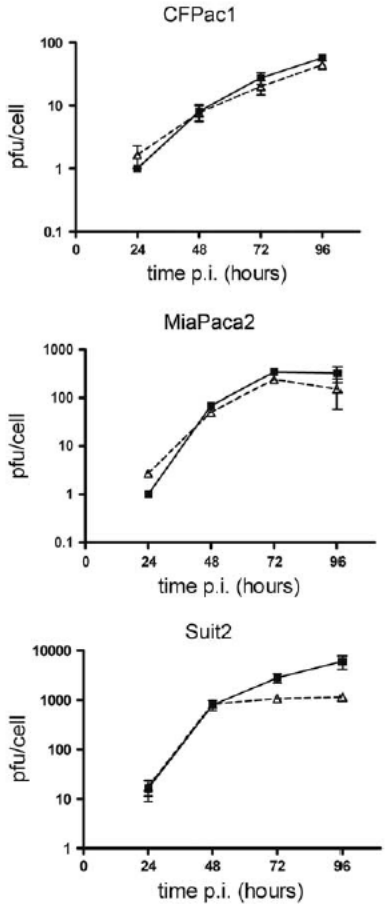

Figure 3 Viral replication of VVLister (Lister vaccine strain of vaccinia virus) in normoxic (solid line) and hypoxic conditions (dashed line) measured by TCID50 (50% tissue culture infective dose) assay of viral burst assays. Cell lines were exposed to normoxic or hypoxic conditions before and after infection with a multiplicity of infection (MOI) = 1 of VVLister. Burst assay samples were collected at 24, 48, 72 and 96 h post-infection. TCID50 assays were performed on CV1 green monkey kidney cells. Experiments were performed in triplicate for each cell line, time point and condition. Results are presented as mean ± standard deviation.

Transgene expression in vaccinia virus vector is not affected by hypoxic conditions

Many replicating viruses used for oncolytic therapy have additional therapeutic transgenes inserted into the viral genome to increase their therapeutic effect. Examples include pro-apoptotic proteins, prodrug-converting enzymes and cytokines.[23] One of the attractions of vaccinia virus over alternative viral vectors is its large capacity for transgene insertion.[17] Hypoxia will modulate the gene expression of any host cell; hence, verifying the effect of hypoxia on transgene expression from replication-competent vaccinia virus is important if this vector is to be of clinical use.[21] We used VVL15 (a recombinant vaccinia

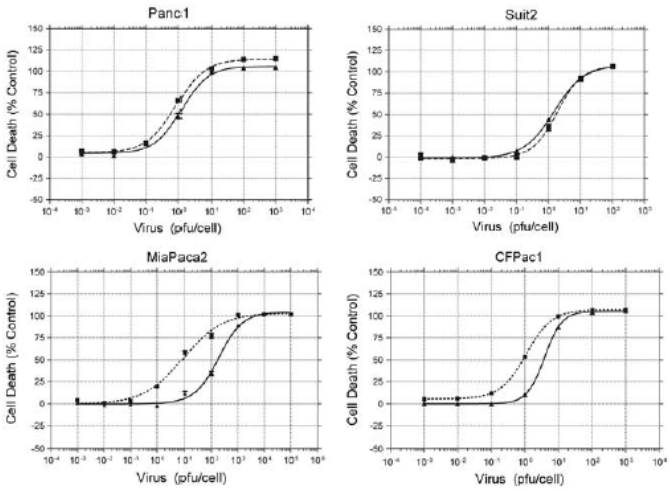

Figure 4 Effect of hypoxia on cytotoxicity of vaccinia virus Lister strain (VVLister). Pancreatic cancer cell lines were pre-treated with hypoxic or normoxic conditions for at least 16 h, then infected with serial dilutions of VVLister and maintained under the same oxygen tension. The infected cells were assayed with MTS (3-(4,5-dimethylthiazol-2-yl)-5-(3-carboxymethoxyphenyl)-2-(4-sulfophenyl)-2H-tetrazolium) reagent at day 6 post-infection at 37 °C with 5% CO_2 for 2 h. Viable cells were determined as a percentage of the non-infected controls and non-linear regression analysis was used to draw dose–response curves. Each assay contained six replicates and results are presented as mean ± standard deviation of four independent experiments (dashed line: hypoxia, solid line: normoxia).

Table 1 Comparison of cytotoxicity of vaccinia virus in normoxia and hypoxia

Cell lines	*EC_{50} (95% CI)*		*P-value*	*Hill slope*	
	20% Oxygen	*1% Oxygen*		*20% Oxygen*	*1% Oxygen*
Panc1	1.21 (1.03–1.41)	0.82 (0.71–0.95)	0.07	1.075	0.9662
Suit2	1.50 (1.24–1.81)	1.88 (1.37–2.59)	0.48	0.924	1.12
MiaPaca2	187.00 (154.39–226.37)	9.15 (7.24–11.58)	<0.00004	0.9555	0.6065
CFPac1	3.89 (3.59–4.20)	1.10 (1.04–1.16)	<0.002	1.66	1.122

Abbreviations: CI, confidence interval; EC_{50}, the concentration of virus required to kill 50% of cells.
The EC_{50} values of vaccinia virus in the four different pancreatic cancer cell lines is presented with 95% CI and *P*-values represent any significant difference between infection in normoxia versus hypoxia. Hill slope values for the dose–response curves are also presented.

virus derived from the VVLister) in which the firefly luciferase reporter gene was inserted into the thymidine kinase region downstream of the early–late vaccinia p7.5 promoter to assess transgene expression. The levels of luciferase activity after infection of four pancreatic cancer cell lines were detected by the Live Imaging System IVS200 (Xenogen, Alameda, CA, USA) at multiple time points, as opposed to isolated readings or early time points, as used in other studies to produce more representative data on gene expression.[24,25] As shown in Figure 5, luciferase expression was largely unaffected by hypoxia. Only two of the four cell lines tested showed a significant difference between normoxic and hypoxic cells at two isolated time points. There was a decrease at 24 h and increase at 48 h in luciferase expression for CFPac1 and Panc1, respectively. However, this difference was not sustained at later time points. This result suggests that hypoxia does not compromise transgene expression from replication-competent vaccinia virus.

Discussion

Wild-type vaccinia virus has been well characterized, and much data on the molecular biology, genome sequence, viral life cycle and immunology have been reported. Vaccinia virus is an appealing candidate agent for oncolytic virotherapy because of these inherent properties. Besides several other attractive qualities (such as fast and efficient replication with rapid cell-to-cell spread; natural tropism for tumours; strong lytic ability; large cloning capacity; well-defined molecular biology; safety in human beings; and good stability[26–29]), a defining feature that we showed in the present study is that hypoxia does not significantly affect viral gene expression, viral replication, cytotoxicity and even enhances the tumour-killing activity in some tumour cell lines.

We have shown here that VVLister shows comparable efficacy in infection, replication and transgene expression,

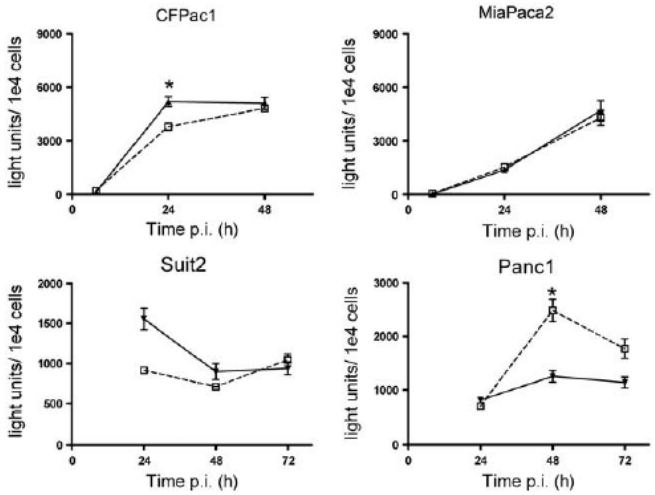

Figure 5 The effect of hypoxia on transgene expression from VVL15. Cells were infected with 1 pfu per cell of VVL15 and luciferase activity was measured at the time points indicated. All experiments were performed in triplicate and results represent the data from three separate experiments. Results are presented as mean ± s.d. (solid line and triangle = 20% pO_2, dashed line and square = 1% pO_2. Light units, photons per second per cm^2. *$P < 0.05$). pfu, plaque-forming unit.

regardless of the ambient oxygen concentration. It is important to highlight that hypoxic cells used in these experiments had been exposed to reduced oxygen concentration for at least 16 h before infection, which is more likely to reflect cellular adaptation to hypoxia and model clinical vaccinia virus infection than shorter exposure times that have been used for the study of other oncolytic viruses.[12,24] In addition, we found that effective tumour cell lysis was maintained after infection of hypoxic PDAC cell lines, and in half of the cell lines tested, there was a statistically significant improvement in viral cytotoxicty. This is an important result given that tumour lysis is the ultimate goal of oncolytic therapy.

Many groups have tried to target hypoxic fractions of tumours using hypoxia-specific promoters often containing hypoxia-response elements that facilitate Hif-1α binding and downstream gene transcription. Unfortunately, such promoters are invariably less powerful drivers of gene expression than constitutive viral promoters, and result in lower levels of gene expression and viral replication relative to wild-type viruses.[30,31] Our results show that vaccinia virus has the capacity to infect and replicate in hypoxic tumour cells without the need for such approaches. A recent report from Connor *et al*.[24] showed that oncolytic vesicular stomatitis virus has comparable viral replication in normoxic HeLa cells compared with those exposed to 1% O_2 for 2 h before infection and only a slight reduction of viral-induced cytopathic effect was seen on semi-quantitative analysis. The availability of other oncolytic viruses that are not significantly attenuated in hypoxia in comparison with adenoviral strains is a welcome finding. However, our results suggest a several-fold, statistically significant improvement in the oncolytic potential of vaccinia virus in some pancreatic cell lines exposed to hypoxic conditions. The underlying mechanisms are not clear, which warrants further investigation. Connor *et al*.[24] conclude that their results suggest an advantage of RNA viruses over DNA viruses in targeting hypoxic tumour cells because of a greater reduction of DNA synthesis in hypoxic cells. Vaccinia virus is a double-stranded DNA virus and similar to vesicular stomatitis virus replicates in the cytoplasm, encodes its own polymerases and is consequently less dependent on host gene and protein expression. Our alternative conclusion is that it is a cytoplasmic life cycle, with a reduced dependence on host gene and protein expression, rather than the nucleic acid construction of the viral genome that dictates the efficacy of oncolytic viruses in hypoxia.

In summary, we report the comparable efficacy of oncolytic vaccinia virus (including direct cancer cell killing and transgene expression) in both normoxic and hypoxic pancreatic tumour cells. These results suggest that vaccinia virus may be a potent therapeutic vector for targeting pancreatic cancer and potentially other hypoxic tumour types.

Materials and methods

Cells and tissue culture conditions

All cell lines were obtained from Cancer Research UK Central Cell Services and maintained in Dulbecco's modified Eagle's medium containing 0.06 μg l^{-1} penicillin and 0.1 μg l^{-1} streptomycin with 10% fetal calf serum. Cell lines were cultured at 37 °C with 5% CO_2 unless otherwise specified. Similarly, low passage numbers were used for each experiment.

Viral stocks and viral infection

The Lister vaccine strain of vaccinia virus (VVLister) and the recombinant luciferase-expressing vaccinia viruses

(VVL15) were constructed and kindly provided by Professor Istvan Fodor (Loma Linda University Campus, Loma Linda, CA, USA). VVL15 was constructed by the insertion of the firefly luciferase and the lacZ reporter genes into the thymidine kinase region of VVLister downstream of the early–late vaccinia p7.5 promoter.[32] Cells were trypsinized, replated and exposed to either normoxic or hypoxic conditions for 16 h before any viral infection. Infections were performed using a MOI = 1 pfu per cell unless otherwise specified.

Hypoxia

For this study, hypoxia is defined as 1% oxygen, which is an oxygen concentration of ~7 mm Hg. This was achieved using a hypoxic incubator maintained at 94% nitrogen, 5% CO_2 and 1% oxygen (Heto-Holten Cell Chamber 170, Surrey, UK).

Immunoblotting

Nuclear extracts were isolated using the NE-PER nuclear and cytoplasmic extraction reagents (Pierce, Rockford, IL, USA) according to the manufacturer's instructions. Whole cell lysates were prepared by removing adherent cells using a cell scraper, washing cells in 1 ml of phosphate-buffered saline at 4 °C and centrifuging at 2000 r.p.m. for 5 min at 4 °C. After the removal of phosphate-buffered saline, cells were resuspended in 50 µl of NP40 cell lysis buffer (50 mM Tris, pH7.4, 150 mM NaCl, 10 mM Ca^{2+}), protease inhibitor cocktail (Roche Applied Science, Mannheim, Germany) and 1% Nonidet P40 (Sigma Chemicals Co., Poole, UK) before storage at −80 °C. Total protein concentration was determined using the BCA protein assay (Pierce), and equal amounts of protein were electrophoresed on a reducing denaturing 10% polyacrylamide gel. Proteins were transferred by electroblotting to a polyvinylidene fluoride membrane (Immobilon-P, Millipore, Bedford, MA, USA). Non-specific binding was blocked using 5% bovine serum albumin in phosphate-buffered saline-Tween 20 (0.1% Tween-20). Antibodies were incubated in 3% bovine serum albumin in phosphate-buffered saline-Tween 20. The murine monoclonal Hif-1α antibody (AbCam Plc, Cambridge, UK) was used at a dilution of 1:750. The rabbit polyclonal vaccinia virus coat protein antibody (MorphoSys UK Ltd, Bath, UK) was used at a dilution of 1:1000. The PCNA (proliferating cell nuclear antigen) antibody (Santa Cruz Biotech Inc, Santa Cruz, CA, USA) was used at a dilution of 1:1000. The β-actin antibody was used at a dilution of 1:3000 (AbCam Plc). The appropriate anti-mouse or anti-rabbit secondary antibody (Santa Cruz Biotech Inc) was used at a dilution of 1:1000. Chemiluminescent detection was performed using ECL detection reagent (GE Healthcare, Buckinghamshire, UK) according to the manufacturer's instructions.

Vaccinia virus replication assay

Cells were seeded in triplicate at a density of 2×10^5 cells. All plates were incubated overnight in normoxic or hypoxic conditions. Plates were infected 16 h later with VVLister at a MOI = 1 pfu per cell. Cells and supernatant were harvested using a cell scraper. Samples were freeze-thawed thrice and then centrifuged. The viral titre in each sample was determined by measuring the $TCID_{50}$ on indicator CV1 green monkey kidney cells. The cytopathic effect on CV1 was determined by light microscopy 10 days after infection. The Reed–Muench accumulate method was used to calculate the TCID50 value for each sample.[33] Triplicates were used for each time point and each replicate had cytopathic effect assayed twice. Viral burst titres were converted to pfu per cell based on the number of cells present at viral infection.

MTS Assay

Cells were seeded in medium supplemented with 5% fetal calf serum in 96-well plates, and maintained under hypoxic or normoxic conditions for 16 h before infection. On the day of infection, medium containing serial dilutions of vaccinia virus was added to each well. Cell viability was measured at 6 days by the MTS assay to assess vaccinia virus cytotoxicity. The MTS assays were carried out by adding 20 µl of the reagent provided in CellTiter96 Aqueous Nonradioactive cell proliferation assay kit (Promega, Madison, WI, USA) to each well and the plates were incubated at 37 °C with 5% CO_2 for 2–3 h. Hypoxic plates were always incubated in the hypoxic chamber for the entire duration of the experiment. Cell viability was determined by measuring the absorbance or optical density at 490 nm using an Opsys MR 96-well plate absorbance reader (Dynex, Chantilly, VA, USA), and a dose–response curve created by non-linear regression using Prism (GraphPad Software, La Jolla, CA, USA), allowing calculation of EC_{50} for each cell line and oxygen condition. The cell viability was measured as a percentage of viable cells remaining in the infected wells against viable cells remaining in the non-infected wells. Each assay contained six replicates and each assay was repeated four times.

Reporter gene expression detected by IVIS camera in vitro

Cells were infected with VVL15 for 24, 48 or 72 h and the luciferase activity measured using an IVIS camera (*In Vivo* Imaging System; Xenogen Corp., Alameda, CA, USA). Approximately 5×10^4 cells were seeded in 0.5 ml of media with 10% fetal calf serum in 24-well plates. Cells were incubated in normoxic or hypoxic conditions as indicated for 16 h. Cells were harvested from control plates and the mean number of cells per well was used to calculate the amount of virus required for infection. Cells were infected with a MOI of 1 pfu per cell of VVL15 in Dulbecco's modified Eagle's medium with 5% fetal calf serum. At 24, 48 and 72 h after infection, luciferase expression was determined as per the manufacturer's instructions. Media was replaced with 150 µg ml^{-1} D-luciferin (Xenogen Corp.) in serum-free medium at 37 °C and luminescence was measured two minutes later. Light emission was quantified as the sum of all detected photon counts within uniform-sized regions of interest with each well manually defined during post-data acquisition image analysis. This was measured in photons per second per cm^2 ($p\,s^{-1}\,cm^{-2}$) using Living Image software (Xenogen Corp.). The mean light emission per cell ($p\,sec^{-1}\,cm^{-2}$ per cell) was calculated using the number of cells infected at time 0 and compared for each MOI at 24, 48 and 72 h.

Statistical analysis
The unpaired students *t*-test was used for all statistical analysis unless otherwise specified.

Conflict of interest

The authors declare no conflict of interest.

Acknowledgements

This project is supported by Cancer Research UK (C633-A6253/A6251), and Barts and The London Research Advisory Board. We are very grateful to Professor Istvan Fodor of Loma Linda University, Loma Linda, CA, USA, for providing the viruses.

References

1 Harris AL. Hypoxia–a key regulatory factor in tumour growth. *Nat Rev Cancer* 2002; **2**: 38–47.
2 Hiley CT, Green MML, Shanks JH, Bottomley IC, West CML, Cowan RA *et al*. Expression of vascular endothelial growth factor (VEGF) in locally invasive prostate cancer is prognostic for radiotherapy outcome. *Int J Radiat Oncol Biol Phys* 2007; **67**: 84–90.
3 Hutchison GJ, Valentine HR, Loncaster JA, Davidson SE, Hunter RD, Roberts SA *et al*. Hypoxia-inducible factor 1alpha expression as an intrinsic marker of hypoxia: correlation with tumor oxygen, pimonidazole measurements, and outcome in locally advanced carcinoma of the cervix. *Clin Cancer Res* 2004; **10**: 8405–8412.
4 Ghaneh P, Costello E, Neoptolemos JP. Biology and management of pancreatic cancer. *Postgrad Med J* 2008; **84**: 478–497.
5 Koong AC, Mehta VK, Le QT, Fisher GA, Terris DJ, Brown JM *et al*. Pancreatic tumors show high levels of hypoxia. *Int J Radiat Oncol Biol Phys* 2000; **48**: 919–922.
6 Sun HC, Qiu ZJ, Liu J, Sun J, Jiang T, Huang KJ *et al*. Expression of hypoxia-inducible factor-1 alpha and associated proteins in pancreatic ductal adenocarcinoma and their impact on prognosis. *Int J Oncol* 2007; **30**: 1359–1367.
7 Yokoi K, Fidler IJ. Hypoxia increases resistance of human pancreatic cancer cells to apoptosis induced by gemcitabine. *Clin Cancer Res* 2004; **10**: 2299–2306.
8 Hawkins LK, Lemoine NR, Kirn D. Oncolytic biotherapy: a novel therapeutic platform. *Lancet Oncol* 2002; **3**: 17–26.
9 Mulvihill S, Warren R, Venook A, Adler A, Randlev B, Heise C *et al*. Safety and feasibility of injection with an E1B-55 kDa gene-deleted, replication-selective adenovirus (ONYX-015) into primary carcinomas of the pancreas: a phase I trial. *Gene Therapy* 2001; **8**: 308–315.
10 Hecht JR, Bedford R, Abbruzzese JL, Lahoti S, Reid TR, Soetikno RM *et al*. A phase I/II trial of intratumoral endoscopic ultrasound injection of ONYX-015 with intravenous gemcitabine in unresectable pancreatic carcinoma. *Clin Cancer Res* 2003; **9**: 555–561.
11 Pipiya T, Sauthoff H, Huang YQ, Chang B, Cheng J, Heitner S *et al*. Hypoxia reduces adenoviral replication in cancer cells by downregulation of viral protein expression. *Gene Therapy* 2005; **12**: 911–917.
12 Shen B, Hermiston T. Effect of hypoxia on Ad5 infection, transgene expression and replication. *Gene Therapy* 2005; **12**: 902–910.
13 Shen BH, Bauzon M, Hermiston TW. The effect of hypoxia on the uptake, replication and lytic potential of group B adenovirus type 3 (Ad3) and type 11p (Ad11p). *Gene Therapy* 2006; **13**: 986–990.
14 Fenner F. *Smallpox and Its Eradication (History of International Public Health, No. 6)*. World Health Organization: Geneva, 1988.
15 Smith GL, Moss B. Infectious poxvirus vectors have capacity for at least 25 000 base pairs of foreign DNA. *Gene* 1983; **25**: 21–28.
16 Schramm B, Locker J. Cytoplasmic organization of POXvirus DNA replication. *Traffic* 2005; **6**: 839–846.
17 Thorne SH. Oncolytic vaccinia virus: from bedside to benchtop and back. *Curr Opin Mol Ther* 2008; **10**: 387–392.
18 Townsley A, Weisberg A, Wagenaar T, Moss B. Vaccinia virus entry into cells via a low-pH-dependent endosomal pathway. *J Virol* 2006; **80**: 8899–8908.
19 Swietach P, Vaughan-Jones RD, Harris AL. Regulation of tumor pH and the role of carbonic anhydrase 9. *Cancer Metastasis Rev* 2007; **26**: 299–310.
20 Masson N, Ratcliffe PJ. HIF prolyl and asparaginyl hydroxylases in the biological response to intracellular O(2) levels. *J Cell Sci* 2003; **116**: 3041–3049.
21 Kraggerud SM, Sandvik JA, Pettersen EO. Regulation of protein synthesis in human cells exposed to extreme hypoxia. *Anticancer Res* 1995; **15**: 683–686.
22 Hay JG. The potential impact of hypoxia on the success of oncolytic virotherapy. *Curr Opin Mol Ther* 2005; **7**: 353–358.
23 Bhattacharyya M, Lemoine NR. Gene therapy developments for pancreatic cancer. *Best Pract Res Clin Gastroenterol* 2006; **20**: 285–298.
24 Connor JH, Naczki C, Koumenis C, Lyles DS. Replication and cytopathic effect of oncolytic vesicular stomatitis virus in hypoxic tumor cells *in vitro* and *in vivo*. *J Virol* 2004; **78**: 8960–8970.
25 Shen B, Bauzon M, Hermiston T. The effect of hypoxia on the uptake, replication and lytic potential of group B adenovirus type 3 (Ad3) and type 11p (Ad11p). *Gene Therapy* 2006; **13**: 986–990.
26 Poland GA, Grabenstein JD, Neff JM. The US smallpox vaccination program: a review of a large modern era smallpox vaccination implementation program. *Vaccine* 2005; **23**: 2078–2081.
27 Roenigk Jr HH, Deodhar S, St Jacques R, Burdick K. Immunotherapy of malignant melanoma with vaccinia virus. *Arch Dermatol* 1974; **109**: 668–673.
28 Kim JH, Oh JY, Park BH, Lee DE, Kim JS, Park HE *et al*. Systemic armed oncolytic and immunologic therapy for cancer with JX-594, a targeted poxvirus expressing GM-CSF. *Mol Ther* 2006; **14**: 361–370.
29 Park BH, Hwang T, Liu TC, Sze DY, Kim JS, Kwon HC *et al*. Use of a targeted oncolytic poxvirus, JX-594, in patients with refractory primary or metastatic liver cancer: a phase I trial. *Lancet Oncol* 2008; **9**: 533–542.
30 Binley K, Iqball S, Kingsman A, Kingsman S, Naylor S. An adenoviral vector regulated by hypoxia for the treatment of ischaemic disease and cancer. *Gene Therapy* 1999; **6**: 1721–1727.
31 Binley K, Askham Z, Martin L, Spearman H, Day D, Kingsman S *et al*. Hypoxia-mediated tumour targeting. *Gene Therapy* 2003; **10**: 540–549.
32 Hung CF, Tsai YC, He L, Coukos G, Fodor I, Qin L *et al*. Vaccinia virus preferentially infects and controls human and murine ovarian tumors in mice. *Gene Therapy* 2007; **14**: 20–29.
33 Reed LJ, Muench H. A simple method of estimating fifty percent endpoints. *Am J Hyg* 1938; **27**: 493–497.